INSTITUTO SUPERIOR TÉCNICO
Universidade Técnica de Lisboa

Data Rate Performance Gains in UMTS Evolution to LTE at the Cellular Level

Pedro Atanásio Carreira

Dissertation submitted for obtaining the degree of
Master in Electrical and Computer Engineering

Jury

Supervisor:	Prof. Luís M. Correia
Co-Supervisor:	Eng. Ricardo Dinis
President:	Prof. José Bioucas Dias
Member:	Prof. António Rodrigues

October 2011

To the Ones I love

Acknowledgements

First of all, I would like to thank Professor Luís Correia, for giving me the opportunity to work on this thesis. His discipline and supervision are reflected on the final work presented. Furthermore, the expertise felt within GROW and the interesting works presented within the group gave rise to what I found to be a compelling environment to learn and develop a critical attitude about research topics presented. Also, the partnership established with a national telecom operator allowed for additional motivation and interest in the development of the work.

To Optimus, namely Eng. Luís Santo, Eng. Ricardo Dinis and Eng. Sérgio Gonçalves, for their initial work planning and for their friendly and always available attitude, despite their limited time. Being able to conduct measurements in a live LTE cluster brings great added value to the work performed, and the technical support provided throughout thesis development largely contributed to the work success.

To the Professors who have contributed for my personal development, namely Prof. Ana Fred, who allowed me to learn on such interesting topics as data clustering, Prof. António Rodrigues and João Sobrinho, for their always available and friendly attitude, intrinsically combined with good teaching. Also to Prof. Rui Castro for the friendly attitude and for the great relationship he is able to maintain with students, even if they have not actually been students of his.

To my new and long time friends in RF II, Diogo Silva and Tiago Gonçalves, Ricardo Batista and João Pato, I would like to show my gratitude for the basement discussions and help provided. Being able to troubleshoot problems while always finding a genuine interest in the topic largely contributed for the presented work. Especially Ricardo and João, friends and colleagues for a longer period, their attitude together with their friendship allowed for the most pleasant journey throughout the whole MSc degree.

To my friends Sílvio Rodrigues, Ricardo Grizonic, João Falcão, Henrique Silva and João Meireles who followed me during the journey in IST, the good friendship and experiences lived together have largely contributed to my personal enrichment, as well as to take the most out of life itself. All the good moments will be kept, and many more will come. To the many other friends, to whom I got closer and more distanced during different times along the study period at IST, I would like to say thank you for contributing to my journey.

At last, but not least, I would like to say thank you to my closest family, my Parents and Sister, but also to the whole family for being always there for me. Their understanding and love was vital to me along this period, and of the furthermost importance for the completion of this work.

Abstract

Mobile communications technologies are aiming at responding to the growing demand for higher connectivity. Performance of recent 3G and 4G systems, UMTS/HSPA+ and LTE, is evaluated regarding the number of users. LTE measurements were taken and system implementation features analysed. A simulator for UMTS and LTE was built based on the results, considering both single- and multi-user scenarios. DL average throughputs of 40 Mbps and 69 Mbps, for UMTS and LTE, are obtained for single-user. Interference coordination and additionally higher order MIMO in LTE increase data rates by factors up to 1.39 and 2.31. Rising average throughput ratio between UMTS and LTE is proved to follow a logarithmic law with the number of users in DL. In UL, average data rates of 11 Mbps and 68 Mbps, for UMTS and LTE, are observed for one user. Interference coordination provides gains up to a factor of 1.5. Approximately stable UMTS to LTE gains are obtained for more than 5 users. Higher data rate variations were measured across the cell in LTE compared to UMTS, for UL and DL. Apart from very particular scenarios, LTE provides for the best UL and DL coverage in the typical multi-user scenarios studied, across all environments.

Keywords

LTE, UMTS/HSPA+, Capacity, Throughput, Coverage, QoS

Resumo

As comunicações móveis enfrentam actualmente a exigência de maior conectividade. Nesse sentido é feita uma análise de performance dos sistemas 3G e 4G, UMTS/HSPA+ e LTE, em ambiente multi-utilizador. Efectuaram-se medidas de LTE e analisaram-se características de implementação. Foi construído um simulador com base nos resultados, para os cenários mono- e multi-utilizador. Obtiveram-se débitos binários médios de 40 Mbps e 69 Mbps, para UMTS e LTE, para um utilizador no DL. O recurso a coordenação de interferência e adicionalmente a configurações avançadas de MIMO aumenta os débitos por factores de até 1.39 e 2.31. Prova-se que os rácios de débito médio entre UMTS e LTE seguem uma lei logarítmica com o número de utilizadores. No UL, medem-se débitos médios de 11 Mbps e 68 Mbps, em UMTS e LTE, apesar do uso de coordenação de interferência em LTE permitir ganhos de até 1.5. São medidos ganhos aproximadamente constantes de UMTS para LTE para mais de 5 utilizadores em UL. É medida uma maior variação de débito ao longo da célula em LTE do que em UMTS, para UL e DL. À parte de cenários muito particulares, o LTE oferece ainda uma melhor cobertura nos cenários típicos de multi-utilizador, para qualquer ambiente.

Palavras-chave

LTE, UMTS/HSPA+, Capacidade, Débito, Cobertura, QoS

Table of Contents

List of Figures

List of Tables

List of Acronyms

3G	3rd Generation
3GPP	3rd Generation Partnership Project
4G	4th Generation
AMC	Adaptive Modulation Coding
AWGN	Additive White Gaussian Noise
BER	Bit Error Rate
BLER	Block Error Rate
BS	Base Station
CCH	Common Channel
CDF	Cumulative Distribution Function
CDMA	Code Division Multiple Access
CN	Core Network
CP	Cyclic Prefix
CPC	Continuous Packet Connectivity
CQI	Channel Quality Indication
CS	Circuit-Switched
CSI	Channel State Information
CSV	Comma-Separated Values
DCH	Dedicated Channel
DL	Downlink
DPCCH	Dedicated Physical Control Channel
DPCH	Dedicated Physical Channels
DS-CDMA	Direct-Sequence CDMA
DSCH	Downlink Shared Channel
E-DCH	Evolved-DCH
EIRP	Equivalent Isotropic Radiated Power
eNB	Evolved Node B
EPA	Extended Pedestrian A
EPC	Evolved Packet Core Network
EPS	Evolved Packet System
ETU	Extended Typical Urban
E-UTRAN	Evolved UTRAN
EVA	Extended Vehicular A
FACH	Forward Access Channel

FDD	Frequency Division Duplexing
FTP	File Transfer Protocol
GBSB	Geometrically Based Single Bounce
GGSN	Gateway GPRS Support Node
GMSC	Gateway MSC
GPRS	General Packet Radio Service
GSM	Global System for Mobile Communications
GUI	Graphical User Interface
HARQ	Hybrid Automatic Repeat Request
HLR	Home Location Register
HO	Handover
HOM	Higher Order Modulation
HSDPA	High Speed Downlink Packet Access
HS-DPCCH	High-Speed Dedicated Physical Control Channel
HS-DSCH	High-Speed Downlink Shared Channel
HSPA	High Speed Packet Access
HSPA+	HSPA Evolution
HS-PDSCH	High-Speed Physical Downlink Shared Channel
HSS	Home Subscription Server
HS-SCCH	High-Speed Shared Control Channel
HSUPA	High Speed Uplink Packet Access
ICIC	Inter-Cell Interference Coordination
IMS	IP Multimedia Sub-system
IP	Internet Protocol
IPTV	IP Television
ISD	Inter-Site Distance
ISI	Inter-Symbol Interference
L1	Layer-1
L2	Layer-2
LoS	Line of Sight
LTE	Long Term Evolution
MAC	Medium Access Control
MBMS	Multimedia Broadcast Multicast Service
MCS	Modulation and Coding Scheme
ME	Mobile Equipment
MIMO	Multiple Input Multiple Output
MISO	Multiple Input Single Output
MM	Mobility Management
MME	Mobility Management Entity
MRC	Maximal Ratio Combining

MMOG	Multimedia Online Gaming
MSC	Mobile Switching Centre
MT	Mobile Terminal
NB	Node B
NLoS	Non-LoS
OFDM	Orthogonal Frequency Division Multiplexing
OFDMA	Orthogonal Frequency Division Multiple Access
OLSM	Open Loop Spatial Multiplexing
OVSF	Orthogonal Variable Spreading Factor
PAR	Peak-to-Average-power-Ratio
PBCH	Physical Broadcast Channel
P-CPICH	Primary Common Pilot Channel
PCRF	Policy and Charging Resource Function
PDCCH	Physical Downlink Control Channel
PDSCH	Physical Downlink Shared Channel
PDU	Protocol Data Unit
P-GW	Packet Data Network Gateway
PMI	Pre-coding Matrix Indicator
PRACH	Physical Random Access Channel
PS	Packet-Switched
PSS	Primary Synchronisation Signal
PUCCH	Physical Uplink Control Channel
PUSCH	Physical Uplink Shared Channel
QAM	Quadrature Amplitude Modulation
QoS	Quality of Service
QPSK	Quadrature Phase Shift Keying
RACH	Random Access Channel
RB	Resource Block
RF	Radio Frequency
RI	Rank Indicator
RLC	Radio Link Control
RMG	Relative MIMO Gain
RNC	Radio Network Controller
RRC	Radio Resource Control
RRM	Radio Resource Management
RSRP	Reference Signal Reference Power
RTT	Round Trip Time
SAE	System Architecture Evolution
SAE-GW	SAE Gateway
SC-FDMA	Single Carrier Frequency Division Multiple Access

SF	Spreading Factor
SFBC	Space-Frequency Block Coding
SGSN	Serving GPRS Support Node
S-GW	Serving Gateway
SIMO	Single Input Multiple Output
SINR	Signal-to-Interference-plus-Noise Ratio
SIR	Signal-to-Interference-Ratio
SISO	Single Input Single Output
SNR	Signal-to-Noise-Ratio
SSS	Secondary Synchronisation Signal
TDD	Time Division Duplexing
TTI	Transmission Time Interval
UE	User Equipment
UFR	Universal Frequency Reuse
UL	Uplink
UMTS	Universal Mobile Telecommunications System
USIM	UMTS Subscriber Identity Mobile
UTRAN	UMTS Terrestrial Radio Access Network
VLR	Visitor Location Register
VoIP	Voice over IP
WCDMA	Wideband CDMA
WiMAX	Worldwide Interoperability for Microwave Access

List of Symbols

α	Downlink orthogonality factor
γ_s	Subcarrier activity factor of cell s
Δf	Subcarrier spacing
$\overline{\varepsilon_r}$	Mean relative error
$\overline{\varepsilon_r^2}$	Mean square error
η	Load factor
$\overline{\eta_{DL}}$	Average DL load factor value across the cell
η_{sch}	Scheduler efficiency
μ	Mean value
ν	Non-centrality parameter of the Rice distribution
ρ_N	SNR
ρ_{IN}	SNIR
$\rho_{N\ ICIC}$	SNR employing ICIC schemes
φ	Incidence angle
σ	Standard deviation
τ_{FF}	Fast fading coherence time
τ_{SF}	Slow fading coherence time
a_{pd}	Average power decay
B	Bandwidth of the total RBs allocated, in LTE, or R_c, in UMTS
B_k	Bandwidth allocated to user k
$\bar{B}_u$	Average bandwidth of the RBs allocated per user
C_{MIMO}	Capacity of the MIMO system
$corr(Z,Y)$	Correlation between random variables Z and Y
$cov(Z,Y)$	Covariance between random variables Z and Y
C_{SISO}	Capacity of the SISO system
d	Distance between user and BS
E_b	Energy per bit
E_c	Energy per chip stream
f	Frequency
F	Noise figure of the receiver
g_a	Array gain
G_{div}	Diversity gain

G_{ICIC}	ICIC scheme gain
$G_{M/S}$	Relative MIMO Gain
G_{MHA}	Masthead amplifier gain
$G_{multi-user\ div}$	Capacity gain obtained due to multi-user diversity
G_P	Processing gain
G_{pos}	Capacity gain obtained due to users' positioning in the cell
$G_{r\ div}$	Gain of the receiving antenna, including diversity
G_r	Gain of the receiving antenna
G_{SIMO}	Relative SIMO gain
G_t	Gain of the transmitting antenna
h_b	BS height
H_B	Buildings' height
$\left\|H_{k_j}^{s}\right\|$	Channel gain from the serving cell s to user k, transmitting in RB j
$\left\|H_{k_{m_j}}^{s_n}\right\|$	Channel gain from the serving cell s_n to user k_m, transmitting in RB j
h_m	MT height
I_{rat}	Ratio of inter- to intra-cell interferences power
K	Rice parameter
k_d	Dependence of the multiscreen diffraction loss versus distance
L_0	Free space loss
L_{COST231}	COST231-Walfisch-Ikegami propagation losses
L_{Link}	Link loss
L_c	Cable losses between transmitter and antenna
L_p	Pathloss
$L_{p\ ind}$	Pathloss due to indoor propagation
$L_{p,k}$	Pathloss from serving BS to user k
$L_{p,k,s}$	Pathloss from user k in cell s to the serving BS
$\mathrm{L_{p,}}_s$	Pathloss from BS s to the user
$L_{p\ máx}$	Maximum pathloss without attenuation or losses
$L_{p\ out}$	Pathloss due to outdoor propagation
$L_{p\ total}$	Total pathloss
L_{ref}	Propagation model losses
L_{rm}	Approximation for the multi-screen diffraction loss
L_{rt}	Rooftop-to-street diffraction and scatter loss
L_u	User losses
m	Modulation order
M	Total margin
M_F	Total fading margin

M_{FF}	Fast fading margin
M_I	Interference margin
$\overline{M_I}$	Average interference margin
M_{SF}	Slow fading margin
N	Total noise power
N_0	Noise power spectral density
N_{BS}	Number of neighbouring BSs
N_R	Number of receiving antennas
N_{RB}^{DL}	Number of RBs used in DL
N_{RB}^{UL}	Number of RBs used in UL
N_{RB}^{u}	Number of user RBs
N_{RF}	Noise power at the receiver
N_{TA}	Timing offset between UL and DL radio frames at the UE in units of T_S
N_{rat}^{eNB}	Ratio between users close to eNB and total number of users
N_{sc}^{RB}	Number of subcarriers per resource block
$N_{streams}$	Number of MIMO streams
N_{symb}^{SF}	Number of symbols per sub-frame
N_{symb}^{slot}	Number of symbols per time slot
N_T	Number of transmitting antennas
N_u	Number of users
N_z	Number of samples of dataset Z
P_I	Interference power
$P_{I_{inter}}$	Received inter-cell interference power
$P_{I_{inter}}^{DL}$	Received DL inter-cell interference power
$P_{I_{inter}}^{UL}$	Received UL inter-cell interference power
$P_{I_{intra}}$	Received intra-cell interference power
$P_{I_{intra}}^{DL}$	Received DL intra-cell interference power
$P_{I_{intra}}^{UL}$	Received UL intra-cell interference power
$P_{I_{inter,max\,s}}$	Maximum interference power of cell s
P_{T_X}	Total transmission power
$P_{T_X}^{DL}$	Total BS transmitted power
$P_{T_X,k}^{DL}$	BS transmitted power to user k
$P_{T_X,s}^{DL}$	BS s transmitted power
$P_{T_X,k}^{UL}$	UE transmitted power to BS
$P_{T_X,k,s}^{UL}$	Transmitted power from user k in adjacent cell s
$P_{T_X}^{Con}$	Power allocated to the common channels
$P_{T_X}^{Ded}$	Power allocated to the dedicated channels

$P_{T_{X_j}}^{s}$	Transmit power from cell s, transmitting in RB j
$P_{T_{X_j}}^{s_n}$	Transmit power from cell s_n, transmitting in RB j
P_{DSCH}	Received power of the DSCH
$P_{HS-DSCH}$	Received power of HS-DSCH
$P_{Rx\,min}$	Receiver sensitivity
$P_{S\&C}$	Signalling and control power
P_r	Power available at the receiving antenna
P_t	Power fed to the transmitting antenna
r	Cell radius
R_b	Data bit rate
$\bar{R}_b$	Average user data bit rate
R_c	Chip rate
SF_{16}	HS-PDSCH Spreading Factor of 16
T_S	Sample period
T_{SF}	Sub-frame period
T_{slot}	Time slot duration
v	User activity factor
$\bar{v}$	Average user activity factor
$\bar{x}$	Mean value of x
w_B	Inter Buildings Distance
w_s	Street width
z_i	Sample i of variable z

List of Software

MATLAB	Computational Math Tool
Microsoft Visual C++ 2010	ANSI C++ Integrated Development Environment
Microsoft Excel 2007	Calculation and graphical chart tool
Microsoft Word 2007	Text editor software
Microsoft Powerpoint 2007	Presentation software
Microsoft Visio 2007	Design tool (e.g. diagrams, flowcharts, etc)

Chapter 1

Introduction

The present chapter introduces the theme of this dissertation, in particular, over a contextual and motivational perspective, while simultaneously providing an overview of the assumptions established for the work development. Furthermore, it establishes the scope for the work performed together with its main contributions, followed by the detailed presentation of the work's structure.

1.1 Overview

Mobile communications have known, in recent years, great technological developments that have had important social and economical impacts. No matter where, how old or for what cost, societies in general have been eager to be part of the emerging highly connected information world. The demand for an always on connection to Web services and personal communications services has supported the development of broadband connection services. Particularly, for cellular systems in Europe, this is directly reflected in a huge appetite for mobile broadband capable systems, namely the Universal Mobile Communications Systems (UMTS), in its latest High Speed Packet Access Evolved (HSPA+) version, marketed as a 3rd Generation (3G) technology, and the Long Term Evolution (LTE) system, marketed as a 4th Generation (4G) one, Figure 1.1. While UMTS's initial release came out around the year 2000, LTE was standardised in 2007, both by the 3rd Generation Partnership Project (3GPP), and initial standards for LTE Advanced have been later introduced in 2010.

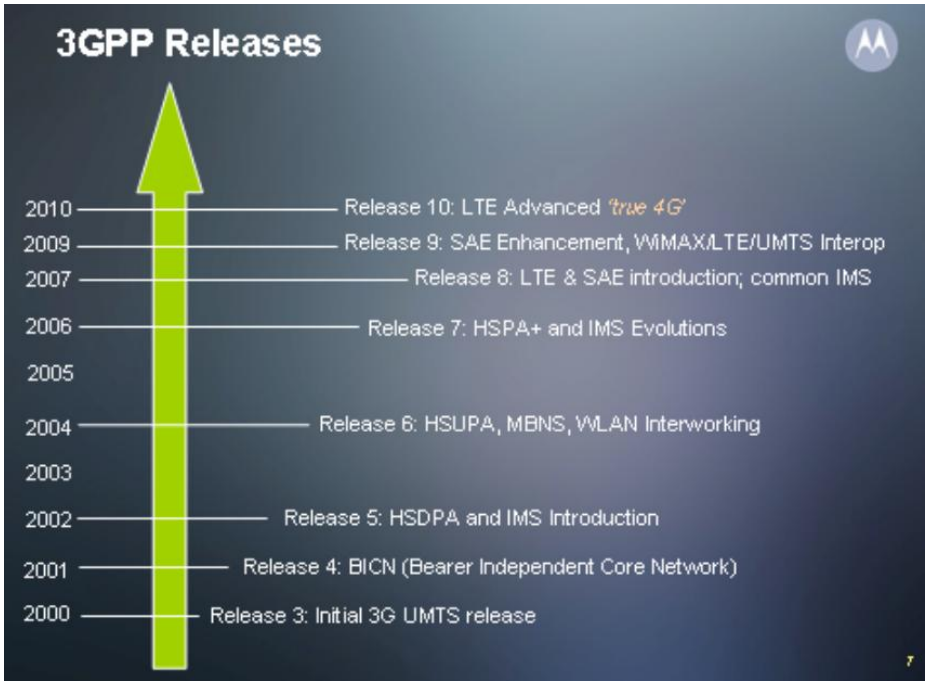

Figure 1.1. 3GPP's mobile communications systems' releases (extracted from [Moto09]).

As for HSPA+, specified in 2006 in 3GPP's Release 7, it is the natural upgrade from the High Speed Packet Access (HSPA), providing backward compatibility with all former UMTS evolutions. Based on Wideband Code Division Multiple Access (WCDMA), it supports both data and voice services. Enhanced features include optimal performance for single and aggregated 5 MHz carriers, while it also enables Multiple Input Multiple Output (MIMO) schemes for data rate improvements, currently allowing for a theoretical maximum of 42 Mbps in Downlink (DL), and 11.5 Mbps in Uplink (UL).

In LTE, specified in 3GPP's Release 8 in 2008, significantly different technologies are employed, both

in the air interface and core network, aiming at bringing higher spectral efficiency and the network closer to the world of Internet Protocol (IP). LTE uses Orthogonal Frequency Division Multiplexing (OFDM) for radio access, together with more advanced MIMO schemes, providing for theoretical maximum data rates of 326 Mbps and 86 Mbps, for DL and UL, respectively.

Performance and usability of mobile handsets has improved together with a wide adoption of 3G dongles. As a consequence, mobile data traffic has been increasing exponentially, Figure 1.2-a), and the number of subscribers continues to grown considerably, as well as usage rates. The emergence of new applications, such as Multimedia Online Gaming (MMOG), Web 2.0 and Video Streaming, is in many cases responsible for this unprecedented increase. All together, a growing traffic placed on 3G networks is bringing significant network congestion in urban areas, and many operators are reporting that a significant portion of their cell sites are already running over capacity, despite having enabled all their UMTS carriers, [Moto09].

Simultaneously, as data services are following a growth curve similar to the one seen for wire line data, the average revenue per user is falling almost as rapidly, Figure 1.2-b). Thus, wireless network operators in virtually every market have been analysing the need to change the way they deliver services.

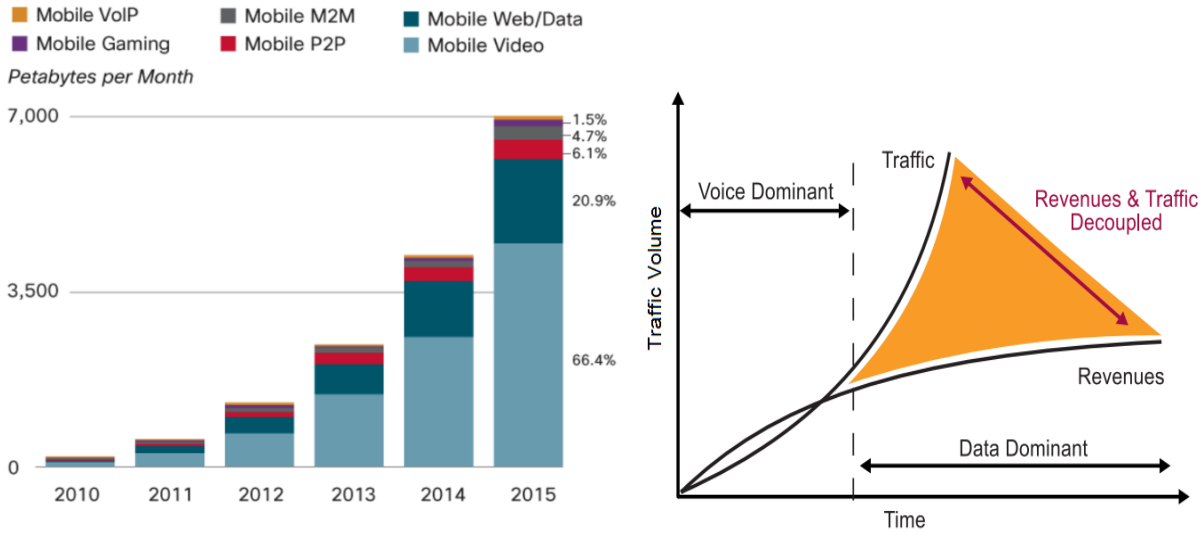

(a) Global mobile data traffic growth per year (adapted from [Cisc11]).

(b) Traffic growth versus revenue in mobile communications ([Open10]).

Figure 1.2. Trends on the evolution of the telecom market.

Once an operator has deployed all of its UMTS carriers, it is faced with the need to provide additional capacity, which can only be achieved by adding more cells sites or by means of an LTE network overlay. Many operators have been lead to deploy LTE to meet the needs of the wireless broadband mass market, and allow for bandwidth-hungry applications to be supported cost effectively with better user experience. A solution could be to initially promote LTE for the heaviest data users, e.g., laptop subscribers, relieving the congestion on the 3G network for lighter users, e.g., smartphone subscribers, Figure 1.3.

According to the study case by [Moto09], this strategy would allow to deliver mass market wireless broadband, minimise proliferation of cell sites, and enhance consumer experience by relieving congestion, while further leveraging high performance LTE for early adopters. Higher data rates, flat rate tariff and continually improving coverage are thus perfectly reachable, i.e., by initially adopting the high capacity LTE in addition to an HSPA network.

Furthermore, it is expected that LTE capacity and lower cost per bit allow for high quality video streaming on any type of mobile devices. Mobile operators with fixed line broadband networks that are already offering Television over IP (IPTV) like services will also be able to leverage these assets on LTE. Rich media solutions connected to the LTE core network will give operators the ability to converge broadcasting, video on demand, innovative applications and advertisements solutions into their LTE service, and hence provide the opportunity for faster investment recovery.

With the envisaged throughput and latency targets complemented by an emphasis on simplicity, spectrum flexibility, added capacity and lower cost per bit, LTE is destined to provide a greatly improved user experience. Furthermore it is expected to deliver new revenue generating mobile services that will excite users and help operators drive competitive advantage and benefit their mobile broadband services profitability.

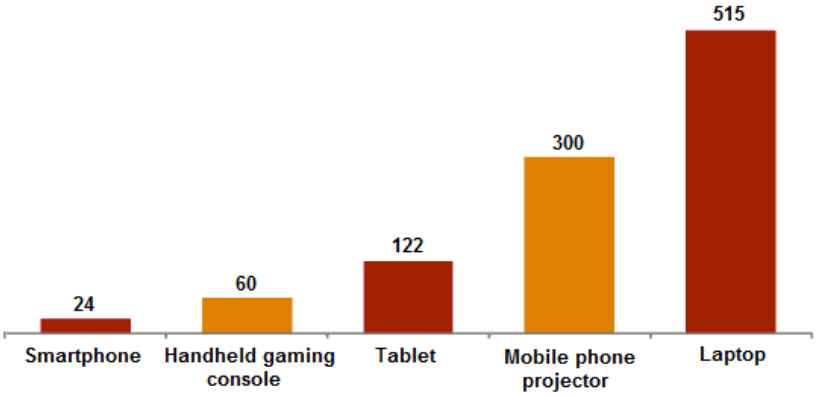

Figure 1.3. Mobile device data traffic multiplier, based on data equivalents of monthly feature phone traffic (adapted from [Cisc11]).

Faced with the described market trends and the current economical situation, Portuguese operators have been carefully analysing the new opportunities generated by the system, together with the first tests on recently installed LTE clusters. In most cases, operators have recently deployed UMTS/HSPA+ and in some cases even double carrier HSPA+. However, the settlement of a new system architecture and network planning is still required in the near future, and should prove to be worthwhile from the operators' view point.

Real data rate performance gains over the average system cell are thus of great interest to the operator, in order to provide sustainable decision on the migration. Preparing the network to meet the growing subscribers' hunger for bandwidth demands a strategic and focused approach, and only by making careful, well-planned choices in next generation technology will today's operators survive in an increasingly competitive market.

1.2 Motivation and Contents

The main scope of this thesis is to compare two systems: UMTS/HSPA+ and LTE. As LTE looks for its place as the successor to UMTS, an analysis of the system's transmission characteristics over varying environment, channel, cell load and coverage for different services is determinant for migration analysis. Therefore, the aim of the analysis is to study, for both DL and UL, capacity and coverage aspects, taking data rate gains as a reference.

The main contribution of this thesis is the development of a model for two different analysis: one to evaluate maximum data rates obtained, allowing for computing data rate gains from UMTS/HSPA+ to LTE, and the other to analyse maximum cell range, providing the use of a given service. Supported by measurements performed in a live LTE network, one can have a very good comparison of the two technologies at stake.

For work development, a partnership was established with Optimus, a Portuguese mobile operator. The collaboration had the important role of providing assistance on several technical details and insights on the technologies, as well as supporting the measurements' campaign performed.

The present thesis is composed of 5 chapters, including the present one. Chapter 2 presents an introduction to UMTS/HSPA+ and LTE. UMTS basic concepts are overviewed, and key features of the releases under study emphasised. Particularly, radio interface measurement grades are out looked, regarding coverage and capacity. A similar analysis follows then, for LTE, in a subsequent section. At the end, a full side by side comparison of the two systems is presented, enhancing key strengths and weaknesses of the two systems, followed by an overview of the current state of the art on the topic.

Chapter 3 introduces the developed models used for simulation. The single cell model is explained, for both single- and multi-user scenarios, for analysis over different channel, environment, cell load and service coverage scenarios. UMTS and LTE systems' modules developed for both DL and UL are also described together with the propagation and channel simulation modules. The simulator assessment is presented at the end.

In Chapter 4, LTE measurements' and simulations' single-user results are taken under an exhaustive analysis, where the influence of varying environment, channel and cell load is mainly considered. Finally the full comparison with capacity and coverage results for UMTS/HSPA+ is done, for a multi-user scenario, and for both DL and UL.

Chapter 5 concludes the present dissertation, where a critical analysis is drawn followed by the main work conclusions. Furthermore, suggestions for future work are outlined and paths for further research on next generation mobile communications' solutions are enlightened. Finally, a set of annexes closes the present document, with supplementary information, when the need for the global comprehension of the problem exists.

Chapter 2

Basic Concepts

This chapter provides an overview of UMTS, focusing on system architecture, radio interface, coverage and capacity, and general performance. In the following the LTE system is analysed in a similar way, drawing comparisons with UMTS. Finally, a brief comparison between the two systems is drawn and state of the art on the subject presented.

2.1 UMTS

This section overviews the fundamental concepts regarding UMTS in its most recent form. First, the system architecture is presented, together with its main elements. A brief description of the radio interface follows, basic concepts of coverage and capacity are overviewed, and finally a performance analysis is drawn. This section is based on [HoTo07] and [3GPP10a].

2.1.1 Network Architecture

UMTS's network architecture, Figure 2.1 was first defined in 3GPP's Release99, remaining unchanged in later releases. It consists of a number of network elements that can be grouped into three sub-networks: User's Equipment (UE), UMTS Terrestrial Radio Access Network (UTRAN) and Core Network (CN).

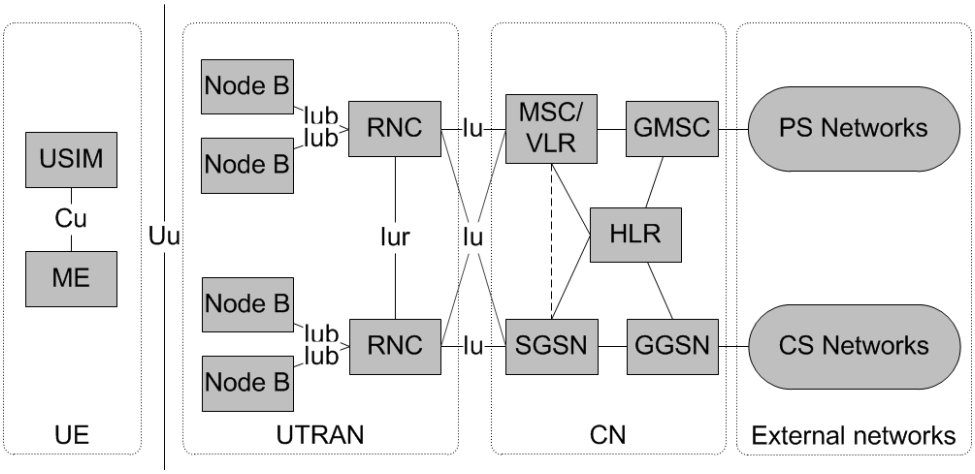

Figure 2.1. UMTS network architecture (adapted from [HoTo07]).

The UE is composed by the UMTS Subscriber Identity Mobile (USIM), and by the Mobile Equipment (ME) or Mobile Terminal (MT), connected through the Cu interface. The USIM contains user-specific information and an authentication key used in access to the network. The ME is the UMTS terminal, which incorporates the protocol stack of the radio interface, as well as the operating elements for the user interface.

The UTRAN encapsulates all tasks connected with transmission of information over radio, and consists of the Node Bs (NBs), the Base Stations (BSs), and the Radio Network Controller (RNC). The Node B converts the data flow between the Iub and Uu interfaces, dealing with the radio channels and the RNC that owns and controls the radio resources in its domain, connecting to the NB and also to the CN through the Iu interface. RNCs are connected through the Iur interface.

The UMTS CN is based on the GSM network, providing the switching, routing, transport and database functions for user traffic. The CN contains Circuit-Switched (CS) elements such as: the Mobile

Switching Centre (MSC), a central switching node of the CS domain of the CN, responsible for switching the CS transactions, namely voice; and the Gateway MSC (GMSC), a switch on the connection between the CN and the external CS networks. Regarding Packet-Switched (PS) elements it includes: the Serving General Packet Radio Service (GPRS) Support Node (SGSN), a central switching node of the PS domain in the CN, responsible for the delivery of data packets from and to the BSs; and the Gateway GPRS Support Node (GGSN), a switch with functionality close to that of GMSC, but connecting the CN to the external PS networks.
Furthermore, two elements exist that are both CS and PS based: theHome Location Register (HLR), a database located in the users' home system that stores the users' service profiles, such as associated authorisations and keys in a connection; and the Visitor Location Register (VLR), a distributed database that saves temporary information about the active users in the geographical area allocated to it, preventing the central database to be interrogated for all the subscriber information each time a new subscriber roams into a location area.

2.1.2 Radio Interface

UMTS's WCDMA radio interface is based on Direct-Sequence Code Division Multiple Access (DS-CDMA), a spread spectrum air interface, with a chip rate of 3.84 Mcps leading to a radio channel of 4.4 MHz and separation of 5 MHz. This access method allows for very high and variable bandwidths, low delay, smooth mobility for voice and packet data and inter-working with existing GSM/GPRS networks. As defined in [3GPP10a], in 3GPP's Release 99, the frequency bands for Europe are [1920, 1980] MHz for UL and [2110, 2170] MHz for DL.

In UMTS, two types of codes are used for spreading and WCDMA multiple access: channelisation and scrambling, [Corr08]. Channelisation codes are used in DL for UE separation, whilst in UL they distinguish between physical data and control channels. The sequence of chips is multiplied by the user's information, associating to a spreading factor the use of an Orthogonal Variable Spreading Factor (OVSF) code, and obtaining a wide spectrum signal. Codes allow to maintain orthogonality between them and to vary the Spreading Factor (SF). Scrambling is used on top of spreading, so it does not change the signal bandwidth, and enables sector separation in DL, and UE separation in UL.

UMTS also provides for power management and soft and softer handovers. Power management is achieved using closed loop power control in both UL, to avoid using excessive power and increasing interference, and DL, taking in account a margin of the cell limits, and using outer loop power control to dynamically adjust the Signal-to-Interference-Ratio (SIR), saving in system capacity. Soft and softer Handovers (HOs) take place in a user transition between cells or sectors of a cell, respectively, allowing for the combining of the received user signal in the RNC or BS, respectively.

High Speed Downlink Packet Access (HSDPA) and High Speed Uplink Packet Access (HSUPA), together known as HSPA, are evolutions of 3GPP's Release 99 being defined in Release 5 and Release 6, respectively. With HSDPA, scheduling control and link adaptation based on physical layer retransmissions were moved from the RNC to the BS, guaranteeing fast link adaptation and fast channel-dependent scheduling, [HoTo09]. Furthermore, the duration of the transmission, named

Transmission Time Interval (TTI), is defined to be 2 ms to achieve a short round-trip delay for the operation between UE and BS for retransmissions, [HoTo07].

For user data transmission, a fixed SF of 16 is specified for HSDPA, as 15 channelisation codes are available per UE in the High-Speed Physical Downlink Shared Channel (HS-PDSCH), and the last channelisation code is reserved for the High-Speed Shared Control Channel (HS-SCCH). HSUPA also introduces new channels for scheduling and retransmission control, as well as for data transmission; for further information refer to [HoTo06].

HSDPA does not support soft handover or fast power control. Release 6 initially defines that, in case of good channel conditions, the use of 16 Quadrature Amplitude Modulation (QAM) for HSDPA is possible, and also that a Hybrid Automatic Repeat Request (HARQ) with soft combining scheme is used, meaning that the UEs store data from previous transmissions to enable joint decoding of retransmissions. While in the DL BSs can be asynchronous and sequence numbering is necessary, the HARQ used in HSUPA is fully synchronous and also operating in soft handover.

HSPA evolution, also known as HSPA+, is defined in Release 7, further extended in Releases 8 and 9, and is targeted to improve end user performance by lower latency, lower power consumption, and higher data rates along with including inter-working features with LTE. In line with the greater use of UMTS/HSPA for packet data transmission, HSPA+ mainly introduces:

- Higher Order Modulation (HOM) and MIMO.
- Advanced G-Rake receivers.
- Superior interference cancellation techniques.
- Multi-Carrier HSDPA and Dual-Carrier HSUPA.
- Layer 2 optimisation
- Flat Architecture.

In theory, a number of ways exist to push the peak data rate higher: increase the bandwidth used, adopt HOM schemes or use multi-stream MIMO transmission. HOM was included in Release 7, specifying the modulation schemes of 16QAM for UL and 64QAM for DL, and MIMO in the DL was also included. Considering that the rate doubles from Quadrature Phase Shift Keying (QPSK) to 16QAM and increases by 50% from 16QAM to 64QAM, and that an increase of 6 dB in Signal-to-Interference-plus-Noise Ratio (SINR) is required for each transition, one can conclude that HOMs can be used only in favourable channel conditions.

Further resorting to MIMO, i.e., the use of multiple antennas and spatial multiplexing to receive multiple transport blocks in parallel, provides for a linear increase of the theoretical peak data rates with the number of transmitted data streams. Exploiting multipath MIMO allows also for improving link reliability and achieving higher spectral efficiency, all without consuming extra radio frequency. The 3GPP MIMO concept for HSPA+ uses two transmit antennas in the BS and two receive antennas in the MT, and uses a closed loop feedback from the MT for adjusting the transmit antenna weighting. The preferred antenna weights are delivered from UE to NB on a High-Speed Dedicated Physical Control Channel (HS-DPCCH) together with Channel Quality Information (CQI), and the information

on used antenna weights in DL is signalled on HS-SCCH.

As shown in Figure 2.2, the peak bit rate with 64QAM is 21.1 Mbps, rising to 28.0 Mbps with MIMO, whereas using 64QAM and MIMO together provide a rise from 14Mbps to 42 Mbps, [HoTo09]. The 16QAM capability in UL enables to push the peak bit rate to 11.5 Mbps, although MIMO is not used in this link, mainly because it obliges the UE to have two power amplifiers. In DL, HOM helps to improve the spectral efficiency because there is a limited number of orthogonal resources. The same is not true for UL, since there is a large availability of codes. Thus, in UL, using 16QAM is a peak data feature and not a capacity feature.

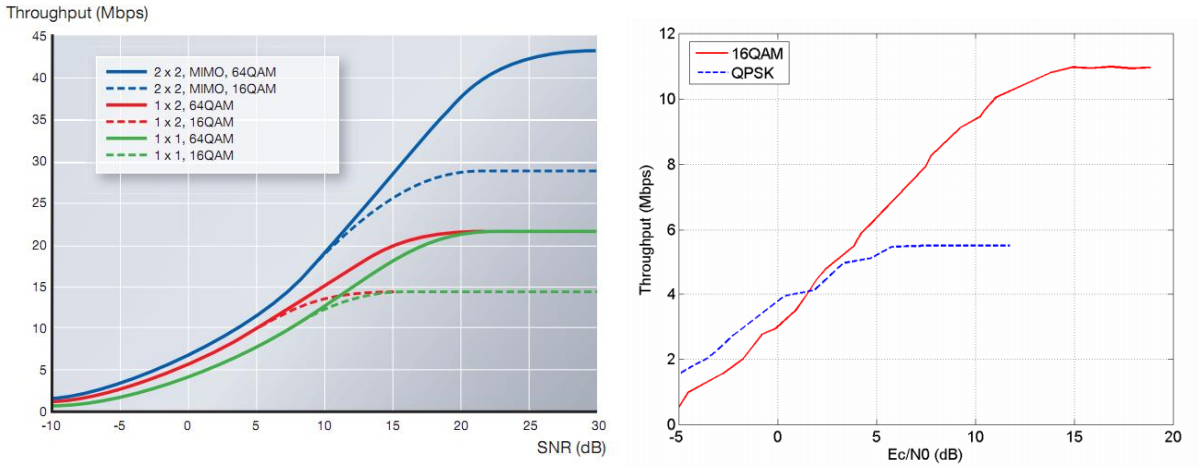

(a) DL achievable throughputs regarding HOM schemes and MIMO configurations.

(b) UL achievable throughputs regarding HOM schemes.

Figure 2.2. Ninetieth percentile throughput as a function of Signal-to-Noise-Ratio (SNR) in Pedestrian A-channel (extracted from [BEGG08]) and Throughput as a function of E_c/N_0 in Pedestrian A channel (extracted from [PWST07]).

Moreover, MTs and BSs requirements are constantly being improved to raise system performance. As Release 6 introduced the use of receive diversity antennas (two antenna Rake receiver type 1) and one-antenna linear equaliser (type 2), Release 7 also introduced a combination of linear equalisers with receive diversity antenna (type 3), based on a two-antenna chip-level equaliser [HoTo07]. The enhanced terminal receivers improve the single-user data rates and together with all other Release 7 features the cell capacity is nearly doubled compared with Release 6. Release 8 brings also an advanced receiver, with inter-cell interference cancellation support.

Multi-Carrier HSDPA and Dual-Carrier HSUPA capabilities are introduced in HSPA+, respectively in Release 10, [3GPP10b], and Release 9, [Seid09]. Taking the combination of two or four carriers instead of one, Multi-Carrier HSDPA allows user data rate to be easily doubled or quadrupled mostly when the loading is low, [JBGB09]. The BS can optimise the transmission based on CQI reporting, similarly as in MIMO closed loop feedback for antenna weighting. As for Dual-Carrier HSUPA, a more limited set of scenarios is defined for its use, combining two adjacent carriers for transmission of UL physical channels and Dedicated Physical Control Channel (DPCCH) [Seid09].

Although both Dual-Carrier HSDPA and MIMO solutions are targeted to boost data rates, and can

provide the same peak rate of 42 Mbps with 64QAM modulation, MIMO can improve spectral efficiency due to two antenna transmission, while the Dual-Carrier HSDPA brings some improvement to the high loaded case with frequency domain scheduling and a larger trunking gain. Also, whilst the Dual-Carrier solution improvement is available over the whole cell area equally, MIMO only improves the data rates mostly close to the Node B, where dual stream transmission is feasible.

This analysis is summarised in Table 2.1, where it is also highlighted that Dual-Carrier can be implemented with a single 10 MHz power amplifier per sector, while MIMO requires two separate power amplifiers, besides the additional Radio Frequency (RF) equipment. This suggests that Dual-Carrier HSDPA makes it easier to upgrade the network.

Table 2.1. Benchmarking of Dual carrier HSDPA and MIMO (adapted from [HoTo09]).

Feature \ Technique	Dual Carrier	MIMO (2×2)
Peak bit rate [Mbps]	42	42
Spectral efficiency improvement [%]	20 (frequency domain scheduling and larger trunking gain)	10 (two antenna transmissions)
Data rate gain	Similar gain over the whole cell area	Largest gain close to Node B
Node B Amplifiers	Single power amplifier per sector	Two power amplifiers per sector
UE RF requirements	Possible with one antenna terminal	Two antennas required

HSPA+ brings the theoretical peak data rates per carrier up to 42 Mbps in DL and 11.5 Mbps in UL, together with improvements in capacity, coverage, latency times and spectral efficiency. A comparison between HSPA+ main features in DL and UL is presented in Table 2.2.

Table 2.2. Feature comparison of the HSPA+ achievements in DL and UL directions.

Feature \ Protocol	Evolved HSDPA	Evolved HSUPA
Variable Spreading Factor	No	Yes
Fast Power Control	No	Yes
BS based scheduling	Yes (multipoint to point)	Yes (point to multipoint)
Adaptive Modulation	Yes	No
Soft Handover	No	Yes
Fast L1 HARQ	Yes	Yes
TTI length [ms]	2	10, 2
Modulation	QPSK, 16QAM, 64QAM	QPSK, 16QAM
Theoretical peak data rate [Mbps]	42 (MIMO 2×2, 64QAM)	11.5 (SISO, 16QAM)

Presently in Portugal, operators have deployed HSPA+, offering DL data rates up to 21.6 Mbps using 64QAM or even 43.2 Mbps using Dual-Carrier HSDPA and 64QAM [Voda10]. Meanwhile, trials

combining 64QAM, MIMO and Dual-Carrier HSDPA have proved to achieve 84 Mbps or even 168 Mbps for DL, just using 64QAM and Multi-Carrier combining eight carriers [Eric11].

2.1.3 Capacity and Coverage

In this thesis, the main performance parameter of interest is the data rate, associated to given coverage and capacity. Nevertheless, interference is a primordial factor to take into account in this analysis of the communications system.

The limiting factors on system capacity are mainly three [Corr10]: the number of available codes in DL, the system load (interference constrains in both UL and DL), and the shared DL transmission power. As the number of available channelisation codes is limited by SF, the number of simultaneous active users in the cell is limited by this number. The maximum value for SF is limited to ensure a minimum Quality of Service (QoS), whereas high SF values would allow unbearable interference levels. In practice, for the total number of available codes in HSDPA, users would be required to be very near the BS and in perfect channel conditions, and so this does not represent a real limit.

On the other hand, the trade-off between capacity and interference is of key importance in cellular networks, shown by the expression for the interference margin [Corr10]:

$$M_{I\,[\mathrm{dB}]} = -10\log\left(1-\eta\right) \tag{2.1}$$

where:

- η: load factor, assuming values in [0,1].

The load factor depends on the services, being distinct for UL and DL due to the traffic asymmetry between them and the different transmission powers that characterise each transmitter. The more load is allowed in the system, the larger is the interference margin needed, and the smaller is the coverage area. For coverage-limited cases a smaller interference margin is suggested, while in capacity-limited cases a larger interference margin should be used. Typical values for the interference margin in the case of coverage limitation are 1 to 3 dB, corresponding to 20-50% load, [HoTo07].

Alternatively to an interference margin, intra-cell and inter-cell interferences can be computed using expressions (2.2) and (2.3) for the DL, and (2.4)and (2.5) for UL, [EsPe06].

$$P_{I_{intra},k}^{DL} = \left(P_{T_X} - P_{T_X,k}\right) \times (1-\alpha) \times L_{p,k} \tag{2.2}$$

where:

- α: code orthogonality factor (typically [50, 90] %);
- P_{T_X}: total BS transmitted power;
- $P_{T_X,k}$: BS transmitted power to user k;
- $L_{p,k}$: pathloss from serving BS to user k;

$$P_{I_{inter}}^{DL} = \sum_{s=1}^{N_{BS}} P_{T_X,s}^{DL} \times (1-\alpha) \times L_{p,s} \tag{2.3}$$

where:

- N_{BS}: number of neighbouring BSs;
- $P_{T_X,s}^{DL}$: BS s transmitted power;
- $\mathrm{L_{p,s}}$: pathloss from BS s to the user.

Providing results based on measurements in an urban environment, the orthogonality factor has been characterised by [PeMo02] as correlated with delay spread, due to multipath, or further as a function of user's distance to BS, as shown in Figure 2.3. A clear drop of the orthogonality factor can be seen with distance, in an environment with high multipath propagation, resulting in higher interference margins for higher distances to the BS.

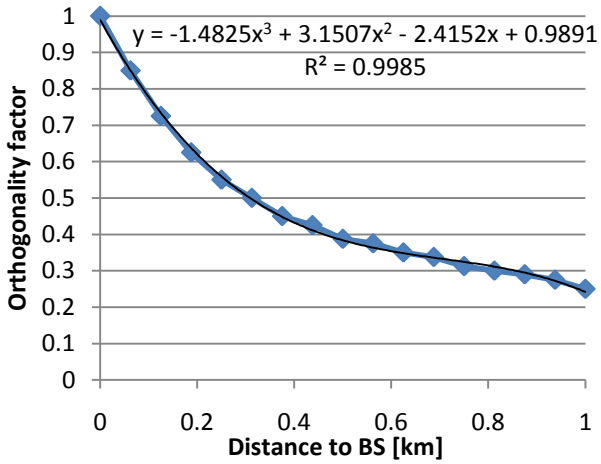

Figure 2.3. Orthogonality factor, α, as a function of user's distance to BS (extracted from [PeMo02]).

For UL, the activity factor for a certain service is considered for each user as shown in:

$$P_{I_{intra}}^{UL} = \sum_{k=1}^{N_u} P_{T_X,k} \times L_{p,k} \times v \tag{2.4}$$

where:

- $P_{T_X,k}$: UE transmitted power to BS;
- v: user activity factor;

$$P_{I_{inter}}^{UL} = \sum_{s=2}^{N_{BS}} \sum_{k=1}^{N_u} P_{T_X,k,s}^{UL} \times L_{p,k,s} \times v \tag{2.5}$$

where:

- $P_{T_X,k,s}$: transmitted power from user k in adjacent cell s;
- N_{u_s}: number of users in adjacent cell s;
- $L_{p,k,s}$: pathloss from user k in cell s to the serving BS.

As the BS transmitting power is shared, in DL, cell coverage is limited by its maximum value. The BS transmission power is expressed in [HoTo07] by:

$$P_{T_{X_{[\mathrm{W}]}}} = \frac{N_0 \cdot R_c \cdot \bar{L}_p \cdot \sum_{j=1}^{N_u} v_j \frac{(E_b/N_0)_j}{G_{P_j}}}{(1 - \overline{\eta_{DL}}) \cdot N_{streams}} \tag{2.6}$$

where:

- E_b: energy per bit;
- N_0: noise power spectral density at the MT;
- G_{P_j}: processing gain for user j;
- v_j: activity factor for user j;
- N_u: Number of users;
- R_c: chip rate, 3.84 Mcps in UMTS;
- $\overline{\eta_{DL}}$: average DL load factor value across the cell;
- $N_{streams}$: number of streams, in case of MIMO;
- $\bar{L}_p$: average pathloss between BS and MT.

When increasing the BS transmitter power, the reciprocal interference between DL user channels will also rise, hence, it is not an efficient solution for the increase of cell capacity. Most typical capacity upgrade solutions are more power amplifiers, allocation of more carriers or transmitting diversity with a second power amplifier per sector.

Combining (2.1), (2.6) and assuming an average activity factor, SNR and processing gain, the average number of user in the cell can be obtained for a given maximum BS transmission power:

$$N_u = \frac{P_{T_X}}{\bar{R}_b \cdot N_0 \cdot \overline{(E_b/N_0)} \cdot \bar{v} \cdot \bar{L}_p \cdot \overline{M_I}} \tag{2.7}$$

where:

- $\bar{R}_b$: average user bit rate;
- $\overline{(E_b/N_0)}$: average user energy per bit to noise power spectral density ratio;
- $\bar{v}$: average user activity factor;
- $\overline{M_I}$: average interference margin.

One can note from (2.7) that the number of users depends on the BS transmission power, on the average user bit rate, and on the interference margin and on pathloss. The last two are responsible for the trade-off between capacity, (2.7), and coverage in UMTS. Regarding the average energy per bit, it is defined for a given Modulation and Coding Scheme (MCS), required for a given Block Error Rate (BLER). Both the required Bit Error Rate (BER) and average user activity are mainly service dependent, being defined for given classes of service.

2.1.4 Performance Analysis

In UL and DL, performance analysis depends highly on network algorithms, deployment scenarios, UE transmitter capability, Node B performance and capability, and type of traffic. Furthermore, it is of extreme relevance for the system dynamic adaptation, as it has effect in interference-based radio resource management functionalities, such as HO control, power control, admission control, load control and packet scheduling functionalities.

Different metrics for performance, at the radio link level, are used according to the operating Release, and in particular HSUPA and HSDPA. While Release 99 typically used E_b/N_0 as performance metric,

for HSDPA that is not a suitable metric as bit rate on HS-DSCH is varied every transmission time interval using different modulation schemes, effective code rates, and a number of HS-PDSCH codes. Defining the average HS-DSCH SINR as the narrowband SINR after de-spreading the HS-PDSCH, it is then possible to express it for a single-antenna Rake receiver as, [Pede05]:

$$\rho_{IN} = SF_{16}\frac{P_{HS-DSCH}}{P_{I_{intra}} + P_{I_{inter}} + N_{RF}} \tag{2.8}$$

where:

- SF_{16}: HS-PDSCH spreading factor of 16;
- $P_{HS-DSCH}$: received power of the HS-DSCH, summing over all active HS-PDSCH codes;
- $P_{I_{intra}}$: received intra-cell interference;
- $P_{I_{inter}}$: received inter-cell interference;
- N_{RF}: received noise power.

One should note from (2.8) that even with given fixed inter- and intra-cell-interferences, SINR is not constant, depending on factors like orthogonality, through intra-cell interference, or UE receiver capabilities. Still, the UE uses the SINR estimate to report back to the BS, allowing it to select the UEs for transmission and select data rate, i.e., transport format, for each transmission and link. Adaptive Modulation Coding (AMC) is then employed in HSDPA to change the modulation scheme on a burst-by-burst basis per link, concerning the radio channel quality.

HS-DSCH SINR is the key measure for describing link performance in HSDPA and reflects the narrow band SINR as experienced by the UE, independently of the number of HS-PDSCH codes, modulation scheme, antenna configuration and effective code rate. This measure is also used to obtain a certain BER or BLER target for a given number of HS-PDSCH codes, and for the modulation and coding scheme per TTI, or; in the other hand, used to determine bit rate due to link adaptation in HSDPA, as shown in Figure 2.2.

The HS-DSCH link level performance with the maximum of 15 codes is shown in Figure 2.4 as a function of the HS-DSCH wideband carrier-to-interference ratio C/I, i.e., the received power of HS-DSCH divided by noise and interference without de-spreading. The HS-DSCH data rate is compared to the maximum error-free data rate given by the Shannon capacity formula for bandwidth of 3.84 MHz in UMTS. Only an approximate 2 dB difference is seen between the two curves, mainly due to decoder limitations and receiver estimation inaccuracies, [HoTo06].

HSUPA performance depends on multiple factors, such as UE transmitter capabilities, network algorithms, BS performance, type of services, and scenario environment [Jaci09]. Thus, the BS can estimate the UL channel quality based on the received SINR, i.e., based on E_c/I_0. A high E_c/I_0 at the BS is required in order to achieve the lowest delays and higher data rates, despite leading to an UL noise increase, thus, decreasing cell coverage. For this reason, a maximum level for the UL noise may be defined for macro-cells, ensuring a certain coverage area, but limiting data throughput.

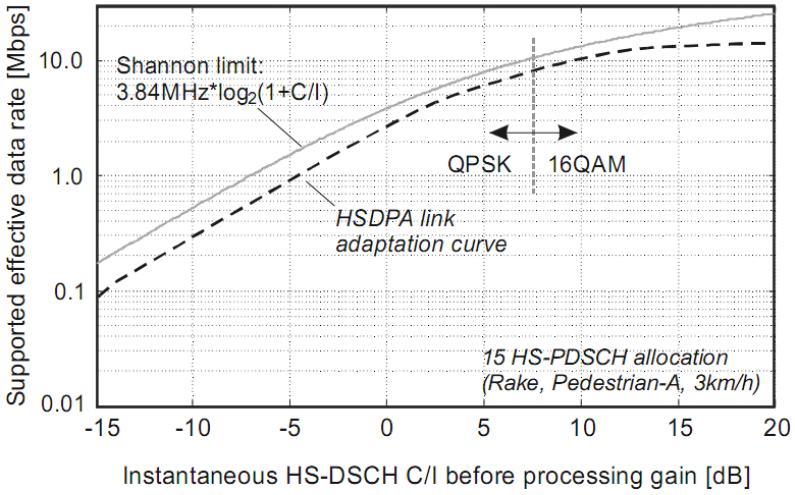

Figure 2.4. HSDPA data rate compared with the Shannon limit as a function of an average HS-DSCH carrier and interference power ratio (extracted from [HoTo06]).

2.2 LTE

This section presents the fundamental concepts regarding LTE. The network architecture is presented, with its main elements. A description of the radio interface follows, and basic concepts of coverage and capacity are analysed. This section is based on [HoTo09] and [3GPP10c].

2.2.1 Network Architecture

The evolution towards LTE was carried out in a request for: optimised PS services, optimised support for higher throughputs, hence, higher end user bit rates, improvement in response times for activation and set-up and, improvement in packet delivery delays. Additionally, on a system's perspective, overall simplification of the system compared to legacy systems, towards a flat architecture, and optimised inter-working with them at the access network layer were also considered.

Network architecture and functionalities are based on a basic architecture configuration of LTE, as possible interoperability with legacy systems is not shown, [HoTo09]. Figure 2.5 shows the division of the System Architecture Evolution (SAE) into three main high level domains: User Equipment (UE), Evolved UTRAN (E-UTRAN) and Evolved Packet Core Network (EPC).

The new architectural development in LTE is limited to the E-UTRAN and the EPC (i.e., Radio Access and Core Networks), while UE and External Networks domains remain architecturally intact, despite some functional evolution. UE, E-UTRAN and EPC together represent the IP Connectivity Layer, or Evolved Packet System (EPS). This layer is optimised to provide IP based connectivity, as all services will be offered on top of IP. Also, in transport, IP technologies are dominant and everything is designed to be operated on top of this layer. Unlike UMTS, the core network does not contain a CS domain,

neither direct connection to CS networks.

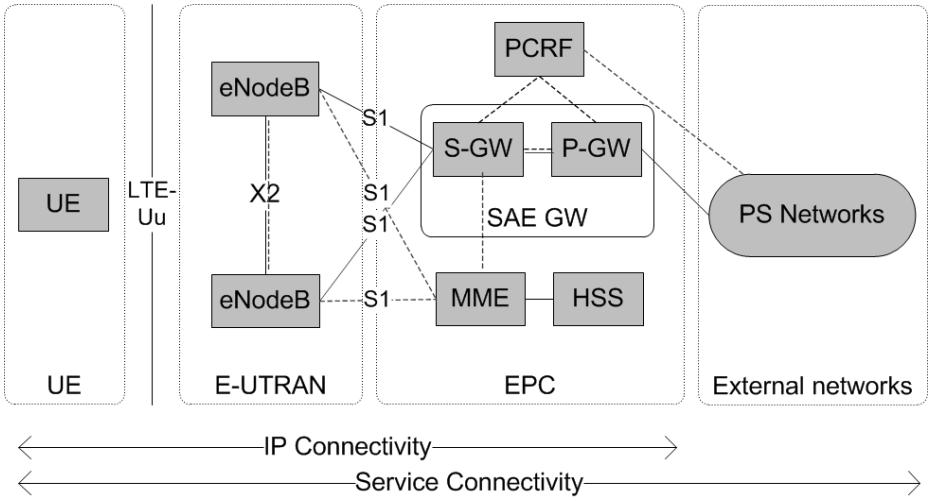

Figure 2.5. Basic System Architecture of LTE (adapted from [HoTo09]).

The development in E-UTRAN is concentrated in one node, the evolved Node B (eNB). It collapses all radio functionalities, i.e., eNB is the termination point for all radio related protocols. The E-UTRAN, as a network, is simply a mesh of eNBs connected to neighbouring eNBs through the X2 interface and interacting with the UE through the LTE-Uu. Communication between eNBs is carried through this interface, e.g., regarding radio and HO, eliminating large data flow through the RNCs, as in UMTS.

eNB accounts for Radio Resource Management (RRM), Mobility Management (MM), bearer handling, user plane data delivery, handovers, security settings and securing and optimising radio interface delivery to the UEs. The eNB also takes part in user plane tunnels for UL and DL data delivery, in the interface, with the Serving Gateway (S-GW), through S1.

Functionally, the EPC is equivalent to the packet switched domain of existing 3GPP networks, despite the different arrangement of functions, performed by distinct nodes in a new architecture configuration. The EPC contains elements, such as: the Mobility Management Entity (MME), the main control element in the EPC, responsible for authentication and security, MM, and managing subscription profile and service connectivity; the S-GW, supporting user plane tunnel management and switching; the Packet Data Network Gateway (P-GW), which is the edge router between the EPS and the external packet data networks, and acts as the IP point of attachment for the UE; the Policy and Charging Resource Function (PCRF), responsible for policy and charging control; and the Home Subscription Server (HSS), constituting subscription data repository for all permanent user data.

Figure 2.5 also shows the so called SAE Gateway (SAE-GW), representing the combination of the two gateways, S-GW and P-GW, defined for the user plane handling in EPC. However, implementing them together as SAE-GW represents one possible deployment scenario, as the standards define the interface between them and all operations have also been specified for them to be separate.

The Services domain may include various sub-systems, categorised by type as: IP Multimedia Sub-system (IMS) based operator services, non-IMS based operator services and other services not provided by the mobile network operator, e.g., services provided through the internet. Further analysis

about service level systems is out of the scope of this thesis, but particularly for IMS, the preferred service machinery for LTE/SAE, the interested reader should refer to [HoTo09] and [PoMa09].

2.2.2 Radio Interface

For LTE, two multiple access techniques are employed: Orthogonal Frequency Division Multiple Access (OFDMA) for DL and Single Carrier Frequency Division Multiple Access (SC-FDMA) with Cyclic Prefix (CP) for UL. OFDMA allows the access of multiple users on the available bandwidth by dynamically assigning each user to a specific time-frequency resource. Using SC-FDMA, the same technique is employed, but with the distinguishing feature that it leads to a single-carrier transmit signal, while OFDMA is a multi-carrier transmission scheme. LTE supports both Frequency Division Duplexing (FDD) and Time Division Duplexing (TDD), although only FDD is addressed in this thesis due to its wide adoption in the majority of European networks. According to the specifications, there are 17 frequency FDD bands and 8 TDD bands of LTE spectrum allocated [3GPP10d]. In Europe, and particularly in Portugal, regulation has been issued under public consultation for the auction of the 800 MHz, 900 MHz, 1800 MHz, 2.1 GHz and 2.6 GHz frequency bands [ANAC11].

The difference in the access techniques chosen for DL and UL is mainly related with the characteristics of better efficiency power and lower Peak-to-Average-power-Ratio (PAR). Compared to OFDM, SC-FDMA in UL ultimately maximises battery life for the MT as a reduction of 2 dB in PAR is achieved comparing to OFDMA, [Zeme08]. Additionally, the CP avoids Inter-Symbol Interference (ISI), and can be chosen to be normal or extended so to be slightly longer than the longest delay spread in the radio channel. This approach allows for simple frequency-domain processing, such as channel estimation and equalisation, with advantages both in UL and DL.

Channel estimation is necessary in LTE, both in UL and DL, as the receiver still has to deal with the channel impact for the individual subcarriers that have experienced frequency dependent phase and amplitude errors. The estimation is done through the use of pilot or reference symbols, which facilitate coherent channel estimation and allow reverting channel impact for each subcarrier, e.g., by using a frequency domain equaliser.

In DL, it is allowed for scalable carrier bandwidths, from 1.4 up to 20 MHz, with subcarrier spacing of 15 kHz [3GPP10c]. In LTE, the concept of a Resource Block (RB) is used, which is a block of 12 subcarriers in one slot, i.e., 180 kHz in the frequency domain. Each time slot is 0.5 ms long, a group of 2 slots is a sub-frame of 1 ms (or the TTI) and each frame is 10 ms. Furthermore, a transport block is a group of resource blocks with a common modulation or coding. The physical interface is a transport block, which corresponds to the data carried in a period of time allocated to a particular UE. Multiple UEs can be serviced on DL at any particular time in one transport block.

The time domain structure of the frame used in LTE is, in most respects, the same for FDD and TDD, Figure 2.6. Some differences exist between the two duplex modes, most notably the presence of a special sub-frame in case of TDD. Nevertheless, LTE's physical layer, like the general system, is designed for maximum efficiency of the packet-based transmission, and for this reason, there are only

shared channels in the physical layer to enable a dynamic resource utilisation.

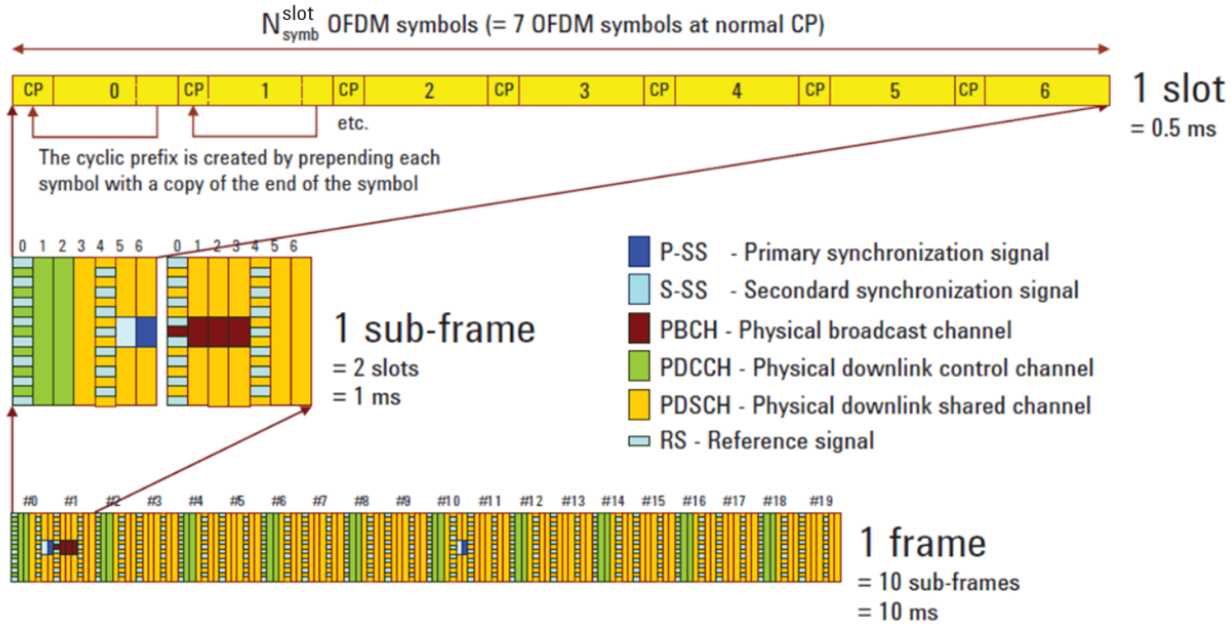

Figure 2.6. DL frame structure type 1, for FDD and TDD (adapted from [Agil07]).

LTE's DL and UL are composed of physical channels and physical signals. Physical channels carry information from higher layers, and are used to carry user data, as well as user control information; physical signals do not carry information from higher layers, and are used for cell search and channel estimation purposes. Examples of the latter are the Primary Synchronisation Signal (PSS) and the Secondary Synchronisation Signals (SSS), transmitted in the 1st and 11th slots of the 10 ms frame, used for cell search and synchronisation of the UE to the network. Reference symbols, referred earlier, are spread over the entire bandwidth and used for channel estimation. As for physical channels to which main transport channels are mapped, there is: the Physical Downlink Control Channel (PDCCH) with functions of scheduling and resource allocation, HARQ related data and also power control commands for the UL; the Physical Downlink Shared Channel (PDSCH) and the Physical Broadcast Channel (PBCH) both for user data and system information, respectively, as in WCDMA.

For UL, the same frame size, sub-frame size and slots are used, although channel allocation differs. Although the Physical Uplink Control Channel (PUCCH) and the Physical Uplink Shared Channel (PUSCH) have similar functions as in DL, the new Physical Random Access Channel (PRACH) is used for random access transmission, the only non-synchronised transmission in LTE's UL.

For the frame structure presented in Figure 2.6 and using normal CP, an RB aggregates 12 consecutive subcarriers and 7 consecutive OFDM symbols in a slot. For extended CP, the number of subcarriers is the same, but 6 OFDM symbols are transmitted per slot. As shown, a CP is appended to each symbol as a guard interval. An RB corresponds to one slot (T_{slot} =0.5 ms) in the time domain, i.e., N_{symb}^{slot}=7 at normal CP, and 180 kHz (12 subcarriers × 15 kHz spacing) in the frequency domain. Thus, the number of available RBs can range from 6, when the transmission bandwidth is 1.4 MHz, to

100, when it is 20 MHz.

For LTE, power control only exists for UL, and does not control absolute power, but rather the power spectral density, for a particular device. Furthermore, the use of orthogonal resources in UL facilitates the use of a slower rate for power control, unlike WCDMA systems where fast power control is required. The key motivation in LTE is, hence, to reduce terminal power consumption and also to avoid overly large dynamic range in the eNB receiver, rather than to mitigate interference.

Besides optimisation in time and frequency domains, antenna optimisation through MIMO is the key enabler of a high data rate in LTE. For this reason, plain SISO transmission is not supported as UEs are required to have at least two receiving antennas and the SIMO case constitutes then the simplest scheme. Further information on MIMO for LTE is presented in Annex D.

2.2.3 Capacity and Coverage

Theoretical bit rates, can be obtained for DL using:

$$R_{b_{[\mathrm{Mbps}]}} = \frac{N_{sc}^{RB} \cdot N_{RB}^{u} \cdot N_{symb}^{SF} \cdot \log_2(m) \cdot N_{streams}}{10^3 \cdot T_{SF_{[\mathrm{ms}]}}} \tag{2.9}$$

where:

- N_{sc}^{RB}: number of subcarriers per resource block (assumed 12 for 15 kHz subcarrier spacing);
- N_{RB}^{u}: number of user resource blocks;
- m: order of the modulation considered;
- N_{symb}^{SF}: number of symbols per sub-frame (14 symbols for normal CP or 12 for extended CP);
- $N_{streams}$: number of streams, in case of MIMO;
- T_{SF}: sub-frame period, 1 ms.

As seen in (2.9), end-user throughput depends on parameters like modulation and MIMO configurations used, directly related with channel conditions, CP size used, and number of resource blocks allocated for a certain user. However, note also that user throughput depends additionally on the overhead amount due to synchronisation and reference signals as well as control channels.

Moreover given the dynamic allocation of time-frequency resources in the eNB, the multi-user scheduling strategies are directly related to user data rates and user capacity, both at the cellular and system level. Main capacity limiting factors include the number of resource blocks, scheduler implementation efficiency, inter-cell interference, MIMO, and supported modulation and coding schemes.

To maximise service delivery for the user, a variety of resource scheduling algorithms may be applied by the eNB, depending on the optimisation criteria required, searching for a fair balance between throughput maximisation for delay-tolerant applications against QoS for delay applications. The prioritisation of data will typically consider the corresponding traffic classes, as shown in [HoTo09]. For this, multi-user diversity is an important factor, especially if the user density is high, in which case the multi-user diversity gain will enable the scheduler to achieve a high capacity, even with tight delay

constraints.

Nevertheless, system throughput and capacity are still limited by inter-cell interference, especially considering cell edge users. As LTE was designed to operate with a frequency reuse factor of one, interference coordination is required. As always, the DL resource allocation strategy is also constrained by the total transmission power of the eNB. The impact on the achievable data rate, for a user k transmitting in sub-frame j, can be expressed by, [SeTB09]:

$$R_{b_j} = B_k \log_2 \left[1 + \frac{P_{T_{X_j}}^{S} \left| H_{k_j}^{s} \right|^2}{N_{RF} + \sum_{i \neq s} P_{T_{X_j}}^{S} \left| H_{k_j}^{i} \right|^2} \right] \tag{2.10}$$

$$B_{[\mathrm{Hz}]} = \Delta f_{[\mathrm{Hz}]} \cdot N_{sc}^{RB} \cdot N_{RB}^{u} \tag{2.11}$$

where:

- $P_{T_{X_j}}^{s}$: transmit power from cell s, transmitting in RB j;
- $\left| H_{k_j}^{s} \right|$: channel gain from the serving cell s to user k, transmitting in RB j;
- B_k: bandwidth of the total RB's allocated to user k;
- Δf: subcarrier spacing (assumed 15 kHz).

The channel gain $|H_k^s(j,n)|$ captures the random signal attenuation due to pathloss, fading and other effects in the channel. In order to further increase the data rates that can be provided for users at the cell edge, the scheduling strategy may take interference from and to adjacent cells into account. Considering a scenario with two cells (s_1 and s_2) with one active user per cell (k_1 and k_2), the total achievable bit rate of the two users is given by:

$$R_{b_j} = B_{k_{1,2}} \left[\log_2 \left(1 + \frac{P_{T_{X_j}}^{s_1} \left| H_{k_{1_j}}^{s_1} \right|^2}{N_{RF} + P_{T_{X_j}}^{s_2} \left| H_{k_{1_j}}^{s_2} \right|^2} \right) + \log_2 \left(1 + \frac{P_{T_{X_j}}^{s_2} \left| H_{k_{2_j}}^{s_2} \right|^2}{N_{RF} + P_{T_{X_j}}^{s_1} \left| H_{k_{2_j}}^{s_1} \right|^2} \right) \right] \tag{2.12}$$

where:

- $B_{k_{1,2}}$: bandwidth allocated simultaneously to users k_1 and k_2;
- $P_{T_{X_j}}^{s_n}$: transmit power from cell s_n, transmitting in RB j;
- $\left| H_{k_{m_j}}^{s_n} \right|$: channel gain from the serving cell s_n to user k_m, transmitting in RB j.

In this situation, it can be shown that the optimal power allocation for maximum capacity is obtained when either BSs are operating at maximum power in the same RB, e.g., when each user is located near its respective eNB, Figure 2.7-a), or one of them is turned off completely in that RB, e.g., users are located close to the edge of their respective cells, Figure 2.7-b), [SeTB09].

In practice, this means that the eNB scheduler will exploit this result by treating users in different ways, depending on whether they are cell-centre or cell-edge users. Inter-Cell Interference Coordination (ICIC) is assumed to be managed in the frequency domain rather than in the time one so to avoid to interfere with the HARQ process, particularly in UL where it is synchronous.

Moreover, considering the single-cell capacity, an estimate for the number of active users in a cell, in a given instant, can be given by:

$$N_u = \frac{B_{[\mathrm{Hz}]} \cdot \eta_{sch} \cdot G_{pos} \cdot G_{multi-user\ div}}{\bar{B}_{u\ [\mathrm{Hz}]}} \tag{2.13}$$

where:

- B: total bandwidth available;
- G_{pos}: capacity gain obtained due to users' positioning in the cell;
- $G_{multi-user\ div}$: capacity gain obtained due to multi-user diversity;
- $\bar{B}_u$: average bandwidth of the RBs allocated per user;
- η_{sch}: scheduler efficiency, chosen in [0,1].

For a given scheduling instant, the scheduler considers the total available bandwidth, scheduling RBs to active users with a given efficiency, as shown in (2.13), taking into account the scheduling inefficiency due to constraining service QoS for each RB, and optimisation criteria for the scheduler implementation inefficiency. Capacity gains can still be obtained by exploiting multi-user diversity, namely in used services and position inside the cell.

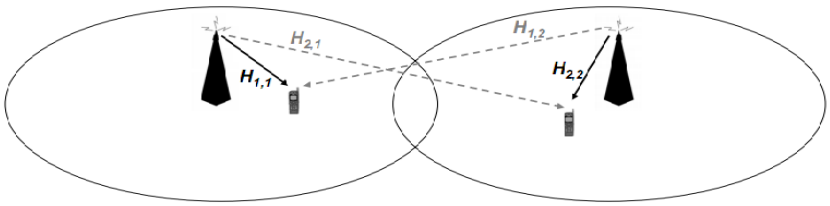

(a) Users close to eNBs.

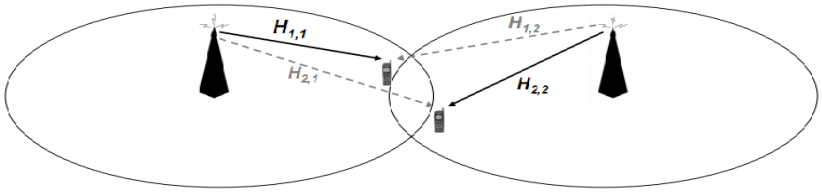

(b) Users close to cell edge.

Figure 2.7. Inter-Cell Interference Coordination limit cases (extracted from [SeTB09]).

For UL, the scheduling algorithm chosen along with FDM resource allocation with fine granularity has a direct impact in system and cell capacity [SeTB09]. In high SINR conditions, the maximum achievable capacity can be limited by the minimum amount of transmission resource allocated to each single UE. Besides coordination, other interference mitigation techniques used are inter-cell interference randomisation, frequency domain spreading and slow power control.

2.2.4 Performance Analysis

As in UMTS, peak data rates are available only in extremely good channel conditions. The practical data rate in LTE is nevertheless limited by the amount of inter-cell interference and noise in the

network. For LTE, the Downlink Shared Channel (DSCH) SINR is taken as performance metric, simply written as a function of interference and random noise, adapted from [SaNC10]:

$$\rho_{IN} = \frac{P_{DSCH}}{\sum_{s=1}^{S} \gamma_s P_{I_{inter,max\,s}} + N_{RF}} \tag{2.14}$$

where:

- P_{DSCH}: DSCH received power;
- γ_s: subcarrier activity factor of the cell s;
- $P_{I_{inter,max\,s}}$: maximum inter-cell interference power, at the edge of the cell s;
- N_{RF}: Noise power.

One can note from (2.14) the trade-off between network capacity, limited by inter-cell interference, and the SINR, which is directly correlated to the average obtained throughput. Full orthogonality is assumed inside a cell, even though in reality non-idealities such as inter-symbol interference due to short CP, inter-carrier interference due to Doppler spread, or transmit signal waveform distortion due to transmitter non-linearities may result in own-signal interference. Inter-cell interference mainly exists, being largely dependent on the scheduler, that might allocate the same subcarriers in different cells, if link adaptation feedback information makes it worth of.

In practice, both adaptive modulation and coding, as well as the frequency domain packet scheduler, rely on channel state information. Link adaptation in DL is primarily based on CQI feedback from users in the cell, while in UL Channel State Information (CSI) is estimated based on the reference signals transmitted by the UE. Furthermore, Rank Indicator (RI) and Pre-coding Matrix Indicator (PMI) are relevant to MIMO operation, which should only be taken when SINR is above 10 dB [SaNC10].

As defined in initial requirements, LTE provides a high spectral efficiency, Figure 2.8, although Shannon's capacity bound cannot be reached in practice due to several implementation issues. Together, requirements on the leakage between adjacent channels and practical filter implementation reduce bandwidth occupancy to 90%. Additionally, CP, pilot overhead for channel estimation, and dual antenna transmission overhead further reduce bandwidth efficiency, to around 83% [HoTo09].

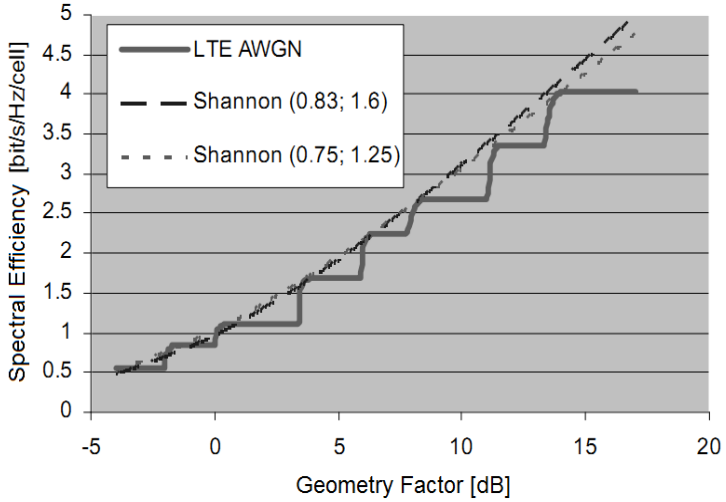

Figure 2.8. LTE spectral efficiency as a function of the geometry factor (extracted from [HoTo09]).

Still, high spectral efficiency is achieved in both links. Although LTE's link budget in DL has several similarities with UMTS and maximum pathloss is similar, in UL some differences exist, namely, smaller interference due to referred orthogonality inside the cell and a capacity gain due to MIMO availability. Thus, LTE itself does not provide any increase in coverage, and link performance at low data rates is not much different in LTE than in UMTS. Even so, beamforming techniques can be additionally used to improve coverage and capacity, and to increase spectral efficiency [DEFJ06].

2.3 Comparison between UMTS and LTE

This section presents the comparison of fundamental concepts between UMTS and LTE, together with a critical analysis of the effects on end user performance. First, a systems comparison is performed and differences explained. An overview of works presented on the subject follows.

2.3.1 Performance Analysis

Both UMTS, in its latest HSPA+ version, and LTE are optimised for PS, coping with the trends for next generation mobile communications systems. Relevant initial demands for LTE, presented in 3GPP's Release 8, were:

- Higher peak data rates and user throughput.
- Better coverage and capacity across the cell.
- Better spectrum efficiency.
- Reduced latency.
- Better support for mobility.

With LTE, demands for higher data rates are achieved through the use of OFDM/OFDMA, which allows flexible channel bandwidth usage and supports higher bandwidth allocation per user under low load scenarios. This flexibility does not exist in UMTS. Furthermore, coverage and capacity enhancements exist from UMTS to LTE. Due to users' orthogonality within a cell, LTE performance in terms of spectral efficiency and available data rates is more limited by inter-cell interference compared to UMTS, where transmission suffers from intra-cell interference caused by multipath propagation, which bring in the need for more complex equalisers.

Additionally, through the use of OFDMA, there is no need for fast power control as in UMTS, improving therefore both system performance and user throughput at the cell edge. However, a smoother distribution of SINR values is expected between cell centre and edge users in UMTS due to power control, whereas in LTE a wider performance gap is seen between cell centre and edge users.

Figure 2.9 illustrates the DL capacity and sector throughput gains from UMTS/HSPA+ to LTE across a cell. The significant capacity improvements seen are directly related with the benefits of OFDM and a more efficient air interface, namely better interference management, frequency selective fading gain,

better multipath signal handling, lower control overhead and improved HARQ operation. Table 2.3 shows also a performance comparison regarding the mean user cell throughput and cell edge user throughput for both UTRA and E-UTRA, UMTS and LTE Radio Access Networks (RANs), taking a UTRA configuration as baseline. Notice that, together with the major gains in mean user throughput for different antenna configurations, also large gains are achieved at cell edge both in DL and, particularly for UL, where the use of ICIC schemes allows for high interference reduction.

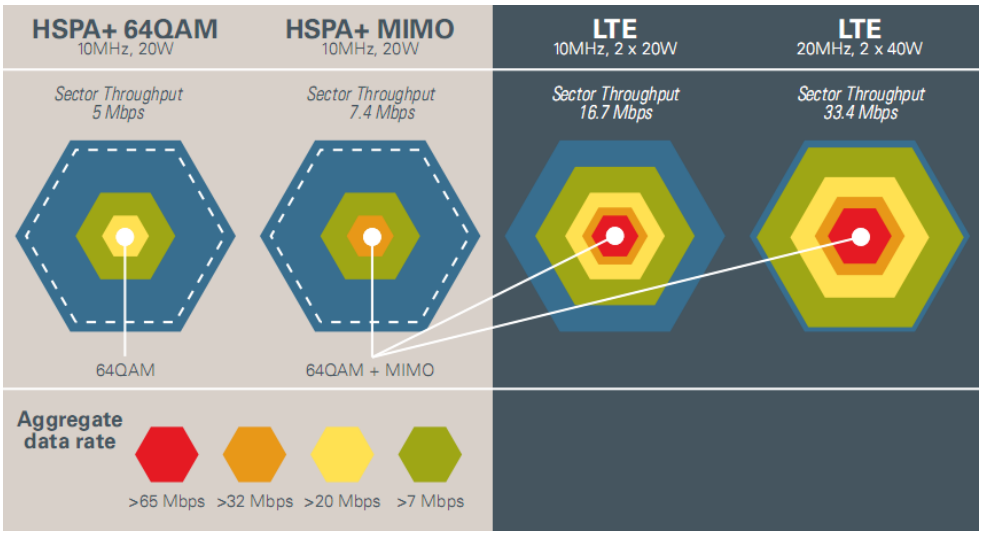

Figure 2.9. Throughput comparison between UMTS and LTE across the cell (extracted from [Moto10]).

Table 2.3. DL user throughput performance for 500 m Inter-Site Distances (ISD), (adapted from [3GPP09]).

System and MIMO configuration	DL				UL			
	UTRA		E-UTRA		UTRA		E-UTRA	
	1×2	2×2	4×2	4×4	1×2	1×2	1×4	2×2
Mean User Throughput (× UTRA)	×1.0	×3.2	×3.5	×5.0	×1.0	×2.2	×3.3	×2.3
Cell-Edge User Throughput (× UTRA)	×1.0	×2.7	×3.0	×4.4	×1.0	×2.5	×5.5	×1.1

Spectrum efficiency is also impacted in LTE due to frequency domain packet scheduling, enabling the scheduler to choose the best subcarriers for transmission based on CQI reports, and by the use of CP, that makes interference cancelation easier to apply in multi-carrier systems. Although CQI reporting is used in both UMTS and LTE, that is, returning the best MCS for usage, in LTE it further gives support for scheduling, being more efficient with the increase of channel bandwidth as shown in Table B.3. Additionally, LTE benefits from the use of a second indicator, the PMI, which is used in conjunction with MIMO and indicates to the BS the available pre-coding MIMO matrices to accomplish the best performance.

A spectrum efficiency comparison is presented in Table 2.4 for both DL and UL, considering two case scenarios. Effective spectral efficiency gains of up to 5 in DL and around 3 in UL can be achieved for the analysed case, making use of complex MIMO configurations as described.

Table 2.4. DL and UL spectrum efficiency performance 500 m ISD (adapted from [3GPP09]).

System and MIMO configuration	DL				UL			
	UTRA		E-UTRA		UTRA		E-UTRA	
	1×2	2×2	4×2	4×4	1×2	1×2	1×4	2×2
Spectral Efficiency [bps/Hz/cell]	0.53	1.69	1.87	2.67	0.33	0.74	1.10	0.78
Spectral Efficiency (×UTRA)	×1.0	×3.2	×3.5	×5.0	×1.0	×2.2	×3.3	×2.3

Latency reduction in LTE is achieved by making use of a shorter TTI, improved scheduling and simpler system architecture than in UMTS. The IP-based flat architecture used in LTE has fewer components than the legacy architecture used in UMTS. Further, with radio related functions such as admission control, scheduling and dynamic resource allocation, or also mobility management, header compression and packet retransmissions being performed in the BS, instead of the RNC in UMTS, performance gains are obtained and latency reduced, as highlighted in the comparison on Figure 2.10.

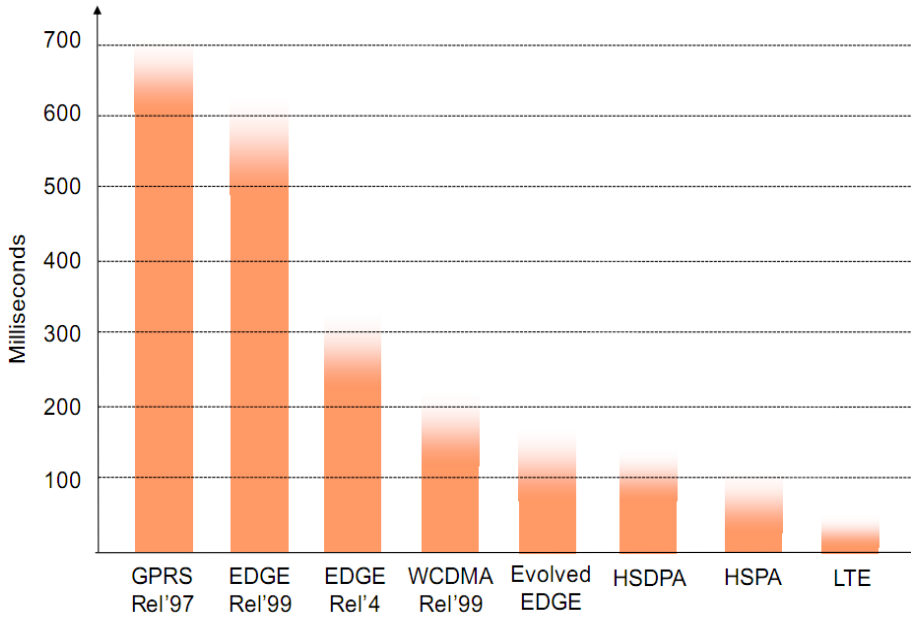

Figure 2.10. Latency for different technologies (extracted from [Rysa10]).

Due to LTE architecture and network management, good support for mobility is also provided mostly to E-UTRAN architecture, in a simpler and more flexible way, although the number of handovers will likely increase compared to UTRAN. For an extensive analysis refer to [HoTo09]. A summary on the major features of the two systems is presented in Table 2.5.

Table 2.5. Major features comparison, under analysis in this thesis, between UMTS and LTE (adapted from [HoTo07], [HoTo09], [Moto07] and [ANAC11]).

Feature \ System	UMTS	LTE
Duplex mode	FDD	
Multiple Access	WCDMA	OFDMA (DL) / SC-FDMA (UL)
Frequency [MHz]	[1920, 1980] for UL; [2110, 2170] for DL	Bands around 800, 900, 1800, 2100 and 2600
Switching map	Circuit and Packet Switched	Packet Switched IP-based
Scheduling	Time Domain	Time and Frequency Domains
Mobility [km/h]	Up to 250	Up to 350
Channel Bandwidth [MHz]	5	1.4, 3, 5, 10, 15, 20
Minimum frame size [ms]	2	1
Modulation	QPSK, 16QAM, 64QAM (DL); QPSK, 16QAM (UL)	QPSK, 16QAM, 64QAM (DL); QPSK, 16QAM, 64 QAM (UL)
DL Theoretical Peak Data Rate [Mbps]	42 (MIMO 2×2, 64QAM)	326 (20 MHz, MIMO 4×4, 64QAM)
UL Theoretical Peak Data Rate [Mbps]	11.5 (SISO, 16QAM)	86 (20 MHz, MIMO 2×2, 64QAM)

2.3.2 State of the Art

A brief overview of the state of the art is presented, emphasising the importance of the work performed. Works on simulators' development and measurements campaigns have been published on LTE, at different levels, as well as studies with different solutions for providing the mobile broadband of the future.

In [MWIB09] a simulator is developed using MATLAB, for DL physical layer simulation in single-cell single-user, single-cell multi-user and multi-cell multi-user scenarios. Main features include AMC, MIMO transmission, multiple users and scheduling, together with a diversity of channel models available for simulation. Throughput results per RB are cross-analysed considering different BLER, CQI and MIMO transmission scenarios. Moreover, [IkWR10] goes one step further providing a system level simulator, based on the former link level simulator. This way, it is possible to analyse effects of cell planning and scheduling, inherently dealing with interference in LTE. Both link and system levels simulators are freely-available for academic research, although not open-source.

In [PGBC10], an open-source framework for LTE simulation at network level is presented. Both single-cell and multi-cell simulations can be run. Handover procedures are considered, supporting users' mobility. QoS differentiation is performed by introducing an EPS bearer and typical application services considered. Additionally, protocol stack functionalities, both user-plane and control-plane, are

considered for MAC, RLC, Packet Data Convergence Protocol (PDCP) and IP layers. Remarkable resource management features, namely bandwidth management, frequency reuse scheme selection, frame structure selection and radio resource scheduling are available for simulation.

Additionally, manufactures have led trial tests on future LTE system. [Eric08] shows LTE performance results on the field. MIMO gains are measured in realistic environments and good system performance verified for varying bandwidth, antenna configuration, channel and service, using two kinds of terminals. Increases of 50% and 113% at the median are further measured in [Eric10] at cell centre and cell edge, from 2×2 MIMO to 4×4 MIMO. [Noki09] also shows similar measurements' results over mobility scenarios, terminal category, antenna configuration, modulation scheme, layer-1 and IP layer and QoS bearer.

Focusing on LTE specific features, [Duar08] extensively analyses different technologies in UMTS evolution to LTE, whereas [Jaci09] studied both systems over a network perspective, evaluating effects when varying bandwidth, frequency band, service user profiles and the use of adaptive modulation. In the latter, higher average network throughput of 13.5 Mbps and average ratio of served users of 72% are presented, compared to 9.8 Mbps and 66% in UMTS/HSPA+.

In an alternative approach, some studies have been conducted using a combination of different technologies including or excluding LTE, as the next mobile communications system. Whereas [Perg08] studies the deployment of Worldwide Interoperability for Microwave Access (WiMAX) as an alternative to UMTS in the specific scenario of Mobility, [VeCo11] goes ahead in presenting a solution for the resource management in a heterogeneous network solution using UMTS, Wi-Fi and WiMAX.

Despite the rich research on the subject, space still exists for specific analyses. While simulation provides for an accurate analysis regarding LTE's system features, in practice either due to varying implementation decisions taken by the equipment's manufacturer, varying system planning and consequent deployment, different environment characteristics, or simply to practical matters on users' behaviour and usage profile, among other factors, obtained results differ drastically. Although provided with adequate planning tools, operators still have the need for studies of more practical value.

On the other hand, manufacturer's measurements vary deeply with implementation aspects, left unspecified by 3GPP and also with the study conditions. Additionally, manufacturer's in general have the obvious interest of providing for the best results on the gains with the new technology, pushing the migration into the next generation systems. In this sense, trial deployments are conceded to operators in lab environment, with the objective of showing the best of all possible results.

Thus, by presenting a capacity and coverage study based on both simulation and measurements in a live LTE network, this thesis is expected to be of great practical value for operators and manufacturers in general. Furthermore, as a new model is developed for LTE simulation, embedded in LTE measurements results, the work contributes for research on the topic inside the academic community. Additionally, by comparing theoretical and measurements' results and further comparing them to the legacy UMTS system, in typical environments, the analysis provides support on the operators' decision of migration to the next generation system.

Chapter 3

Models Description

In this chapter, an overview of the Single Cell model and the UMTS/LTE simulator is presented. The former is intended to provide an analysis of an average system cell, regarding data rate performance and cell range for UMTS and LTE, in the case of a certain service required by the user. The multi-user scenario in one cell is then also considered by simply extending the single-user scenario. The chapter concludes with the assessment of the simulator.

3.1 Single-Cell Model

This section presents the single-cell model, used to evaluate data rate performance of HSPA+ and LTE. The model is initially applied for the single-user scenario, Figure 3.1, and used to analyse system performance in terms of capacity and coverage, allowing the user to make full use of a certain service. Later on, the multi-user scenario is also considered by making a simple extension of this model.

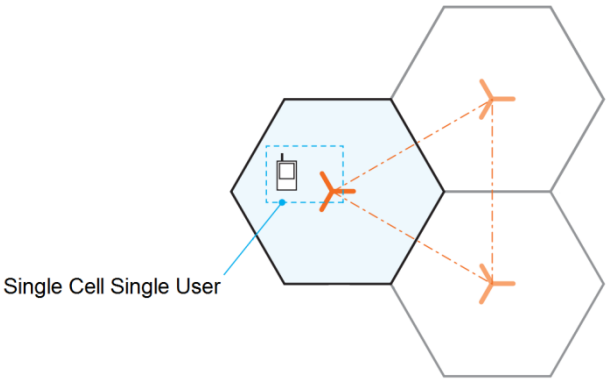

Figure 3.1. Single-cell single-user model.

For a given distance to the BS, maximum physical layer throughput is computed, within a set of parameters. Total resource availability is assumed for the unique user in the cell, and perfect propagation conditions are considered. Maximum physical throughput depends on several parameters, namely:

- Modulation scheme.
- Antenna MIMO configuration.
- Total BS and MT transmission power.
- BS and MT antenna gains.
- Frequency.
- Bandwidth.
- Environment, e.g., rural, urban.
- Channel, e.g., pedestrian, vehicular.

Apart for all parameters, one should also not forget that for the maximum throughputs obtained at the physical layer, a reduction should be considered due to coding rate, bandwidth efficiency, CP in LTE, pilot overhead, and dedicated and common control channel. Using a link budget analysis based on the expressions in Annex A, the SNR may be obtained. Then, by mapping it onto the throughputs for different MIMO and modulation schemes, using the expressions in Annex B, the maximum physical throughput is computed.

The Extended Pedestrian A (EPA) channel and Pedestrian A channel are considered in Annex B, respectively for LTE and UMTS, assigned to pedestrian and indoor users due to static (or almost) characteristics. For the vehicular channels, the Extended Vehicular A (EVA) channel and Vehicular A channel can be extrapolated from the pedestrian channels. Additionally, for LTE, the Extended Typical Urban (ETU) channel is also available for typical outdoor urban environments.

MIMO and modulation schemes for transmission are considered to be dependent on the channel and

environment conditions, as well as on the systems specific manufacturers' implementation. Hence, modulation and MIMO usage statistics vary according to the manufacturer, for specific environment and channel, according with implementation specifications, and this can be input into the simulator. Moreover, MIMO schemes are often used in good SINR conditions, allowing for higher gains in high scattering environments, [Opti11]. Therefore, a SINR threshold can be found, for varying environment and channel conditions, over which MIMO transmission is possible.

For maximum throughput analysis, maximum BS and MT transmission power are considered, used when only one user is present in the cell. Also, maximum BS and MT antenna gains are used in order to have maximum throughput. Central frequencies for both directions in each system are also defined having a direct impact in propagation as considered by the pathloss model in Annex C. For UMTS maximum system bandwidth 5MHz is used while for LTE different bandwidth deployments are available, as shown in Table B.3.

Concerning environment influence in SINR, it is reflected in two different components. First, it has an impact on the fading effects, which vary from strong LoS to non-LoS transmission; secondly, it is accounted for in propagation losses computation, depending only on the environment's morphology, e.g., the buildings' height or BS's and MT's heights. Whilst the former regards the varying nature of the transmission channel, through signal fading, the latter captures the nature of the propagation obstacles in the environment. Although both depend on the environment, the two components have a different influence on the instantaneous data rate achieved.

Propagation channels also impact on the instantaneous data rate achieved through the fast and slow fading attenuation margins, considered in the model, for UMTS and LTE. Rice and Lognormal statistical distributions were considered for fading, characterised by the standard deviation and Rice parameter, (A.18), and mean and standard deviation, (A.20), respectively. First, channel coherence time, defined in [Corr10], is considered to vary from the pedestrian to the vehicular channel, directly reflecting a faster varying propagation environment; secondly, standard deviations for fading margins adopted are also different depending on the channel, [Jaci09]. In this way, the channel chosen will directly affect data rates, based on both slow and fast fading influences on SINR.

Regarding signal propagation, pathloss is calculated using link budget analysis detailed in Annex A. From COST231-Walfisch-Ikegami propagation model, Annex C, and making use of (A.2), one has:

$$L_{p\,[\mathrm{dB}]} = EIRP_{[\mathrm{dBm}]} - P_{r\,[\mathrm{dBm}]} + G_{r\,[\mathrm{dBi}]} = L_{0\,[\mathrm{dB}]} + L_{rt\,[\mathrm{dB}]} + L_{rm\,[\mathrm{dB}]} \quad (3.1)$$

where:

- $EIRP$: Equivalent Isotropic Radiated Power;
- L_0: free space loss;
- L_{rt}: rooftop-to-street diffraction and scatter loss;
- L_{rm}: approximation for the multi-screen diffraction loss.

Conversely, for a fixed required throughput value, the maximum distance to the BS, i.e., maximum cell radius, can be obtained. A coverage analysis is thus possible by mapping requested physical throughput onto SINR, Annex B, which provides for computing receiver sensitivity, i.e., the minimum

received power that allows the user to be served with the requested throughput, using (A.13) and (A.14) for LTE and UMTS respectively. Then, manipulating (3.1) and the expressions for L_0 and L_{rt} from the COST231-Walfisch-Ikegami model, Annex C, cell radius can be expressed as:

$$r_{[\mathrm{km}]} = 10^{\frac{EIRP_{[\mathrm{dBm}]} - P_{r\,[\mathrm{dBm}]} + G_{r\,[\mathrm{dBi}]} - L_{\mathrm{COST231[dB]}}}{20 + k_d}} \tag{3.2}$$

where:

- k_d: dependence of the multi-screen diffraction loss versus distance, as described in Annex C;
- L_{COST231}: propagation losses over the propagation model being:

  $$L_{\mathrm{COST231\,[dB]}} = L'_{0\,[\mathrm{dB}]} + L_{\mathrm{rm\,[dB]}} + L'_{\mathrm{rt\,[dB]}} \tag{3.3}$$

  where:

  - $L'_{rt} = L_{rt} - k_d \log_{10}(d_{[\mathrm{km}]})$;
  - $L'_0 = L_0 - 20 \log_{10}(d_{[\mathrm{km}]})$;
  - d: distance between the user and the BS.

For LoS conditions, a similar expression can be also derived, resulting in:

$$r_{[\mathrm{km}]} = 10^{\frac{EIRP_{[\mathrm{dBm}]} - P_{r\,[\mathrm{dBm}]} + G_{r\,[\mathrm{dBi}]} - L^{LoS}_{\mathrm{COST231[dB]}}}{26}} \tag{3.4}$$

where:

- $L^{LoS}_{\mathrm{COST231}}$: propagation losses over the propagation model being:

  $$L^{LoS}_{\mathrm{COST231}} = L_{p\,[\mathrm{dB}]} - 26 \log_{10}(d_{[\mathrm{km}]}) = 42.6 + 20 \log(f_{[\mathrm{MHz}]}) \tag{3.5}$$

  where:

  - f: frequency in use.

For a more realistic analysis, user's performance must be analysed considering the influence of other user's in the cell, namely by taking average intra- and inter-cell interference in both UL and DL into account. A model for the multi-user influence on the single user's performance is then obtained by simply extending the previously developed model, Figure 3.2.

At each time instant in the developed model, users are assumed to be spread over the cell at the approximate same distance from serving BS. Thus, for UMTS, BS power is split equally among active users. Similarly, user's distance is considered for both UL and DL intra-cell interference computation, based on (2.2) and (2.4). Regarding (2.2), the distribution of the orthogonality factor with distance, Figure 2.3, is assumed.

Regarding UMTS inter-cell interference, however, a given ISD is used as reference to compute pathloss attenuation values of interfering adjacent BS, in DL, although subtracting to it the user's distance from its serving BS. For simplicity, only one interfering BS is considered and received interference power is computed as in (2.3). As for UL inter-cell interference, (2.5), users' in neighbouring cell are considered to be at the same average distance of the users' distribution in the cell under analysis, and an estimate of their distance is obtained by subtracting their distance to their

serving BS to the ISD.

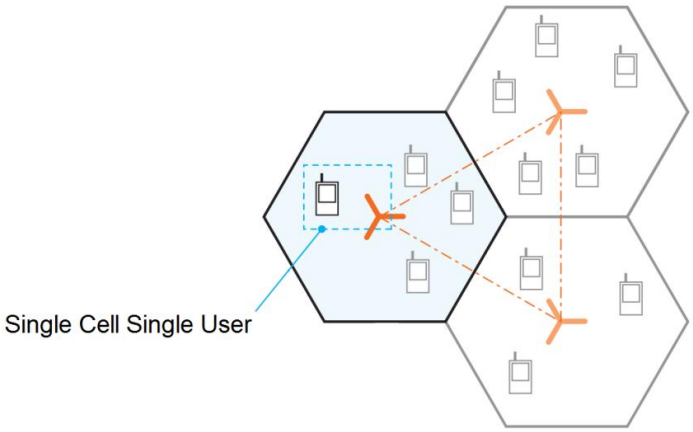

Figure 3.2. Extending the single-cell single-user model to the multi-user case, by mapping other users and BSs as average intra- and inter-cell interference.

For LTE, the major limiting feature is the number of available RBs, for both UL and DL. RBs are equally distributed among users, assuming similar services. No RBs are however denied to the user due to its usage in the neighbouring cell, i.e, the Universal Frequency Reuse (UFR) scheme is assumed. Regarding inter-cell interference affecting user's performance in LTE, similar expressions were used for inter-cell interference computation, the difference being the lack of an orthogonality factor in the expressions for DL inter-cell interference. In any case, others users' LTE UL interference is considered to have smaller impact than interference caused by neighbouring cells, namely due to MT's smaller transmitting power, coordinated RB scheduling and ICIC schemes.

For inter-cell interference mitigation, ICIC schemes such as soft frequency reuse or partial frequency reuse schemes are often referred, [HoTo09]. For any of these, inter-cell interference is reduced, resulting in improved SINR levels in UL and DL, differently for both cell centre and cell edge users, as in [LZZY07] and [XuMK08]. Centre and edge users can be classified based on their SINR, for both UMTS and LTE, or on received Reference Signal Reference Power (RSRP) in LTE, Figure 3.3. An SINR ICIC gain is defined in LTE, (A.9), relative to UFR SINR, assuming different values depending on user positioning.

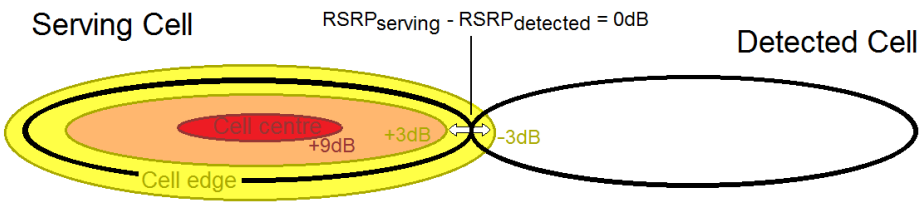

Figure 3.3. Cell centre versus cell edge.

Moreover, power control exists in UMTS UL and DL, and in LTE UL, as referred in Chapter 2. Still, users are considered to be at the same average distance to BS, and so equal resource division is always performed between users. Also as both in capacity and coverage analysis maximum throughput and distance to BS are obtained, there is no reason not to use maximum transmission

power, providing for a straightforward comparison between systems, as long as these assumptions are clearly understood.

Also, both in UMTS and LTE, interference power is considered to be equally spread over the transmission bandwidth, for a realistic analysis under an equally loaded system, reducing SNR for both LTE and UMTS comparing to the single-user's case. Apart from the last considerations, all additional interference due to external factors is considered to be negligible.

3.2 UMTS and LTE Simulator

Specific implementation aspects regarding the developed HSPA+ and LTE simulator are presented in this section. First, the simulator file structure is presented, followed by the description of simulator's implementation features, and finally a global simulator evaluation is performed.

3.2.1 Simulator Overview

The simulator was developed in C++ and is composed by two main components, each one dedicated to one of the two systems, UMTS and LTE, and able to perform both capacity and coverage analyses. Inside each of these, a link budget analysis module exists for both UL and DL. Parallel to the simulators, two separate modules exist, the pathloss propagation model and the channel simulation, used to simulate propagation conditions, Figure 3.4.

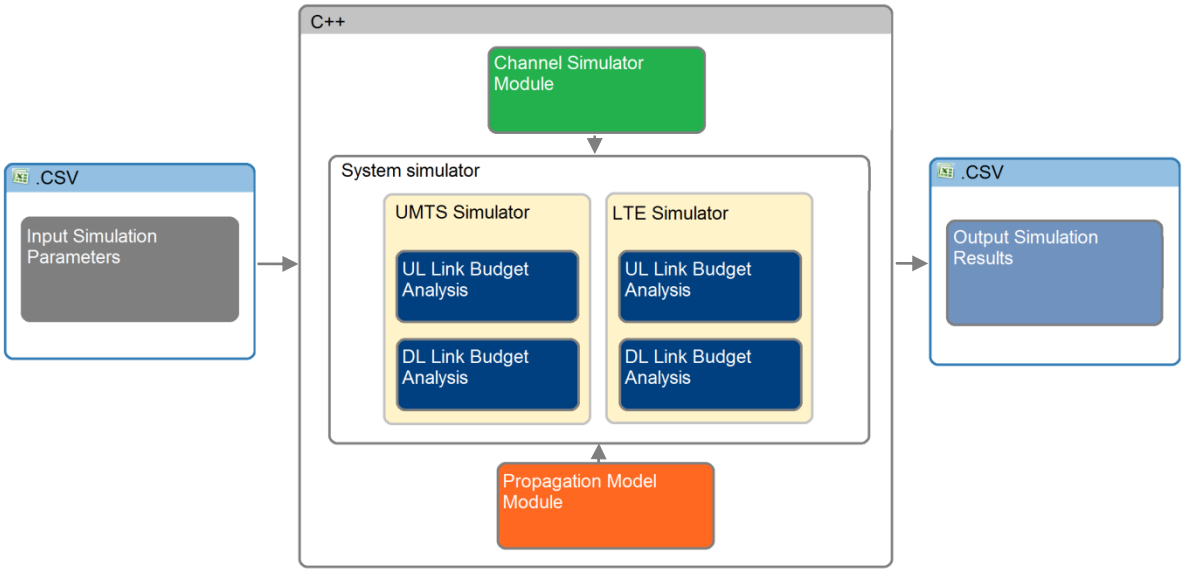

Figure 3.4. UMTS and LTE Simulator's architecture.

The simulator receives the input parameters either directly typed in the interface developed or also by loading Excel input files, in Comma-Separated Values (CSV) format. Output results are always presented in a CSV Excel file, allowing to take advantage of Excel's capabilities for data analysis.

The structure chosen allows for a simpler and isolated implementation of the different modules, particularly for different propagation models or channel simulators. More importantly, however, is that the chosen structure allows for a comparison between systems' performance, by using the same channel simulation, i.e., the same channel conditions generated, repeatedly by any of the two simulators.

Both UMTS and LTE simulation modules receive BS's and UE's features as input for the link budgets' analysis, the system's specific parameters, namely frequencies and bandwidth, and also general simulation parameters, namely UE's positions vector and simulation period. The results computation is performed inside each link module, receiving as inputs the channel simulation and the pathloss results, respectively from the channel simulation and the propagation model modules. Further analysis regarding the developed simulator is presented in the simulator's user manual, Annex E.

3.2.2 UMTS and LTE Implementation Analysis

The modules have the purpose to do the main overall calculations obtaining the coverage and capacity analyses for both systems, through an instantaneous snapshot approach, i.e., for a set of defined time frames. To perform the single cell analysis, some parameters are considered, which can be modified in the simulator:

- BS's transmission power.
- MT's transmission power.
- BS and MT antenna gain.
- Noise figure.
- User and cable losses.
- Signalling & Control power percentage.
- Central frequency.
- Bandwidth.
- Modulation usage.
- MIMO usage threshold.
- Slow and fast fading margins.
- Environment.
- Channel.
- Neighbouring BS's transmission power.
- Neighbouring MT's transmission power.

Radio parameters, such as DL and UL transmission power, MT antenna gain, user and cable losses and noise figure are considered the same for UMTS and LTE, being used in the simulation modules. Specifically for DL and UL transmission powers, the same power was considered for both systems in order to perform a fair comparison. Thus, although MT categories are a relevant constraint to maximum user throughput, this will not be taken into account, assuming that a MT supports all available throughputs.

Additionally, it should be considered that part of the transmission power is used for signalling and control purposes. Namely for UMTS, the BS power split between signalling and control and user data varies with the operating Release, as referred in Section 2.1.3. For LTE DL, one OFDM symbol is discounted per RB and in UL, one SC-FDMA symbol, due to the reference signals, [Jaci09]. Regarding LTE DL signalling, the symbols occupied by the P-SCH and S-SCH are neglected here, since they only account for 12 OFDM symbols in a frame, corresponding to percentages as low as 0.2% in the best case [Duar08].

Frequency and bandwidth, LTE specific variables, together with modulation and antenna configuration are performance key parameters, heavily affecting achievable maximum user data rate. Considering an analysis on the systems' capacity, maximum number of available codes is considered for UMTS (15 codes in DL) whereas for LTE variable bandwidth can be chosen in the simulator, as in Table B.3. The comparison between UMTS and LTE for the same bandwidth (5 MHz) or for maximum system capacity (20 MHz in LTE) is thus possible.

Regarding antenna configurations, different schemes were considered: SISO, SIMO and MIMO. Additionally, for LTE DL also a MISO configuration was taken into account. Maximum physical layer throughput values are given as a function of the measured SNR by the expressions in Annex B, obtained based on the 3GPP documentation and on MIMO models explained in Annex D. For the MIMO configurations of both systems, transmission modes providing for maximum throughputs were considered, i.e., considering spatial multiplexing transmission schemes and not transmit or receive diversity schemes. However, an SINR level was defined as threshold for the usage of MIMO, in particular, for each environment, due to the correlation of MIMO transmissions with the good SINR conditions and with the scattering characteristics of the environment, as referred in Section 3.1.

Regarding modulation, while usage statistics can be specified for different schemes, throughput calculation can also be done for each modulation scheme available and the best scheme, i.e., the one that maximises throughput is chosen, simulating AMC techniques in both LTE and UMTS. While the former is adopted for comparison with measured data, the latter is employed for all other capacity and coverage analysis. Due to lack of information and to the complexity involved, adaptive coding rate is not exploited, and only one coding scheme is considered for each modulation scheme and antenna configuration as shown in Annex B.

Slow and fast fading margins, computed in the channel simulation module, are both probabilistic distributions, given by Rice, (A.18), and Lognormal distributions, (A.20). Distributions' standard deviations, *K* parameter for the Rice distribution, and channel coherence times are all input into the simulator. Fading margins are computed in the channel module, at each coherence time interval, for both UL and DL.

Particularly for Rice fading, different values for the *K* parameter were chosen according to the environment. From the three environments implemented, Axial, Urban and Dense Urban, the Axial benefits from LoS transmission reflected by a higher value for *K*, comparing to the Urban and Dense Urban environments. Apart from this, different building configurations are taken for the Urban and Dense Urban environments, having an influence in obtained pathloss values for these environments.

For the pedestrian and vehicular channels, due to the information available, different implementations were considered inside each system simulator. Regarding UMTS, the pedestrian channel is based on the data for the Pedestrian A channel, as shown in Annex B, and the vehicular channel is also obtained based on this results as detailed in Annex B. For LTE, the pedestrian channel is obtained based on the data for the EPA5Hz channel, and for the vehicular channel the ETU70Hz's results are used for the Urban and Dense Urban environments while the extrapolation based on EPA5Hz's results, similar to UMTS's, is taken for the Axial environment, Annex B.

Interference power is computed differently in each system module, as intra-cell interference exists in UMTS. Regarding inter-cell interference in both systems, it is computed as detailed in Section 3.1, i.e., considering the user distance to the interfering BS, in DL, and the average neighbouring cell users' distance to the serving BS, in UL. Neighbouring BS's and MT's power are also inputted into the simulator, making it possible to consider a neighbouring BS transmitting at 50% of maximum power, for example, reflecting a lower cell load situation. Intra-cell interference only exists in UMTS, and as average users' distance to BS is known, received interference power in UL and DL is simply computed.

For both user and interference power received, the propagation model module computes pathloss, as in Annex C, depending on environment characterisation and distance between emitting and receiving antennas. Conversely, for coverage analysis, the module computes the L_{COST231} and $L_{\mathrm{COST231}}^{LoS}$, used in (3.2) and (3.4).

Furthermore, for simulation, three main parameters are defined as inputs, depending on the type of analysis required. For the capacity analysis, distance to BS statistics, i.e., mean and standard deviation of a Gaussian distribution, and number of cell users are required for single- and multi-user analysis. Differently, for service coverage analysis, service required data rate and number of cell users are inputted, so to obtain maximum cell range, for which the user is still served. Apart from these, also the simulation period is defined for simulation, independently of the performed analysis.

Output results vary depending on the analysis, either capacity or coverage. Instantaneous user's distance to BS, pathloss, fading margins, SINR, throughput, modulation and antenna configuration are output for the first, while pathloss, fading margins, cell range, modulation and antenna configuration for the second, for UL and DL by both UMTS and LTE simulators.

3.3 Simulator Assessment and Model Evaluation

Prior to results analysis, the simulator was assessed, namely regarding the validity of the output and the necessary number of simulations that ensure statistical relevance of the results. For this purpose, statistical parameters such as the average, standard deviation and correlation coefficients of the results were analysed. The simulator, i.e., the implemented model, is further compared with the measured results obtained in subsequent chapters.

Output results mean, standard deviation and correlation coefficient between data sets were obtained using (3.6), (3.7) and (3.8), as defined in [Mora10].

$$\mu = \frac{\sum_{i=1}^{N_z} z_i}{N_z} \tag{3.6}$$

where:

- z_i: sample i;
- N_z: number of samples.

$$\sigma = \sqrt{\frac{1}{N_z}\sum_{i=1}^{N_z}(z_i - \bar{z})^2} \tag{3.7}$$

where:

- $\bar{z}$: average value of sample set z.

$$corr(Z,Y) = \frac{cov(Z,Y)}{\sigma_Z \sigma_Y} \tag{3.8}$$

where:

- $cov(Z,Y)$: covariance between random variables Z and Y, assuming equal number of samples of the two variables, defined as:

$$cov(Z,Y) = \frac{\sum_{i=1}^{N_z}(z_i - \bar{z}) \times (y_i - \bar{y})}{N_z} \tag{3.9}$$

- y_i: sample i; (3.10)

Due to channel coherence times, used to characterise the time varying nature of the channel, i.e., that vary slow and fast fading margins, obtained throughputs and cell service ranges both have a strong randomness associated. Thus, the analysis of both throughput's and cell range's average and standard deviation values for varying simulation period values are shown in Figure 3.5-a) and Figure 3.5-b), for the pedestrian urban single-user scenario in DL. No additional randomness is associated to the vehicular channel, other environments, multi-user scenario or UL direction and so a similar analysis for that case would provide for a similar analysis and the same conclusions. Modulation and MIMO configurations that allow for the highest throughputs are taken and no MIMO SINR threshold is defined for this analysis. The urban pedestrian scenario with 500 m ISD and user distance to BS given by Gaussian distribution with mean 200 m and 100 m for standard deviation are considered. For cell range analysis a required service of 5 Mbps is chosen.

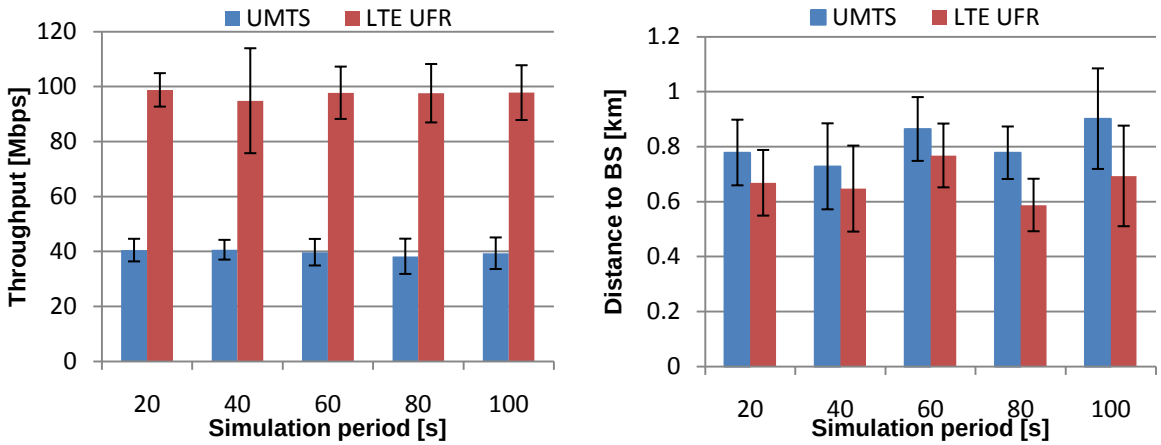

(a) Average user throughput. (b) Average user distance to BS, for 5 Mbps.

Figure 3.5. Capacity and coverage performance results for UMTS and LTE UFR, for varying simulation period.

Slight changes in average throughput value are seen, especially regarding average throughput, with closer standard deviation values for simulation periods higher than 40 s. Thus 60 s simulation period was chosen for further simulations, featuring a fair trade-off between associated error of results and

real simulation time, approximately 5 seconds in an Intel Core2 Duo T7250 2 GHz, 2 GB RAM.

Furthermore, a results analysis regarding throughput and distance to BS is needed for model validation, with average and standard deviations values determined. Results are presented in Figure 3.6, as a function of users' number and summarised also in Table 3.1 and Table 3.2 for UMTS and LTE UFR respectively. For analysis of user's distance to BS, two service data rates are taken under analysis, namely 1 Mbps and 5 Mbps, although similar analyses could be performed for different data rates.

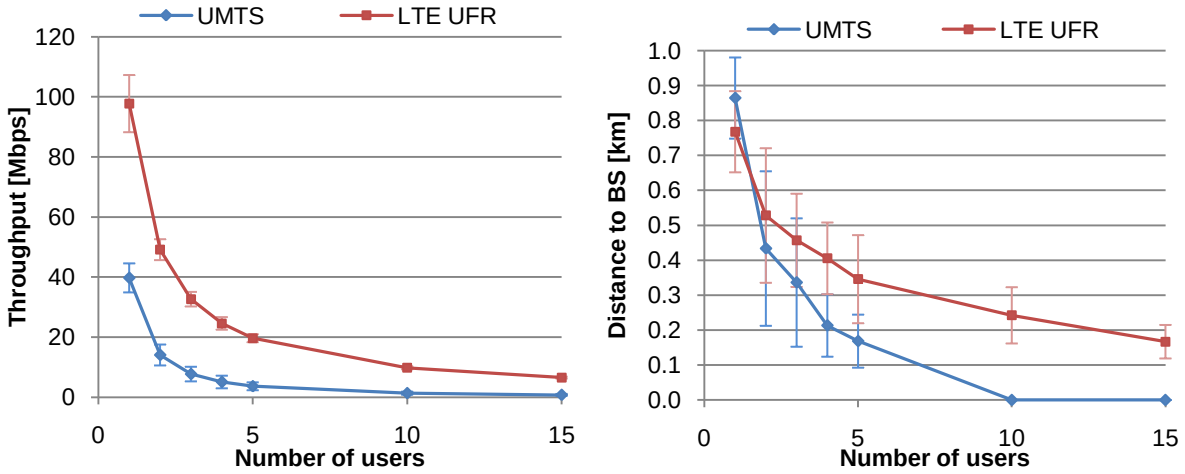

(a) Average user throughput.

(b) Average user distance to BS, for 5 Mbps.

Figure 3.6. Capacity and coverage performance results for UMTS and LTE UFR, for varying number of users.

Table 3.1. User throughput and distance to BS for 1 Mbps and 5 Mbps data rates in UMTS.

Parameter		Number of users							
		1		5		10		15	
		μ	σ	μ	σ	μ	σ	μ	σ
Average throughput [Mbps]		39.7	4.8	3.6	1.3	1.3	0.5	0.8	0.3
Average distance [m]	**1 Mbps**	2044	620	399	169	245	101	265	113
	5 Mbps	864	116	169	76	0	0	0	0

For the single user scenario, average throughputs of 39.7 Mbps and 97.7 Mbps are obtained for UMTS and LTE UFR, respectively, close to the maximum theoretical data rates of 42 Mbps for UMTS, although rather bellow the maximum of 150 Mbps for LTE. Differences are mainly explained by the SINR to throughput mapping models used, that allow maximum data rates of 42 Mbps in UMTS but of only 114 Mbps in LTE. Additionally, fading margins are mainly responsible by simulating the varying nature of the propagation channel, leading to a decrease of the maximum data rates allowed by the models, but giving rise to a more realistic simulation.

Nevertheless, average throughput values decrease with user's number and together with it standard

deviation, naturally, due to the smaller absolute throughput values. A great drop in average throughput is seen from the single- to the multi-user scenario, as expected, in both UMTS and LTE UFR. Whereas for UMTS throughput is mainly reduced by the presence of intra-cell interference, rising with the number of cell users, in LTE the split of available RBs between users also reduces data rates, as it is clearly seen in results in Table 3.2. Smaller growths in intra-cell interference and decreases in RBs per user occur, however, for higher user's number in the multi-user scenario, resulting in smaller decrease in average throughput.

Table 3.2. User throughput and distance to BS for 1 Mbps and 5 Mbps data rates in LTE UFR.

Parameter		**Number of users**							
		1		**5**		**10**		**15**	
		μ	**σ**	**μ**	**σ**	**μ**	**σ**	**μ**	**σ**
Average throughput [Mbps]		97.7	9.5	19.6	1.3	9.8	0.5	6.5	0.3
Average distance [m]	**1 Mbps**	880	236	682	221	531	171	465	176
	5 Mbps	768	116	346	126	243	81	167	48

Regarding cell range, for any of the considered services, it decreases with users' number but also with the absolute value of the required service throughput. For higher user's number, users' may even not be served, as it is seen with UMTS for more than 10 users, due to the limited BS transmission power and limiting intra- and inter-cell interference power levels. Regarding LTE the limitation is still in the number of RB's per user. Nevertheless, UMTS still provides for higher cell ranges for the single-user scenario in 1 Mbps and in 5 Mbps assured data rates.

Chapter 4

Results Analysis

This chapter presents the results from the LTE measurements campaign performed as well as the simulator results for both UMTS and LTE. Measurements results are initially analysed, describing the scenario used and drawing different analysis regarding SNIR and physical throughput. A comparison between measurements' and simulations' results is then performed, comparing SINR and throughput for varying channel and environment. Finally, UMTS's and LTE's simulation results are compared, and performance gains computed, presenting conclusions on systems' capacity and coverage.

4.1 Scenarios Description

For the performed analysis, different environment, channel and load conditions were considered. Regarding the first, three different environments are defined:

- The Axial environment is characterised by strong Line of Sight (LoS) with the serving eNB and thus the best propagation conditions. As a consequence, BSs are highly distanced from each other, and low cell overlap occurs.
- The Urban environment is defined mainly by multipath coverage, although LoS might occur sporadically, due to moderate building concentration. Due to higher pathloss, BSs are less distanced when comparing to the Axial environment.
- The Dense Urban environment, where high building concentration occurs, is also where strong multipath exists and big cell overlap occurs due to closer installed eNBs.

The defined environments have both an effect in pathloss and in neighbouring cells interference. Default and recommended values of COST231-Walfisch-Ikegami are described in Annex C, for pathloss calculation. Whereas for the Axial environment COST231-Walfisch-Ikegami's expression for LoS conditions is used, for urban environments no LoS is considered to prevail and environment characterisation is assumed as in Table 4.1. Furthermore, different ISDs characterise the environments. ISDs obtained in the measurements scenario, presented in Subsection 4.2.1 and with values shown in Table F.2, are used as reference for each environment in all analysis performed.

Table 4.1. COST231-Walfisch-Ikegami's environment parameters for the urban scenarios, [Opti11].

Parameter \ Environment	Urban	Dense Urban
BS Height (h_b) [m]	30	30
MT Height (h_m) [m]	1.5	1.5
Buildings Height (H_B) [m]	23	23
Street Width (w_s) [m]	35	30
Inter Buildings Distance (w_B) [m]	75	50
Incidence Angle (φ) [°]	90	90

Also, two different channel scenarios are defined: the pedestrian and vehicular channels. The pedestrian stands for a static user (or almost, 3 km/h in ITU Pedestrian A channel) at the street level with low attenuation margins; the vehicular for users moving at high-speed, normally considered 50 km/h. These channels were taken for each of the defined environments, and associated SNIR-to-throughput mapping is considered as available in Annex B.

Due to the random nature of the propagation channel, multipath terrain and buildings configurations, associated signal fading and degradation is accounted by defined fast and slow fading margins, respectively. Both for single- and multi-user scenarios, a statistical modelling for the fading margins is employed, as referred in Subsection 3.2.2. Different default values are assumed for fading characterisation in pedestrian and vehicular channels for both systems, Table A.1, Table A.2 and Table A.3.

The default parameters used for link budget simulations are presented in Table 4.2 for UMTS and LTE. Frequency bands used are based on [Opti11]. One can further note different Signalling and Control Power percentage values for both systems according to the analysis in Chapter 2. All modulation and MIMO schemes present in 3GPP's reports on throughput-SINR traces are available.

Table 4.2.Default values used in UMTS and LTE link budgets (based on [Jaci09], [EsPe06], [HoTo09], [PoPo10] and [Opti11]).

Parameter		**UMTS**		**LTE**	
		DL	**UL**	**DL**	**UL**
BS Transmission Power [dBm]		46	-	46	-
MT Transmission Power [dBm]		-	24	-	24
Frequency Band [MHz]		2110	1920	2600	
Bandwidth [MHz]		5		20	
Modulations		QPSK, 16QAM, 64QAM	QPSK, 16QAM	QPSK, 16QAM, 64QAM	QPSK, 16QAM, 64QAM
Antenna Configurations		SISO, SIMO, MIMO	SISO	SISO, SIMO, MISO, MIMO	SISO, MISO, MIMO
MT Antenna Gain [dBi]		1			
BS Antenna Gain [dBi]		18			
User Losses [dB]		1			
Cable losses between emitter and antenna [dB]		2			
Noise Figure [dB]		9	7	7	5
Signalling and Control Power [%]		40	15	28.5	10
MIMO Threshold [dB]		17.3		16	
ICIC Gain [dB]	**Cell centre user**	-		6	
	Cell edge user			10	

Maximum BS and MT antenna gains of 18 dBi (with a 65º half power beam width) and 1 dBi, respectively, are assumed for both systems, [Jaci09]. Despite the dependence with frequency, equal values were assumed, allowing for a fair comparison between systems and a simpler analysis.

Additionally, both equipment gains are manufacturer dependent and may vary according to the type of hardware.

Identical transmission power values were also set in order for a fair system's comparison. Actually, some HSPA+ sites exist that are already being supplied by 40 W. However, general values are below this target, according to [Jaci09], namely 43 or 44.7 dBm for macro-cells. For LTE, BSs are commonly deployed with 46 dBm maximum transmission power, [Opti11].

As the human body absorbs energy, a body loss margin of 1 dB is established. Moreover, losses generated by feeders, connectors and all external equipment between the antenna and the BS receiver are considered. Although varying with the equipment type and manufacturers and operators implementation issues, a margin of 2 dB is used.

A 5 MHz bandwidth is assumed for UMTS transmission whereas for LTE the maximum of 20 MHz is used. Although the same bandwidth could be considered, for LTE the system is designed to allow for higher bandwidths, differently than for UMTS, and thus one should not restrict itself to a comparison using 5 MHz LTE. Nevertheless, if the latter scenario is the case, the same results are applicable although dividing maximum throughputs obtained by a factor of 4, assuming equal spectral efficiency for 5 and 20 MHz, Table B.3.

A SINR threshold level is defined for both systems, above which MIMO transmission can be scheduled. For UMTS, the reference threshold value was adapted from [Bati08], where it was considered as SINR threshold for the maximum throughputs in DL for HSPA+. For LTE, the assumed value is obtained in Section 4.2, based on measurements results.

Additionally for LTE ICIC variant, a higher SINR gain is considered for cell edge users than for cell centre users, based on results in [LZZY07] and [XuMK08]. Although different gain values could be assumed, depending on the environment, due to different interference levels felt in each environment, for simplicity no differences are here assumed. Moreover, the obtained gain in SINR is largely dependent on the ICIC scheme chosen, e.g. soft frequency reuse or partial frequency reuse schemes, and in practical implementation considerations. Again, a simple but meaningful solution is preferred.

Interference power is computed as defined by the Single-Cell model developed, both intra- and inter-cell. However, although users in the cell under study are considered to be at maximum load, i.e., transmitting with maximum power in both UL and DL, neighbouring cells are considered to serve the same amount of users but at 50% of maximum transmitted power, [Opti11]. Therefore, in DL, neighbouring BS's maximum transmitted power is 42.97 dBm, Table 4.3, and in UL, neighbouring MTs' maximum transmitted power is 21 dBm, 50% of the respective MT power in Table 4.2.

Regarding the coverage analysis, i.e., distance to BS as a function of number of users' analysis, different services were considered to provide a broader coverage of vast types of services possible. Particularly, three service types were considered: a Web service, for UL and DL, requiring typical data rates of 1 Mbps according to [Jaci09]; a video streaming service, for DL, with typical maximum throughput values of 5 Mbps for MPEG-2's primary distribution according to [Pere11]; and a File Transfer Protocol (FTP) service, considering a possible requested throughput of 10 Mbps, Table 4.4.

For a comparative coverage analysis between different service data rate values, no mixed service profile was considered.

Table 4.3. Neighbouring BS's transmitted power, regarding cell load, [Opti11].

Cell load [%]	Neighbouring BS transmitted power [dBm]
0	41.20
50	42.97
75	44.73
100	46.00

Table 4.4.Default required service data rates considered for coverage analysis (based on [Jaci09] and [Pere11]).

Service / Throughput	Typical [Mbps]	Considered [Mbps]
Web	[1.024, $R_{b\,max}$]	2
Video Streaming	[0.032, 10]	5
FTP	[0.512, $R_{b\,max}$]	10

Non-real time applications such as Web, Video Streaming and FTP typically present an asymmetrical nature, as they mostly request information executed by users to remote servers. Nevertheless, in the scenario developed, the defined service data rates will be considered for both DL and UL. Also, different QoS levels characterise each of these services, required for a suitable end-user satisfaction rate. However, as each service will be analysed separately, the same priority is assumed for all users, performing the same service, and thus an accurate and simple analysis is possible.

Finally, regarding users' distance to the serving BS, a Gaussian distribution with the same average and standard deviations values as measured in Section 4.2, shown in Table F.1, is considered in Sections 4.3 to 4.4, for an accurate comparison between theoretical and simulation results and also a realistic comparative scenario for UMTS and LTE performance analysis.

4.2 LTE Measurements Results Analysis

Measurements results on LTE are presented in this section. The measurements scenarios are first detailed in Subsection 4.2.1. Results are then cross-analysed for varying environment, channel, modulation and antenna schemes, user's position in the cell and system's load and distance to serving BS, over Subsection 4.2.2 until Subsection 4.2.7.

4.2.1 Measurements Scenarios

In the framework of this thesis, a plan for measurements was carried out, in cooperation with Optimus. Measurements for the DL single-user in the cell scenario were then performed in Optimus' LTE cluster in the city of Porto, Figure G.1, considering the Axial, Urban and Dense Urban environments, defined in Section 4.1.

Measurements were performed, for both UL and DL, using a maximum of two outdoor antennas for the UE and equipment specifications in Table 4.5. The antennas were installed on the top of Optimus measurement vehicle, considering a recommended distance of about the same order of magnitude of the propagation wavelength and positioned with a 45º angle between them, as shown in Figure 4.1-a). The antennas were connected to a MT Probe equipment, Figure 4.1-b), used together with a laptop for data acquisition and storage. Also a GPS receiver was used, for collecting data on positioning.

Table 4.5. Equipment used in LTE live measurements.

Feature	Value
Central frequency for UL / DL [MHz]	2510 / 2630
Maximum bandwidth [MHz]	20
UE category	5 (QPSK,16QAM,64QAM in UL and DL)
System's MIMO capabilities	1Tx 1Rx Single Stream 1Tx 2Rx Receive Diversity 2Tx2 Rx Space-Frequency Block Coding 2T2R Open-Loop Spatial Multiplexing
ICIC schemes	None

(a) Two antennas used in the measurements.

(b) MT Probe equipment used for data acquisition.

Figure 4.1. Measurements equipment used.

A UDP stream was used to create a continuous data stream, for both UL e DL directions. For the latter, a server was used from Optimus' back office, provided that the connections upstream in the core network were not constraining maximum achievable data rates. The control plane data was then

acquired on the UE's side.

For all three environments, measurements were taken mainly in the middle of the streets, where possible. Both static and mobility measurements were taken in this set. Moderate average velocity for mobility measurements was found around 20 km/h for different environments, as shown in the Probability Distribution Function (PDF) and Cumulative Distribution Function (CDF) of user's speed in Figure 4.2-a), taking into account obvious traffic constraints.

Selected measurement areas were scattered for varying distances to serving BS, as shown in Figure 4.2-b) and further in Table F.1, and over the different environment wide areas, seeking to cover different propagation conditions. Distances between BS's statistics are summarised for each environment in Table F.2, measured as shown in Figure G.2 to Figure G.4.

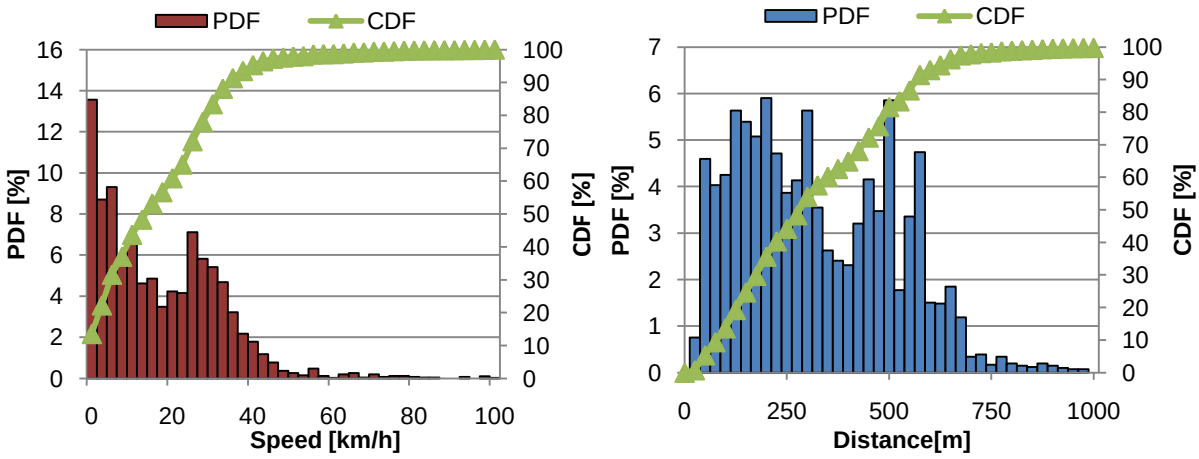

(a) UE's speed.

(b) Distance to serving eNB.

Figure 4.2. Mobility measurements statistics for 0% cell load measurements over all the environments.

For the Axial environment, measurements were taken in the main avenue and neighboring streets, at varying distances from serving BS, mainly in locations were strong LoS was present or diffraction on at most one building top was likely to occur. In both Urban and Dense Urban environments, measurements were taken closer to installed BSs when compared to the Axial environment, avoiding high pathlosses to limit results. Varying street configurations were covered, as results for the latter environments are known to be more dependent on these configurations. Although initial static measurements spots were not chosen over the routes used for the drive tests, shown in Figure G.5, for the present analysis only the results over these routes are considered. For each environment, the same route was also considered when varying load.

For a broad analysis of coverage, extended measurements were made, shown in Figure G.6, besides the static and mobility ones performed inside the cluster. The latter route was used for drive tests both on DL and UL, going from the cluster center over to the cluster's surroundings and until an area where residual coverage was measured. A broader range of channel conditions and SINR values is then measured, not obtained when measuring close to the serving BS.

Regarding the data collected, a filter was applied to cut off data obtained during HO procedures, based on Radio Resource Control (RRC) measurement control messages, used for HO decision, and

on the system events reported by the manufacturer's software used. Also, apart for coverage measurements, results corresponding to very low throughput values, i.e. under the threshold of 0.5 Mbps, were not considered, as these were determined to be associated to connection establishment or other procedures that are not under study.

Further, regarding the limitations of the GPS receiver used, it was seen that cases were where the system's measurements were taken without associated GPS coordinates. Careful interpolation of the GPS coordinates was performed in these cases, where possible, based on adjacent measurement points. Taking into account that the measurements' data was acquired in the UE each second and that the described GPS blackouts were bursty, the interpolation method is considered to be acceptable.

Apart from this matter, measurements' data on position showed a fairly good precision for the measurements performed in the drive tests, but noticeable positioning errors when performing static measurements. Furthermore, these limitations make it impossible to make accurate measurements of channel variations in time or in space, interesting for environment and channel characterisation.

Load measurements were also performed making use of a system function for load simulation, made available by the equipment's manufacturer, mainly acting on BSs' transmitted power. Interference in this way is equally spread over the whole transmission bandwidth available. Power levels for the three load sets analysed, 50%, 75% and 100% load, are specified in Table 4.3, compared to the case with no load, i.e., only control channels exist. Note that in the LTE scenario studied, the 0% cell load situation does not correspond to no transmitted power in neighboring cells, but instead to transmitted power allocated to the common reference signals, transmitted by the BS at all times, and that correspond to 33% of the total available power in the BS. However, for simplicity, this case is said to correspond to 0% load.

For accurate environment comparison, environment characterisation was made in loco, taking into account the users' surroundings. For the Axial environment, LoS propagation is prevalent in most cases and is the only propagation considered. Regarding Urban and Dense Urban environments, non-LoS is likely and propagation occurs mostly by diffraction on the buildings' tops, located between the BS and the user's street. Urban and Dense Urban environments measured showed in general, buildings with similar heights, without noticeable isolated higher buildings or other irregular building patterns over the landscape. Therefore, the measured environments are coherent with the scenarios developed in Section 4.1.

For the record, it is also worth mentioning that one of the BSs, serving in the Axial environment, proved to have lower data rate values than expected, and in an agreement with Optimus, the measurements regarding this BS were excluded from this study.

4.2.2 Environment

PDFs and CDFs obtained from static measurements' results are presented in Figure 4.3, Figure 4.4 and Table 4.6, for different environments regarding both measured average SINR and measured average throughput. Similar results are also obtained for the mobility measurements, Figure F.1,

Figure F.2 and Table F.3.

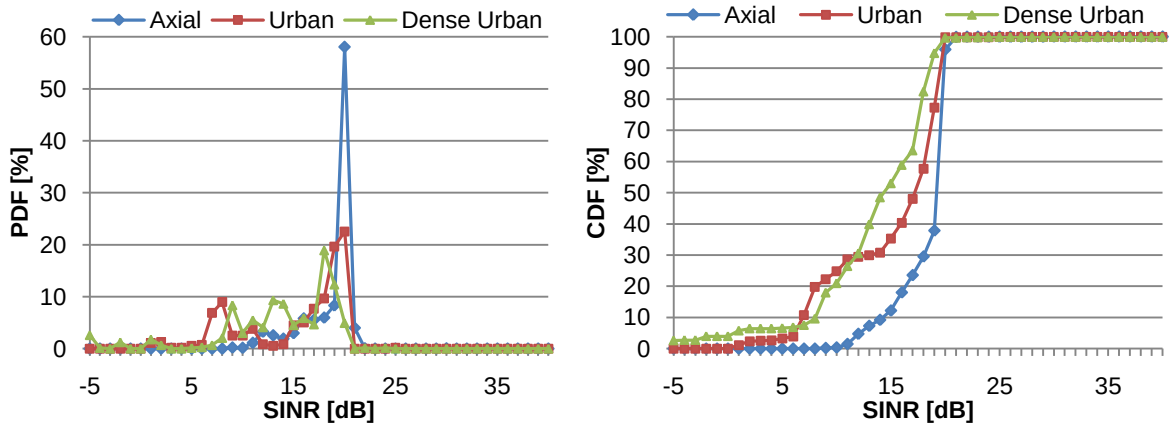

(a) PDF. (b) CDF.

Figure 4.3. SINR statistics of DL static measurements results for different environments.

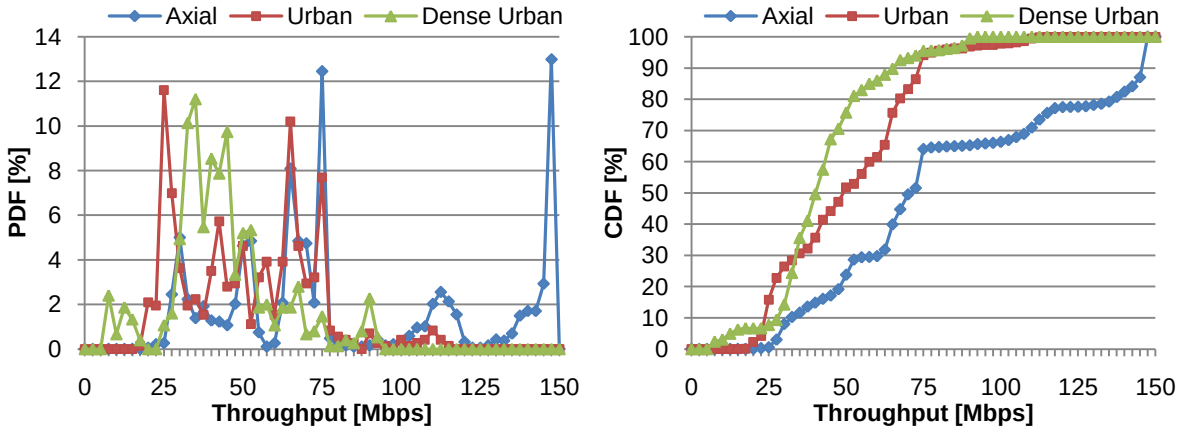

(a) PDF. (b) CDF.

Figure 4.4. Throughput statistics of DL static measurements results for different environments.

Regarding the considerable differences in SINR, these have an obvious direct impact on the achievable throughput. Figure 4.5 shows the comparison between the number of allocations of both the Space-Frequency Block Coding (SFBC) scheme, a transmit-receive diversity scheme, and the Open Loop Spatial Multiplexing (OL SM) scheme, a 2×2 MIMO scheme for the static measurements. Similar results are also obtained for the mobility measurements, Figure F.3.

Table 4.6. SINR's and throughput's mean and standard deviation, for different environments.

Parameter \ Environment	Axial	Urban	Dense Urban
μ_{SINR} [dB]	18.11	14.80	13.31
σ_{SINR} [dB]	2.44	5.18	5.72
$\mu_{Throughput}$ [Mbps]	82.04	49.75	42.26
$\sigma_{Throughput}$ [Mbps]	39.67	20.72	16.60

It is seen that for the Axial environment, MIMO is by far more used than the SFBC scheme, 46% of the times, when comparing to other environments, 7% and 9% for Urban and Dense Urban environments respectively. This happens mainly due to the higher SINR values measured for the Axial environment.

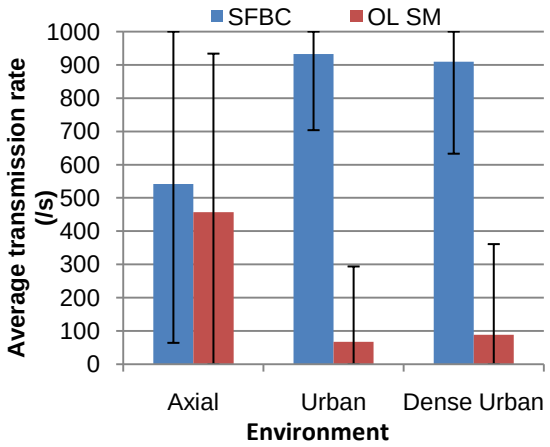

Figure 4.5. Transmission mode statistics analysis for static measurements in different environments.

An estimate of threshold value for the usage of the OL SM transmission scheme can be obtained by the analysis of the average number of allocation times as a function of SINR, presented on Figure 4.6-a), Figure 4.7-a) and Figure 4.7-b) for the mobility measurements obtained in the three environments. Additionally, a polynomial fitting is also shown over the data.

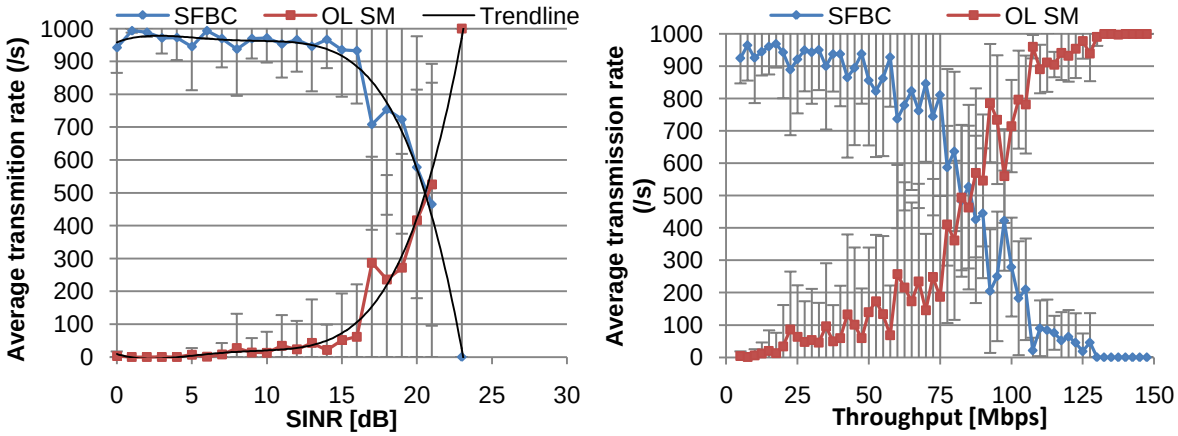

(a) SINR. (b) Throughput.

Figure 4.6. Transmission mode analysis versus SINR and throughput, for mobility measurements in the Axial environment.

Considering the threshold of 10% MIMO transmissions, it can be seen that for the Axial environment it corresponds to an approximately 16 dB of SINR. For the Urban and Dense Urban environments, a similar threshold can be measured for SINR values around 17 dB and 16.5 dB, respectively. For Rank1 SINR a diversity gain of 1 dB and for Rank2 SINR a loss of 7 dB is added on top of average SINR, considering the results in Figure F.4.

Considering the results in Figure 4.3-a), the average SINR value for the Axial environment is found to be above the MIMO threshold, with 82% of measurements above SINR of 16 dB, justifying thus the greater average throughput values in Figure 4.3-b) when comparing to the Urban and Dense Urban

environments.

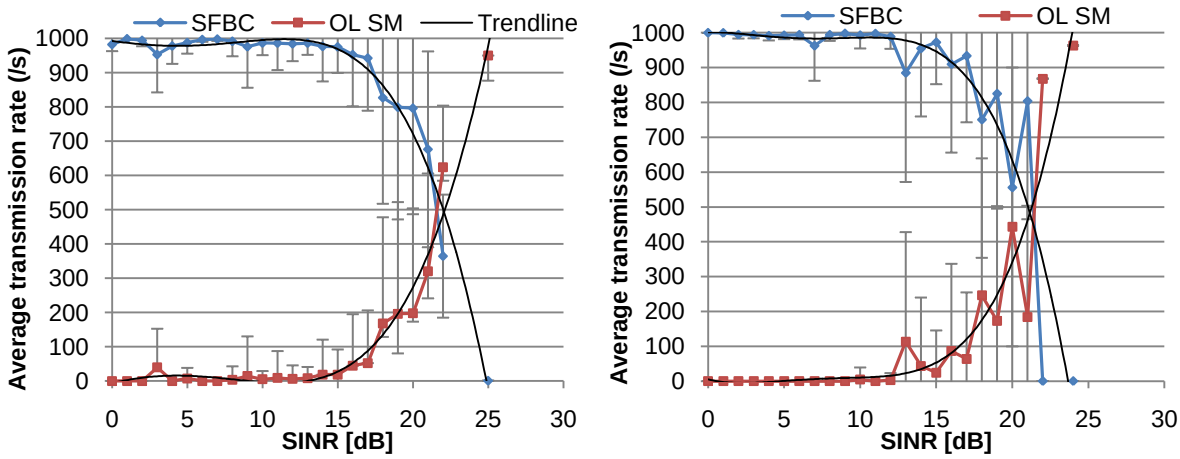

(a) Urban. (b) Dense Urban.

Figure 4.7. Transmission mode versus SINR analysis, for mobility measurements in the Urban and Dense Urban environments.

Thus, although MIMO transmission takes advantage of spatial diversity in the environment for multiplexing transmission streams, as it exists in the Urban and Dense Urban environments, results show that it is in the Axial environment that MIMO is more used. Although stronger LoS transmission exists for the latter, and hence a weaker multipath transmission component, better conditions for MIMO transmission are found allowing for a boost in throughput rates, as shown in Figure 4.6-b). Achieved throughput rates of over 100 Mbps in the Axial environment, are only possible due to the use of MIMO.

4.2.3 Mobility

By taking the measurements obtained in mobility, according to the distribution in Figure 4.2-a) and the static measurements, a comparison in done in terms of SINR and throughput distributions for the Axial, Urban and Dense Urban environments, as shown in Figure F.5, Figure 4.8 and Figure F.6, respectively. Table 4.7 summarises results for all environments.

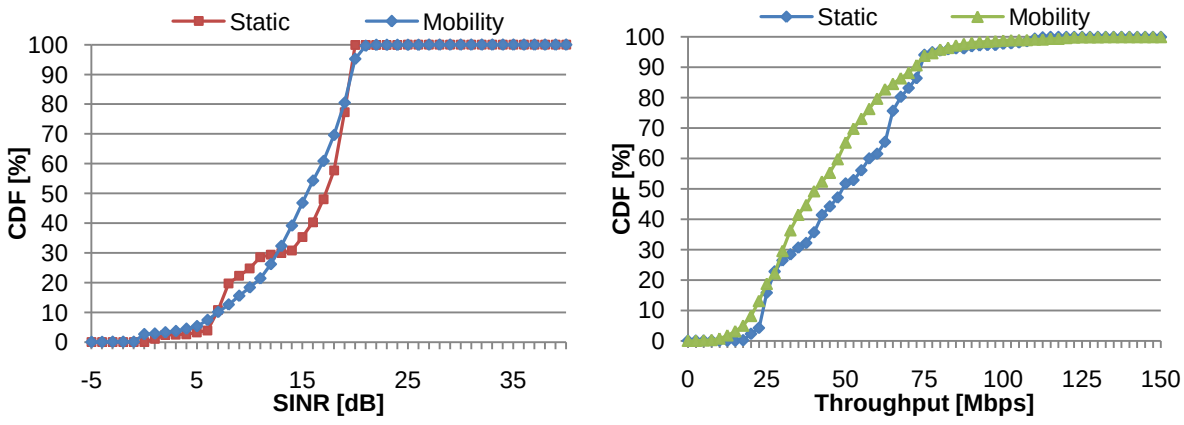

(a) SINR. (b) Throughput.

Figure 4.8. CDFs of DL mobility and static measurements' results for the Urban environment.

For the Axial environment, a noticeable difference exists regarding the two measurement scenarios, a gain of 3.7 dB in average SINR from the static to the mobility scenario and of 73% in average throughput. Also, taking into account the results in Figure 4.6-a), it can be found that for the mobility case the SINR threshold for MIMO usage is not always achieved, 24% comparing to 62% for the static case, and justifying why throughput is strongly affected.

One can conclude that the fast varying environment, due to mobility, can have a great impact for this environment. However, it should be also noted that the static measurements' locations chosen have a great influence in this analysis, and although these were chosen over the drive test's route used for the mobility measurements, a more extensive set of static measurements should be taken for a more reliable analysis.

Regarding the Urban and Dense Urban environments, Figure 4.8 and Figure F.6,smaller differences can be seen, 0.05 dB and -0.87 dB in the average SINR from static to mobility scenarios, and 14% and 9% in the average throughput. Hence, for the Urban and Dense Urban environments, a smaller effect of mobility on the measurements is shown, comparing to the Axial environment. Being the latter characterised by strong LoS transmission, it might be said that environments where LoS transmission occurs are more affected by mobility than environments where multipath transmission is dominant.

Table 4.7. SINR's and throughput's mean and standard deviation for static and mobility scenarios.

Parameter \ Environment	**Axial**		**Urban**		**Dense Urban**	
	Static	**Mobility**	**Static**	**Mobility**	**Static**	**Mobility**
μ_{SINR} [dB]	18.11	14.41	14.80	14.75	13.31	14.18
σ_{SINR} [dB]	2.44	5.40	5.18	4.53	5.72	4.57
$\mu_{Throughput}$ [Mbps]	82.04	47.30	49.75	43.72	42.26	38.84
$\sigma_{Throughput}$ [Mbps]	39.67	30.24	20.72	20.08	16.60	14.09

4.2.4 Modulation and Antenna Configuration

An analysis of the transmission modulation used is also performed, based on the results of the MCS used in the static and mobility scenarios, Figure 4.9-a) and Figure F.7 respectively. In a first analysis results are presented for both the non-MIMO and MIMO transmissions.

For static measurements results a dominant usage of 64QAM is seen for all three environments. 16QAM modulation is the second most used modulation scheme, by far separated from the QPSK modulation, only marginally used. The great usage of higher order modulations can be justified by the good SINR environments, with SINR average values of 18.11 dB, 14.80 dB and 13.31 dB despite their differences.

Similar results are also evidenced for mobility measurements in Figure F.7, although not as expressive

due to poorer channel conditions, and in which cases lower order modulations are thus used, Figure 4.9-b). Great differences can be seen, however, comparing the modulation usage results for a real life in use network, as presented in [Bati11] for the UMTS system, where other users coexist and such good channel conditions and a fully dedicated BS are not possible.

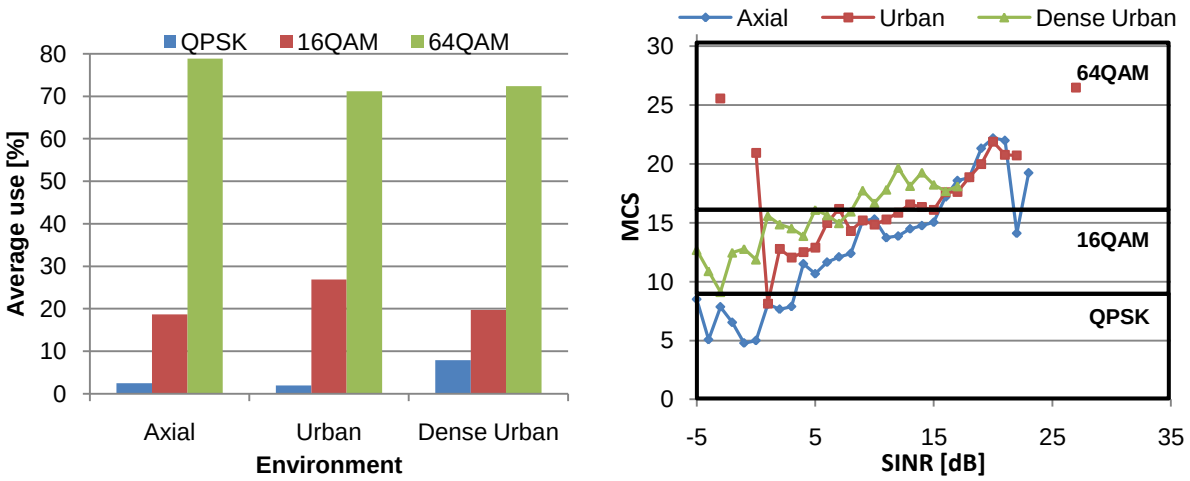

(a) Average modulation usage. (b) Average MCS as a function of SINR.

Figure 4.9. Modulation schemes analysis in DL static measurements' results for different environments.

Regarding MIMO usage, i.e. OL Spatial Multiplexing, versus transmit-receive diversity transmission using SFBC, it was seen in Figure 4.5 that it is mainly reliant on good SINR levels. Nevertheless, significant differences exist between static and mobility measurements, for the latter refer to Figure F.3, mainly in the Axial environment precisely due to the SINR levels for each case, Figure F.5.

4.2.5 Cell Edge vs. Cell Centre

Based on measurements, a cell centre and edge performance analysis was made, based on the measured RSRP. The relation with the distance to BS is shown in Figure 4.10 for the Axial environment. Despite the poor fitting, Table F.4, a clear trend is seen to exist, namely the decrease of the difference between serving and detected RSRP with distance rise.

Nevertheless, SINR and throughput results are presented in Figure 4.11 for the Urban environment and in Figure F.8 and Figure F.9, Annex F, for the remaining environments. Table 4.8 summarises results obtained over all environments. It is seen that, in the case where no ICIC is used, a decrease of 5.65 dB, 4.74 dB and 4.97 dB in average SINR exists from cell centre to cell edge in the Axial, Urban and Dense Urban environments, respectively, with associated decrease of 54%, 55% and 41% in average throughput.

The higher and lower SINR values associated to cell centre and cell edge reflect also that it is possible to use SINR as an indicator of cell edge and cell centre results, such as it happens when the geometry factor is employed, defined in [HoTo09] as an average wide-band SINR. Hence, for all the three environments, a SINR threshold of around 15 dB to 16 dB can be defined for separating cell edge

users from cell centre users, as approximately 80%, 76% and 79% the cell edge measurements are bellow this value and 80%, 87%, 88% of cell centre measurements are above it.

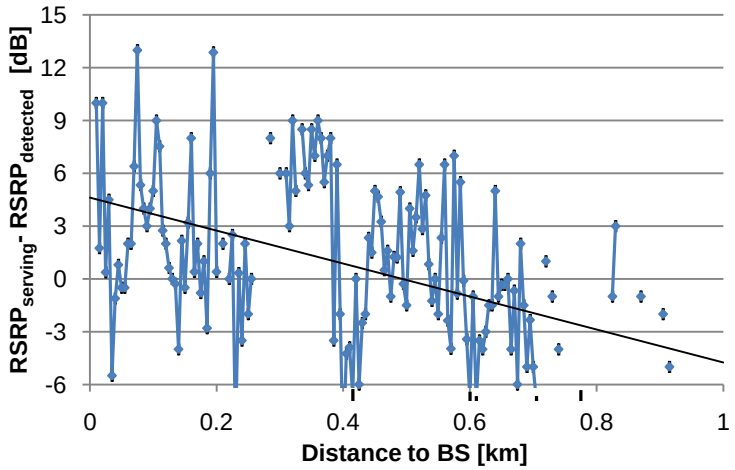

Figure 4.10. Serving and neighbouring cell RSRP difference as a function of distance to BS for the Axial environment, based on mobility measurements.

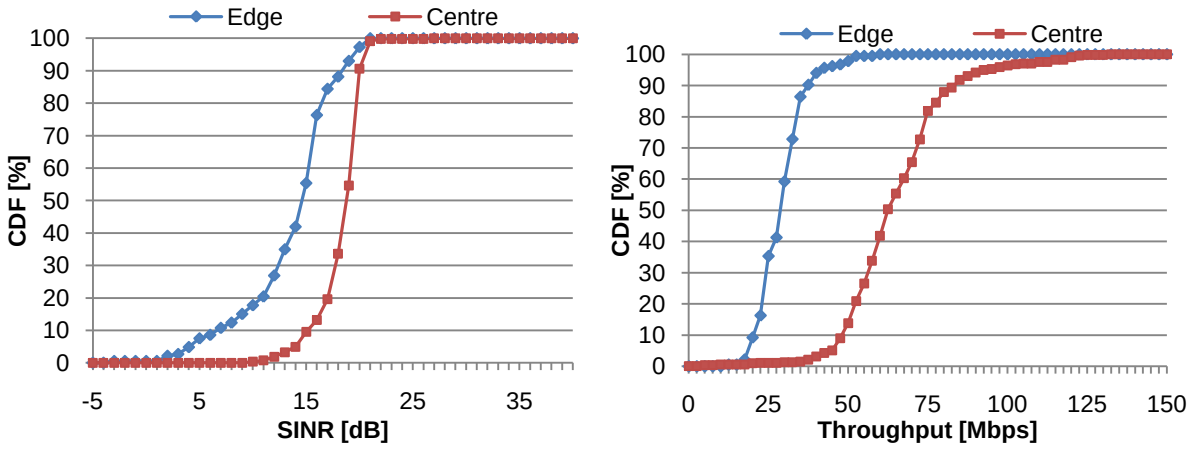

(a) SINR. (b) Throughput.

Figure 4.11. Cell edge versus cell edge statistics, from mobility measurements in the Urban environment.

Table 4.8. SINR's and throughput's mean and standard deviation for cell edge versus cell centre, for the mobility scenario.

Parameter \ Environment	Axial		Urban		Dense Urban	
	Cell edge	Cell centre	Cell edge	Cell centre	Cell edge	Cell centre
μ_{SINR} [dB]	11.82	17.47	13.46	18.20	11.93	16.90
σ_{SINR} [dB]	5.38	3.54	4.39	2.05	5.36	2.20
$\mu_{Throughput}$ [Mbps]	31.04	68.10	28.83	64.68	30.96	52.38
$\sigma_{Throughput}$ [Mbps]	16.06	30.60	7.23	16.40	7.94	10.79

4.2.6 Cell Load and Capacity

Considering the presence of cell load as described in Chapter 4.1, results of measured average SINR and throughput are presented in Figure 4.12 and Table 4.9 for the Urban environment whereas similar results are shown for the Axial and Dense Urban environments, respectively, in Figure F.10 and Table F.5, and Figure F.11 and Table F.6.

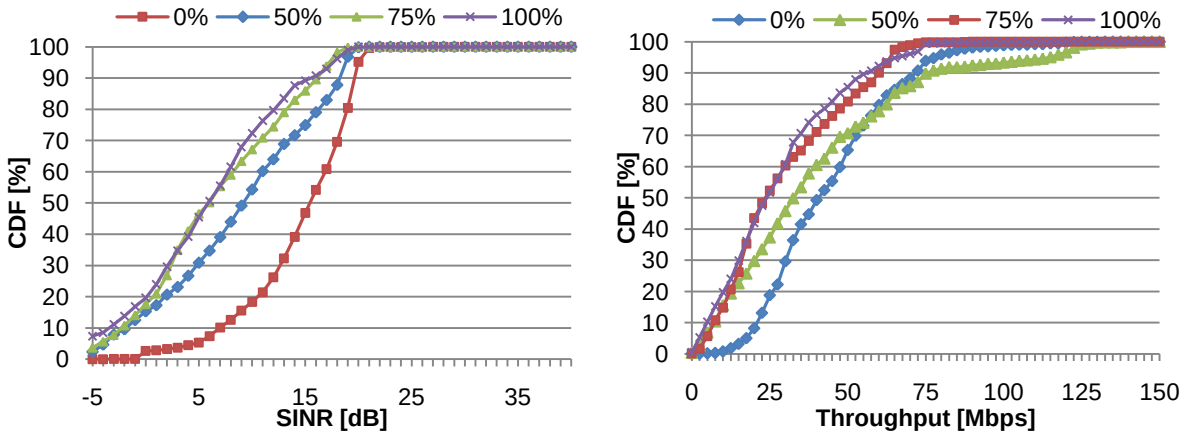

(a) SINR. (b) Throughput.

Figure 4.12. CDFs of DL measurements results, for varying load, in the Urban environment.

For the Axial environment, an approximate decrease of 4.48 dB, 3.47 dB and 7.40 dB in the average SINR is seen from the 0% load environment, to 50%, 75% and 100% load scenarios. Regarding throughput, the decrease in the average throughput is of approximately 15%, 9% and 28% from the 0% load to the 50%, 75% and 100% scenarios.

In the Urban environment, an approximate decrease of 6.04 dB, 8.29 dB and 8.87 dB in the average SINR and of 10%, 33% and 37% in the average throughput is presented from 0% load to 50%, 75% and 100% load scenarios. The relative decreases in average SINR and throughput are thus in its majority higher than for the Axial environment, as shorter distances between neighbouring BSs create potentially higher interference power levels.

Table 4.9. SINR's and throughput's mean and standard deviation for varying load scenarios in the Urban environment.

Parameter \ Load	0%	50%	75%	100%
μ_{SINR} [dB]	14.75	8.71	6.46	5.88
σ_{SINR} [dB]	4.53	7.21	6.65	6.78
$\mu_{Throughput}$ [Mbps]	43.72	39.44	29.12	27.39
$\sigma_{Throughput}$ [Mbps]	20.08	30.24	19.01	19.14

Regarding the Dense Urban environment, an approximate decrease of 7.99 dB, 9.16 dB and 9.69 dB in the average SINR is shown from the 0% load to the 50%, 75% and 100% scenarios whilst the decrease in the average throughput is of approximately 30%, 38% and 39%. The relative decreases in

average SINR and throughput are hence the highest of the three environments, following the trend presented also for the Urban environment, where shorter ISDs imply potentially higher interference power and lower SINR values.

Furthermore, the effect of cell load in the modulation schemes used for transmission can also be measured for the Axial, Urban and Dense environments, as shown in Figure 4.13 and Figure 4.14, for varying load levels.

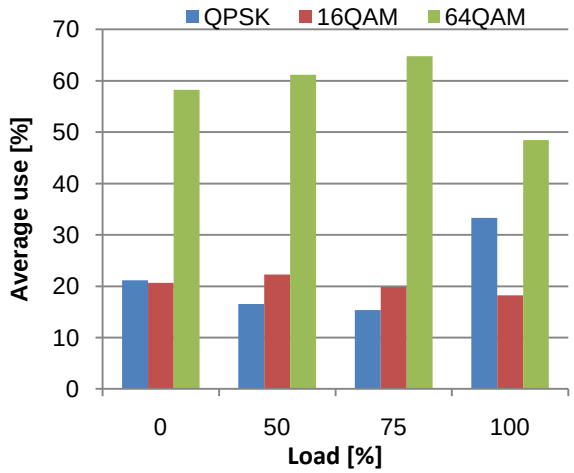

Figure 4.13. Modulation schemes average use regarding cell load for the Axial environment.

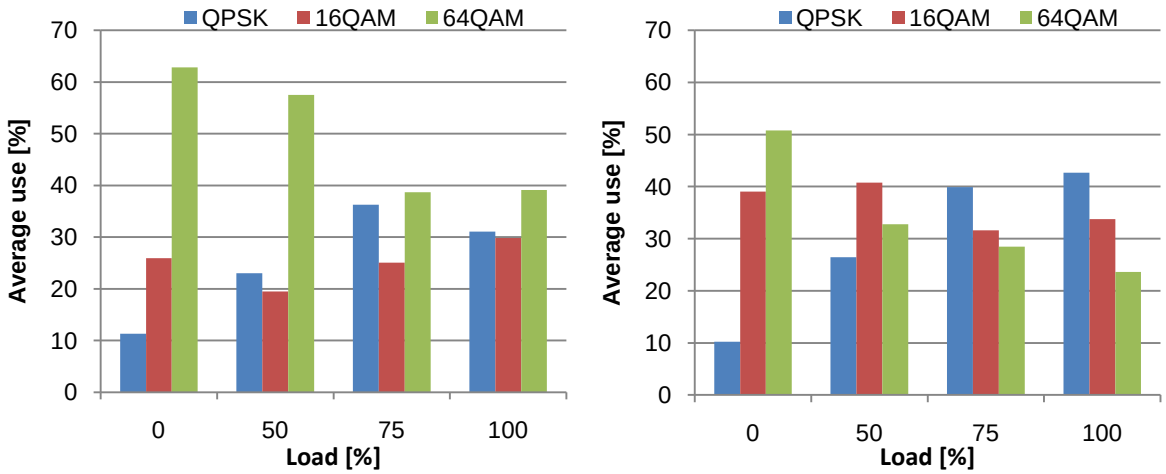

(a) Urban. (b) Dense Urban.

Figure 4.14. Modulation schemes average use regarding cell load for the Urban and Dense Urban environments.

For the Axial environment, larger differences are seen for the 100% load scenario, where a decrease of 10% on 64QAM and an increase of 12% on QPSK were measured regarding the 0% scenario. Regarding the Urban and Dense Urban environments, changes in modulation usage are even clearer for increasing load levels, with decreases of 20% and 24% on 64QAM usage, respectively, and increases of 33% and 27% on QPSK usage from 0% to 100% load scenario. The difference between the modulation schemes used in the Axial, Urban and Dense Urban environments is thus, in accordance with the SINR differences measured.

Regarding MIMO usage, SINR levels for 0%, 50%, 75% and 100% load scenarios in mobility are all

below the MIMO SINR threshold, defined in Subsection 4.2.2. Hence, differences in MIMO usage for varying load are hardly seen, and similar low MIMO usage levels occur. Even so, from 0% to the 50% load scenario a decrease of 16% and 12% was measured for the Axial and Dense Urban environments and the same decrease was also maintained for 75% and 100% load scenarios, for all the environments.

Further regarding cell centre versus cell edge performance, the difference in measured average SINR and average throughput between cell centre and cell edge is shown in Figure 4.15, as a function of load.

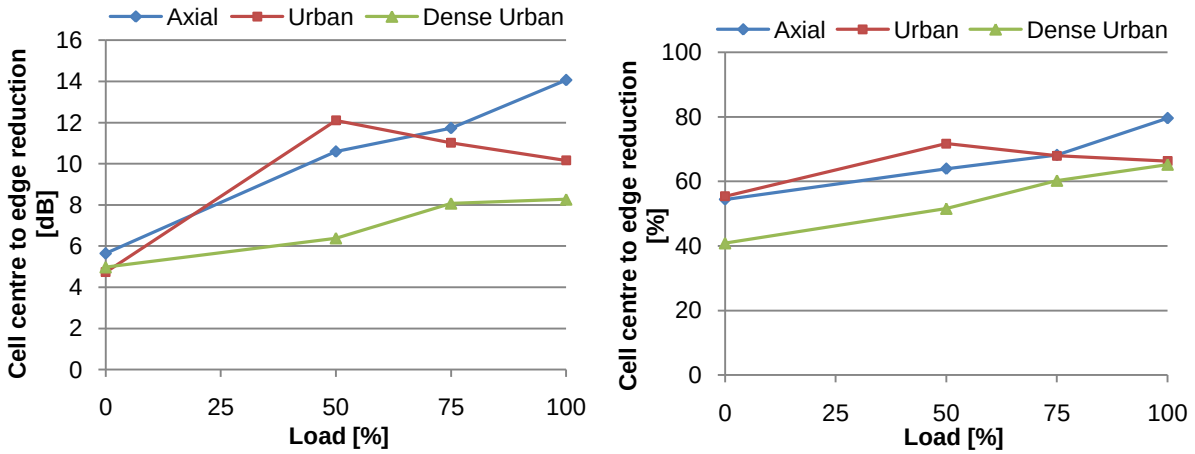

(a) SINR. (b) Throughput.

Figure 4.15. Performance differences between cell centre and cell edge as a function of cell load, for varying environment.

Apart from the Urban environment, the gap between cell edge and cell centre performances increases with system load, as interference in cell edge leads average SINR and average throughput to decrease while cell centre sees a smaller influence, Figure F.13 and Figure F.14. Greater losses are particularly seen in the average SINR in Figure 4.15-a), of 14 dB, 10 dB and 8 dB for the 100% load scenario for the Axial, Urban and Dense Urban environments, but also reduction of 80%, 66% and 65%, respectively, in throughput. Despite higher inter BS distance, LoS conditions for the Axial environment favour higher interference from neighbouring cells, especially in cell edge, whereas in Urban and Dense Urban environments higher building concentration provides for lower interference levels.

4.2.7 Coverage

Furthermore, a performance analysis was carried, in a drive test going from the LTE cluster centre into the surrounding area, extending the system coverage. Whilst inside the cluster inter-cell interference limited DL SINR measured, as shown in the cell edge-centre analysis, pathloss, or more generally, link loss as defined in (A.4), is now constraining average SINR and throughput, Figure 4.16.

Figure 4.16 presents measured link loss and SINR as a function of distance. Figure 4.16-b) shows average throughput as a function of distance. For both cases, a decrease can be seen when distance

to serving BS rises, while in the former a clear correlation between link loss and average SINR is seen. A correlation coefficient, defined as in [Mora10], between link loss and SINR of 0.85 is obtained, proving that there is a relationship between the two for significance levels as low as 10%, [Neag11]. Further, approximate decreases of 35 dB in link loss, 19 dB in average SINR and 84% in average throughput are seen when moving from BS proximity to a distance of 1.5 km. A consistent throughput reduction is though seen until the distance of 1 km, proven to be the transition point, and a distinct variation rate is seen from this range on.

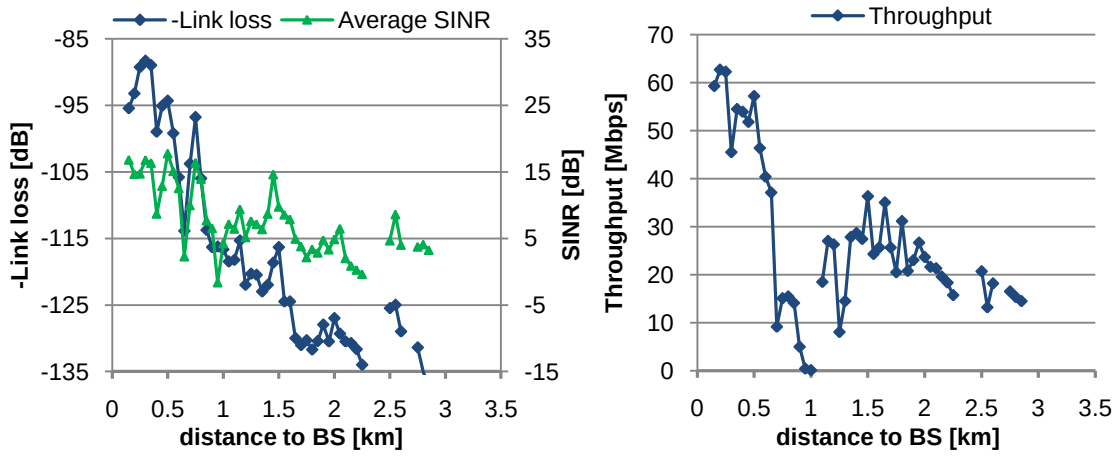

(a) Link loss and SINR. (b) Throughput.

Figure 4.16. Link loss, average SINR and average throughput as a function of distance to serving BS.

Also, measured average DL throughput can be obtained as a function of average SINR, using coverage measurement results and drive tests' results for varying environment, Figure 4.17. Similar results are seen, between results outside and inside the cluster, for varying environment, found to be inside the standard deviation margins of coverage measurements.

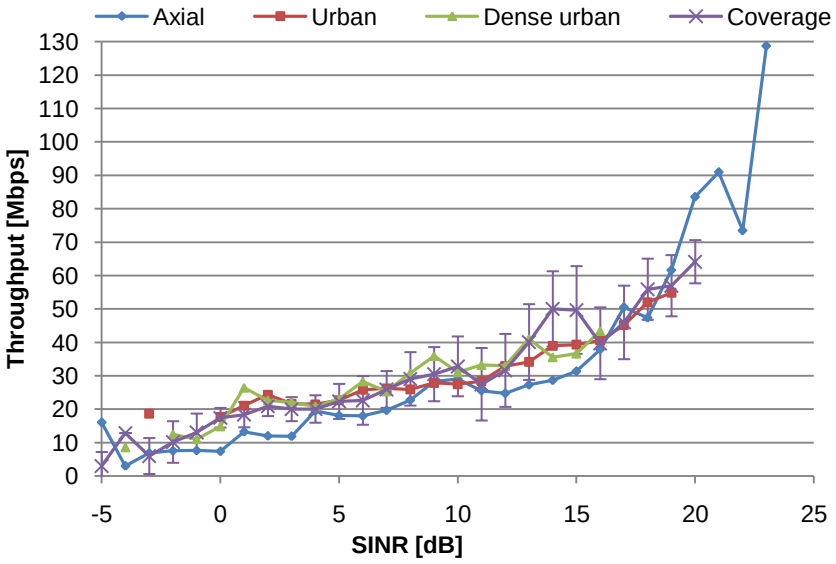

Figure 4.17. Average DL throughput as a function of average SINR.

4.3 LTE Simulation Results Comparison

Simulated and measured results are presented in Figure 4.18 for the pedestrian channel and static measurements, respectively, in terms of average SINR and throughput, for varying environment. Average and standard deviation values are shown for the theoretical, i.e. simulation, results compared with measurement's results.

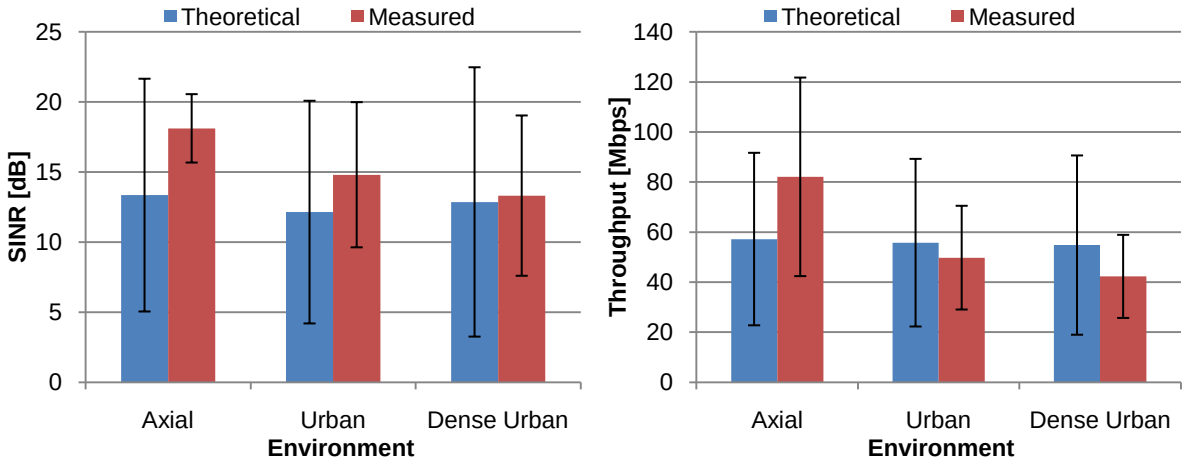

(a) SINR. (b) Throughput.

Figure 4.18. Simulated and measured results, respectively for the pedestrian channel and static measurements.

Regarding average SINR, differences of approximately 4.76 dB, 2.66 dB and 0.45 dB are seen for the Axial, Urban and Dense Urban environments, and of 40%, -12% and -30% in average throughput. Nevertheless, for SINR, after correcting the distribution mean by this value, rather consistent distributions can be seen as shown in Figure F.15 and Figure F.16, Annex F, where simulated and measured PDFs for SINR are shown.

The higher differences seen for the Axial environment can be mainly justified by the distance to BS distribution considered in the simulations (as no data over the distance to BS was collected for this measurement scenario). Therefore, the distance distribution considered was the same used for the vehicular analysis, which can correspond to wider distances to the serving BS. Moreover, for all environments, maximum user throughput in simulations is directly constrained by the expressions in Annex B (maximum throughput value is of 114.52 Mbps, Figure B.6, lower than measured values, as seen in standard deviation for the Axial environment).

Regarding the vehicular channel, results for the Urban environment are presented in Figure 4.19 for varying neighbouring cells' load. Results for Axial and Dense Urban environments are presented in Figure F.17 and Figure F.18. For the 0% load scenario, differences bellow 0.9 dB, 1.4 dB and -1.0 dB in average SINR and bellow 18%, -1.6% and 1.6% in average throughput are shown for Axial, Urban and Dense Urban environments. Considering higher load scenarios, differences in SINR no higher than 1.8 dB, 3.7 dB and 5.1 dB and no higher than 30%, 16% and 23% in average throughput are seen in Axial, Urban and Dense Urban results, respectively.

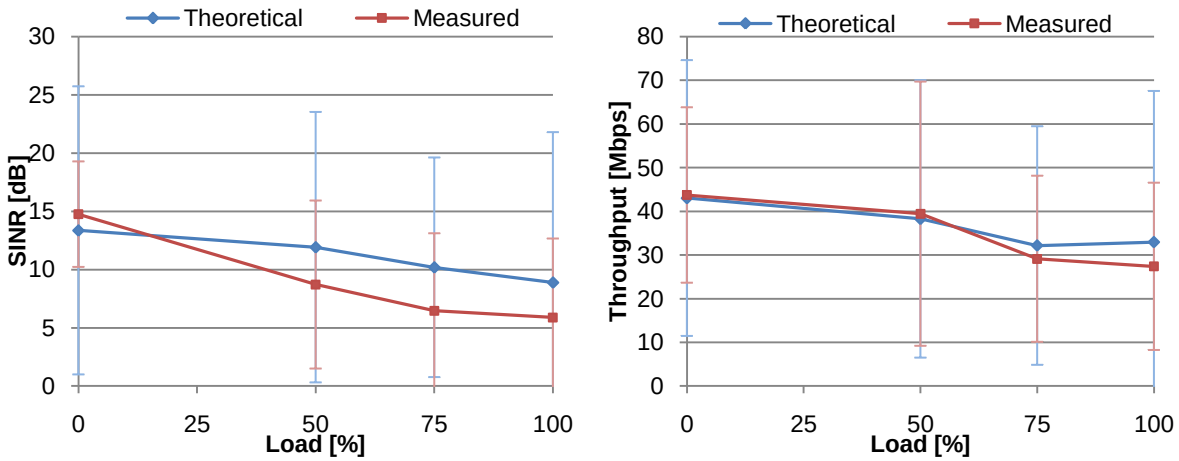

(a) SINR. (b) Throughput.

Figure 4.19. Simulated and measured results for the Urban vehicular scenario in DL, for varying load.

Correlation coefficients between measured and simulated results, defined as in [Mora10], are presented in Table 4.10, regarding average SINR and throughput. According to [Neag11], correlation is seen for the Urban environment and for throughput in the Dense Urban environment, for a significance level of 10%, as correlation coefficients above 0.9 are seen. For the remaining results, the null hypothesis cannot be rejected, most strikingly for the Axial environment, and thus a statistically significant relationship is not proved to exist.

Table 4.10. Correlation coefficients between measured and simulated results, for varying environment.

Parameter \ Environment	Axial	Urban	Dense Urban
$corr_{SINR}$	0.89	0.94	0.88
$corr_{Throughput}$	0.72	0.97	0.98

Furthermore, the variation of average SINR and average throughput values across the cell can be cross-analysed for theoretical and measured data. Cell centre to edge reduction in average SINR and average throughput are presented in Figure 4.20 for the Urban environment, while similar results are presented in Figure F.19 and Figure F.20 for the remaining environments. Absolute results for cell edge and cell centre obtained through simulation are also presented in Figure F.21 to Figure F.23.

Despite visible differences in the absolute SINR losses, revealing a wider variation from cell edge to centre in simulation results, similar trends are nevertheless evident with varying neighbouring cell load, Table 4.11. Differences between theoretical and measured SINR losses are likely to be associated to the higher varying nature of the channel for the mobility scenario, i.e., considered fading margins' standard deviations may differ significantly from the real channel's variation. Thus, one can conclude that, for the significance level of 10%, theoretical and measured results can be considered correlated for the Axial environment, regarding throughput, whereas for the remaining no correlation is seen, most strikingly for the Urban scenario.

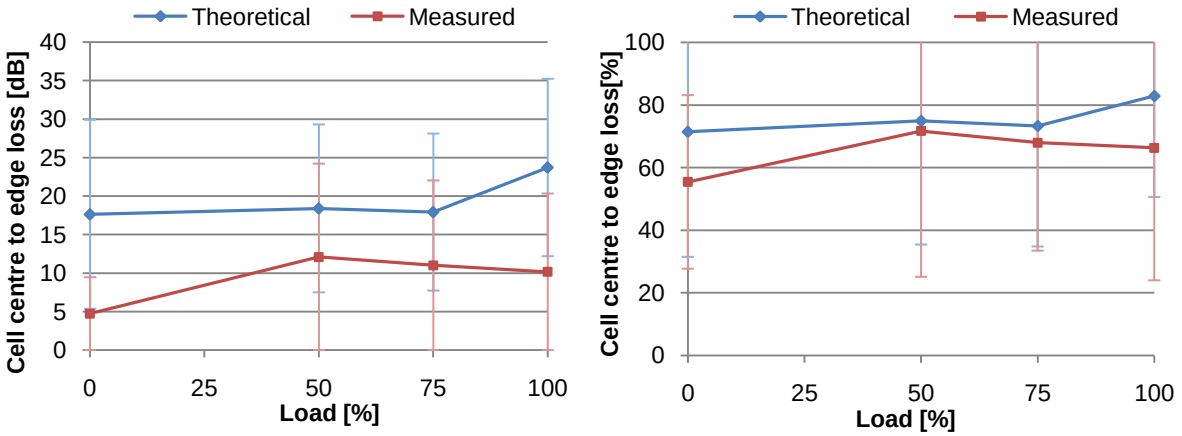

(a) SINR. (b) Throughput.

Figure 4.20. Simulated and measured performance differences between cell centre and cell edge in the Urban vehicular scenario, for varying load.

Table 4.11. Correlation coefficients between measured and simulated results of cell centre to cell edge reduction, for varying environment in mobility.

Parameter \ Environment	Axial	Urban	Dense Urban
$corr_{SINR}$	0.76	0.23	0.57
$corr_{Throughput}$	0.91	0.36	0.70

4.4 UMTS vs. LTE Results Analysis

In this section, UMTS and LTE multi-user simulation results on capacity and coverage, for different service data rates, are analysed, and performance gains from UMTS to LTE obtained. First, results are analysed for the DL, in Subsection 4.4.1, followed by a similar analysis for UL in Subsection 4.4.2.

4.4.1 Downlink Performance Analysis

Regarding DL capacity, an analysis of SINR, Figure 4.21, and data rate, Figure 4.22 to Figure 4.24, was performed for the pedestrian channel of all environments.

For the DL, while inter-cell interference limits LTE's SINR, remaining constant for the same neighbouring cell transmitted power, in UMTS also intra-cell interference is responsible for SINR variation with the number of users. It is seen that UMTS provides for the highest SINR of the single-user scenario. Nevertheless, only in the Dense Urban scenario is LTE UFR's SINR lower than UMTS's for more than one user, namely for two users, although LTE ICIC still allows for the highest SINR values. The high SINR for the single user scenario in UMTS is obviously obtained due to the absence of intra-cell interference, in which case UMTS will take advantage of the processing gain to boost

average SINR values, (A.8).

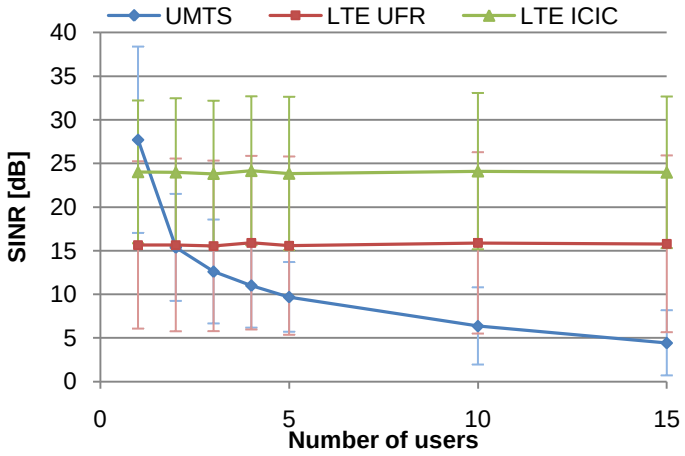

Figure 4.21. LTE and UMTS DL SINR for the Urban pedestrian scenario, for varying users' number.

Regarding environment, slight differences in SINR are seen from the Axial to the Urban environment and furthermore to the Dense Urban, Figure 4.21. While for the former differences no higher than 1 dB exist, losses of up to 3 dB are seen in a transition from the Urban to the Dense Urban environments, especially for LTE, due to higher inter-cell interference power levels caused by higher cell overlap. Although LoS in the Axial environment also helps to boost interference from neighbouring cells, high ISDs still help to reduce received interference power.

Hence, while UMTS is mainly limited by intra-cell interference in multi-user scenarios, LTE suffers a substantially higher impact of growing inter-cell interference, especially in Dense Urban environments. Furthermore, the effect of the processing gain in UMTS provides for greater SINR values in the case of two cell users and similar SINR values for the three users' case, thus improving SINR in scenarios of limited number of users. Nevertheless, LTE provides for better data rate results over all environments, Figure 4.22 to Figure 4.24.

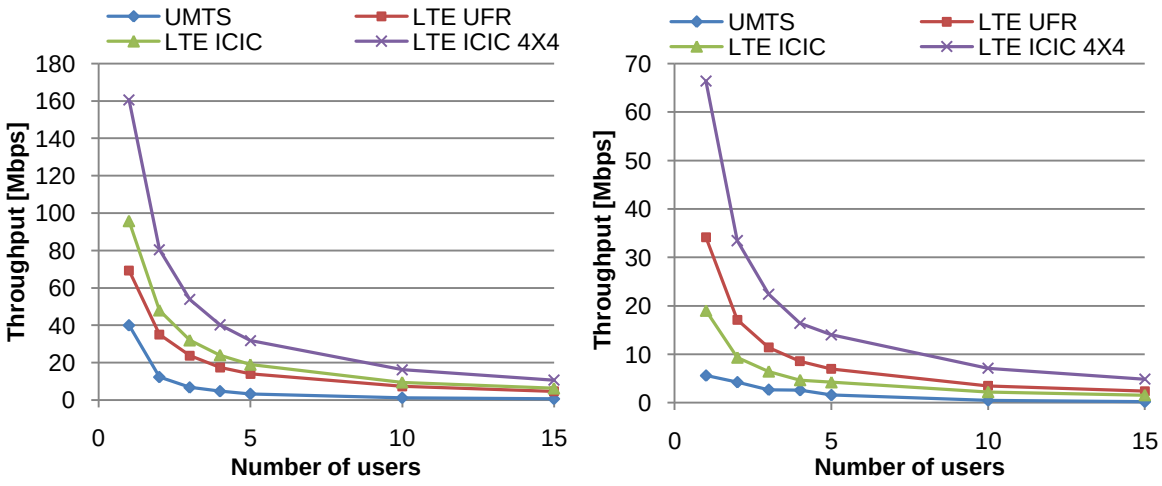

(a) Average. (b) Standard deviation.

Figure 4.22. LTE and UMTS DL throughput for the Axial pedestrian scenario, for varying users' number.

For UMTS, the average data rate of 40 Mbps obtained for single-user scenario in UMTS is extremely close to the maximum throughput of 42 Mbps. While for LTE UFR, LTE ICIC and LTE ICIC 4×4 average throughput values of 69 Mbps, 96 Mbps and 160 Mbps are obtained in the Axial environment, maximum theoretical values would be of approximately 150 Mbps and 300 Mbps for MIMO 2×2 and 4×4, respectively. An increase by a factor of 1.39 and 2.31 is obtained through the user of ICIC and when using ICIC combined with higher order MIMO, respectively.

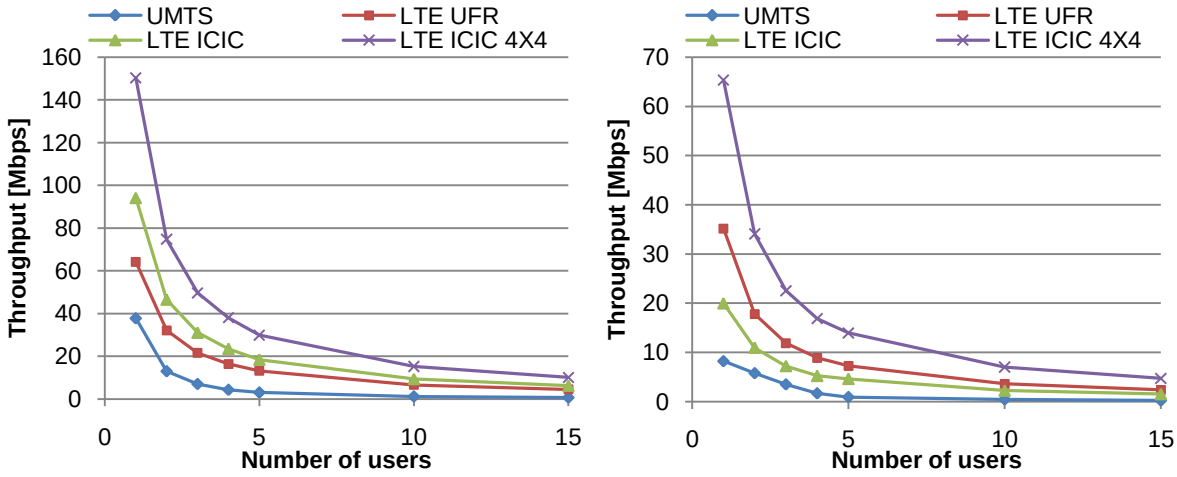

(a) Average. (b) Standard deviation.

Figure 4.23. LTE and UMTS DL throughput for the Urban pedestrian scenario, for varying users' number.

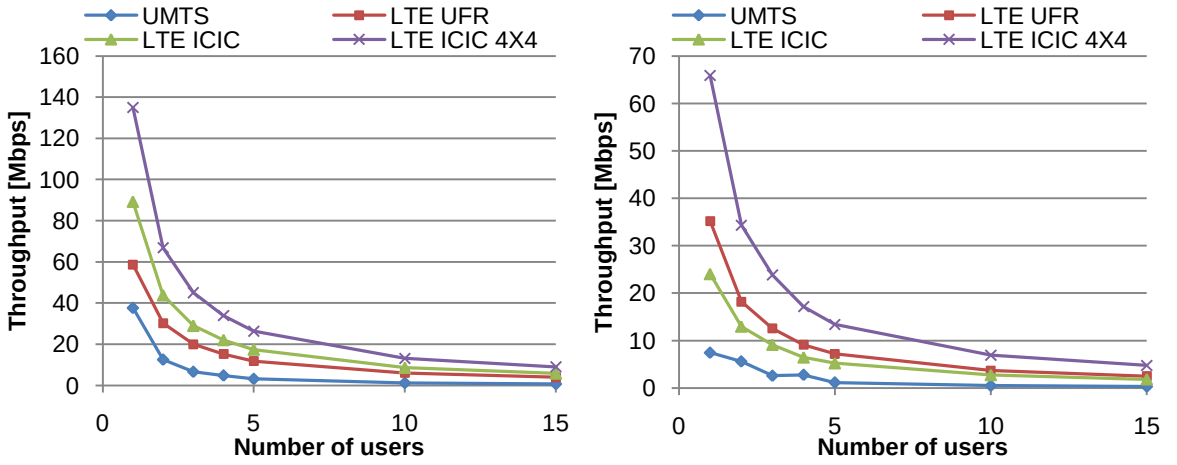

(a) Average. (b) Standard deviation.

Figure 4.24. LTE and UMTS DL throughput for the Dense Urban pedestrian scenario, for varying users' number.

Although these maximum values might be reached in some cases, as seen by taking into account standard deviation values obtained, Figure 4.22-b), limitations in throughput exist provided by the SINR to throughput mapping models considered, Annex B, or even by system specific constraints, taken from measurements and used in simulation, such as the MIMO SINR threshold. While the former has a major impact in both average and standard deviation values obtained, by restricting maximum data rate values to 114 Mbps and 258 Mbps, the latter may also diminish throughput gains

by restricting MIMO usage to good SINR conditions in the considered scenarios.

Nevertheless, considering the results obtained, slight differences are seen from the Axial to the Urban environment, in accordance with the SINR results obtained, with reduction levels lower than 10% in all cases. Differently, in a transition from the Urban to the Dense Urban environment, slightly higher reductions are obtained, though always lower than 14% in all cases, reflecting the same correspondence with SINR losses previously referred.

LTE over UMTS throughput ratios of 1.70, 2.49 and 3.98 are obtained for LTE UFR, LTE ICIC and LTE ICIC 4×4 in the single-user Urban environment, Figure 4.25. In the multi-user scenario, whereas for two users ratios rise to 2.47, 3.58 and 5.75, for three users ratios of up to 3.07, 4.42 and 7.07 are seen for LTE UFR, LTE ICIC and LTE ICIC 4×4, respectively. Although absolute throughput drops in both systems with the number of users, the lack of intra-cell interference and BS power split in LTE provides for a smoother decrease comparing to UMTS. This rising trend in the throughput gains is maintained even for higher number of users.

Similar results are also obtained for the Axial and Dense Urban environments, Figure F.25, with differences of 0.44, 0.31 and 0.90 in throughput ratios from Urban to Axial, and of -0.14, -0.12 and -0.40 in Urban to Dense Urban environments, respectively using LTE UFR, LTE ICIC and LTE ICIC 4×4. For the multi-user case, LTE UFR throughput gains are also increased in Axial, to 2.85 and 3.51 for two and three cell users, and in Dense Urban environments, to 3.90 and 4.73.

These results are explained by the slightly lower SINR values obtained in the Urban and Dense Urban environments that may not be enough to overcome the SINR MIMO threshold imposed. While in UMTS average SINR values are below the threshold for all multi-user scenarios, in LTE average values are above the considered threshold for the Axial environment but not for the Urban and Dense Urban cases. Therefore, while in general UMTS data rates are obtained without the use of MIMO, in LTE data rates would be leveraged in the Axial environment by using MIMO, less frequently employed in the Urban and Dense Urban scenarios considered.

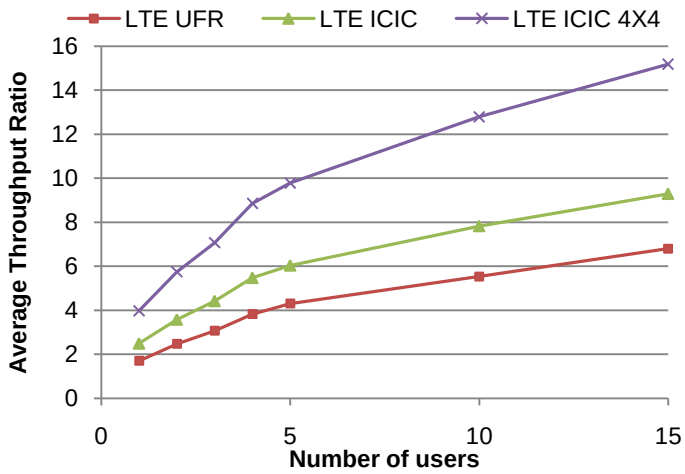

Figure 4.25. UMTS to LTE throughput ratio for the Urban pedestrian scenario, for varying users' number.

For all environments, ratio values grow rapidly with users' number, for all LTE variants considered, proving to follow a logarithmic law, as shown in Figure 4.25, for the Urban environment. Whereas similar higher SINR values were obtained for the Axial and Urban environments, and in data rate a similar reduction was seen in the transitions Axial-Urban and Urban-Dense Urban, the highest throughput ratios are obtained for the Axial environment, due to the best propagation conditions that boost MIMO usage rates. Similar but lower ratios are seen for both the Urban and Dense Urban environments.

Regarding cell coverage, obtained results are presented for the Urban environment in Figure 4.26-a), Figure 4.26-b) and Figure 4.27, respectively, for users performing the typical Web, Video streaming and FTP services defined. Results for LTE 4×4 ICIC are not presented as these were equal to LTE ICIC, and thus 4×4 MIMO does not help to boost coverage in the scenario considered. A comparison with results for the Axial and Dense Urban environments is shown in Figure F.26 and Figure F.27, for LTE UFR.

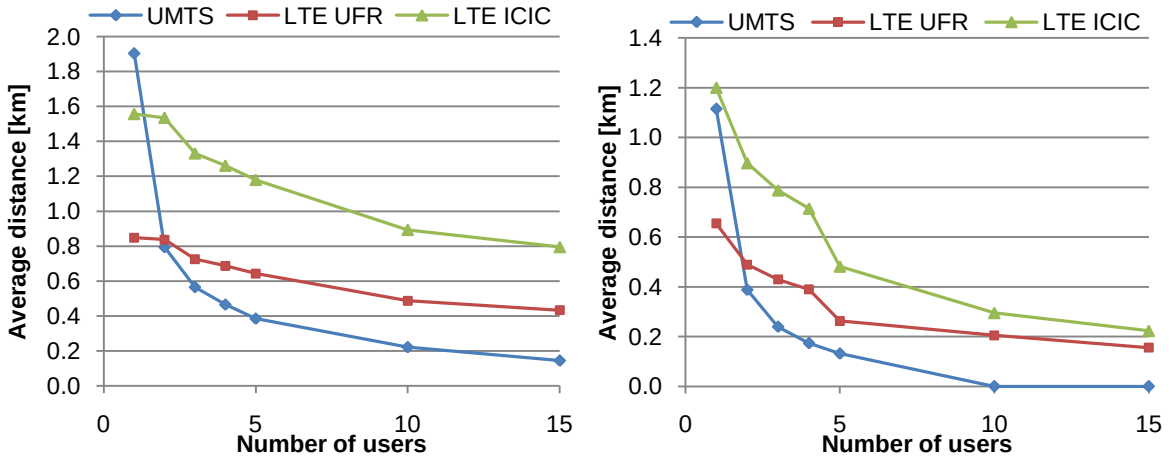

(a) 1Mbps. (b) 5Mbps.

Figure 4.26. LTE and UMTS coverage results for the Urban pedestrian scenario, for required 1Mbps and 5Mbps throughput service.

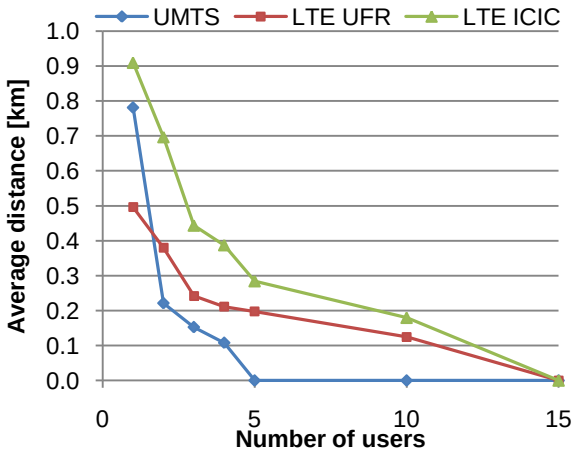

Figure 4.27. LTE and UMTS coverage results for the Urban pedestrian scenario, for required 10Mbps throughput service.

It is seen that higher cell ranges are obtained for the single user scenario in UMTS compared to LTE UFR and even higher than in LTE ICIC for the Web service. However for the multi-user case, maximum users' distance to BS in UMTS is always below the maximum values for LTE UFR and LTE ICIC for all services. Also, a steeper decline in range is seen in UMTS than in LTE with the number of cell users, which is again explained by the rise of UMTS's intra-cell interference and moreover by BS power split between users.

Conversely, LTE benefits from user orthogonality inside the cell, while having a wider bandwidth to serve more users. The decrease in LTE's coverage with the number of users comes then by the limited number of RBs available. For more users, less RBs can be allocated to each user and thus higher SINR values are needed to serve the user. For 5 users, coverage ratios of 1.67 and 2.00, i.e., gains of 67% and 100%, are obtained with LTE UFR regarding UMTS, for the 1 Mbps, 5 Mbps service data rates, and of 3.06 and 3.67 using LTE ICIC, while for a 10 Mbps service LTE is the only option.

Considerable differences are measured for varying environment on maximum distance to BS for different environments. Reference to the Urban environment, an increase in LTE UFR coverage of 84% is seen to the Axial and a reduction of 32% to the Dense Urban environments in the case of 5 users at 1 Mbps, of 24% and 36% at 5 Mbps and of 10% and 36% at 10 Mbps. The higher differences are mainly explained by high pathloss in the Urban and Dense Urban environments, and between these, mainly by the ISD difference that allows for higher interference power in the Dense Urban environment. Nevertheless, regardless of the environment, higher cell ranges are generally obtained by LTE comparing to UMTS, for any number of users over all environments.

Apart from the previous analysis, it is of great interest to take a measure on the variation of SINR and throughput depending on user's position in the cell. Due to fast power control in UMTS, the distribution of BS power, in DL, and each UE's power, in UL, depends on the UE's distance to the serving BS. In an optimal power control scheme, no difference exists between cell edge users and cell centre users.

Furthermore, whereas for a cell centre user intra-cell interference tends to be higher, near cell edge inter-cell interference rises, and thus the difference between the two tends to vanish, Figure F.28, obtained by considering the same cell centre to edge threshold as for LTE. However, in LTE, as no power control is employed for DL, system performance is heavily impacted by users' position in the cell and thus cell edge user's performance differs drastically when compared to a cell centre user.

Figure 4.28 shows cell centre to edge reduction, in SINR and throughput, for the environments under study using LTE UFR. As BS's power is not split between users and neighbouring BS's power is considered to the same no matter the number of users in the cell, cell centre to edge SINR losses will be independent of the number of users in our case.

Hence, for any number of users, a drop in SINR of 13.96 dB, 14.9 dB and 16.0 dB is measured from cell edge to cell centre for the Axial, Urban and Dense Urban environments, giving rise to throughput reduction of 57.4%, 56.5% and 54.6%, respectively. The usage of ICIC schemes allows for SINR gains of 6dB in cell edge and 10 dB in cell centre, improving throughput edge-to-centre gap to 18.1%, 18.4% and 22.8%, Figure F.29. The high losses in SINR, compared to measurements' results in

Subsection 4.2 for instance, are mainly due to the user's distance to BS distribution, but are also strongly dependent on fading margins distribution, particularly on the standard deviation values considered. Throughput levels obtained are then strongly correlated with SINR values.

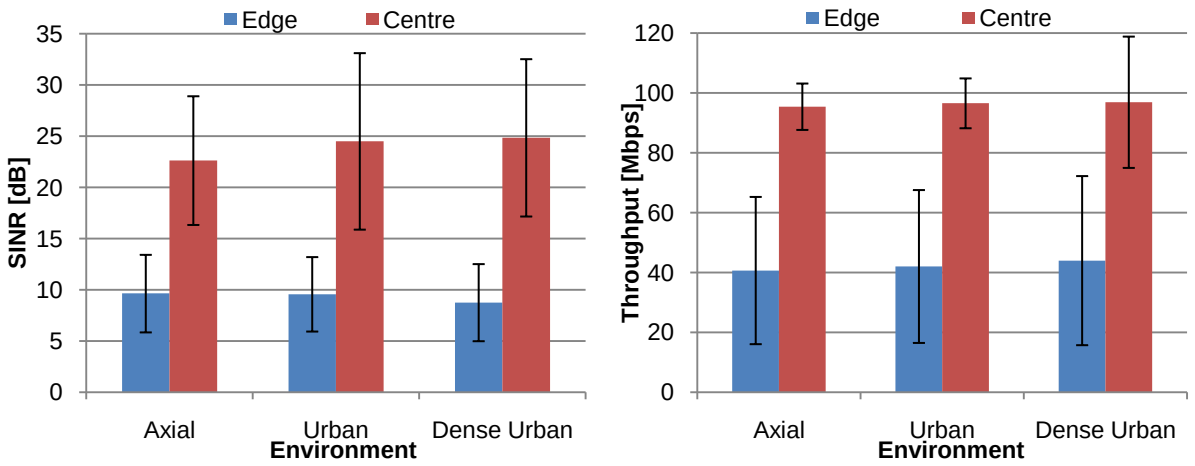

(a) SINR. (b) Throughput.

Figure 4.28. Performance differences between cell centre to cell edge for the pedestrian channel with LTE UFR.

Despite the strong dependence of the results on fading margins' distributions, the Dense Urban environment is where measured SINR differences are the highest, mainly explained by high cell overlapping and thus lower SINR values in cell edge, and the highest SINR values in cell centre. The Urban environment follows, with a slight reduction in SINR difference, due to less interference in cell edge and higher interference in cell centre and finally the Axial environment, where the lowest difference is seen.

Although differences of approximately 1 dB from the Axial to the Urban environments and from the Urban to the Dense Urban environments exist, corresponding differences of only 1% and 2% are seen in cell centre to edge throughput. Thus it is concluded that, despite the simplicity of the analysis, no significant changes are seen in cell centre to edge differences for varying environment and an average throughput decrease of 56% is considered for any environment.

Figure F.30 shows even that cell centre to edge transition happens at the approximate distance of 220 m, 180 m and 120 m for the Axial, Urban and Dense Urban environments, respectively. While for the Axial environments high ISDs help to enlarge the cell centre area, LoS propagation conditions also provide for shorter transition distance, shorter than half the ISD value. Regarding the Urban and Dense Urban environments, shorter ISDs are responsible for smaller cell centre and cell edge areas, with cell edge distances shorter than half the ISD.

4.4.2 Uplink Performance Analysis

For UL, a similar analysis was performed for a full study of the limits and gains of UMTS to LTE in both directions. A capacity analysis regarding SINR, Figure 4.29, and throughput, Figure 4.30 and Figure 4.31, is performed as a function of the users' number, for the pedestrian channel.

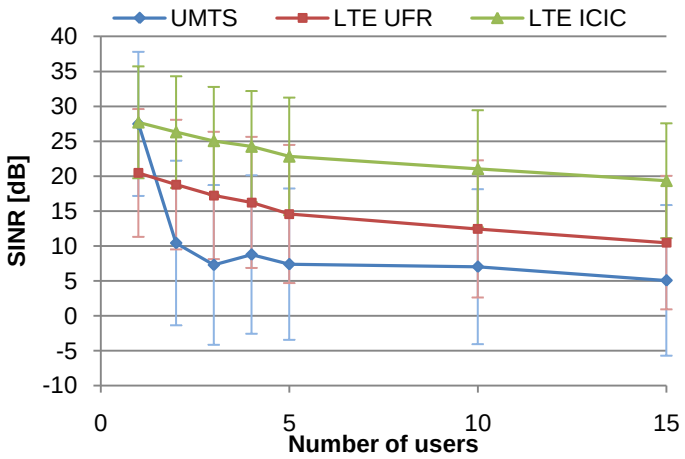

Figure 4.29. LTE and UMTS UL SINR for the Urban pedestrian scenario, for varying users' number.

Similarly to the DL, inter-cell interference limits LTE's SINR, although for the UL transmitted interference power is not constant, but varies with the number of users in the neighbouring cell and their position. For UMTS, however, the strongest limitation is intra-cell interference.

Regarding environment, differences in SINR of less than 0.7 dB exist in UMTS from the Axial to the Urban scenario, Figure F.31, except for the single user case, and differences no higher than 5 dB exist for LTE UFR and 4 dB for LTE ICIC in all cases. In the transition from Urban to Dense Urban environments, similar results to the Axial-Urban transition are seen for UMTS, whereas for LTE differences bellow 8 dB in UFR and below 7 dB with ICIC are measured. The variations, higher in absolute value for LTE than in DL, are mainly explained by the dominance of intra-cell as limit in UMTS's UL, no matter the environment, and the impact of ISDs and environment propagation, i.e., pathloss of each environment, in LTE UL.

In fact, as our multi-user analysis considers all users in the cell at the same average distance to the serving BS, it is natural that, whatever the environment pathloss, both the user's signal as the own-cell users' signals will suffer the same pathloss and thus UMTS's UL SINR will remain approximately constant for any environment. The exception is obviously the single user case, where only inter-cell interference exists, and where considerably different SINR values are obtained for varying environment. Similarly to UMTS's single user's scenario, LTE's UL interference is created by other-cell users and thus interference varies with their distance to the BS in our cell.

Thus, while in UMTS approximately constant SINR values are obtained across environments, in LTE, by the increase of inter-cell interference from the Axial to the Urban and further to the Dense Urban environment, LTE UFR suffers SINR losses as high as 8 dB, in this last transition. The use of ICIC schemes helps to reduce inter-cell interference, especially in UL. As example, interference rise in LTE leads in the Dense Urban environment to obtain higher SINR in UMTS than in LTE UFR for more than 5 cell users. Average gains of up to 9 dB by using ICIC allow for SINR improvement in this case.

Nevertheless, regarding throughput results in Figure 4.30 and Figure 4.31, it is seen than for all environments LTE provides for higher data rates. Maximum theoretical data rates of 11.5 Mbps for UMTS and 75 Mbps for LTE, Subsection 2.3, are approximately reached for all environments in UMTS

and for the Axial and Urban environments in LTE. As a consequence lower standard deviation values are obtained, not exceeding 1 Mbps in UMTS and not higher than 7 Mbps in most cases for LTE. In accordance with the SINR results seen, measurable decreases no higher than 3% for UMTS, up to 20% in LTE UFR and bellow 10% in LTE ICIC occur from the Axial to the Urban environment and no higher than 6% for UMTS, up to 40% LTE UFR and below 27% in LTE ICIC exist from the Urban to the Dense Urban environment.

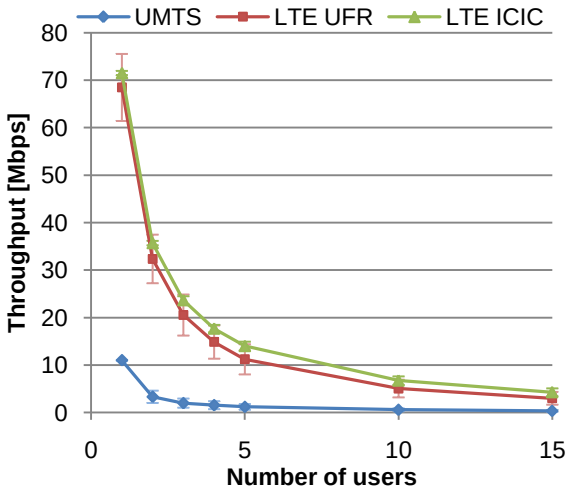

Figure 4.30. LTE and UMTS UL throughput for the Axial pedestrian scenario, for varying users' number.

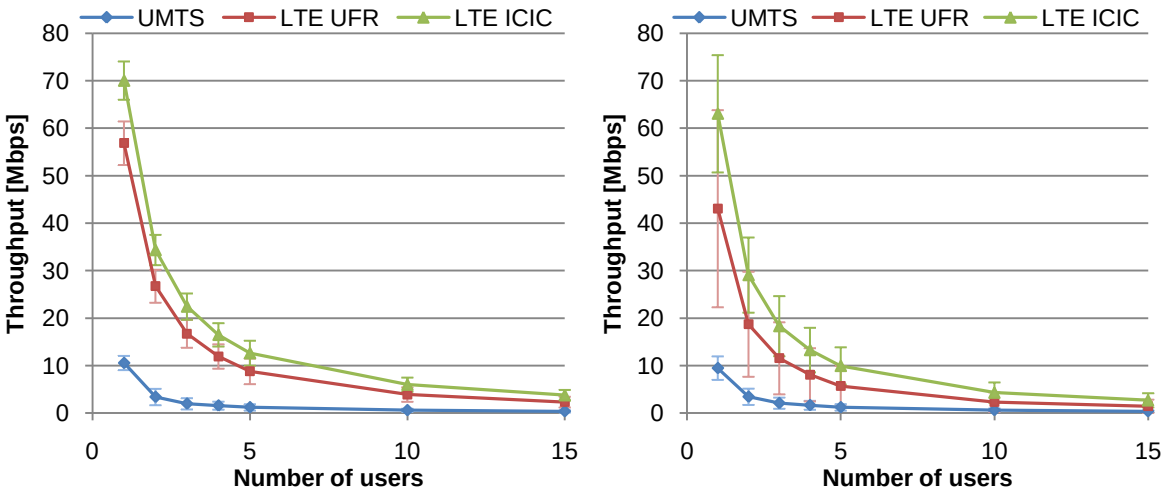

(a) Urban. (b) Dense Urban.

Figure 4.31. LTE and UMTS UL throughput for the Urban and Dense Urban pedestrian scenarios, for varying users' number.

Furthermore, for the Urban environment, Figure 4.32, a throughput ratio of 5.38 is obtained for a single user in LTE UFR, and up to 6.63 employing ICIC. For the case of more own cell and neighbouring cell users absolute values decrease steeply, especially for a number of users lower than five. In contrast, UMTS to LTE UFR throughput ratios rise, to 7.88 and 8.50 in the case of two and three users, and to 10.13 and 11.41 when ICIC is employed. For higher users' number, however, throughput differences see a lower increase, almost reaching a constant value. This is due to the marginal low values

provided by UMTS in high cell load, together with a less rapid decrease of throughput in LTE due to smoother transition in RBs split for growing number of users.

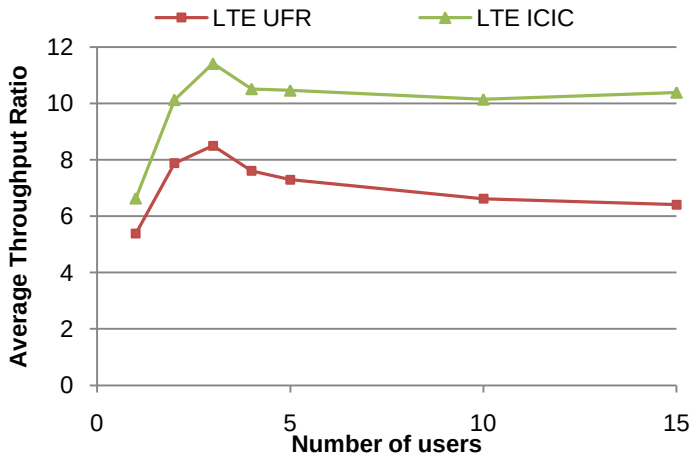

Figure 4.32. UMTS to LTE throughput ratio for the Urban pedestrian scenario, for varying users' number.

Differences of 0.85 and -0.13, to the Axial, and of -1.69 and 0.15, to the Dense Urban environments exist for LTE UFR and LTE ICIC, Figure F.32, in the single-user case. Although for the Axial environment differences between ratios of up to 3 exist for both UFR and ICIC, obtained for 15 users, in the Urban and Dense Urban environments the use of ICIC provides for great improvement in SINR and thus throughput values and ratios obtained, allowing for differences of throughput ratios of at least 3 in all multi-user scenarios.

For cell coverage analysis, results are presented in Figure 4.33-a), Figure 4.33-b) and Figure 4.34 for the Urban environment, respectively for the three typical service throughputs defined. Similar results are presented in Figure F.33 and Figure F.34, where LTE UFR results for Axial and Dense Urban environments are plotted for comparison against the Urban environment.

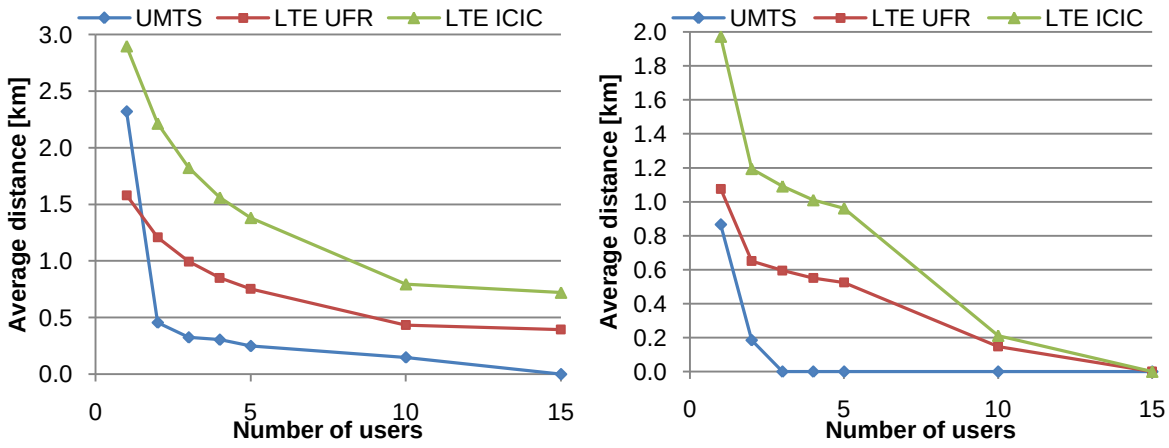

(a) 1Mbps.

(b) 5Mbps.

Figure 4.33. LTE and UMTS coverage results for the Urban pedestrian scenario, for required 1Mbps and 5Mbps throughput service.

Independently of the considered service throughput, in general LTE provides for higher cell ranges

than UMTS, the exception being the single user case for the required 1 Mbps Web service throughput. Benefitting from the lack of intra-cell interference for the smallest required throughput of our analysis, only for this case performs UMTS better. However, a steep decline in coverage is seen from the single user to the multi-user scenario, where intra-cell interference appears, cell ranges dropping to ranges below 0.5 km for 1 Mbps, 0.2 km for 5 Mbps and for the case of 10 Mbps UMTS can no longer serve users.

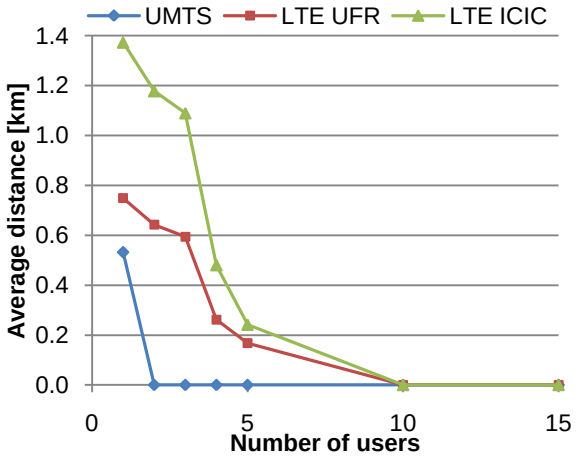

Figure 4.34. LTE and UMTS coverage results for the Urban pedestrian scenario, for required 10Mbps throughput service.

While for UMTS the coverage limit is strongly related with the intra-cell interference felt, in LTE inter-cell interference but mainly the number of RBs available, needed to serve users with the throughput requested, are the limit in coverage. As in DL, a steep drop in average range is seen until 5 users in the cell, approximately for all service throughputs, and a smoother drop exists beyond that, reflecting the referred effect of the division of the total available RBs by 2, 3, 4, 5 or more users.

Compared to the Urban environment, cell range gains of 77%, 43% and 46% exist to the Axial environment in a LTE UFR scenario of 5 users for 1 Mbps, 5 Mbps and 10 Mbps, respectively, and losses of 50%, 52% and 51% are obtained for the Dense Urban environment. The former higher gains are mainly explained by the high ISD that, despite LoS propagation, help to reduce inter-cell interference. Conversely, for the Dense Urban environment, smaller distances exist between other-cell users and the BS in our cell, thus providing for interference rise and great cell range reduction.

Similarly to DL, an analysis of system's performance across the cell is done for UL. As for UMTS, power control in UL also provides for a fair distribution of power across the cell, Figure F.35. Although power control exists for LTE, its aim is only to save MT's power when possible. Thus, in the case of maximum coverage analysis, differences in SINR and throughput are likely to exist. Differently from DL, however, UL inter-cell interference varies with the number of active users in neighbouring cell and thus an analysis for different number of users is required.

SINR and throughput performance, for cell centre and cell edge, is presented in Figure 4.35 for LTE UFR in the Urban environment. Similar analyses are presented for the Axial and Dense Urban environments in Figure F.36 and Figure F.37. SINR differences of around 14 dB are seen, growing for

higher users' numbers, whereas for throughput, a reduction of 31%, for the single user case, up to 60% and 64% in the case of 10 and 15 users are obtained. The growth in losses is largely due to the growth in inter-cell interference, though slight for the Urban environment. ICIC in UL can however provide for increase of SINR for centre and edge users, resulting in an almost similar data rate performance, throughout the whole cell. Regarding the Axial and Dense Urban environments, lower and higher SINR differences are seen, respectively, with up to 3 dB difference to the Urban environment.

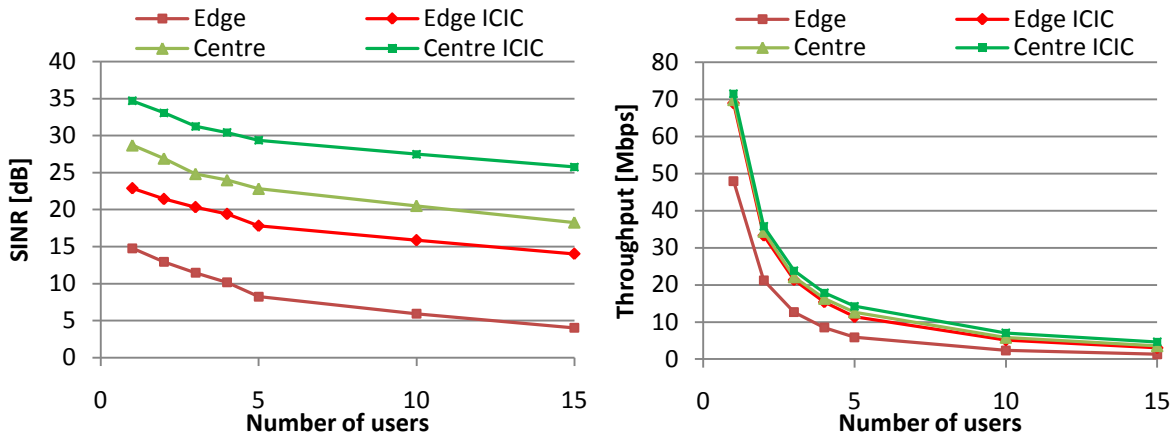

(a) SINR. (b) Throughput.

Figure 4.35. Performance difference between cell centre to cell edge in the LTE UFR Urban pedestrian scenario, for varying number of users in the cell.

Furthermore Figure F.38 shows the cell centre to edge transition for the single-user case. For the Urban and Dense Urban environments, transition occurs at 250 m and 140 m, approximately, closer to half the ISD value than for DL, whereas for the Axial environment cell centre region is extended beyond 500 m.

Chapter 5

Conclusions

This chapter concludes the present dissertation, compiling a discussion and a critical analysis of the results, presenting the future evolution possibilities of mobile communications, as well as mid-term future research areas.

The main objective of this thesis is to evaluate UMTS/HSPA+ and LTE cellular performance, in terms of data rate gains, especially regarding capacity and coverage aspects, in different scenarios regarding channel, environment and the number of users. To accomplish this goal, information was gathered on both UMTS/HSPA+ and LTE. Higher bandwidth, better spectrum efficiency and more advanced MIMO schemes allow for higher data rates in LTE than with UMTS, although smoother performance variation across the cell exists for UMTS.

Based on literature results for both UMTS and LTE, a model was developed and implemented: the Single Cell model, considering both single- and multi-user scenarios. Two separate components were considered in the simulator for UMTS and LTE, based on a link budget analysis and literature results for computing throughput from SINR. COST231-Walfisch-Ikegami propagation model was used to calculate propagation losses and a channel model was built for computing Rice and Lognormal fading margins, based on literature studies.

Afterwards, the multi-user approach was considered evolving from the single user one. This extension to more than one user provides for a more realistic analysis, where different cell load scenarios can be considered. An important difference from the single to the multi-user scenario is resource sharing, namely available codes in UMTS and RBs in LTE, and further DL transmission power in UMTS. Additionally, interference in both systems directly increases with cell load.

Study scenarios were defined, in cooperation with the telecommunications operator Optimus. Axial, Urban and Dense Urban environments under the pedestrian and vehicular scenarios where characterised. Further, neighbouring cells load levels were defined for DL, namely by defining BS transmission power levels. Finally, for the coverage analysis, typical service data rates were defined, for relevant services described.

A LTE measurements' campaign was then conducted in a Portuguese city, where a cluster has been deployed. DL performance data was collected for the single user case, across the scenarios defined. Common QPSK, 16QAM and 64QAM modulations were available and up to MIMO 2×2 was possible. Varying load scenarios were measured. However no ICIC schemes were deployed. The maximum bandwidth of 20MHz was taken.

Measurements results are analysed regarding varying environment, channel, modulation schemes and antenna configuration, user positioning in the cell, cell load scenarios and coverage scenarios. Average throughput values of 82 Mbps, 50 Mbps and 42 Mbps are obtained for static Axial, Urban and Dense Urban environments, respectively, and of 47 Mbps, 44 Mbps and 39 Mbps for mobility scenario. For the Axial environment, throughputs are boosted mainly due to MIMO transmission, with average transmission percentages of 46%, compared to 7% in Urban and 9% in Dense Urban environments. Static and mobility results are in most cases similar, except for the Axial environment where measurements spots choices heavily influenced results.

Regarding modulation, 64QAM is the preferred scheme, with 74% average usage over all environments for the static scenario, followed by 16QAM with 22% and QPSK with 4%. The selection of HOM schemes is attributed to the lack of load in the system, only used by one user, allowing for low

BER levels. Regarding antenna configurations, SINR MIMO thresholds of 16 dB, 17 dB and 16.5 dB exist for Axial, Urban and Dense Urban environments, above which more than 10% of MIMO usage occurs.

Users' position in the cell is determined to heavily impact obtained data rate, with throughput reductions of 54%, 55% and 41% measured from cell centre to cell edge in Axial, Urban and Dense Urban environments, respectively. A cell centre to edge threshold of 15 dB to 16 dB in SINR was found to exist for all environments measured.

System load, in the form of inter-cell interference, also heavily reduces data rate performance. Throughput reduction of 10%, 33% and 37% was measured in the Urban environment for 50%, 75% and 100% load scenarios, regarding the one with 0% load. Similar results were obtained for the remaining environments. Higher reductions are seen in the Urban compared to the Axial and in the Dense Urban compared with the Urban environments mainly due to smaller ISDs, higher cell overlapping and thus higher interference levels.

Furthermore, a reduction in HOM and MIMO usage rates is seen, for rising load, namely due to SINR reduction. Regarding cell centre to edge transition, data rate reduction tends to increase also for higher load conditions, with higher difference associated to cell edge users compared to cell centre ones, due to increase in interference.

Based on measurements' results obtained, namely for the same modulation usage distribution and MIMO SINR threshold for each environment, simulation results were obtained. The same distribution for user distance to BS, ISD and neighbouring BS power were taken. For both pedestrian and vehicular channels, results are found to be consistent with static and mobility measurements. Similar average results are obtained for the former, covered by the measured standard deviation, and correlation is obtained for the latter, in most cases, for a confidence level of 10%. Nevertheless, higher standard deviation values are obtained in simulated results, for both the pedestrian and vehicular channels, suggesting high standard deviation values assumed for the fading margins, mainly responsible by SINR variation.

Being the simulator validated against measurements results, simulations results were obtained for UMTS and LTE, for performance comparison. For LTE the deployment of ICIC schemes for UL and DL and additionally MIMO 4×4 schemes for DL were also considered.

For DL, average 42 Mbps, 69 Mbps, 96 Mbps and 160 Mbps data rates are obtained using UMTS, LTE UFR, LTE ICIC and LTE ICIC 4×4 and 11 Mbps, 68 Mbps and 72 Mbps using UMTS, LTE UFR, LTE ICIC for UL in the Axial environment for single-user. High throughputs are mainly explained by low inter-cell interference existing in this scenario and no intra-cell interference in UMTS. Both for UL and DL data rates drop rapidly with the number of users. RBs split in LTE and intra-cell interference rise in UMTS, for UL and DL, and BS power division in UMTS's DL justify the performance drop.

Varying environment, decreases in throughput no higher than around 10% exist in DL from the Axial to Urban and from the Urban to the Axial environments, for both UMTS and LTE, and bellow 6% and 27% in UL, for UMTS and LTE, respectively. Especially for the UL, neighbouring cell users' are

responsible for steep interference rise in Urban and Dense Urban environments, due to the shortest ISDs.

DL throughput ratios of 1.73, 2.39 and 4.01 are obtained from UMTS to LTE UFR, LTE ICIC and LTE ICIC 4×4, for the single-user in the Axial environment. Similar gains are obtained for the Urban and Dense Urban environments in single user scenario. For increasing number of users, throughput gains increase rapidly and the highest gains are obtained for the Axial environment, followed by the Urban and Dense Urban environments. Moreover, average throughput ratio's growth in DL proves to follow a logarithmic law with the number of users, for all analysed environments.

The rapid growth in data rate gains is explained by the increase in intra-cell interference and BS power split in UMTS, providing for a drop in SINR and hence data rate. Conversely, for LTE, SINR remains constant for higher number of users, and only the division of available RBs constrains users' data rates. Furthermore, by deploying an ICIC scheme and further using 4×4 MIMO, throughput gains are significantly improved.

In UL, higher throughput ratios are obtained, of 6.23 and 6.5, respectively employing LTE UFR and LTE ICIC in the single user Axial scenario. For the multi-user case throughput ratios rise due to intra-cell interference rise in UMTS, lowering throughputs, and due to a smaller throughput reduction in LTE, due to RBs split between users. For the Urban environment, a decrease is seen to 5.83 and 6.63 throughput ratios for LTE UFR and LTE ICIC and 4.54 and 6.65 for the Dense Urban. For the multi-user scenario similar differences are maintained, justified by higher inter-cell interference in Urban and Dense Urban environments.

Regarding DL coverage, cell ranges of 0.64 km, 0.26 km and 0.20 km are seen with LTE UFR in 5 users' Urban scenario, respectively for required 1 Mbps and 5 Mbps 10 Mbps. For UMTS ranges of 0.39 km and 0.13 km, for 1 Mbps and 5 Mbps, are allowed in the same scenario, while for 10 Mbps users cannot be served. For UL, cell ranges of 0.25 km and 0.75 km are seen with UMTS and LTE UFR, for serving 5 users at 1 Mbps in the Urban environment, while for higher data rates only LTE is able to serve all users. Also, for the majority of single- and multi-users scenarios, over all environments, it is even seen that, for the same throughput, coverage limitations are not imposed by the UL but by the DL in both systems.

Benefiting from orthogonality inside the cell and a wider bandwidth LTE provides for higher cell ranges despite higher inter-cell interference comparing to UMTS. Additionally, no BS power split occurs in LTE DL, which reduces cell range in UMTS for the same power sensitivity.

Moreover, while in UMTS DL cell centre to edge performance tends to be similar by means of power control, for LTE UFR 56% throughput drops occur from cell centre to cell edge, for the Urban environment with small differences to the Axial and Dense Urban environments. For UL high losses are also measured, of approximately 54% and 60% for 5 and 10 cell users. Nevertheless, the centre-to-edge gap can be significantly reduced by the use of ICIC schemes, to approximately 18% in DL and to 20% and 27% in UL with 5 and 10 cell users, respectively.

Existing variations in centre-to-edge gap are more significant from the Axial to the Urban and Dense

Urban environments and further more in UL than DL namely due to smaller ISDs that boost inter-cell interference in cell edge. Moreover, while in DL cell centre to edge transition is determined to occur at the distances 180 m and 120 m respectively for Urban and Dense Urban environments, in UL the transition occurs at 250 m and 140 m. Thus a greater cell centre region is measured for UL than DL.

All in all, through the analysis of UMTS versus LTE performance it is seen that, apart from very particular scenarios, higher performance is obtained by the use of LTE especially in the multi-user case. However, considering different scenarios, e.g. different ISDs, user's distribution in the cell, BS and MT transmitted powers in cell load and building concentration, results will certainly vary.

As LTE deployment examples start to emerge, and demand for the next generation technology grows, this thesis is of great practical value. Data rate gains from UMTS to LTE are determined for both systems and performance aspects analysed, providing for an in depth study across the scenarios of interest. Furthermore, as LTE presents new challenges at the network management level, gains on SINR and throughput provided by ICIC and advanced antenna configurations are estimated and analysed.

Nevertheless, in future work, the impact of varying ICIC schemes should be analysed in more depth, providing for a more accurate estimation of the gains associated to the different resource managing schemes and algorithms, both at the cell and network level. The improvement that can be obtained will have a great impact on the overall LTE system performance, affecting capacity and coverage results. Similarly, MIMO configurations also boost performance if proper channel conditions are met, and associated gains for LTE are in need to be studied with a base on real world data, especially for advanced antenna configurations.

In a more global perspective, end-users are only concerned about having reliant broadband connection. The use of other solutions such as hybrid UMTS and LTE system with seamless overlay between the two, UMTS and Wi-Fi, or other combinations that may also make use of WiMAX are of great interest to the operators, manufacturers and any companies related to the mobile communications market. The deployment of the next generation systems, converging to a single platform based on IP, opens a diversity of options carrying different trade-offs between performance and associated costs, adequate for a variety of distinct case studies.

Annex A – Link Budget

The description in Annex D of COST231-Walfisch-Ikegami was made in the perspective of an outdoor propagation in the radio link between BS and MT. For indoor cases an extra attenuation could then added, reflecting building/obstacle penetration, obtaining thus the total attenuation, (A.1).

$$L_{p_{[\mathrm{dB}]}} = L_{p\ out_{[\mathrm{dB}]}} + L_{p\ ind_{[\mathrm{dB}]}} \tag{A.1}$$

where:

- $L_{p\ out}$: pathloss due to outdoor propagation;
- $L_{p\ ind}$: pathloss due to indoor propagation.

The link budget used in this thesis is based on the one on Release 99, as presented in [Jaci09], adapted to HSPA+ and LTE.

The pathloss can be calculated by:

$$L_{p_{[\mathrm{dB}]}} = P_{t_{[\mathrm{dBm}]}} + G_{t_{[\mathrm{dBi}]}} - P_{r_{[\mathrm{dBm}]}} + G_{r_{[\mathrm{dBi}]}} = EIRP_{[\mathrm{dBm}]} - P_{r_{[\mathrm{dBm}]}} + G_{r_{[\mathrm{dBi}]}} \tag{A.2}$$

where:

- L_p: pathloss;
- P_t: transmitting power at antenna port;
- G_t: transmitting antenna gain;
- P_r: available receiving power at antenna port;
- G_r: receiving antenna gain.

If diversity is used, G_r is given by:

$$G_{r\ div_{[\mathrm{dB}]}} = G_{r_{[\mathrm{dBi}]}} + G_{div_{[\mathrm{dB}]}} \tag{A.3}$$

where:

- G_{div}:diversity gain.

The diversity gain defined is mainly dependent on the diversity type applied and on the propagation environment. Typical values stand for 2 or 3 dB for 2 antennas and for SIMO configuration. Assuming minimally correlated signals, a measure of the maximum values is given by the antenna array, (D.5), or considering a Maximal Ratio Combining (MRC) scheme, (D.6), taken in this thesis.
Apart from pathloss, also link loss can be defined as:

$$L_{Link_{[\mathrm{dB}]}} = P_{t_{[\mathrm{dBm}]}} - P_{r_{[\mathrm{dBm}]}} = L_{p_{[\mathrm{dB}]}} - G_{t_{[\mathrm{dBi}]}} - G_{r_{[\mathrm{dBi}]}} \tag{A.4}$$

The Equivalent Isotropic Radiated Power (EIRP) can be calculated for DL by (A.5), and for UL by (A.6).

$$EIRP_{[\mathrm{dBm}]} = P_{Tx_{[\mathrm{dBm}]}} - L_{c_{[\mathrm{dB}]}} + G_{t_{[\mathrm{dBi}]}} - P_{S\&C_{[\mathrm{dBm}]}} \quad \text{(A.5)}$$

$$EIRP_{[\mathrm{dBm}]} = P_{Tx_{[\mathrm{dBm}]}} - L_{u_{[\mathrm{dB}]}} + G_{t_{[\mathrm{dBi}]}} - G_{MHA_{[\mathrm{dB}]}} - P_{S\&C_{[\mathrm{dBm}]}} \quad \text{(A.6)}$$

where:

- P_{Tx}: total BS or MT transmission power at the remote radio head output;
- L_c: cable losses between transmitter and antenna;
- L_u: user losses;
- G_{MHA}: masthead amplifier gain, being 0 dB in the MU comparison, while in SU is set to 3 dB; the use of near antenna amplifier provides cable loss compensation and consequent diminish of noise figure;
- $P_{S\&C}$: signalling and control power.

SINR can be computed using the results from EIRP and pathloss expressions, respectively for LTE and HSPA+:

$$\rho_{N_{[\mathrm{dB}]}} = EIRP_{[\mathrm{dBm}]} + G_{r_{[\mathrm{dBi}]}} - L_{p_{[\mathrm{dB}]}} - N_{[\mathrm{dBm}]} \quad \text{(A.7)}$$

$$\rho_{IN_{[\mathrm{dB}]}} = EIRP_{[\mathrm{dBm}]} + G_{r_{[\mathrm{dBi}]}} - L_{p_{[\mathrm{dB}]}} - N_{[\mathrm{dBm}]} + G_{p_{[\mathrm{dB}]}} \quad \text{(A.8)}$$

where:

- N: total noise power;
- G_p: processing gain, equal to 16 for HSPA+ DL and variable for UL.

Specifically for LTE, a SINR gain due to employing an ICIC scheme can be defined:

$$\rho_{N\ ICIC\ [\mathrm{dB}]} = \rho_{N_{[\mathrm{dB}]}} + G_{ICIC_{[\mathrm{dB}]}} \quad \text{(A.9)}$$

where:

- G_{ICIC}: ICIC gain, relative to the scenario with no ICIC, varying depending on user's position in the cell.

Total noise power, defined for the computation of SINR, is given by:

$$N_{[\mathrm{dBm}]} = N_{RF_{[\mathrm{dBm}]}} + M_{I_{[\mathrm{dB}]}} \quad \text{(A.10)}$$

where:

- N_{RF}: average noise power at the receiver is given by:

$$N_{RF\ [\mathrm{dBm}]} = -174 + 10\log\left(B_{[\mathrm{Hz}]}\right) + F_{[\mathrm{dB}]} \quad \text{(A.11)}$$

- M_I: interference margin;
- B: bandwidth of the total RB's allocated, while in UMTS equals R_c;
- F: noise figure of the receiver.

Alternatively, total interference power can be computed instead of using the interference margin as given by:

$$N_{[\mathrm{dBm}]} = (N_{RF} + P_I)_{[\mathrm{dBm}]} \quad \text{(A.12)}$$

where:

- P_I: total interference power.

The LTE receiver sensitivity can be approximately defined as:

$$P_{Rx\,min_{[\mathrm{dBm}]}} = N_{[\mathrm{dBm}]} + \rho_{N_{[\mathrm{dB}]}} \quad \text{(A.13)}$$

where:

- ρ_N: Signal to Noise Ratio (SNR);
- N: total noise power

The HSPA+ receiver sensitivity can be approximated by:

$$P_{Rx\,min_{[\mathrm{dBm}]}} = N_{[\mathrm{dBm}]} - G_{p_{[\mathrm{dB}]}} + \rho_{N_{[\mathrm{dB}]}} \quad \text{(A.14)}$$

where:

- N: total noise power.

For the sensitivity calculation, E_b/N_0 is necessarily obtained from the interpolation of E_c/N_0:

$$\frac{E_b}{N_{0\,[\mathrm{dB}]}} = \frac{E_c}{N_{0\,[\mathrm{dB}]}} + G_{p_{[\mathrm{dB}]}} \quad \text{(A.15)}$$

In HSPA+ UL, manipulating (B.10) and (B.11), E_c/N_0 for a certain user's distance is given by:

$$\frac{E_b}{N_{0\,[\mathrm{dB}]}} = P_{Rx\,min_{[\mathrm{dBm}]}} - N_{[\mathrm{dBm}]} \quad \text{(A.16)}$$

Despite the losses caused from radio propagation, some margin values must be preset to adjust link calculations, where (stands for the total fading margin defined:

$$M_{F_{[\mathrm{dB}]}} = M_{SF_{[\mathrm{dB}]}} + M_{FF_{[\mathrm{dB}]}} \quad \text{(A.17)}$$

where:

- M_{SF}: slow fading margin;
- M_{FF}: fast fading margin.

Fast and slow fading are modelled by Rice and Log-Normal distributions respectively, in order to guarantee more realistic results as well as to account for the randomness associated to the radio channel over MU scenarios.

The expressions for the PDF of the Rice and Lognormal distributions can be found in [Corr10], while the expressions (A.18) and (A.20) were also derived based on [Corr10]:

$$z_i = \sqrt{(x_i \cdot \sigma_{Rice})^2 + (y_i \cdot \sigma_{Rice} + \nu)^2} \quad \text{(A.18)}$$

where:

- x_i: sample of a Gaussian distribution with mean μ_X and standard deviation σ_X;
- y_i: Gaussian random variable with mean μ_Y and standard deviation σ_Y;
- σ_{Rice}: standard deviation of the Rice distribution,
- ν: non-centrality parameter of the Rice distribution, obtained as a function of the Rice parameter, K:

$$\nu = \frac{K}{z_i} \tag{A.19}$$

where:

K: Rice parameter, as defined in [Corr10].

$$w_i = e^{x_i \cdot \sigma_{Log} + \mu_{Log}} \tag{A.20}$$

where:

- x_i: sample of a Gaussian distribution with mean μ_X and standard deviation σ_X;
- σ_{Log}: standard deviation of the Lognormal distribution;
- μ_{Log}: mean of the Lognormal distribution.

The standard deviations taken to describe the fading phenomena are stated on Table A.1, knowing that those values depend on variables such as pathloss, environment, weather conditions, etc. The values taken for the Rice parameter, K, are shown in

Table A.2, mainly varying with the presence of LoS, in the Axial environment, or inexistence of it, in the Urban and Dense Urban environments. Channel coherence times are shown in Table A.3.

Table A.1. Distributions and standard deviations for slow and fast fading margins (extracted from [Jaci09]).

Standard Deviation	**Channel**	
	Pedestrian	**Vehicular**
$\boldsymbol{M_{FF}}$ **[dB]**	Rice Distribution	
	4	2
$\boldsymbol{M_{SF}}$ **[dB]**	Log-Normal Distribution	
	4	7

Table A.2. Rice parameter (based on [GGEM09] [Jaci09]).

Environment	**Axial**	**Urban**	**Dense Urban**
$\boldsymbol{K}$ **[dB]**	10	2.5	2.5

Table A.3. Channel coherence time values.

Coherence time	Channel	
	Pedestrian	Vehicular
τ_{FF} [ms]	35	3
τ_{SF} [ms]	10.000	10.000

The total fading margin was included in the total pathloss expression, computed using (A.17), whereas $L_{P\ máx}$ means the maximum pathloss achieved without any attenuation or losses during the radio propagation, calculated using the COST231-Walfisch-Ikegami propagation model, Annex C.

$$L_{p\ total_{[\mathrm{dB}]}} = L_{p\ máx_{[\mathrm{dB}]}} + M_{F\ [\mathrm{dB}]} \tag{A.21}$$

The total pathloss is the one considered for the computation of SINR, (A.7) and (A.8), that is then mapped on the instantaneous throughput obtained using the expressions in Annex B. Furthermore, considering the coverage analysis, the instantaneous maximum cell range is determined via (3.2) and (3.4), considering the maximum pathloss that allows for the minimum SINR that still allows for the required instantaneous throughput values, again mapped using the expressions in Annex B.

Annex B – SINR and Data Rate Models

This Annex presents the HSPA+ and LTE models, used to determine SINR and throughput for each system for several system configurations. The considered models are referred to the throughput over the physical layer of each system, not considering overhead load and Block Error Rate (BLER).

B.1 UMTS/HSPA+

For UMTS, theoretical throughput values were already presented in Figure 2.2 for a Pedestrian A channel. Nevertheless, exact expressions are presented to precise SINR, ρ_{IN}, as a function of Throughput, R_b, Figure B.1 and Figure B.2, and vice-versa, Figure B.3 and Figure B.4, for several antenna configuration and modulation schemes, in DL and UL directions. These interpolations were mainly extracted from [Jaci09] and [Bati11]. Due to the relevance of interference in CDMA systems, SINR is considered and not SNR.

The results are presented here for a Pedestrian A channel. Due to the relevance of the study of different radio channels, present in the real environment, different radio channel models should also be considered. The Vehicular A channel is, in this sense, a usual reference model, and it can be further be obtained by shifting down the Pedestrian A channel curves presented in 1 dB.

It is worth noticing that the interpolations made bear relative mean errors not greater than 5%, considered reasonable for this study. Furthermore, the following models consider 15 HS-PDSCH codes, contrary to the real 14 HS-PDSCH available for traffic, as there were found no results for the latter number of codes.

Due to lack of suitable data, expressions for QPSK modulation in DL were extrapolated from the ones for 16QAM, considering the relation between the number of bits per symbol of the two modulation schemes. Thus, for SISO configuration and QPSK, in DL, SINR is given by the obtained expression:

$$\rho_{IN_{[\mathrm{dB}]}} = \begin{cases} 40.94{R_b}^3 - 92.91{R_b}^2 + 76.12R_b - 27.1, & 0.35485 \le R_{b\,[\mathrm{Mbps}]} < 0.75 \\ 0.00765{R_b}^5 - 0.1346{R_b}^4 + 0.8984{R_b}^3 - & \\ -2.988{R_b}^2 + 7.849R_b - 9.467, & 0.75 \le R_{b\,[\mathrm{Mbps}]} < 6.6057 \\ 10.69{R_b}^2 - 140.1R_b + 470.4, & 6.6057 \le R_{b\,[\mathrm{Mbps}]} < 7.1697 \\ 82.58R_b - 576.5, & 7.1697 \le R_{b\,[\mathrm{Mbps}]} \le 7.2 \end{cases} \quad \text{(B.1)}$$

For SISO configuration and 16QAM, in DL, SINR is given by:

$$\rho_{IN_{[\mathrm{dB}]}} = \begin{cases} -0.0541{R_b}^6 + 0.9496{R_b}^5 - 6.7214{R_b}^4 + 24.6466{R_b}^3 \\ -49.805{R_b}^2 + 55.0299R_b - 31.1894, \quad 0.7 \le R_{b\,[\mathrm{Mbps}]} < 4.5 \\ -0.0319{R_b}^2 + 1.7534R_b - 6.9882, \quad 4.5 \le R_{b\,[\mathrm{Mbps}]} < 9.7 \\ 0.1529{R_b}^3 - 5.1218{R_b}^2 + 57.816R_b - 211.471, \quad 9.7 \le R_{b\,[\mathrm{Mbps}]} < 14.4 \end{cases} \tag{B.2}$$

For SISO configuration and 64QAM, in DL, one has:

$$\rho_{IN_{[\mathrm{dB}]}} = \begin{cases} -0.0541{R_b}^6 + 0.9496{R_b}^5 - 6.7214{R_b}^4 + 24.6466{R_b}^3 \\ -49.805{R_b}^2 + 55.0299R_b - 31.1894, \quad 0.7 \le R_{b\,[\mathrm{Mbps}]} < 3.7 \\ 1.3691R_b - 5.8516, \quad 3.7 \le R_{b\,[\mathrm{Mbps}]} < 8.7 \\ 0.9565R_b - 2.3371, \quad 8.7 \le R_{b\,[\mathrm{Mbps}]} < 20 \\ 0.0396{R_b}^2 + 0.0799R_b + 1.9286, \quad 20 \le R_{b\,[\mathrm{Mbps}]} < 21.5 \end{cases} \tag{B.3}$$

For SIMO 1×2 configuration and QPSK, in DL, SINR is given by:

$$\rho_{IN_{[\mathrm{dB}]}} = \begin{cases} -0.1117{R_b}^4 + 1.22{R_b}^3 - 5.102{R_b}^2 + \\ +12.39R_b - 14.96, \quad 0.5018 \le R_{b\,[\mathrm{Mbps}]} < 3.9849 \\ -1.578{R_b}^2 + 15.68R_b - 34.81, \quad 3.9849 \le R_{b\,[\mathrm{Mbps}]} < 4.6567 \\ 0.7205{R_b}^4 - 16.39{R_b}^3 + 139.4{R_b}^2 - \\ -522.9R_b + 732.6, \quad 4.6567 \le R_{b\,[\mathrm{Mbps}]} \le 7.2 \end{cases} \tag{B.4}$$

For SIMO 1×2 configuration and 16QAM, in DL, SINR is given by:

$$\rho_{IN_{[\mathrm{dB}]}} = \begin{cases} -0.0012{R_b}^6 - 0.0171{R_b}^5 + 0.0476{R_b}^4 \\ +0.4255{R_b}^3 - 3.251{R_b}^2 + 10.0299R_b - 17.1838, \quad 1.0 \le R_{b\,[\mathrm{Mbps}]} < 1.8 \\ -0.4437{R_b}^2 + 4.3888R_b - 13.5340, \quad 1.8 \le R_{b\,[\mathrm{Mbps}]} < 3.2 \\ 0.0661{R_b}^4 - 1.2758{R_b}^3 \\ +8.8721{R_b}^2 - 24.7943R_b + 19.3601, \quad 3.2 \le R_{b\,[\mathrm{Mbps}]} < 5.9 \\ -0.1323{R_b}^3 + 2.7646{R_b}^2 - 17.8122R_b + 36.0243, \quad 5.9 \le R_{b\,[\mathrm{Mbps}]} < 8.3 \\ 0.0208{R_b}^3 - 0.6278{R_b}^2 + 7.276R_b - 26.0464, \quad 8.3 \le R_{b\,[\mathrm{Mbps}]} < 13.5 \\ 3.3333{R_b}^2 - 87.6667R_b + 585, \quad 13.5 \le R_{b\,[\mathrm{Mbps}]} < 14.4 \end{cases} \tag{B.5}$$

Considering SIMO 1×2 configuration with 64QAM, in DL, SINR is given by;

$$\rho_{IN_{[\mathrm{dB}]}} = \begin{cases} -0.0012{R_b}^6 - 0.0171{R_b}^5 + 0.0476{R_b}^4 + 0.4255{R_b}^3 \\ -3.251{R_b}^2 + 10.0299R_b - 17.1838, \quad 1.0 \le R_{b\,[\mathrm{Mbps}]} < 2.2 \\ -0.1349{R_b}^2 + 2.7519R_b - 11.4313, \quad 2.2 \le R_{b\,[\mathrm{Mbps}]} < 5.9 \\ -0.0148{R_b}^4 + 0.2876{R_b}^3 \\ -1.6684{R_b}^2 + 2.8789R_b - 0.07, \quad 5.9 \le R_{b\,[\mathrm{Mbps}]} < 7.4 \\ -0.0381{R_b}^2 + 1.7802R_b - 9.1641, \quad 7.4 \le R_{b\,[\mathrm{Mbps}]} < 12.4 \\ -0.0158{R_b}^2 + 1.4815R_b - 9.0373, \quad 12.4 \le R_{b\,[\mathrm{Mbps}]} < 18.5 \\ 0.6466{R_b}^2 - 23.7609R_b + 230.2882, \quad 18.5 \le R_{b\,[\mathrm{Mbps}]} < 21.5 \end{cases} \tag{B.6}$$

For MIMO 2×2 using QPSK, in DL, one has:

$$\rho_{IN_{[\mathrm{dB}]}} = \begin{cases} 47.38{R_b}^5 - 330.9{R_b}^4 + 916.6{R_b}^3 - \\ -1258{R_b}^2 + 859.3R_b - 242.7, \quad 0.8582 \le R_{b\,[\mathrm{Mbps}]} < 1.8506 \\ -0.0055299{R_b}^4 + 0.06641{R_b}^3 - \\ -0.1676{R_b}^2 + 2.205R_b - 7.721, \quad 1.8506 \le R_{b\,[\mathrm{Mbps}]} < 7.23886 \\ 0.2216R_b + 7.896, \quad 7.23886 \le R_{b\,[\mathrm{Mbps}]} < 9.4952 \\ 0.003739{R_b}^5 - 0.1925{R_b}^4 + 3.908{R_b}^3 - \\ -38.84{R_b}^2 + 188.9R_b - 350.6, \quad 9.4952 \le R_{b\,[\mathrm{Mbps}]} \le 14.4 \end{cases} \tag{B.7}$$

For MIMO 2×2 using 16QAM, in DL, one has:

$$\rho_{IN_{[\mathrm{dB}]}} = \begin{cases} -0.0052{R_b}^6 + 0.4179{R_b}^5 - 1.7114{R_b}^4 \\ +10.2135{R_b}^3 - 33.3531{R_b}^2 + 58.6222R_b - 50.9322, \quad 1.7 \le R_{b\,[\mathrm{Mbps}]} < 3.4 \\ -0.0642{R_b}^2 + 1.9468R_b - 10.8835, \quad 3.4 \le R_{b\,[\mathrm{Mbps}]} < 5.6 \\ -0.0579{R_b}^2 + 2.1091R_b - 12.0231, \quad 5.6 \le R_{b\,[\mathrm{Mbps}]} < 7.0 \\ -0.0704{R_b}^2 + 2.3595R_b - 13.1371, \quad 7.0 \le R_{b\,[\mathrm{Mbps}]} < 12.0 \\ -0.0043{R_b}^3 + 0.1489{R_b}^2 - 0.8793R_b + 1.6067, \quad 12.0 \le R_{b\,[\mathrm{Mbps}]} < 14.2 \\ -0.0170{R_b}^2 + 1.1714R_b - 6.3410, \quad 14.2 \le R_{b\,[\mathrm{Mbps}]} < 19.3 \\ -0.0016{R_b}^3 + 0.1082{R_b}^2 - 1.6755R_b + 13.4935, \quad 19.3 \le R_{b\,[\mathrm{Mbps}]} < 25.8 \\ 0.5533{R_b}^2 - 28.4577R_b + 381.012, \quad 25.8 \le R_{b\,[\mathrm{Mbps}]} < 28.8 \end{cases} \tag{B.8}$$

For a MIMO 2×2 configuration with 64QAM, for DL, SINR is given by:

$$\rho_{IN_{[\mathrm{dB}]}} = \begin{cases} -0.0673{R_b}^6 + 1.5397{R_b}^5 - 14.3404{R_b}^4 + 69.4089{R_b}^3 \\ -184.0043{R_b}^2 + 255.3831R_b - 154.7503, \quad 1.7 \le R_{b\,[\mathrm{Mbps}]} < 3.5 \\ -0.0202{R_b}^4 + 0.5189{R_b}^3 - 4.7933{R_b}^2 \\ +20.2255R_b - 37.2841, \quad 3.5 \le R_{b\,[\mathrm{Mbps}]} < 6.4 \\ -0.0202{R_b}^4 + 0.5189{R_b}^3 - 0.0579{R_b}^2 \\ +2.1091R_b - 14.0231, \quad 6.4 \le R_{b\,[\mathrm{Mbps}]} < 7.0 \\ -0.0817{R_b}^2 + 2.3595R_b - 13.2108, \quad 7.0 \le R_{b\,[\mathrm{Mbps}]} < 7.8 \\ -0.0933{R_b}^3 + 2.5064{R_b}^2 - 21.1894R_b + 57.9987, \quad 7.8 \le R_{b\,[\mathrm{Mbps}]} < 9.5 \\ 0.8613R_b - 5.1806, \quad 9.5 \le R_{b\,[\mathrm{Mbps}]} < 14.1 \\ -0.0042{R_b}^2 + 0.7262R_b - 2.4267, \quad 14.1 \le R_{b\,[\mathrm{Mbps}]} < 34.5 \\ 0.0482{R_b}^2 - 2.879R_b + 60.0064, \quad 34.5 \le R_{b\,[\mathrm{Mbps}]} < 42.5 \\ 0.2984{R_b}^2 - 21.9131R_b + 417.3976, \quad 42.5 \le R_{b\,[\mathrm{Mbps}]} < 43.2 \end{cases} \tag{B.9}$$

For QPSK, considering now the UL direction, one has:

$$(E_c/N_0)_{[\mathrm{dB}]} = \begin{cases} -3.33R_b - 10.0, \quad 0 \le R_{b\,[\mathrm{Mbps}]} < 1.5 \\ -0.5998{R_b}^2 + 5.0194R_b - 11.1447, \quad 1.5 \le R_{b\,[\mathrm{Mbps}]} < 3.4 \\ -5.2083{R_b}^3 + 62.5{R_b}^2 - 244.7917R_b + 313.5, \quad 3.4 \le R_{b\,[\mathrm{Mbps}]} < 4.2 \\ -4.3821{R_b}^3 + 65.5602{R_b}^2 - 321.7734R_b + 521.6365, \quad 4.2 \le R_{b\,[\mathrm{Mbps}]} < 5.5 \end{cases} \tag{B.10}$$

Considering 16QAM for UL, the obtained interpolation obtained by (C.8) is shown in Figure B.2.

$$(E_c/N_0)_{[\mathrm{dB}]} = \begin{cases} -1.5432{R_b}^3 + 6.9444{R_b}^2 - 6.9444R_b - 3, & 0.6 \le R_{b\,[\mathrm{Mbps}]} < 1.6 \\ 2R_b - 6, & 1.6 \le R_{b\,[\mathrm{Mbps}]} < 3.8 \\ 0.1307{R_b}^4 - 3.041{R_b}^3 + 26.0522{R_b}^2 & \\ -95.8265R_b + 129.0191, & 3.8 \le R_{b\,[\mathrm{Mbps}]} < 7.7 \\ 0.1386{R_b}^3 - 3.5025{R_b}^2 & \\ +30.979R_b - 87.2192, & 7.7 \le R_{b\,[\mathrm{Mbps}]} < 11 \end{cases} \quad \text{(B.11)}$$

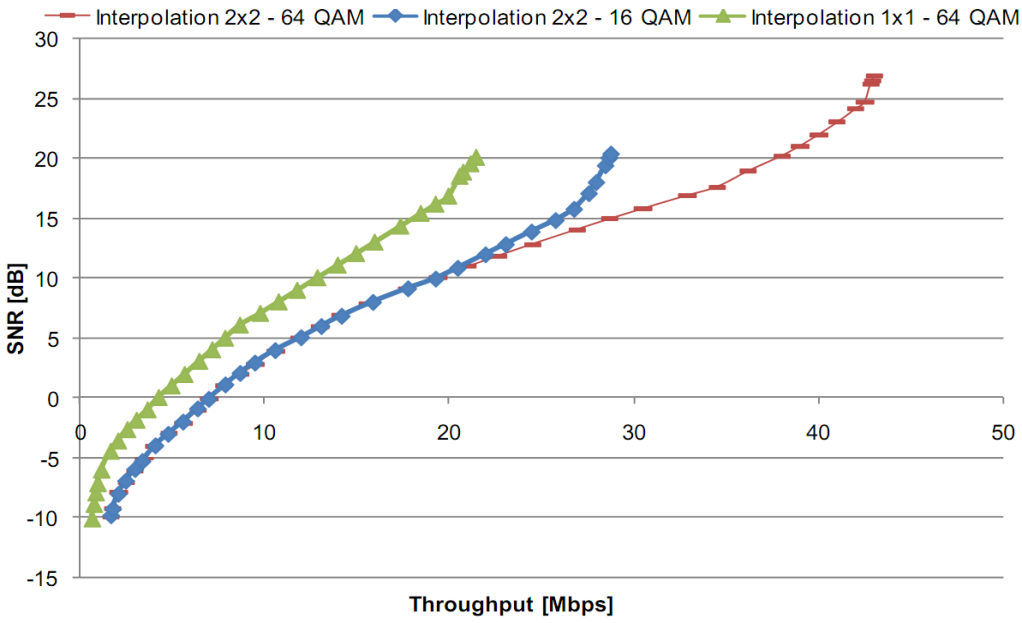

Figure B.1. HSPA+ DL with MIMO configurations – SNR as a function of physical Throughput (extracted from [Jaci09]).

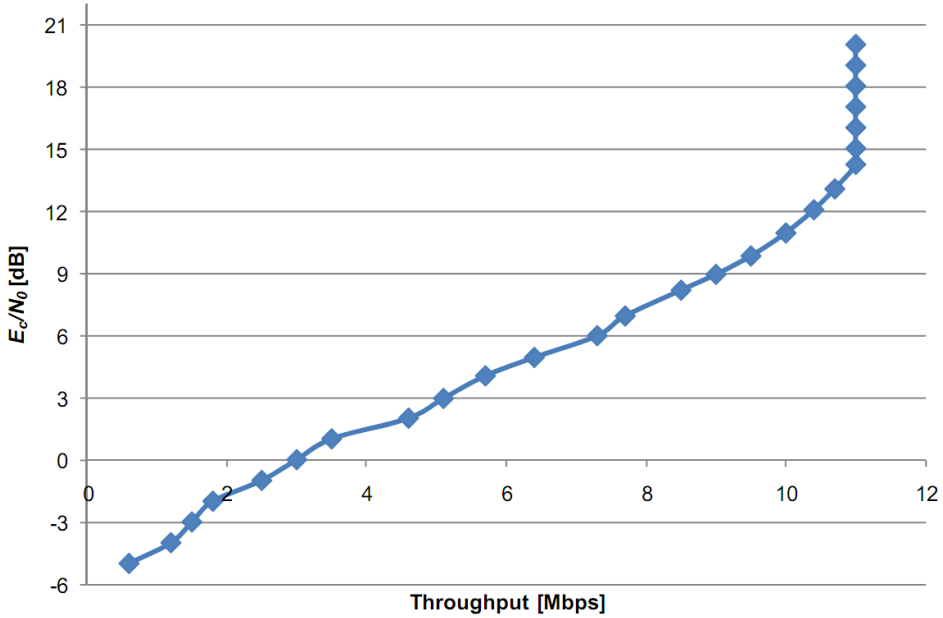

Figure B.2. HSPA+ UL for 16QAM – E_c/N_0 as a function of physical Throughput (extracted from [Jaci09]).

Based on the results of Figure 2.2, the expressions for Throughput as a function of SINR were

obtained, for HSPA+ in DL direction. Expressions for QPSK modulation in DL were once more extrapolated from the ones for 16QAM, and data rate for QPSK is simply considered to be half of the one for 16QAM.

Considering a SISO configuration, with 16QAM, one has for DL:

$$R_{b\,[\mathrm{Mbps}]} = \begin{cases} 0.0143{\rho_{IN}}^2 + 0.3486\rho_{IN} + 2.7657, & -10 \le \rho_{IN_{[\mathrm{dB}]}} < -6 \\ 0.05{\rho_{IN}}^2 + 0.85\rho_{IN} + 4.5, & -6 \le \rho_{IN_{[\mathrm{dB}]}} < -1 \\ 0.0223{\rho_{IN}}^2 + 0.631\rho_{IN} + 4.3203, & -1 \le \rho_{IN_{[\mathrm{dB}]}} < 10 \\ -0.05{\rho_{IN}}^2 + 1.5757\rho_{IN} + 1.9286, & 10 \le \rho_{IN_{[\mathrm{dB}]}} < 18 \\ 14.4, & \rho_{IN_{[\mathrm{dB}]}} \ge 18 \end{cases} \quad \text{(B.12)}$$

For SISO configuration and 64QAM, the DL throughput is given by:

$$R_{b\,[\mathrm{Mbps}]} = \begin{cases} 0.0143{\rho_{IN}}^2 + 0.3586\rho_{IN} + 2.7657, & -10 \le \rho_{IN_{[\mathrm{dB}]}} < -6 \\ 0.0005{\rho_{IN}}^3 + 0.0208{\rho_{IN}}^2 + 0.6167\rho_{IN} + 4.3131, & -6 \le \rho_{IN_{[\mathrm{dB}]}} < 11 \\ -0.0652{\rho_{IN}}^2 + 2.87\rho_{IN} - 9.7048, & 11 \le \rho_{IN_{[\mathrm{dB}]}} < 20 \\ 21.6, & \rho_{IN_{[\mathrm{dB}]}} \ge 20 \end{cases} \quad \text{(B.13)}$$

For SIMO 1×2 configuration, with 16QAM, the DL throughput is obtained using:

$$R_{b\,[\mathrm{Mbps}]} = \begin{cases} 0.03{\rho_{IN}}^2 + 0.7823\rho_{IN} + 5.8266, & -10 \le \rho_{IN_{[\mathrm{dB}]}} < 3 \\ -0.0626{\rho_{IN}}^2 + 1.6255\rho_{IN} + 3.813, & 3 \le \rho_{IN_{[\mathrm{dB}]}} < 13 \\ 14.4, & \rho_{IN_{[\mathrm{dB}]}} \ge 13 \end{cases} \quad \text{(B.14)}$$

Considering a SIMO 1×2 configuration and 64QAM, throughput for DL is given by:

$$R_{b\,[\mathrm{Mbps}]} = \begin{cases} 0.0255{\rho_{IN}}^2 + 0.7265\rho_{IN} + 5.6914, & -10 \le \rho_{IN_{[\mathrm{dB}]}} \le -1 \\ 0.0105{\rho_{IN}}^2 + 0.8517\rho_{IN} + 5.783, & -1 \le \rho_{IN_{[\mathrm{dB}]}} \le 13 \\ -0.0542{\rho_{IN}}^2 + 2.2154\rho_{IN} - 0.9696, & 13 \le \rho_{IN_{[\mathrm{dB}]}} \le 18 \\ 21.6, & \rho_{IN_{[\mathrm{dB}]}} > 18 \end{cases} \quad \text{(B.15)}$$

For MIMO 2×2 configuration, 16QAM, the DL throughput is:

$$R_{b\,[\mathrm{Mbps}]} = \begin{cases} -0.0139{\rho_{IN}}^3 - 0.2714{\rho_{IN}}^2 - 1.3004\rho_{IN} + 1.9524, & -10 \le \rho_{IN_{[\mathrm{dB}]}} \le -5 \\ 0.0021{\rho_{IN}}^3 - 0.0209{\rho_{IN}}^2 + 0.7905\rho_{IN} + 7.0537, & -5 \le \rho_{IN_{[\mathrm{dB}]}} \le 10 \\ -0.0722{\rho_{IN}}^2 + 3.1463\rho_{IN} - 5.2526, & 10 \le \rho_{IN_{[\mathrm{dB}]}} \le 20 \\ 28.8, & \rho_{IN_{[\mathrm{dB}]}} > 20 \end{cases} \quad \text{(B.16)}$$

For MIMO 2×2, with 64QAM, the DL throughput is computed using:

$$R_{b\,[\mathrm{Mbps}]} = \begin{cases} -0.0083{\rho_{IN}}^3 - 0.1357{\rho_{IN}}^2 - 0.2131\rho_{IN} + 4.8057, & -10 \le \rho_{IN_{[\mathrm{dB}]}} \le -6 \\ 0.0005{\rho_{IN}}^4 + 0.0018{\rho_{IN}}^3 + 0.0089{\rho_{IN}}^2 + 0.7812\rho_{IN} + 7.0784, & -6 \le \rho_{IN_{[\mathrm{dB}]}} \le 1 \\ -0.0001{\rho_{IN}}^3 + 0.0657{\rho_{IN}}^2 + 0.5792\rho_{IN} + 7.211, & 1 \le \rho_{IN_{[\mathrm{dB}]}} \le 6 \\ 0.0008{\rho_{IN}}^3 - 0.0593{\rho_{IN}}^2 + 0.8046\rho_{IN} + 6.0472, & 6 \le \rho_{IN_{[\mathrm{dB}]}} \le 17 \\ -0.0757{\rho_{IN}}^2 + 4.3661\rho_{IN} - 19.392, & 17 \le \rho_{IN_{[\mathrm{dB}]}} \le 26.5 \\ 42.2 & , \quad \rho_{IN_{[\mathrm{dB}]}} > 26.5 \end{cases} \tag{B.17}$$

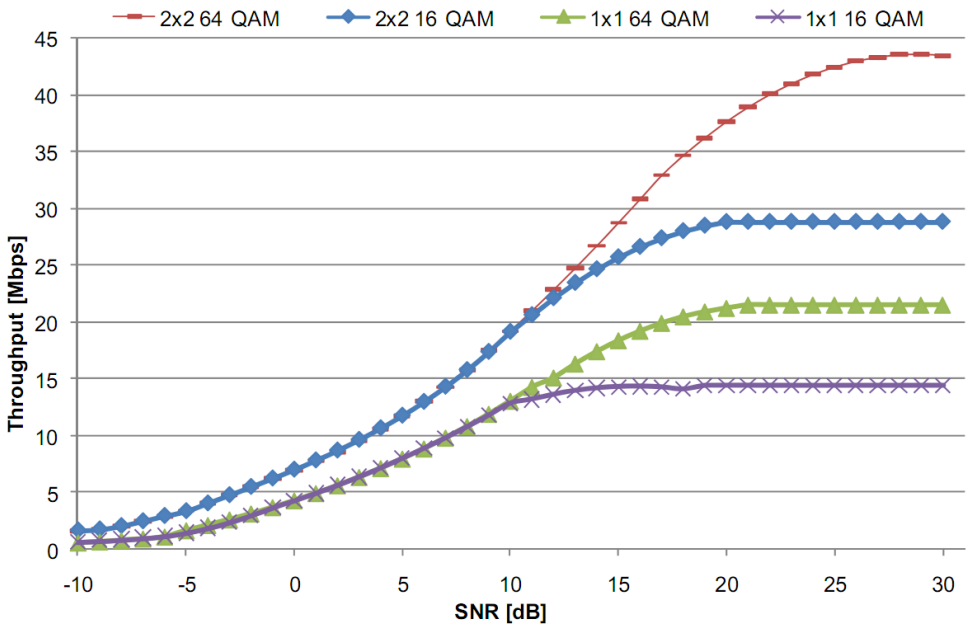

Figure B.3. HSPA+ DL with MIMO and SISO configurations – physical Throughput as a function of SNR (extracted from [Jaci09]).

For QPSK modulation scheme, now for UL, one can define the physical throughput by:

$$R_{b\,[\mathrm{Mbps}]} = \begin{cases} 0.0643(E_c/N_0)^2 + 0.8557(E_c/N_0) + 4.18, & -5 \le (E_c/N_0)_{[\mathrm{dB}]} < -1 \\ -0.05(E_c/N_0)^2 + 0.31(E_c/N_0) + 3.77, & -1 \le (E_c/N_0)_{[\mathrm{dB}]} < 2 \\ 0.0417(E_c/N_0)^3 - 0.5429(E_c/N_0)^2 + 2.5012(E_c/N_0) + 1.04, & 2 \le (E_c/N_0)_{[\mathrm{dB}]} < 6 \\ 5.5, & 6 \le (E_c/N_0)_{[\mathrm{dB}]} < 11 \end{cases} \tag{B.18}$$

Similarly, for 16QAM in UL, the throughput is given by:

$$R_{b\,[\mathrm{Mbps}]} = \begin{cases} -0.0087(E_c/N_0)^4 - 0.0669(E_c/N_0)^3 - 0.0936(E_c/N_0)^2 \\ +0.6056(E_c/N_0) + 3.0522, & -5 \le (E_c/N_0)_{[\mathrm{dB}]} < -3 \\ 0.0333(E_c/N_0)^4 + 0.1(E_c/N_0)^3 \\ -0.0333(E_c/N_0)^2 + 0.4(E_c/N_0) + 3, & -3 \le (E_c/N_0)_{[\mathrm{dB}]} < 1 \\ 0.0583(E_c/N_0)^3 - 0.575(E_c/N_0)^2 \\ +2.3667(E_c/N_0) + 1.66, & 1 \le (E_c/N_0)_{[\mathrm{dB}]} < 5 \\ -0.0003(E_c/N_0)^3 - 0.0195(E_c/N_0)^2 \\ +0.9558(E_c/N_0) + 2.1899, & 5 \le (E_c/N_0)_{[\mathrm{dB}]} < \rho_{IN_{[\mathrm{dB}]}} \le 14 \\ 11, & (E_c/N_0)_{[\mathrm{dB}]} > 14 \end{cases} \tag{B.19}$$

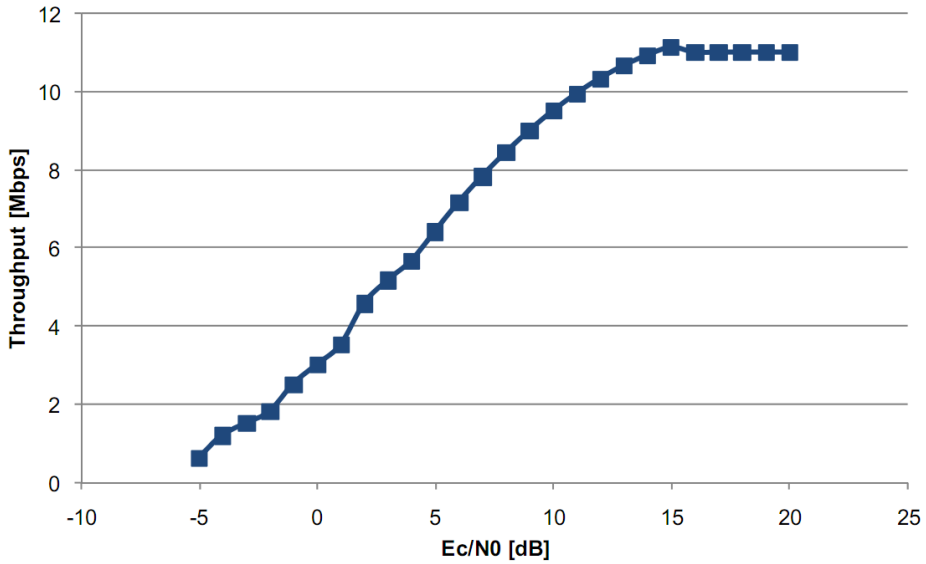

Figure B.4. HSPA+ UL for 16QAM – physical Throughput as a function of SNR (extracted from [Jaci09]).

B.2 LTE

Trial measurements documented by the 3GPP were taken as reference for deriving the expressions for throughput in the physical layer and SNR, similarly to UMTS. The channel models chosen are characterised in terms of the maximum Doppler frequency considered and maximum delay spread, Table B.1. Moreover, Figure B.6 and Figure B.7 show throughput as a function of SNR for the EPA5Hz channel, for some selected modulation schemes and MIMO configurations, respectively in DL and UL directions.

Table B.1. Characterisation of the channel models used, in terms of Doppler frequency spread and delay spread (extracted from [Jaci09]).

Channel Model	Doppler Frequency [Hz]	Delay Spread [ns]
EPA 5Hz	5 (low)	43 (low)
EVA 5Hz	5 (low)	357 (medium)
ETU 70Hz	70 (medium)	991 (high)

DL interpolations are presented based on the results in [Duar08], [Jaci09] and on simulation results presented by 3GPP. SIMO, MISO and MIMO configurations are considered, for 10MHz bandwidth, using normal CP and considering the EPA5Hz channel model, having low delay spreads.

Nevertheless, when results for the considered channel model were not available, an extrapolation was made, based on the results for the EVA5Hz channel, as shown in Table B.2. This happened only for the DL cases of MIMO 4×2 with QPSK and 16QAM modulations and also for MIMO 2×2 using 16QAM. Furthermore, saturation of the curves for higher values of SNIR was done so to assure coherence between different MIMO and modulation configurations.

Conversely, and due to the relevance of considering different radio channel models, the extrapolation factors used to derive results for the EPA5Hz can also be easily used to obtain results for the EVA5Hz channel model. Furthermore, the interpolations here shown present relative mean errors lower or approximately equal to 5%, similarly to the considered interpolations for HSPA+.

Table B.2. Extrapolation EVA5Hz to EPA5Hz (extracted from [Duar08]).

M	$\frac{\text{EPA 5Hz}}{\text{EVA 5Hz}}$	$\bar{\varepsilon}_r$ [%]
QPSK	1.027	5.3
16QAM	1.061	4.6
64QAM	1.04	15.2

Also, results for higher order MISO and MIMO configurations in DL (namely 4×2 and 4×4 but also for 2×2 using QPSK) and simpler SIMO configurations in UL (1×2 and 1×4) were obtained recurring to the Relative MIMO Gain Model, [KuCo08], together with the model for the receive diversity gain, via selection combining, explained in [OeCl08].

To be able to easily obtain results for different bandwidths, throughput for a single RB is considered for the following expressions. An estimate of the channel throughput is obtained by multiplying the average throughput per RB by the number of RBs used for a required channel bandwidth, according to Table B.3.

Table B.3. Transmission band (adapted from [Duar08]).

Channel bandwidth [MHz]	**Number of RBs**	**Transmission bandwidth [MHz]**	**Spectral efficiency [%]**
1.4	6	1.08	77
3	15	2.7	90
5	25	4.5	90
10	50	9	90
15	75	13.5	90
20	100	18.0	90

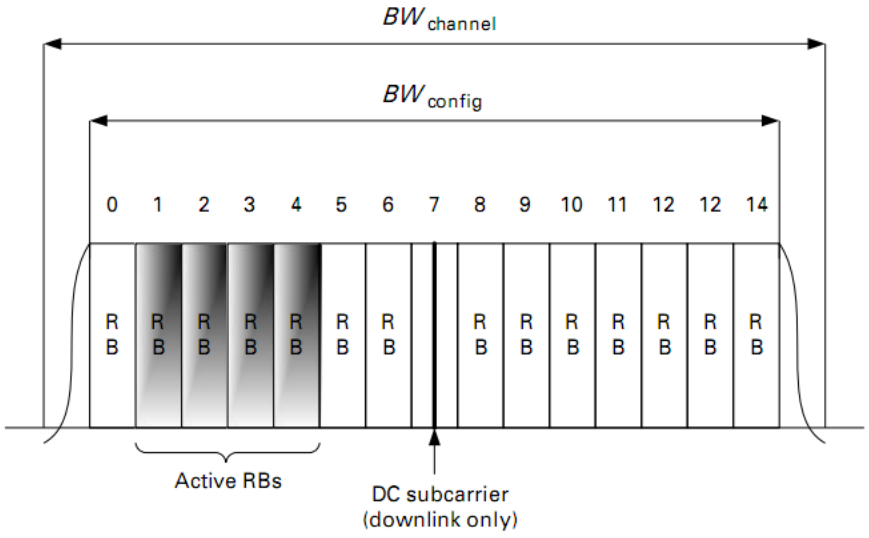

Figure B.5. Channel and transmission bandwidth configuration for a LTE carrier (extracted from [Khan09])

For SIMO 1×2, coding rate of 1/3 and QPSK modulation, SNR in the DL is given by, based on [Duar08]:

- EPA5Hz

$$\rho_{N_{[\mathrm{dB}]}} = \begin{cases} 2.55\times10^{7}{R_b}^{5} - 6.303\times10^{6}{R_b}^{4} + 5.803\times10^{5}{R_b}^{3} - 2.502\times10^{4}{R_b}^{2} + \\ \quad +609.1\,R_b - 12.93, \quad 0.02037304 \le R_{b\,[\mathrm{Mbps}]} < 0.09338800 \\ 7.457\times10^{9}{R_b}^{3} - 2.126\times10^{9}{R_b}^{2} + 2.02\times10^{8}R_b - \\ \quad -6.397\times10^{6}, \quad 0.09338800 \le R_{b\,[\mathrm{Mbps}]} \le 0.096261 \end{cases} \tag{B.20}$$

- ETU70Hz

$$\rho_{N_{[\mathrm{dB}]}} = \begin{cases} -61.62{R_b}^{2} + 104.2\,R_b - 8.231, \quad 0.04145 \le R_{b\,[\mathrm{Mbps}]} < 0.08313 \\ 4.465\times10^{4}{R_b}^{2} - 7476\,R_b + 313, \quad 0.08313 \le R_{b\,[\mathrm{Mbps}]} \le 0.0916893 \end{cases} \tag{B.21}$$

For SIMO 1×2, coding rate of 1/2 and using 16QAM, SNR in DL is obtained, according to the results in [Duar08], by:

- EPA5Hz

$$\rho_{N_{[\mathrm{dB}]}} = \begin{cases} -70.91{R_b}^{2} + 61.37R_b - 5.045, \quad 0.09042 \le R_{b\,[\mathrm{Mbps}]} < 0.2200675 \\ \left(820.7{R_b}^{5} + 1151{R_b}^{4} - 644.9{R_b}^{3} + 180.6{R_b}^{2} - 25.26R_b + 1.412\right)\times10^{8}, \\ \quad 0.2200675 \le R_{b\,[\mathrm{Mbps}]} \le 0.29382 \end{cases} \tag{B.22}$$

- ETU70Hz

$$\rho_{N_{[\mathrm{dB}]}} = \begin{cases} 2968{R_b}^4 - 1233{R_b}^3 - 12.73{R_b}^2 + \\ +93.33R_b - 6.971, \quad 0.08175 \le R_{b\,[\mathrm{Mbps}]} < 0.27310179 \\ (1664{R_b}^4 - 1824{R_b}^3 + 749.5{R_b}^2 - \\ -136.9R_b + 9.374) \times 10^9, \quad 0.27310179 \le R_{b\,[\mathrm{Mbps}]} \le 0.27500964 \end{cases} \tag{B.23}$$

In SIMO 1×2, coding rate of 3/4 and 64QAM modulation, one gets for DL, [Duar08]:

- EPA5Hz

$$\rho_{N_{[\mathrm{dB}]}} = \begin{cases} -3.891 \times 10^4{R_b}^4 + 1.418 \times 10^4{R_b}^3 - \\ -1756{R_b}^2 + 110R_b - 0.1967, \quad 0.003036 \le R_{b\,[\mathrm{Mbps}]} < 0.152616 \\ -7931{R_b}^3 + 4946{R_b}^2 - 946.6R_b + 62.48, \quad 0.152616 \le R_{b\,[\mathrm{Mbps}]} < 0.25014 \\ 455.2{R_b}^4 - 599.4{R_b}^3 + 246.2{R_b}^2 - \\ -11.18R_b + 6.022, \quad 0.25014 \le R_{b\,[\mathrm{Mbps}]} < 0.637095 \\ 1.547 \times 10^4{R_b}^2 - 1.972 \times 10^4R_b + 6300, \quad 0.637095 \le R_{b\,[\mathrm{Mbps}]} < 0.648575 \end{cases} \tag{B.24}$$

- ETU70Hz

$$\rho_{N_{[\mathrm{dB}]}} = \begin{cases} \left(-9.862{R_b}^4 + 3.195{R_b}^3\right) \times 10^4 - \\ -3458{R_b}^2 + 165.5R_b + 0.8493, \quad 0 \le R_{b\,[\mathrm{Mbps}]} < 0.1428556 \\ 7838{R_b}^3 - 3441{R_b}^2 + 527R_b - 21.91, \quad 0.1428556 \le R_{b\,[\mathrm{Mbps}]} < 0.220953 \\ 198.2{R_b}^3 - 267.3{R_b}^2 + 135.4R_b - 7.904, \quad 0.220953 \le R_{b\,[\mathrm{Mbps}]} < 0.5656632 \\ 2290{R_b}^2 - 2617R_b + 766.5, \quad 0.5656632 \le R_{b\,[\mathrm{Mbps}]} < 0.6068352 \\ (3.684{R_b}^2 - 4.472R_b + 1.375) \times 10^4, \quad 0.6068352 \le R_{b\,[\mathrm{Mbps}]} \le 0.6076992 \end{cases} \tag{B.25}$$

For MIMO 2×2, coding rate of 1/2 and 16QAM, for DL, SNR is obtained based on the results in [3GPP08a], [3GPP08b], [3GPP08c] and [3GPP08d]:

- EPA5Hz

$$\rho_{N_{[\mathrm{dB}]}} = \begin{cases} 683.8{R_b}^3 - 399.4{R_b}^2 + 115.8R_b - 7.195, \quad 0.081909 \le R_{b\,[\mathrm{Mbps}]} < 0.2619 \\ 5.149 \times 10^4{R_b}^5 - 1.056 \times 10^5{R_b}^4 + 8.561 \times 10^4{R_b}^3 - \\ -3.43 \times 10^4{R_b}^2 + 6812R_b - 528, \quad 0.2619 \le R_{b\,[\mathrm{Mbps}]} < 0.52724 \\ 2740{R_b}^2 - 2868R_b + 766.7, \quad 0.52724 \le R_{b\,[\mathrm{Mbps}]} < 0.5507425 \\ 2.851 \times 10^4{R_b}^2 - 3.105 \times 10^4R_b + 8472, \quad 0.5507425 \le R_{b\,[\mathrm{Mbps}]} \le 0.5531 \end{cases} \tag{B.26}$$

- ETU70Hz

$$\rho_{N_{[\mathrm{dB}]}} = \begin{cases} 23.21{R_b}^2 + 27.73R_b - 0.7635, \quad 0.02782 \le R_{b\,[\mathrm{Mbps}]} < 0.23376343 \\ 1.765 \times 10^4{R_b}^3 - 1.391 \times 10^4{R_b}^2 + \\ +3675R_b - 317.4, \quad 0.23376343 \le R_{b\,[\mathrm{Mbps}]} < 0.3024 \\ 1.019 \times 10^4{R_b}^4 - 1.595 \times 10^4{R_b}^3 + \\ +9329{R_b}^2 - 2396R_b + 237.4, \quad 0.3024 \le R_{b\,[\mathrm{Mbps}]} < 0.5155584 \\ 197.8R_b - 85.95, \quad 0.5155584 \le R_{b\,[\mathrm{Mbps}]} < 0.5206152 \\ (3.909{R_b}^2 - 4.0689R_b + 1.059) \times 10^5, \quad 0.5206152 \le R_{b\,[\mathrm{Mbps}]} < 0.5232 \end{cases} \tag{B.27}$$

For MIMO 2×2, coding rate of 3/4 and 64QAM, based on the results in [3GPP08a], DL SNR is given

by:

- EPA5Hz

$$\rho_{N_{[\mathrm{dB}]}} = \begin{cases} 1.071 \times 10^5 {R_b}^3 - 1.023 \times 10^4 {R_b}^2 + 337.1 R_b + 2.201, \\ 0.000636 \leq R_{b\,[\mathrm{Mbps}]} < 0.0510 \\ -1475 {R_b}^4 + 1090 {R_b}^3 - 283.9 {R_b}^2 + \\ +52.07 R_b + 4.943, \quad 0.0510 \leq R_{b\,[\mathrm{Mbps}]} < 0.3522 \\ 97.69 {R_b}^3 - 179 {R_b}^2 + 118.4 R_b - 10.72, \quad 0.3522 \leq R_{b\,[\mathrm{Mbps}]} < 0.7042 \\ 158.6 {R_b}^3 - 418.5 {R_b}^2 + 380.9 R_b - 98.1, \quad 0.7042 \leq R_{b\,[\mathrm{Mbps}]} < 1.0780 \\ (3.49 {R_b}^3 - 11.55 {R_b}^2 + 12.75 R_b - 4.689) \times 10^4, \quad 1.0780 \leq R_{b\,[\mathrm{Mbps}]} < 1.1434 \end{cases} \tag{B.28}$$

- ETU70Hz

$$\rho_{N_{[\mathrm{dB}]}} = \begin{cases} 3.69 \times 10^4 {R_b}^3 - 5182 {R_b}^2 + 269 R_b + 0.8425, 0 \leq R_{b\,[\mathrm{Mbps}]} \leq 0.07103922 \\ -10.14 {R_b}^3 + 5.678 {R_b}^2 + 24.37 R_b + 5.248, \ 0.07103922 \leq R_{b\,[\mathrm{Mbps}]} \leq 0.858 \\ 243.1 {R_b}^3 - 675.3 {R_b}^2 + 643.7 R_b - 184.8, 0.858 \leq R_{b\,[\mathrm{Mbps}]} \leq 1.1452 \end{cases} \tag{B.29}$$

In the case of the UL direction main results regarding MIMO 2×2 and 4×4 configurations in [Duar08] were used, updated in some cases with the results documented by the 3GPP.

For MIMO 2×2, coding rate of 1/3 and QPSK, considering the UL direction, SNR is given by:

- EPA5Hz

$$\rho_{N_{[\mathrm{dB}]}} = \begin{cases} 4.798 \times 10^4 {R_b}^3 - 8140 {R_b}^2 + 529.2 R_b - 15.86, \quad 0.0366 \leq R_{b\,[\mathrm{Mbps}]} \leq 0.094 \\ 1.363 \times 10^6 {R_b}^2 - 2.572 \times 10^5 R_b + 1.214 \times 10^4, \quad 0.094 \leq R_{b\,[\mathrm{Mbps}]} \leq 0.0959 \end{cases} \tag{B.30}$$

- ETU70Hz

$$\rho_{N_{[\mathrm{dB}]}} = 6.801 \times 10^5 {R_b}^3 - 1.582 \times 10^5 {R_b}^2 + +1.234 \times 10^4 - 321.6, \quad 0.0672 \leq R_{b\,[\mathrm{Mbps}]} \leq 0.0959 \tag{B.31}$$

Similarly, for MIMO 2×2, coding rate of 3/4 and 16QAM, UL, SNR is given by:

- EPA5Hz

$$\rho_{N_{[\mathrm{dB}]}} = \begin{cases} 88.31 {R_b}^3 - 92.67 {R_b}^2 + 59.18 R_b - 2.797, \quad 0.0512 \leq R_{b\,[\mathrm{Mbps}]} \leq 0.3351 \\ 4.633 \times 10^4 {R_b}^3 - 5.37 \times 10^4 {R_b}^2 + \\ +2.077 \times 10^4 R_b - 2670, \quad 0.3351 \leq R_{b\,[\mathrm{Mbps}]} \leq 0.4291 \end{cases} \tag{B.32}$$

- ETU70Hz

$$\rho_{N_{[\mathrm{dB}]}} = (3.039 {R_b}^5 - 3.477 {R_b}^4 + 1.484 {R_b}^3) \times 10^4 - 2901 {R_b}^2 + +301.9 R_b - 11.58, \quad 0.1181 \leq R_{b\,[\mathrm{Mbps}]} \leq 0.4197 \tag{B.33}$$

For MIMO 2×2, coding rate of 5/6 and 64QAM, UL, SNR is given by:

- EPA5Hz

$$\rho_{N_{[\mathrm{dB}]}} = \begin{cases} 349.5R_b - 0.04397, & 0.0001 \le R_{b\,[\mathrm{Mbps}]} \le 0.0087 \\ 17.51{R_b}^2 + 22.23R_b + 2.654, & 0.0087 \le R_{b\,[\mathrm{Mbps}]} \le 0.3914 \\ \left(3.567{R_b}^5 - 9.618{R_b}^4 + 10.29{R_b}^3 - 5.447{R_b}^2 + 1.43R_b\right) \times 10^4 \\ \quad -1474, & 0.3914 \le R_{b\,[\mathrm{Mbps}]} \le 0.716 \end{cases} \quad \text{(B.34)}$$

- ETU70Hz

$$\rho_{N_{[\mathrm{dB}]}} = (3.698{R_b}^5 - 5.411{R_b}^4 + 2.953{R_b}^3) \times 10^4 - 7377{R_b}^2 + \\ +880.9R_b - 36.38, \quad 0.1244 \le R_{b\,[\mathrm{Mbps}]} \le 0.4952 \quad \text{(B.35)}$$

For a MIMO 2×4 configuration, coding rate of 1/3 and QPSK, in UL, SNR is given by:

- EPA5Hz

$$\rho_{N_{[\mathrm{dB}]}} = \begin{cases} 515.2R_b - 48.44, & 0.0940 \le R_{b\,[\mathrm{Mbps}]} \le 0.095978 \\ 4.545 \times 10^4 R_b - 4362, & 0.095978 \le R_{b\,[\mathrm{Mbps}]} \le 0.096 \end{cases} \quad \text{(B.36)}$$

- ETU70Hz

$$\rho_{N_{[\mathrm{dB}]}} = \begin{cases} 79.88R_b - 4.469, & 0.081 \le R_{b\,[\mathrm{Mbps}]} \le 0.0935 \\ 444.8R_b - 38.6, & 0.0935 \le R_{b\,[\mathrm{Mbps}]} \le 0.0958 \\ 1.09 \times 10^4 R_b - 1040, & 0.0958 \le R_{b\,[\mathrm{Mbps}]} \le 0.0959 \end{cases} \quad \text{(B.37)}$$

For MIMO 2×4, coding rate of 3/4 and 16QAM, UL, SNR is obtained by:

- EPA5Hz

$$\rho_{N_{[\mathrm{dB}]}} = \begin{cases} 12.32R_b + 5.255, & 0.304 \le R_{b\,[\mathrm{Mbps}]} \le 0.3852 \\ 957.7{R_b}^2 - 723R_b + 146.4, & 0.3852 \le R_{b\,[\mathrm{Mbps}]} \le 0.4335 \end{cases} \quad \text{(B.38)}$$

- ETU70Hz

$$\rho_{N_{[\mathrm{dB}]}} = \left(2.911{R_b}^4 - 4.109{R_b}^3 + 2.158{R_b}^2\right) \times 10^4 - \quad \text{(B.39)}$$

$$-4974R_b + 434, \quad 0.287 \le R_{b\,[\mathrm{Mbps}]} \le 0.4506$$

For the case of MIMO 2×4, coding rate of 5/6 and 64QAM, UL, SNR is given by:

- EPA5Hz

$$\rho_{N_{[\mathrm{dB}]}} = \begin{cases} 11.41R_b + 10.6, & 0.5611 \le R_{b\,[\mathrm{Mbps}]} \le 0.6487 \\ 639.6{R_b}^2 - 836.8R_b + 291.7, & 0.6487 \le R_{b\,[\mathrm{Mbps}]} \le 0.7208 \end{cases} \quad \text{(B.40)}$$

- ETU70Hz

$$\rho_{N_{[\mathrm{dB}]}} = 1439{R_b}^3 - 1729{R_b}^2 + 696.6R_b - 80.02, \qquad 0.2909 \le R_{b\,[\mathrm{Mbps}]} \le 0.5756 \tag{B.41}$$

Considering throughput in the physical layer as a function of the SNR in LTE, interpolated expressions were obtained.

For SIMO 1×2, coding rate of 1/3 and using QPSK, DL throughput is given by, [Duar08] e [3GPP08a]:

- EPA5Hz

$$R_{b\,[\mathrm{bps}]} = \begin{cases} (0.0190{\rho_N}^3 - 0.1455{\rho_N}^2 + 0.3516\rho_N + 9.3388) \times 10^{-2}, & -2 \le \rho_{N_{[\mathrm{dB}]}} < 2 \\ (0.0063\rho_N + 9.6009) \times 10^4, & 2 \le \rho_{N_{[\mathrm{dB}]}} < 4 \\ 96261, & 4 < \rho_{N_{[\mathrm{dB}]}} \le 6 \end{cases} \tag{B.42}$$

- ETU70Hz

$$R_{b\,[\mathrm{bps}]} = \begin{cases} (0.01035\rho_N + 0.08285) \times 10^6, & -4 \le \rho_{N_{[\mathrm{dB}]}} < 0 \\ (0.0001279{\rho_N}^3 - 0.001638{\rho_N}^2 + 0.006616\rho_N + 0.08313) \times 10^6, & 0 \le \rho_{N_{[\mathrm{dB}]}} \le 6 \\ 91484.4, & \rho_{N_{[\mathrm{dB}]}} > 6 \end{cases} \tag{B.43}$$

For SIMO 1×2, coding rate of 1/2 and 16QAM, DL throughput is given by, [Duar08] and [3GPP07]:

- EPA5Hz

$$R_{b\,[\mathrm{bps}]} = \begin{cases} -263.5{\rho_N}^3 + 303{\rho_N}^2 + 26360\rho_N + 90420, & -4 \le \rho_{N_{[\mathrm{dB}]}} < 2 \\ (-0.000945{\rho_N}^4 + 0.0103{\rho_N}^3 - 0.0141{\rho_N}^2 + 0.1696\rho_N + 1.0083) \times 10^5, & 2 \le \rho_{N_{[\mathrm{dB}]}} < 6 \\ (0.0048{\rho_N}^3 - 0.1503{\rho_N}^2 + 1.5644\rho_N - 2.4858) \times 10^5, & 6 \le \rho_{N_{[\mathrm{dB}]}} < 12 \\ 293820, & 12 \le \rho_{N_{[\mathrm{dB}]}} \le 14 \end{cases} \tag{B.44}$$

- ETU70Hz

$$R_{b\,[\mathrm{bps}]} = \begin{cases} (0.002862{\rho_N}^2 + 0.03113\rho_N + 0.07953) \times 10^6, -4 \le \rho_{N_{[\mathrm{dB}]}} \le 0 \\ (1.204{\rho_N}^2 + 12.02\rho_N + 81.75) \times 10^3, & 0 < \rho_{N_{[\mathrm{dB}]}} \le 8 \\ 66{,}41{\rho_N}^2 + 1909\rho_N + 261300, & 8 < \rho_{N_{[\mathrm{dB}]}} \le 14 \\ 275009.64, & \rho_{N_{[\mathrm{dB}]}} > 14 \end{cases} \tag{B.45}$$

For SIMO 1×2, coding rate of 3/4 and 64QAM, DL throughput is obtained by, [Duar08]:

- EPA5Hz

$$R_{b\,[\mathrm{bps}]} = \begin{cases} (-0.1292{\rho_N}^3 + 1.3299{\rho_N}^2 - 0.4279\rho_N + 0.3036) \times 10^4, & 0 \le \rho_{N_{[\mathrm{dB}]}} < 6 \\ (-0.1018{\rho_N}^2 + 2.92\rho_N + 3.8494) \times 10^4, & 6 \le \rho_{N_{[\mathrm{dB}]}} < 10 \\ (0.0585{\rho_N}^2 - 1.0032\rho_N + 6.4581) \times 10^5, & 10 \le \rho_{N_{[\mathrm{dB}]}} < 16 \\ (0.4354\rho_N - 1.6098) \times 10^5, & 16 \le \rho_{N_{[\mathrm{dB}]}} < 18 \\ (-0.0241{\rho_N}^2 + 1.0214\rho_N - 4.33555) \times 10^5, & 18 \le \rho_{N_{[\mathrm{dB}]}} < 22 \\ 647085, & 22 \le \rho_{N_{[\mathrm{dB}]}} \le 26 \end{cases} \quad \text{(B.46)}$$

- ETU70Hz

$$R_{b\,[\mathrm{bps}]} = \begin{cases} 727.4\rho_N, & 0 \le \rho_{N_{[\mathrm{dB}]}} < 2 \\ 127.6{\rho_N}^4 - 3709{\rho_N}^3 + 34850{\rho_N}^2 - 91410\rho_N + 72490, & 2 \le \rho_{N_{[\mathrm{dB}]}} < 10 \\ 3933{\rho_N}^2 - 71940\rho_N + 5.364 \times 10^5, & 10 \le \rho_{N_{[\mathrm{dB}]}} < 18 \\ -100.8{\rho_N}^4 + 9480{\rho_N}^3 - 334300{\rho_N}^2 + 5.239 \times 10^6\rho_N - \\ -30.18 \times 10^6, 18 \le \rho_{N_{[\mathrm{dB}]}} \le 26 \\ 604499.2, \quad , \quad 18\rho_{N_{[\mathrm{dB}]}} > 26 \end{cases} \quad \text{(B.47)}$$

For MIMO 2×2, coding rate of 1/2 and 16QAM, DL throughput is given based on the results in [3GPP08a], [3GPP08b], [3GPP08c] and [3GPP08d]:

- EPA5Hz

$$R_{b\,[\mathrm{bps}]} = \begin{cases} (-0.0348{\rho_N}^3 - 0.0922{\rho_N}^2 + 2.045\rho_N + 8.1909) \times 10^4, & -4 \le \rho_{N_{[\mathrm{dB}]}} < 2 \\ (0.0023{\rho_N}^2 + 2.4658\rho_N + 6.4636) \times 10^4, & 2 \le \rho_{N_{[\mathrm{dB}]}} < 8 \\ (-0.0049{\rho_N}^2 + 0.1405\rho_N + 1.8086) \times 10^5, & 8 \le \rho_{N_{[\mathrm{dB}]}} < 10 \\ (3.8501\rho_N - 9.1235) \times 10^4, & 10 \le \rho_{N_{[\mathrm{dB}]}} < 16 \\ 412.3468{\rho_N}^3 - 2.4976 \times 10^4 + 5.0302 \times 10^5 - 2.8162 \times 10^6, & 16 \le \rho_{N_{[\mathrm{dB}]}} \le 22 \\ 552524, & \rho_{N_{[\mathrm{dB}]}} > 22 \end{cases} \quad \text{(B.48)}$$

- ETU70Hz

$$R_{b\,[\mathrm{bps}]} = \begin{cases} 21.63{\rho_N}^4 - 335.4{\rho_N}^3 + 1058{\rho_N}^2 + 31030\rho_N + 27820, & 0 \le \rho_{N_{[\mathrm{dB}]}} < 10 \\ 330.4{\rho_N}^3 + 18560{\rho_N}^2 + 347600\rho_N - 1.648 \times 10^6, & 10 \le \rho_{N_{[\mathrm{dB}]}} \le 20 \\ 533200, & \rho_{N_{[\mathrm{dB}]}} > 20 \end{cases} \quad \text{(B.49)}$$

Considering MIMO 2×2, coding rate of 3/4 and 64QAM, based on the results in [3GPP08a], throughput in the DL is given by:

- EPA5Hz

$$R_{b\,[\mathrm{bps}]} = \begin{cases} (0.1853\rho_N{}^2 - 0.8564\rho_N + 1.0352) \times 10^4, & 2 \le \rho_{N_{[\mathrm{dB}]}} < 6 \\ (0.0005738\rho_N{}^4 - 0.02762\rho_N{}^3 & \\ +0.4778\rho_N{}^2 - 3.088\rho_N + 6.81) \times 10^5, & 6 \le \rho_{N_{[\mathrm{dB}]}} < 13 \\ (0.0893\rho_N{}^2 - 2.0808\rho_N + 15.3841) \times 10^5, & 13 \le \rho_{N_{[\mathrm{dB}]}} < 19 \\ (0.010304\rho_N{}^2 + 0.16608\rho_N - 1.247) \times 10^5, & 19 \le \rho_{N_{[\mathrm{dB}]}} < 24 \\ -4424\rho_N{}^2 + 281800\rho_N - 3344000, & 24 \le \rho_{N_{[\mathrm{dB}]}} \le 30 \\ 1143420, & \rho_{N_{[\mathrm{dB}]}} > 30 \end{cases} \quad \text{(B.50)}$$

- ETU70Hz

$$R_{b\,[\mathrm{bps}]} = \begin{cases} 36.62\rho_N{}^4 - 387.8\rho_N{}^3 + 2810\rho_N{}^2 - 3080\rho_N - 1.011 \times 10^{-11}, & 0 \le \rho_{N_{[\mathrm{dB}]}} < 8 \\ 80.56\rho_N{}^3 - 3033\rho_N{}^2 + 76910\rho_N - 3.55 \times 10^5, & 8 \le \rho_{N_{[\mathrm{dB}]}} < 24 \\ -2800\rho_N{}^2 + 192700\rho_N - 2.154 \times 10^6, & 24 \le \rho_{N_{[\mathrm{dB}]}} \le 32 \\ 1145200, & \rho_{N_{[\mathrm{dB}]}} > 32 \end{cases} \quad \text{(B.51)}$$

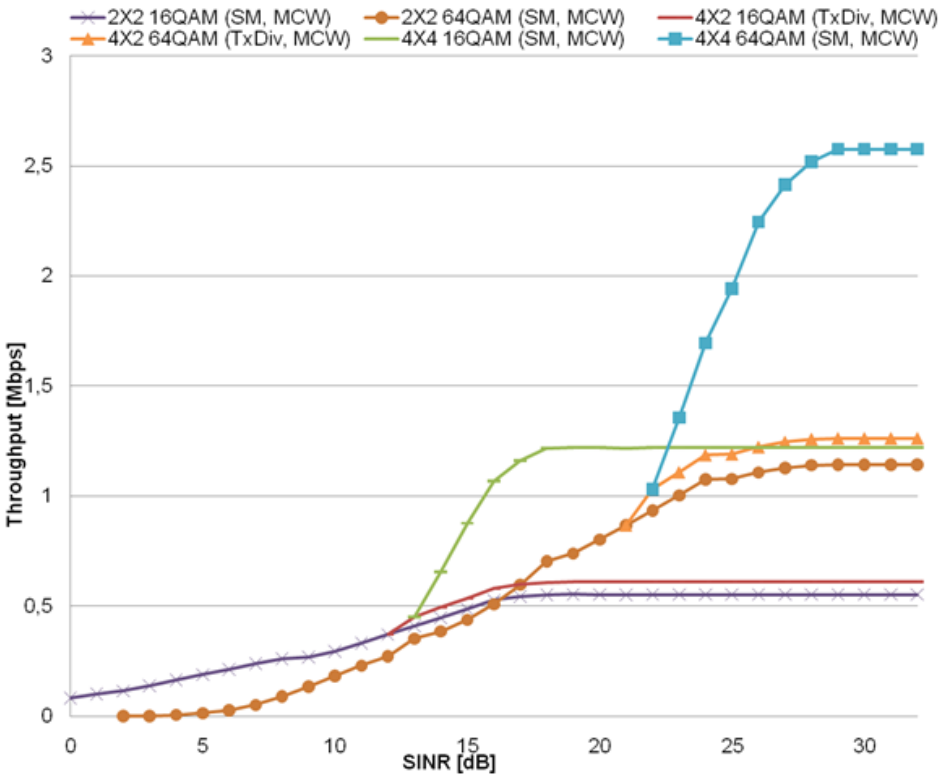

Figure B.6. LTE EPA5Hz downlink physical throughput per RB for two layer 16QAM and 64QAM modulation schemes as a function of SNR.

Considering now the throughput obtained in UL, expressions can be derived in a similar way as for the DL. For a MIMO 2×2, coding rate of 1/3 and QPSK, UL throughput is given, as a function of SNR, by [3GPP08e] and [Jaci09]:

- EPA5Hz

$$R_{b\,[\mathrm{bps}]} = \begin{cases} 69.76\rho_N{}^3 - 1102\rho_N{}^2 + 5475\rho_N + 8.691 \times 10^4, & -2 \le \rho_{N_{[\mathrm{dB}]}} \le 8 \\ 95899, & \rho_{N_{[\mathrm{dB}]}} > 8 \end{cases} \quad \text{(B.52)}$$

- ETU70Hz

$$R_{b\,[\mathrm{bps}]} = \begin{cases} (-0.0567\rho_N{}^2 + 0.8052\rho_N + 6.715) \times 10^4, & 0 \le \rho_{N_{[\mathrm{dB}]}} \le 6 \\ 403.36\rho_N + 92629.84, & 6 \le \rho_{N_{[\mathrm{dB}]}} \le 8 \\ 95856.72, & \rho_{N_{[\mathrm{dB}]}} > 8 \end{cases} \quad \text{(B.53)}$$

For MIMO 2×2, coding rate of 3/4 and 16QAM, UL throughput is given by [3GPP08e], [Duar08]:

- EPA5Hz

$$R_{b\,[\mathrm{bps}]} = \begin{cases} (0.0008773\rho_N{}^2 + 0.01934\rho_N + 0.05122), & 0 \le \rho_{N_{[\mathrm{dB}]}} < 8 \\ (-0.0017\rho_N{}^4 + 0.0425\rho_N{}^3 - 0.317\rho_N{}^2 + 1.905\rho_N + 3.9032) \times 2 \times 10^4, & 8 \le \rho_{N_{[\mathrm{dB}]}} < 12 \\ (-0.0801\rho_N{}^2 + 2.7554\rho_N - 2.1906) \times 2 \times 10^4, & 12 \le \rho_{N_{[\mathrm{dB}]}} \le 18 \\ 429084, & \rho_{N_{[\mathrm{dB}]}} > 18 \end{cases} \quad \text{(B.54)}$$

- ETU70Hz

$$R_{b\,[\mathrm{bps}]} = \begin{cases} (-0.001415\rho_N{}^4 + 0.0515\rho_N{}^3 - 0.6331\rho_N{}^2 + 5.0886\rho_N + \\ +3.7749) \times 10^4, & 2 \le \rho_{N_{[\mathrm{dB}]}} < 14 \\ (-0.0189\rho_N{}^2 + 0.7093\rho_N - 2.4465) \times 10^5, & 14 \le \rho_{N_{[\mathrm{dB}]}} \le 18 \\ 419730, & \rho_{N_{[\mathrm{dB}]}} > 18 \end{cases} \quad \text{(B.55)}$$

For MIMO 2×2, coding rate of 5/6 and 64QAM, UL throughput is given by [3GPP08e] and [Jaci09]:

- EPA5Hz

$$R_{b\,[\mathrm{bps}]} = \begin{cases} 2861\rho_N + 125.8, & 4 \le \rho_{N_{[\mathrm{dB}]}} < 18 \\ -392.8\rho_N{}^2 + 39780\rho_N - 87830, & 18 \le \rho_{N_{[\mathrm{dB}]}} < 24 \\ -3443\rho_N{}^2 + 163300\rho_N - 1.22 \times 10^6, & 18 \le \rho_{N_{[\mathrm{dB}]}} \le 24 \\ 716032, & \rho_{N_{[\mathrm{dB}]}} > 24 \end{cases} \quad \text{(B.56)}$$

- ETU70Hz

$$R_{b\,[\mathrm{bps}]} = \begin{cases} (0.0011719\rho_N{}^4 - 0.035372\rho_N{}^3 + 0.204\rho_N{}^2 + \\ +3.1745\rho_N - 1.554) \times 10^4, & 4 \le \rho_{N_{[\mathrm{dB}]}} < 18 \\ (-0.01165\rho_N{}^2 + 0.6762\rho_N - 4.566) \times 10^5, & 18 \le \rho_{N_{[\mathrm{dB}]}} \le 24 \\ 495240, & \rho_{N_{[\mathrm{dB}]}} > 24 \end{cases} \quad \text{(B.57)}$$

For MIMO 2×4, coding rate of 1/3 and QPSK, UL throughput is given by [Jaci09] and [3GPP08e]:

- EPA5Hz

$$R_{b\,[\mathrm{bps}]} = \begin{cases} (0.0011\rho_N + 4.7978) \times 2 \times 10^4, & 0 \le \rho_{N_{[\mathrm{dB}]}} < 1 \\ \dfrac{4800000}{50}, & \rho_{N_{[\mathrm{dB}]}} > 1 \end{cases} \quad \text{(B.58)}$$

- ETU70Hz

$$R_{b\,[\mathrm{bps}]} = \begin{cases} 40.14{\rho_N}^3 - 596.25{\rho_N}^2 + 2994.3\rho_N + 88386.2, & 2 < \rho_{N_{[\mathrm{dB}]}} \le 3 \\ 44.6{\rho_N}^3 - 662.5{\rho_N}^2 + 3327\rho_N + 90190, & 3 < \rho_{N_{[\mathrm{dB}]}} \le 6 \\ 959356, & \rho_{N_{[\mathrm{dB}]}} > 6 \end{cases} \quad \text{(B.59)}$$

For MIMO 2×4, coding rate of 3/4 and 16QAM, UL throughput is computed as in [3GPP08e] and [Jaci09]:

- EPA5Hz

$$R_{b\,[\mathrm{bps}]} = \begin{cases} (-0.00702{\rho_N}^2 + 0.17811\rho_N + 2.7726) \times 10^5, & 9 < \rho_{N_{[\mathrm{dB}]}} \le 10 \\ (-0.00741{\rho_N}^2 + 0.188005\rho_N + 2.9267) \times 10^5, & 10 < \rho_{N_{[\mathrm{dB}]}} \le 11 \\ (-0.007644{\rho_N}^2 + 0.19394\rho_N + 3.019) \times 10^5, & 11 < \rho_{N_{[\mathrm{dB}]}} \le 12 \\ (-0.0078{\rho_N}^2 + 0.1979\rho_N + 3.0807) \times 10^5, & 12 < \rho_{N_{[\mathrm{dB}]}} < 18 \\ 432000, & \rho_{N_{[\mathrm{dB}]}} > 18 \end{cases} \quad \text{(B.60)}$$

- ETU70Hz

$$R_{b\,[\mathrm{bps}]} = \begin{cases} -7.25{\rho_N}^5 + 260.6375{\rho_N}^4 - 2950.75{\rho_N}^3 + 10216.7{\rho_N}^2 + \\ \quad +27444.15\rho_N + 67684.55, & 10 < \rho_{N_{[\mathrm{dB}]}} \le 11 \\ 371780.89, & 11 < \rho_{N_{[\mathrm{dB}]}} \le 12 \\ 416845.24, & 12 < \rho_{N_{[\mathrm{dB}]}} \le 13 \\ 441630.63, & 13 < \rho_{N_{[\mathrm{dB}]}} \le 14 \\ 4506435, & \rho_{N_{[\mathrm{dB}]}} > 14 \end{cases} \quad \text{(B.61)}$$

Considering a MIMO 2×4, coding rate of 5/6 and 64QAM, UL throughput is given based on the measurements in [3GPP08e] and [Duar08]:

- EPA5Hz

$$R_{b\,[\mathrm{bps}]} = \begin{cases} 648720, & 17 < \rho_{N_{[\mathrm{dB}]}} \le 18 \\ 691968, & 18 < \rho_{N_{[\mathrm{dB}]}} \le 19 \\ 713592, & 19 < \rho_{N_{[\mathrm{dB}]}} \le 20 \\ 720800, & \rho_{N_{[\mathrm{dB}]}} > 20 \end{cases} \quad \text{(B.62)}$$

- ETU70Hz

$$R_{b\,[\mathrm{bps}]} = \begin{cases} (0.000285{\rho_N}^4 - 0.005537{\rho_N}^3 + 0.01017{\rho_N}^2 + 0.38058\rho_N + \\ +0.9) \times 10^5, \quad 12 < \rho_{N_{[\mathrm{dB}]}} \leq 14 \\ (0.000269{\rho_N}^3 - 0.0182{\rho_N}^2 + 0.4118\rho_N - 2.5431) \times 10^6, \quad 14 < \rho_{N_{[\mathrm{dB}]}} \leq 24 \\ 575556, \quad \rho_{N_{[\mathrm{dB}]}} > 24 \end{cases} \tag{B.63}$$

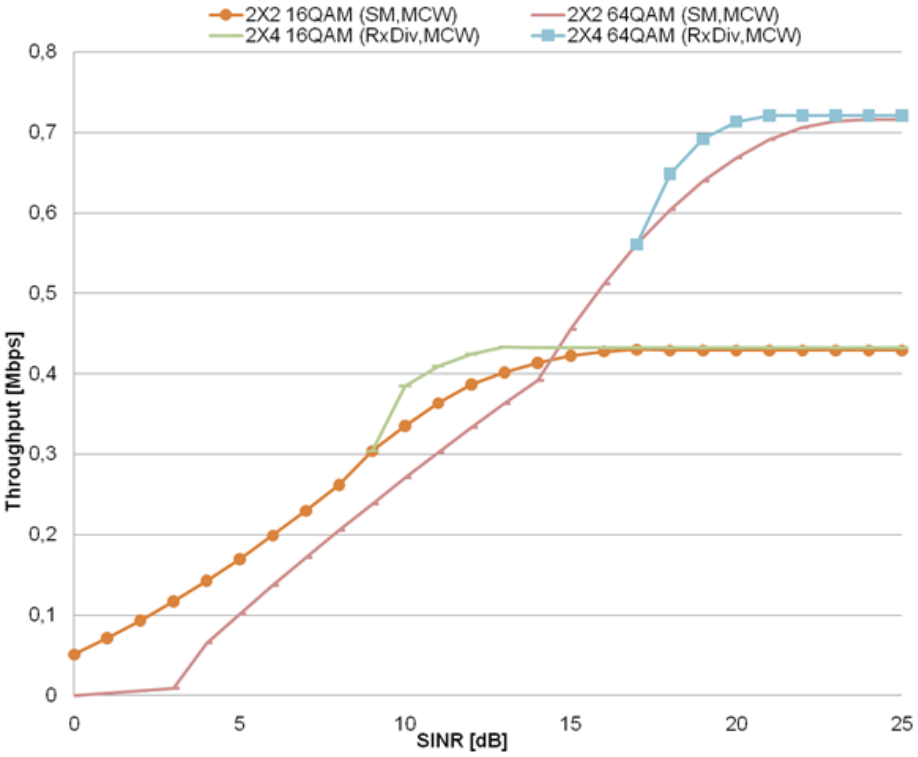

Figure B.7. LTE EPA5Hz uplink physical throughput per RB for two layer 16QAM and 64QAM modulation schemes as a function of SNR.

Annex C – COST231-Walfisch-Ikegami

COST231-Walfisch-Ikegami Model takes both Ikegami and Walfisch-Bertoni models into account, assessed by measurements in European cities. The default situation is shown in Figure C.1.

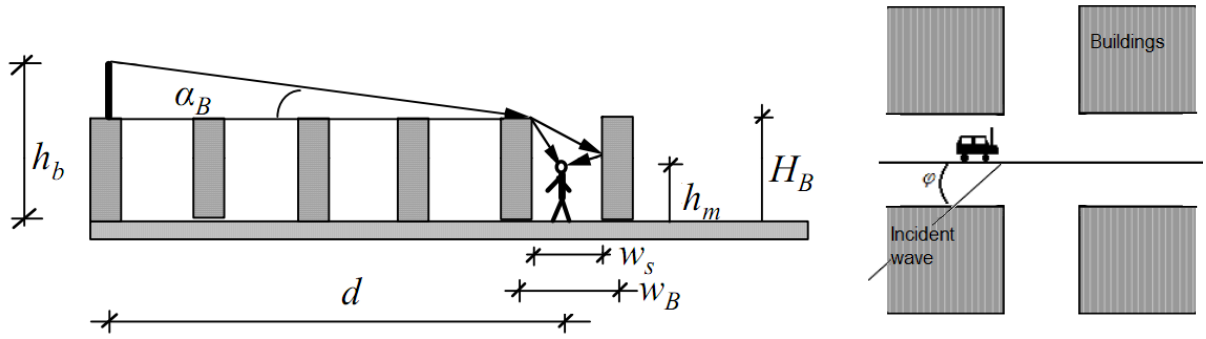

Figure C.1. COST231 Walfisch-Ikegami assumptions and associated definition parameters (extracted from [Corr10]).

The pathloss for Line of Sight (LoS) propagation in a street, i.e., $\varphi = 0$, is given by:

$$L_{p\,[\mathrm{dB}]} = 42.6 + 26\log(d_{[\mathrm{km}]}) + 20\log(f_{[\mathrm{MHz}]}),\ d > 0.02\ \mathrm{km} \quad \text{(C.1)}$$

In other cases, including Non-LoS (NLoS), one has

$$L_{p\,[\mathrm{dB}]} = \begin{cases} L_{0\,[\mathrm{dB}]} + L_{rt\,[\mathrm{dB}]} + L_{rm\,[\mathrm{dB}]}, & L_{rt} + L_{rm} > 0 \\ L_{0\,[\mathrm{dB}]}, & L_{rt} + L_{rm} \le 0 \end{cases} \quad \text{(C.2)}$$

where

- L_0: pathloss in free space propagation,

$$L_{0\,[\mathrm{dB}]} = 32.4 + 20\log(d_{[\mathrm{km}]}) + 20\log(f_{[\mathrm{MHz}]}) \quad \text{(C.3)}$$

- d: distance between BS and MT;
- f: frequency in use;
- L_{rt}: diffraction loss and scatter loss on the rooftop edge to the street;

$$L_{rt\,[\mathrm{dB}]} = L_{bsh\,[\mathrm{dB}]} + k_a + k_d\log(d_{[\mathrm{km}]}) + k_f\log(f_{[\mathrm{MHz}]}) - 9\log(w_{B\,[\mathrm{m}]}) \quad \text{(C.4)}$$

  - w_B: distance between middle points of adjacent street buildings;
  - $L_{bsh\,[\mathrm{dB}]}$: losses due to BS antennas position, whether above of below rooftop level,

$$L_{bsh\,[\mathrm{dB}]} = \begin{cases} -18\log\left(h_{b[\mathrm{m}]} - H_{B[\mathrm{m}]} + 1\right), & h_b > H_B \\ 0, & h_b \le H_B \end{cases} \quad \text{(C.5)}$$

- h_b: BS height;
- H_B: building height.

- k_a: increase of the pathloss for BS antennas below the rooftops of the adjacent buildings,

$$k_a = \begin{cases} 54, & h_b > H_B \\ 54 - 0.8\left(h_{b[\mathrm{m}]} - H_{B[\mathrm{m}]}\right), & d \ge 0.5\mathrm{km}, h_b \le H_B \\ 54 - 1.6\left(h_{b[\mathrm{m}]} - H_{B[\mathrm{m}]}\right), & d < 0.5\mathrm{km}, h_b \le H_B \end{cases} \quad \text{(C.6)}$$

- k_d: dependence of multi-screen diffraction loss versus distance,

$$k_d = \begin{cases} 18, & h_b > H_B \\ 18 - 15\,\frac{h_{b[\mathrm{m}]} - H_{B[\mathrm{m}]}}{H_{B[\mathrm{m}]}}, & h_b \le H_B \end{cases} \quad \text{(C.7)}$$

- k_f: dependence of multi-screen diffraction loss versus frequency,

$$k_f = \begin{cases} -4 + 0.7\left(\frac{f_{[\mathrm{MHz}]}}{925} - 1\right), & \text{urban and suburban} \\ -4 + 1.5\left(\frac{f_{[\mathrm{MHz}]}}{925} - 1\right), & \text{dense urban} \end{cases} \quad \text{(C.8)}$$

- L_{rm}: approximation for multiple screen diffraction loss,

$$L_{rm\,[\mathrm{dB}]} = -16.9 - 10\log\left(w_{s[\mathrm{m}]}\right) + 10\log\left(f_{[\mathrm{MHz}]}\right) + 20\log\left(H_{B[\mathrm{m}]} - h_{m[\mathrm{m}]}\right) + L_{ori[\mathrm{dB}]} \quad \text{(C.9)}$$

- w_s: street width;
- h_m: MT height;
- L_{ori}: street orientation loss,

$$L_{ori\,[dB]} = \begin{cases} -10 + 0.354\varphi, & 0° < \varphi_{[°]} < 35° \\ 2.5 + 0.075(\varphi - 35), & 35° \le \varphi_{[°]} < 55° \\ 4.0 - 0.114(\varphi - 55), & 55° \le \varphi_{[°]} < 90° \end{cases} \quad \text{(C.10)}$$

- φ: street orientation with respect to the direct radio link path.

The model is valid under the defined ranges for

- f ∈ [800, 2000] MHz;
- d ∈ [0.02, 5] km;
- h_b ∈ [4, 50] m;
- h_m ∈ [1, 3] m.

Although the frequency bands for HSPA+ DL are [2110,2170] MHz and for LTE are around 2500 MHz and 2600 MHz, falling off the frequency range considered, this model is still the most adequate model to consider in Urban and Suburban NLoS propagation environments.

The COST231-Walfisch-Ikegami Model standard deviation takes values from 4 dB to 7 dB, and the

error of the model increases as h_b decreases relative to H_B [Corr10]. In absence of specific values, the following are recommended [Corr10]:

- $w_B \in [20, 50]$ m;
- $w_s = w_B/2$;
- $\varphi = 90°$;
- $H_{B\,[\mathrm{m}]} = 3 \times (\#floors) + H_{roof\,[\mathrm{m}]}$;
- $H_{roof\,[\mathrm{m}]} = \begin{cases} 3, & \text{pitched} \\ 0, & \text{flat} \end{cases}$.

Annex D – MIMO Models

Regarding MIMO configurations, Figure D.1, four transmission schemes are possible: SISO, MISO, SIMO and MIMO. In LTE DL, SIMO configurations are employed for transmit diversity while MIMO schemes allow mainly for spatial multiplexing techniques; in UL, SIMO and also Single User MIMO are considered, although requiring two power amplifiers in the MT.

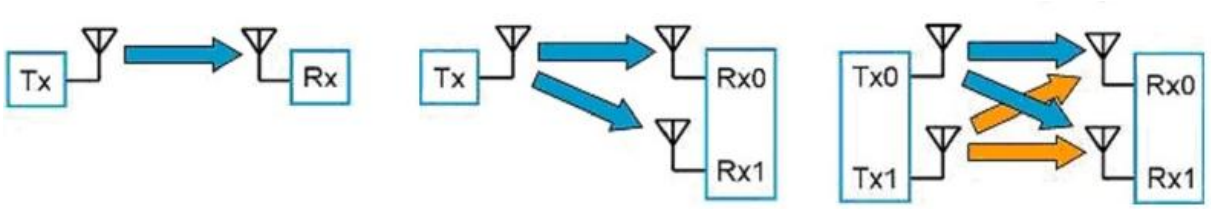

(a) SISO. (b) SIMO. (c) MIMO.

Figure D.1. Different radio transmission schemes, SISO, SIMO, MISO and MIMO (adapted from [Agil11]).

In general, the performance of MIMO is dependent on a number of factors such as the state of the wireless channel (e.g. low versus high scattering), the signal quality (measured by the SINR), the speed of the MT, and the correlation of the received signals at the receiving antennas. Therefore, different MIMO modes will be more effective than others depending on these critical factors.

A key factor to the performance of MIMO is the number of spatial layers of the wireless channel which allows to highly improve spectral efficiency. Spatial layers are born out of the multipath and scattering environment between transmitters and receivers. Simultaneously, the increase in data rate of a MIMO systems is linearly proportional with the minimum number of transmit and receive antennas subject to the rank limit, i.e., the number of independent spatial layers. In plain LoS conditions, the channel matrix rank is one and hence, even with 4 antennas the spectral efficiency of the channel is not increased.

Figure D.2 illustrates the difference between having rank one or rank 2 transmission, for a system with two receiving antennas, by comparing its SINR levels to the reference average SINR measured at the antenna. While the average SINR is measured at the terminal of any of the receiving antennas, rank 1 SINR is the SINR measured after combining the signals received by the two antennas and rank 2 SINR is the one measured separately for each MIMO stream. Hence, when using a rank 1 transmission one is broadly using a receive (or also transmit) diversity scheme, generally adequate for poor channel conditions, obtaining a higher rank 1 SINR. On the other hand, for rank 2 transmission, two ranks or transmission streams are employed and thus, being the user's signal power divided in two streams, measured rank 2 SINR is lower than the average SINR. Although providing for higher transmission rates, the latter is only adequate in good channel conditions.

For LTE, seven MIMO modes are defined for the downlink path [Khan09]:

- Mode 1 - Single stream.
- Mode 2 - Transmit diversity.
- Mode 3 - Open loop spatial multiplexing.
- Mode 4 - Closed loop spatial multiplexing.
- Mode 5 - Multi-User MIMO.
- Mode 6 - Closed loop Rank 1 with pre-coding.
- Mode 7 - Single antenna port.

Using the first mode, a single data stream (codeword) is transmitted on one antenna and received by either one (SISO) or more antennas (SIMO, receive diversity). In the second mode, the same information stream is transmitted on multiple antennas (LTE supports 2 or 4 antennas), being the information coded differently on each antenna by using Space-Frequency Block Codes (SFBC). Employing SFBC, data symbols are repeated over different subcarriers on each antenna. Since it is a single-layer transmission, it does not improve the peak rate but instead the signal quality becomes more robust and lower signal to interference plus noise ratio (SINR) is required to decode the signal.

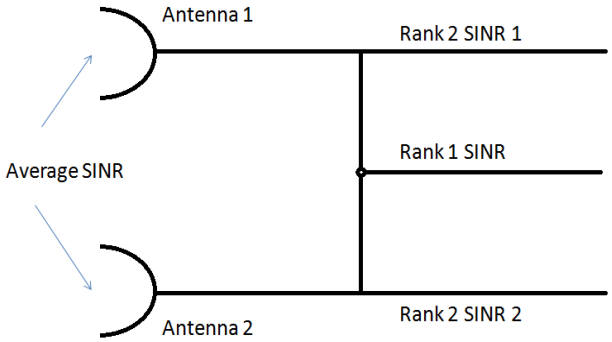

Figure D.2. Average SINR, rank 1 SINR and rank 2 SINR levels (extracted from [Opti11]).

In LTE, modes 3 and 4 are both classified as SU-MIMO schemes, specified for the configuration with two or four transmit antennas in the DL, which support up to two or four layers respectively. For the UL only a maximum of two transmit antennas is possible. As for mode 3, named open loop spatial multiplexing, two information streams (and usually two code words) are transmitted over two or more antennas (up to 4 in LTE). No explicit UE feedback is used, and only the wideband Rank Indication (RI) is transmitted by the UE, besides de CQI, and used by the BS to select the number of spatial layers.

Whereas in mode 3 open loop was employed in mode 4 the Pre-coding Matrix Indicator (PMI) is additionally fed back from the handset to the base station. This feedback mechanism allows the transmitter to pre-code the data to optimise transmission over the wireless channel so the signals at the receiver can be easily separated into the original streams. This method is expected to be the highest performing mode of MIMO in LTE, although both SU-MIMO schemes provide for much better peak throughput than with transmit diversity.

The benefits of open and closed loop spatial multiplexing schemes are mostly achieved when the received signal quality (measured SINR) is at its highest values. Thus, poor SINR conditions at the cell

edge reduce the benefits of spatial duplexing modes and closed-loop rank 1 or transmit diversity become more attractive. Furthermore, transmit diversity is also more attractive than closed-loop and open-loop spatial multiplexing schemes in an environment where signal scattering is low, e.g., in LoS transmission. Moreover, the performance of spatial multiplexing techniques is best in case of low signal correlation, placing restrictions on the placement of the antennas. Beamforming techniques are alternatively effective in high correlation environments, where the signal comes with low angular spread such as in open areas environments.

The speed of the MT also impacts the performance of closed loop MIMO systems. In general, the latter provides better spectral efficiency than open loop spatial multiplexing as channel knowledge is fed back to the transmitter allowing for optimal data stream coding. However, as the speed of the MT increases and channel conditions change more rapidly, this advantage is lost over to the open loop spatial multiplexing mode, which is simpler to implement. Transmit diversity is also robust to speed while its performance in low scattering environment and high SINR does not degrade as with open loop spatial multiplexing. Table D.1 summarises the decision matrix to select MIMO mode most suitable for the usage scenario, from the main modes used.

Table D.1. Decision matrix for the main LTE MIMO modes (adapted from [Tele09]).

MIMO Mode	SINR	Scattering	Speed
Transmit Diversity	Low	Low	High
Open-Loop Spatial Multiplexing	High	High	High
Closed-Loop Spatial Multiplexing	High	High	Low
Closed-Loop Rank=1 Pre-coding	Low	Low	Low

Knowing the MIMO functioning in LTE, the Relative MIMO Gain (RMG) Model was employed in order to predict the capacity improvement of the usage of MIMO configurations, [KuCo08]. Based on the Geometrically Based Single Bounce (GBSB) channel model, the authors derive simulation results for the capacity gains of MIMO, for different configurations.

The RMG is defined as the ratio between the MIMO and SISO throughput capacity of a given radio link:

$$G_{M/S} = \frac{C_{MIMO}}{C_{SISO}} \quad \text{(D.1)}$$

where:

- C_{MIMO}: capacity of the MIMO system;
- C_{SISO}: capacity of the SISO system, given by the Shannon capacity formula:

$$C_{SISO} = \log_2(1 + \rho_N) \quad \text{(D.2)}$$

The RMG model is a statistical model developed to estimate the distribution of the RMG, based on simulation results. This distribution can be modelled by sigmoid functions, which are completely defined by their mean and variance, as further explained in [KuCo08]. Both the mean value and the variance depend on the number of Tx and Rx antennas and on the distance between those.

Furthermore, for a certain number of Tx and Rx antennas, the variance is very low in each cell range, i.e., the slope of the sigmoid function has been assumed to be constant within a cell type.

Table D.2 shows the results approximated for the scenarios with either 2 Tx and/or 2 Rx antennas, used to derive the throughput expressions from the ones in Annex B, Subsection B.2. For these cases, the cell type is not very relevant, hence, the configurations can be defined for all distances between 10 m and 2400 m.

Table D.2. Mean value of μ_{RMG} for systems with N_R=2, independent of cell type (extracted from [KuCo08]).

N_T	μ_{RMG}	$\overline{\varepsilon_r}$ [%]	$\overline{\varepsilon_r^2}$ [%]
2	1.54	1.1	0.1
4	1.70	1.1	0.2
8	1.84	0.4	0.4
16	1.77	-2.1	3.9

For other configurations results of the mean value and variance are presented as a function of the distance between the antennas, Table D.3. For the estimation of the throughput expressions for these MIMO configurations, the maximum value of the mean value was considered.

Table D.3. Mean value of μ_{RMG} for systems with N_T>2 and N_R>2 for different cell types ([KuCo08]).

(a) Pico-cell.

$N_T \times N_R$	range [m]	μ_{RMG}	$\overline{\varepsilon_r}$ [%]	$\overline{\varepsilon_r^2}$ [%]
4×4	10-31	$50.32d_{[\mathrm{km}]}$+1.77	-0.1	0.1
	31-57	3.36		
8×4	10-31	$52.56d_{[\mathrm{km}]}$+1.84	0.0	0.4
	31-57	3.50		
8×8	10-29	$117.59d_{[\mathrm{km}]}$+2.11	2.9	2.6
	29-59	3.36		
16×4	10-28	$76.80d_{[\mathrm{km}]}$+1.28	1.7	1.0
	28-58	3.50		
16×8	10-28	$138.23d_{[\mathrm{km}]}$+1.51	4.2	3.6
	28-58	5.43		
16×16	10-27	$225.37d_{[\mathrm{km}]}$+1.71	5.9	7.5
	27-42	7.86		

Table D.4 (cont.). Mean value of μ_{RMG} for systems with N_T>2 and N_R>2 for different cell types ([KuCo08]).

(b) Micro-cell.

$N_T \times N_R$	range [m]	μ_{RMG}	$\overline{\varepsilon_r}$ [%]	$\overline{\varepsilon_r^2}$ [%]
4×4	57-686	-2.00$d_{[km]}$+3.47	-0.1	0.4
8×4	57-680	-2.08$d_{[km]}$+3.62	0.0	0.4
8×8	59-703	-4.88$d_{[km]}$+5.86	3.0	2.6
16×4	58-692	-2.74$d_{[km]}$+3.66	1.7	1.0
16×8	58-675	-5.42$d_{[km]}$+5.75	4.2	3.6
16×16	42-654	-8.61$d_{[km]}$+8.23	5.9	7.5

(c) Macro-cell

$N_T \times N_R$	range [m]	μ_{RMG}	$\overline{\varepsilon_r}$ [%]	$\overline{\varepsilon_r^2}$ [%]
4×4	686-2400	2.10	-0.1	0.4
8×4	680-2400	2.21	0.0	0.4
8×8	703-2400	2.42	3.0	2.6
16×4	692-2400	1.76	1.7	1.0
16×8	675-2400	2.09	4.2	3.6
16×16	654-2400	2.59	5.9	7.5

For the case of SIMO configurations a similar channel capacity gain can be derived based on the results in [OeCl08]:

$$G_{SIMO} = \frac{\log_2(1 + g_a \cdot \rho_N)}{C_{SISO}} \tag{D.3}$$

where:

- g_a: array gain defined for a certain number N_R of receiving antennas. Considering simple receive diversity scheme via selection combining, it is given by:

$$g_a = \sum_{n=1}^{N_R} \frac{1}{n} \tag{D.4}$$

Assuming receive diversity via Maximal Ratio Combining (MRC), it is defined as:

$$g_a = N_R \tag{D.5}$$

Thus, estimates for the relative SIMO capacity gain are obtained, assuming for this thesis that a MRC scheme is used, allowing for further extending the results in Annex B for SIMO antenna configurations.

Annex E – Simulator User's Manual

This annex includes a reference manual to the Single Cell Model interface, implemented for the simulator. The main objectives behind the Graphical User Interface create (GUI) were to allow a modular edition of the different simulation components of the simulator, easily, fast enough, prone to user's errors and allowing for simulations using input parameters' files or directly put into the simulator by hand.

The interface developed follows the same simulator core structure referred earlier. The simulators' main window shows the four components: channel model simulation, propagation model simulation and the system's simulators', UMTS and LTE, as shown in Figure E.1. For each of the four modules the user can either load the respective parameters input file into the simulator, by using the 'Path' button, or input the parameters himself by hand, by using the 'Input' button.

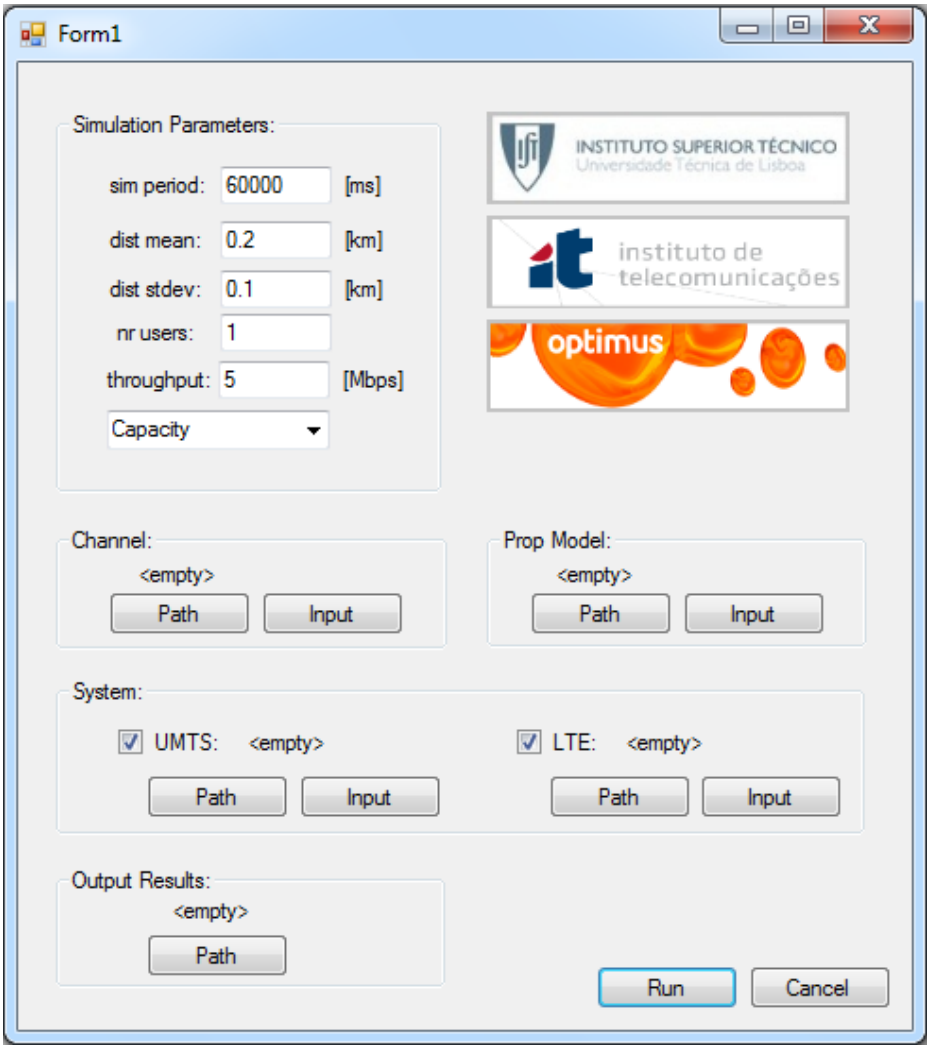

Figure E.1. Main simulator window: simulation parameters, channel, propagation model, systems' and output results path definition..

For the former, the user selects the respective '.csv' files, as input for the respective module, assuring that these follow the normalised simple format, as outlined in the sample files provided with the simulator. For the latter case, a dedicated parameters window will open for each module, already filled in with the default parameters considered. If the use does not load any input file neither inputs the parameters by hand, the default parameters will be the ones considered.

Regarding the systems' simulation, the user is given the option to run the simulation for each system independently or separately for any of the UMTS or LTE systems. For comparison purposes, if the two simulators are used together, both will use the same channel and propagation models selected. This implementation option follows along with the main simulators' objective of comparing the two systems, but if different single simulations of each system with varying channel and propagation models are needed, running the simulator for each system at a time is suggested.

Accordingly, the output results will only be presented for the selected system or systems. The output path for the output file can also be selected by the user, using the specific 'Path' button, as long as the output file name chosen follows the considered '.csv' extension.

For the UMTS and LTE simulators, input windows are the ones presented in Figure E.2 and Figure E.3, respectively, and the input parameters are divided in system parameters and link budget parameters. The default values are the ones already presented in Subsection 4.1.

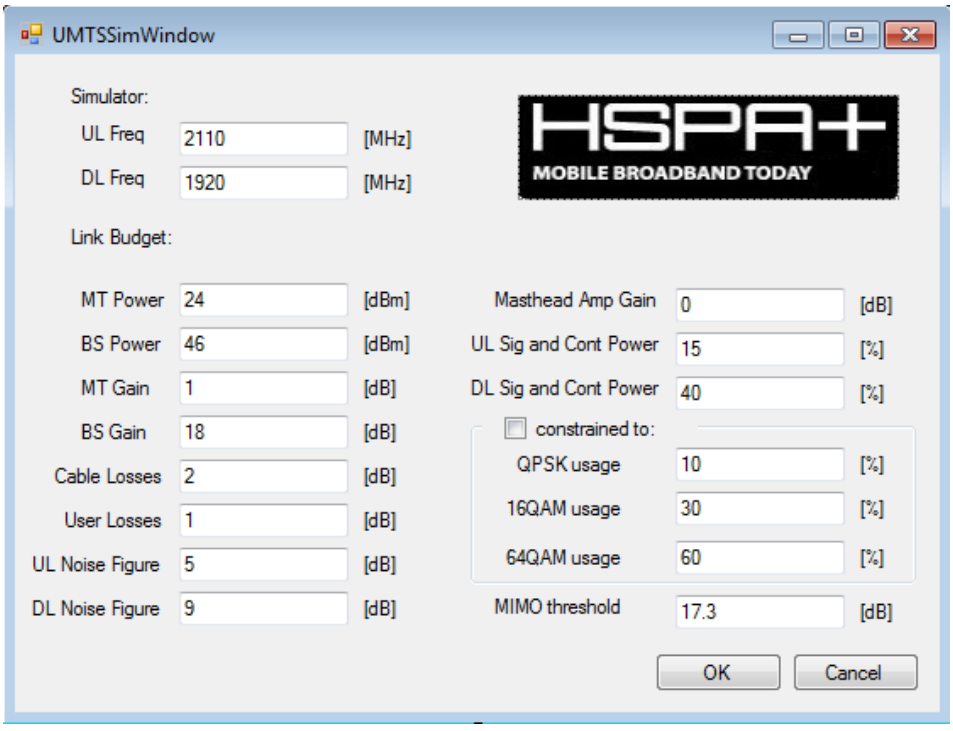

Figure E.2. UMTS/HSPA+ parameters input window.

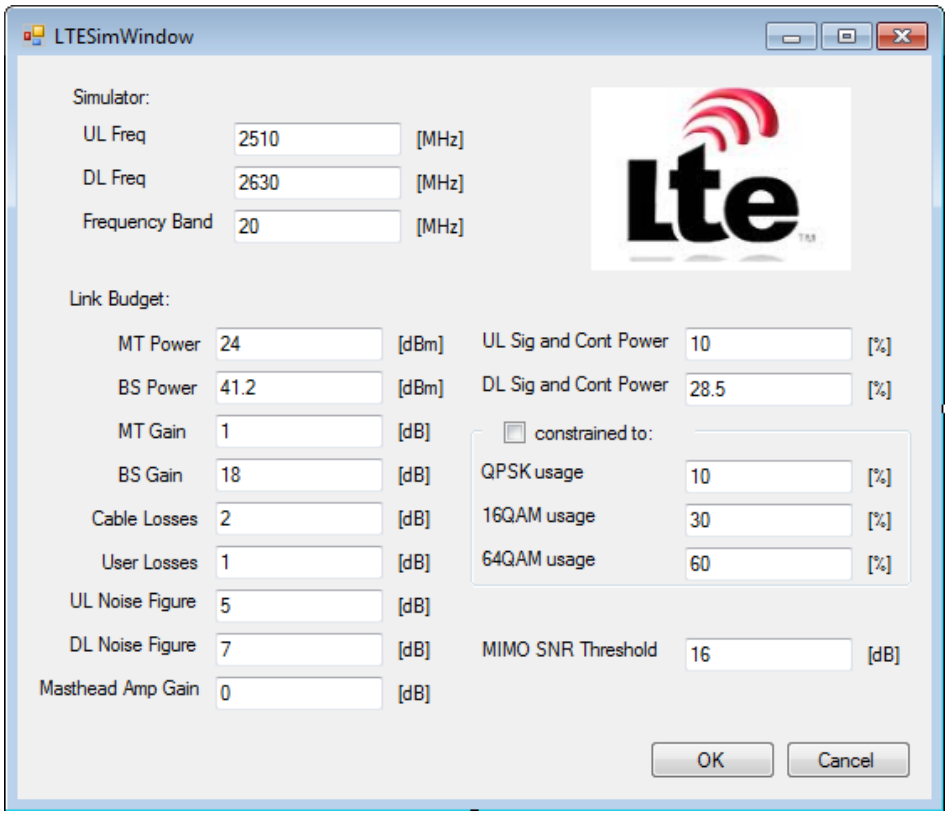

Figure E.3. LTE parameters input window.

Regarding the channel and propagation model simulation, the input windows are the ones shown in Figure E.4. Again, default parameters shown are the ones referred in Subsection 4.1.

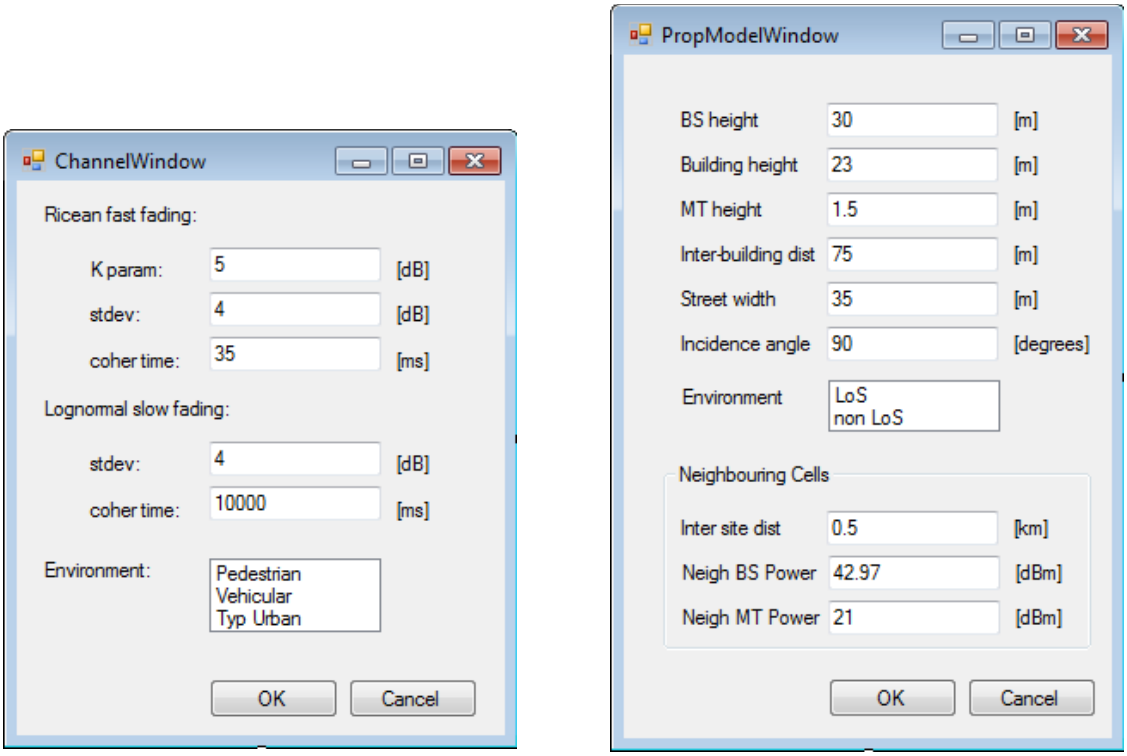

Figure E.4. Channel model and Propagation Model parameters input windows.

Annex F – Additional Results

Additional measured and simulation results, for both UMTS and LTE, are presented in this annex. These were previously referenced throughout previous analyses and constitute a complement to them.

Table F.1. Distance to serving BS mean and standard deviation, for different environments.

Parameter \ Environment	Axial	Urban	Dense Urban
μ_{dist} [km]	0.335	0.314	0.269
σ_{dist} [km]	0.220	0.162	0.190

Table F.2. ISDs for varying environment.

Parameter/Environment	Axial	Urban	Dense Urban
μ_{ISD} [km]	0.816	0.528	0.317
σ_{ISD} [km]	0.192	0.152	0.016

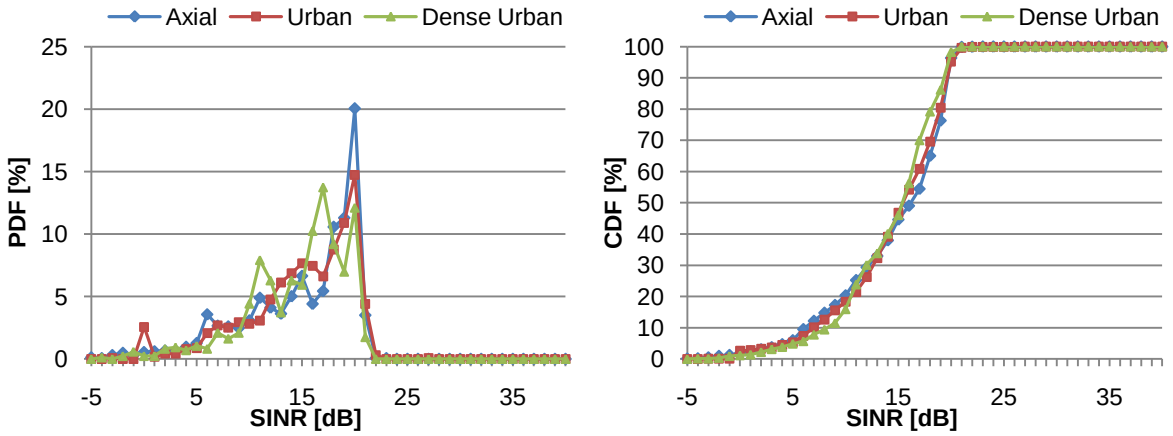

(a) PDF. (b) CDF.

Figure F.1. SINR statistics of DL mobility measurements results for different environments.

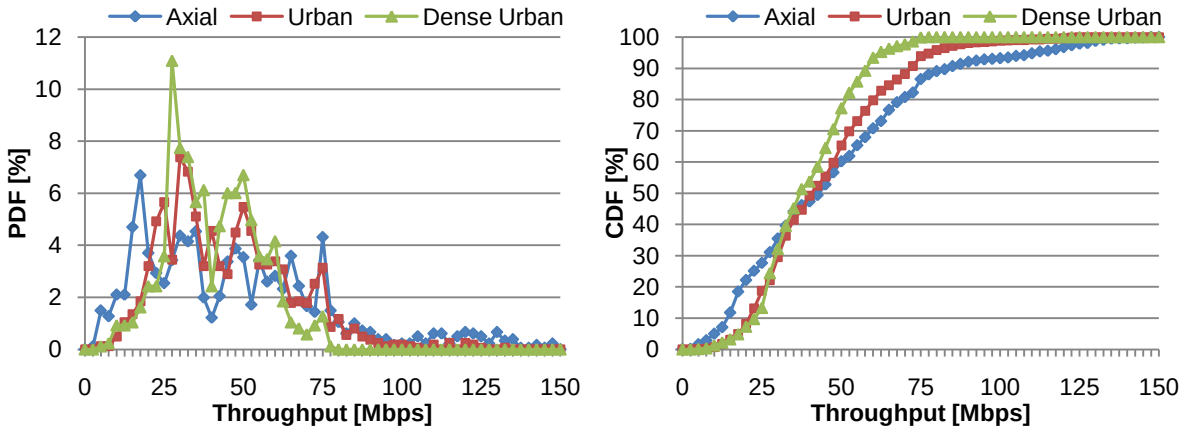

(a) PDF. (b) CDF.

Figure F.2. Throughput statistics of DL mobility measurements results for different environments.

Table F.3. SINR's and throughput's mean and standard deviation of DL mobility measurements, for different environments.

Parameter \ Environment	Axial	Urban	Dense Urban
μ_{SINR} [dB]	14.41	14.75	14.18
σ_{SINR} [dB]	5.40	4.53	4.57
$\mu_{Throughput}$ [Mbps]	47.30	43.72	38.84
$\sigma_{Throughput}$ [Mbps]	30.24	20.08	14.09

Table F.4. Serving cell and detected cell RSRP difference given as a function of distance to BS, obtained by curve fitting.

Fitted equation	R^2
$-0.0064d_{[\mathrm{m}]} + 6.6679$	0.3004

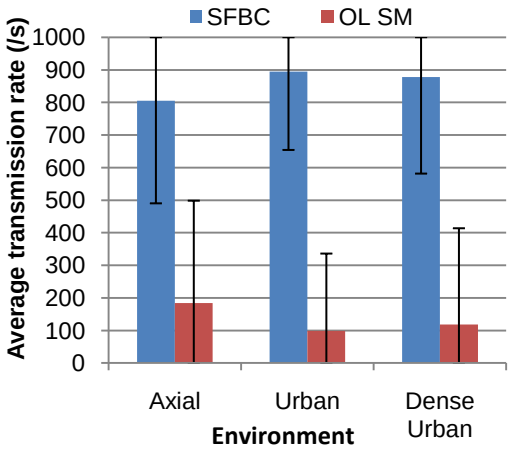

Figure F.3. Transmission mode statistics analysis for mobility measurements in different environments.

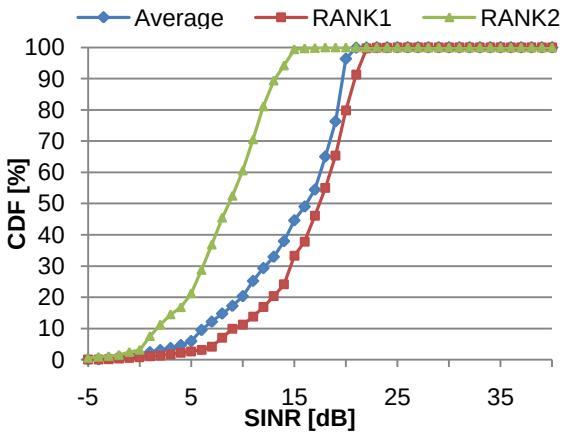

Figure F.4. SINR statistics for average SINR, Rank1 SINR and RANK2 SINR, from mobility measurements in the Axial environment.

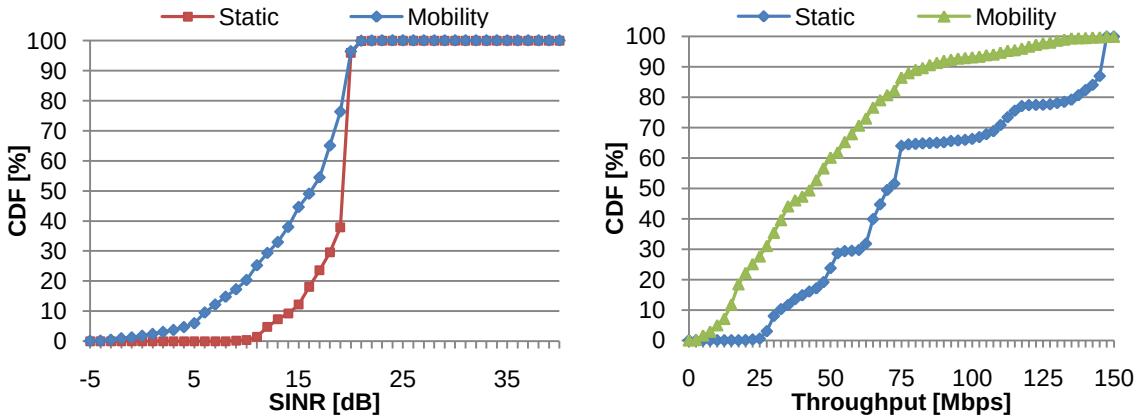

(a) SINR. (b) Throughput.

Figure F.5. CDFs of DL mobility and static measurements' results for the Axial environment.

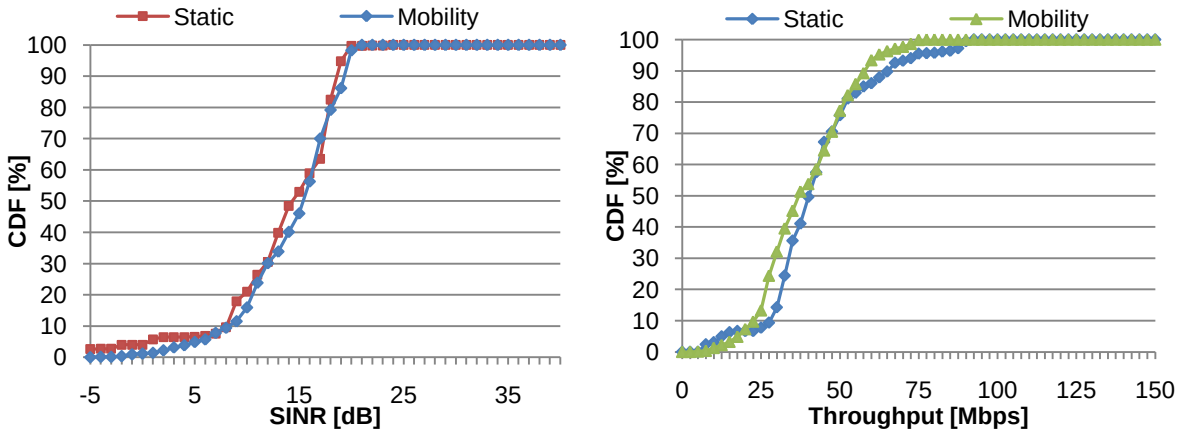

(a) SINR. (b) Throughput.

Figure F.6. CDFs of DL mobility and static measurements results for the Dense Urban environment.

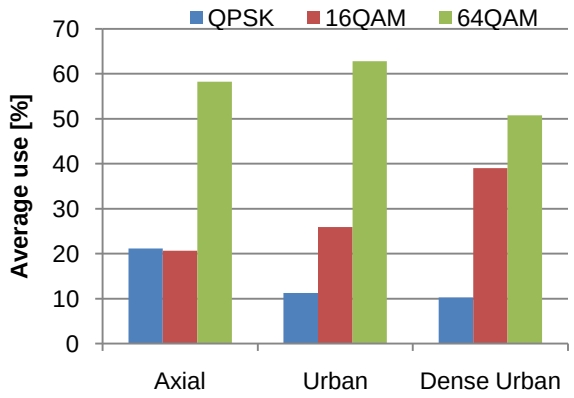

Figure F.7. Average modulation usage analysis of DL mobility measurements' results for different environments.

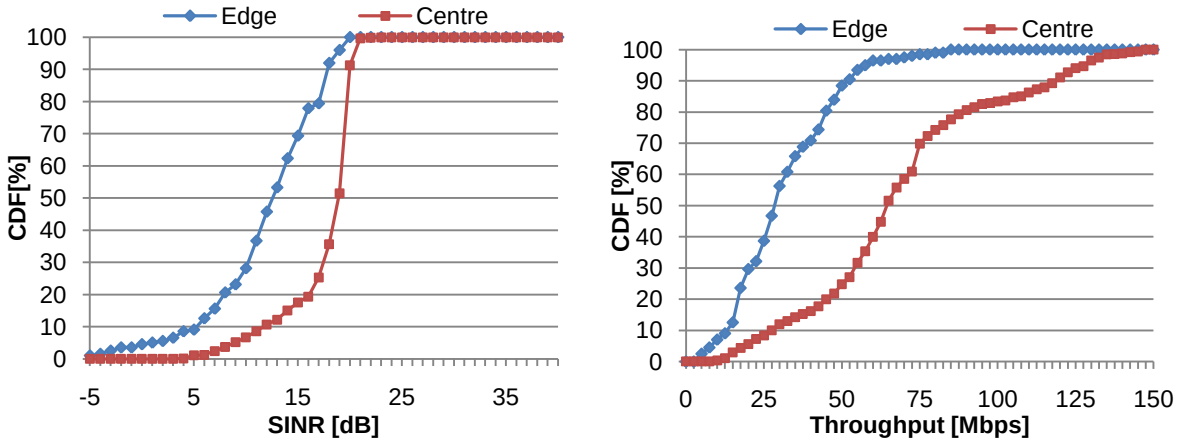

(a) SINR. (b) Throughput.

Figure F.8. Cell edge versus cell edge statistics, from mobility measurements in the Axial environment.

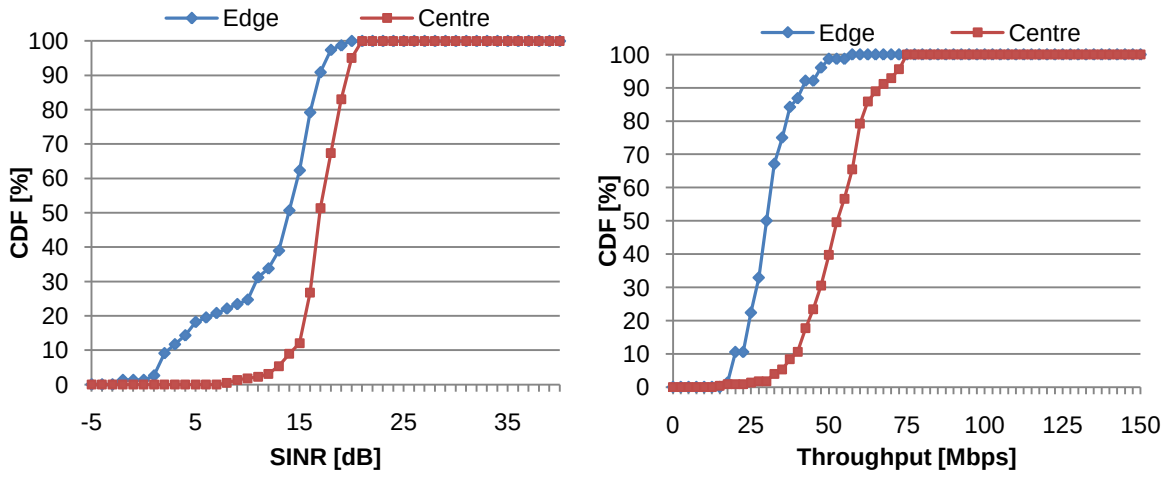

(a) SINR. (b) Throughput.

Figure F.9. Cell edge versus cell edge statistics, from mobility measurements in the Dense Urban environment.

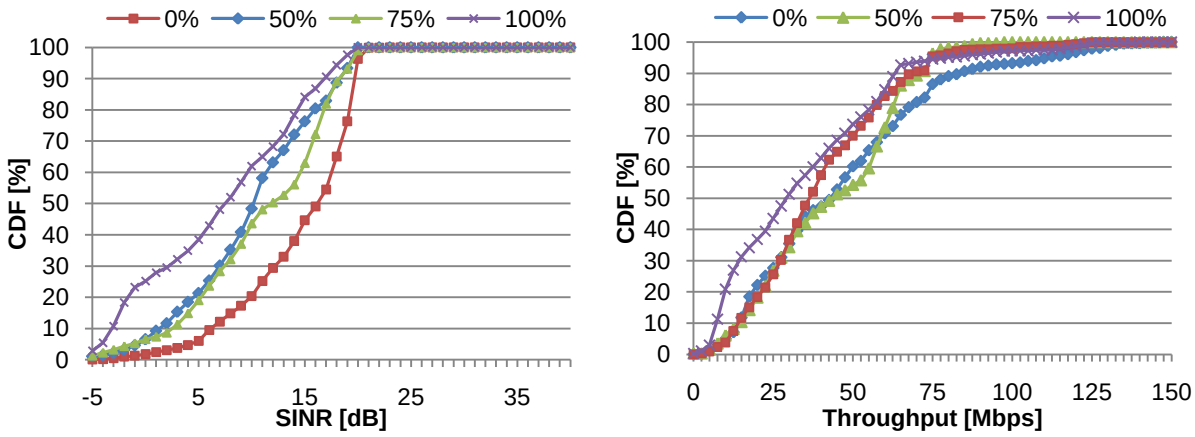

(a) SINR. (b) Throughput.

Figure F.10. CDFs of DL measurements results, for varying load, in the Axial environment.

Table F.5. SINR's and throughput's mean and standard deviation for varying load scenarios in the Axial environment.

Parameter \ Load	0%	50%	75%	100%
μ_{SINR} [dB]	14.41	10.94	9.93	7.01
σ_{SINR} [dB]	5.40	6.39	6.13	7.38
$\mu_{Throughput}$ [Mbps]	47.30	42.89	40.00	34.24
$\sigma_{Throughput}$ [Mbps]	30.24	21.47	21.85	25.85

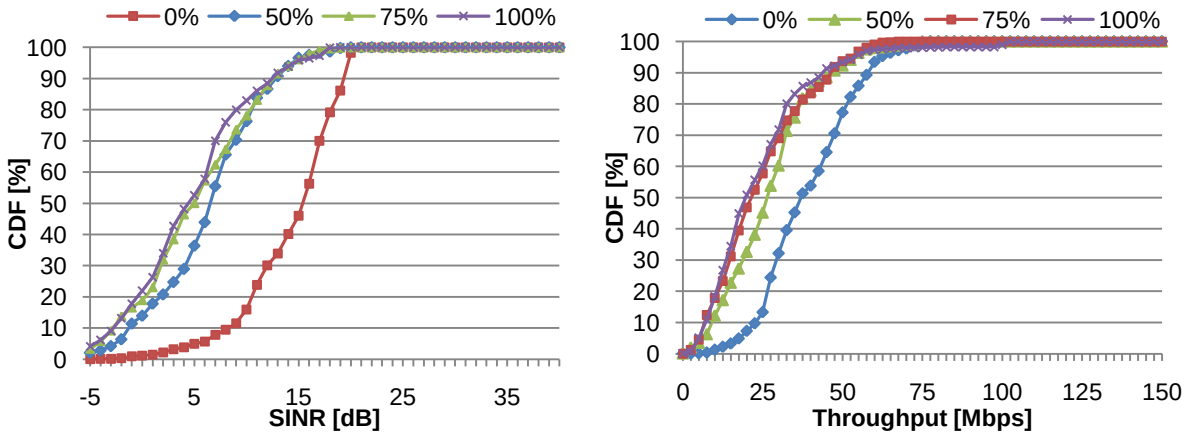

(a) SINR. (b) Throughput.

Figure F.11. CDFs of DL measurements results, for varying load, in the Dense Urban environment.

Table F.6. SINR's and throughput's mean and standard deviation for varying load scenarios in the Dense Urban environment.

Parameter \ Load	0%	50%	75%	100%
μ_{SINR} [dB]	14.18	6.19	5.02	4.49
σ_{SINR} [dB]	4.57	5.20	5.72	5.67
$\mu_{Throughput}$ [Mbps]	38.84	27.25	24.15	23.69
$\sigma_{Throughput}$ [Mbps]	14.09	13.98	14.55	16.92

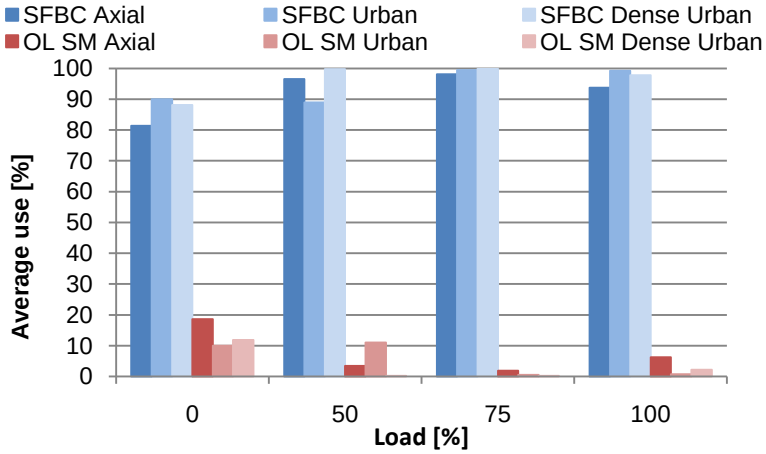

Figure F.12. Transmission mode average use regarding cell load, for different environments.

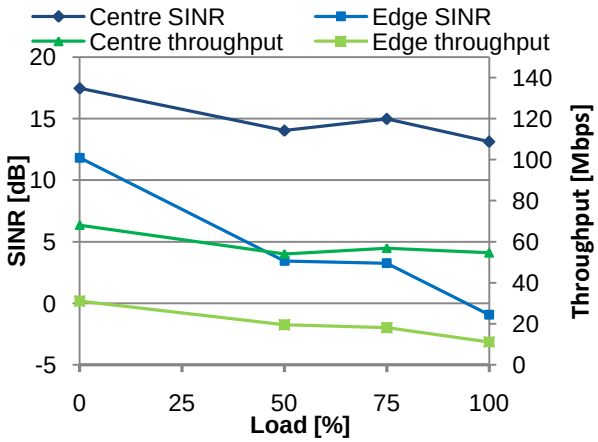

Figure F.13. Cell centre versus cell edge average SINR and average throughput as a function of load, for the Axial environment.

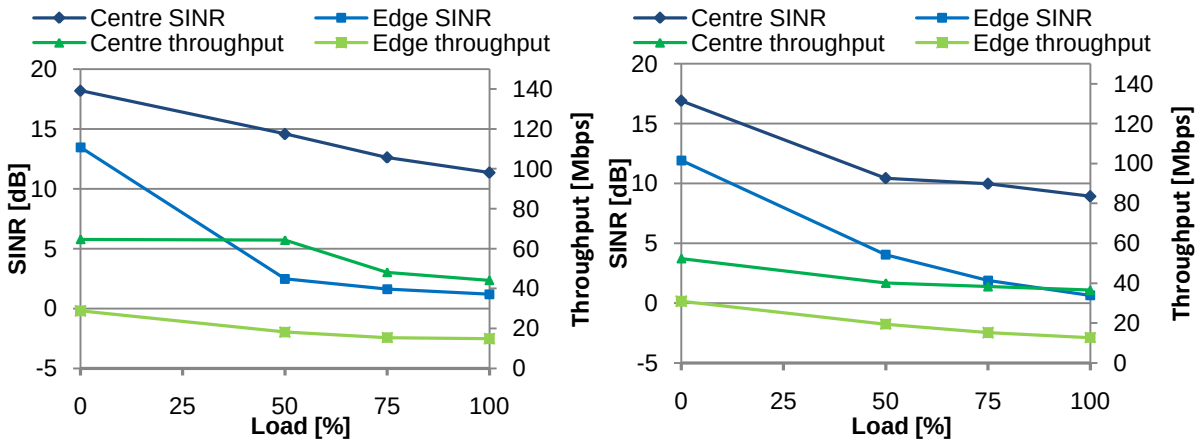

(a) Urban. (b) Dense Urban.

Figure F.14. Cell centre versus cell edge average SINR and average throughput as a function of load, for the Urban and Dense Urban environments.

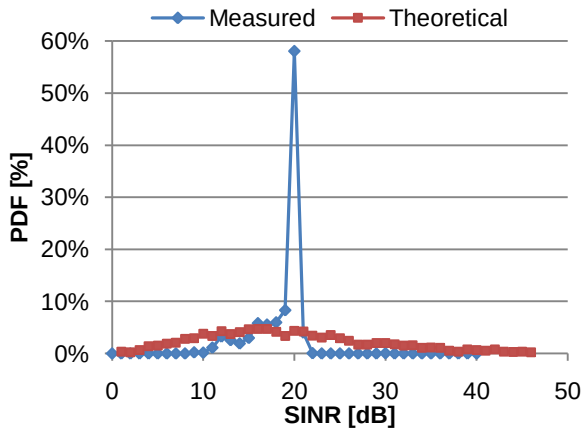

Figure F.15. DL SINR PDFs of measured and simulated results for the Axial pedestrian scenario.

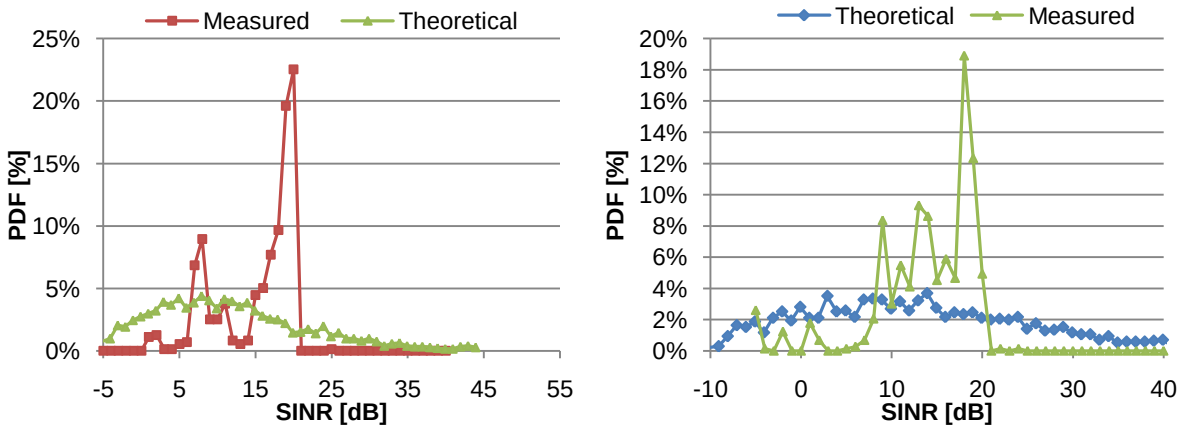

(a) Urban (b) Dense Urban

Figure F.16. DL SINR PDFs of measured and simulated results for the pedestrian channel of the Urban and Dense Urban environments.

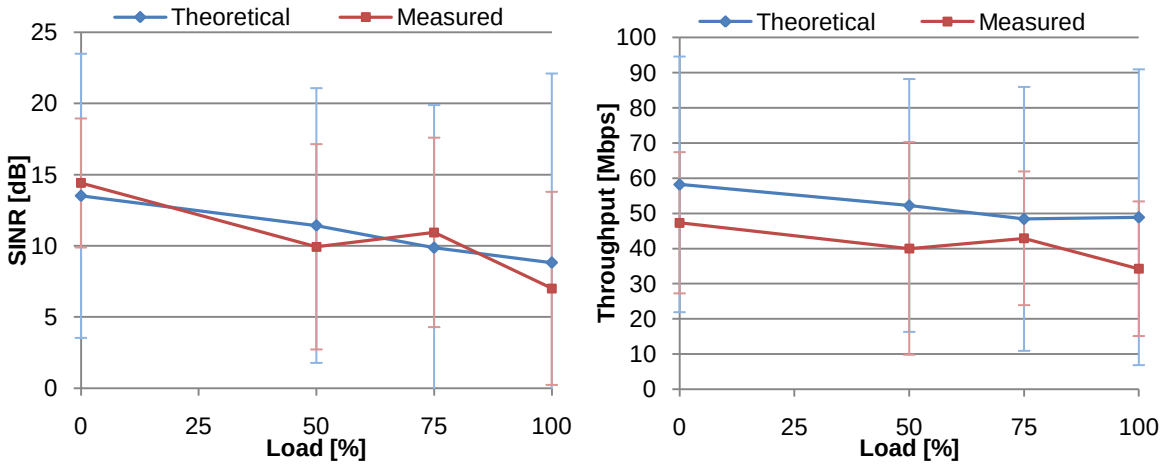

(a) SINR. (b) Throughput.

Figure F.17. Simulated and measured results for the Axial vehicular scenario in DL, for varying load.

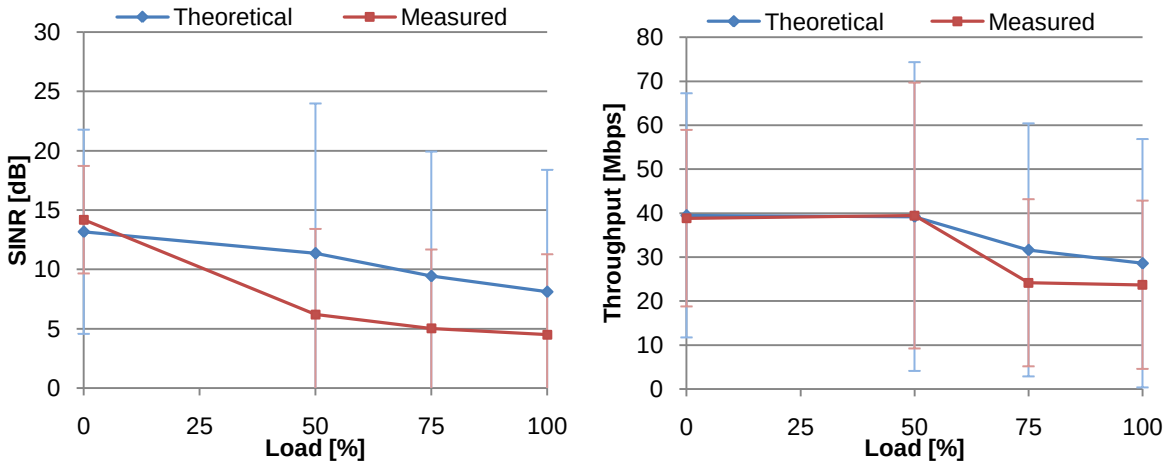

(a) SINR. (b) Throughput.

Figure F.18. Simulated and measured results for the Dense Urban vehicular scenario in DL, for varying load.

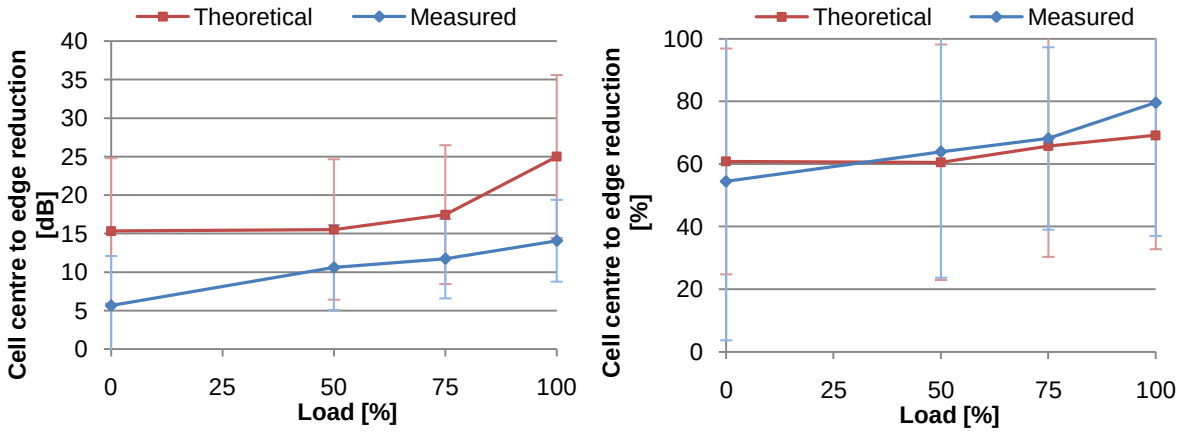

(a) SINR. (b) Throughput.

Figure F.19. Simulated and measured results for the difference between cell centre to cell edge in the Axial vehicular scenario, for varying load.

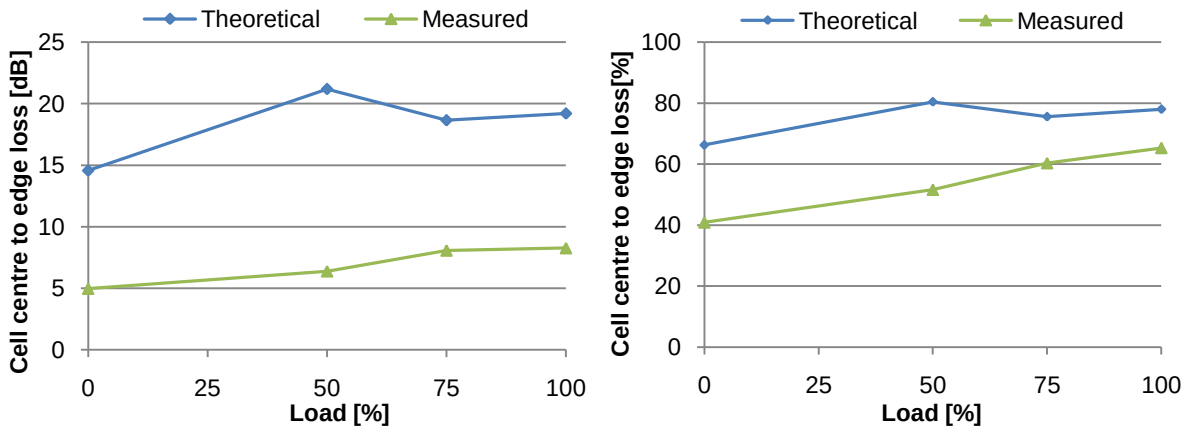

(a) SINR. (b) Throughput.

Figure F.20. Simulated and measured results for the difference between cell centre to cell edge DL in the Dense Urban vehicular scenario, for varying load.

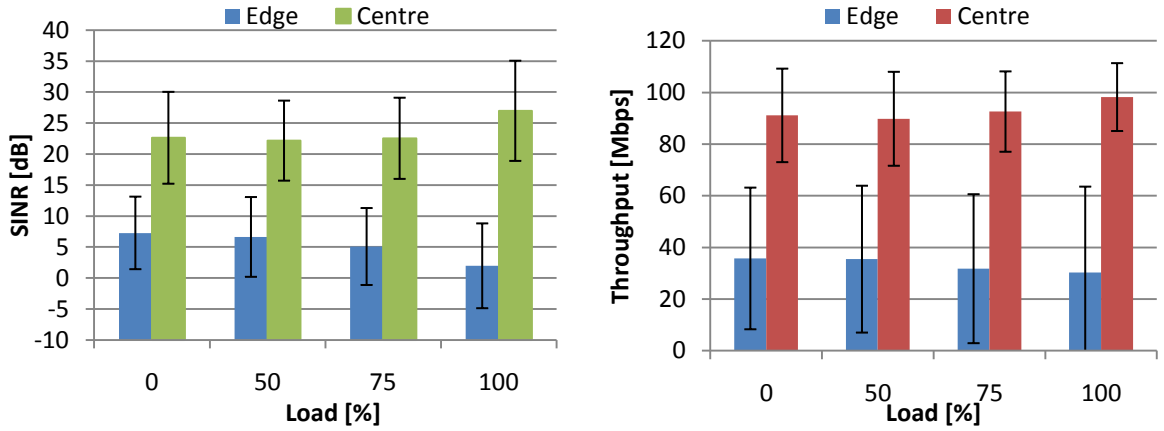

(a) SINR. (b) Throughput.

Figure F.21. Simulated cell edge versus cell centre results for DL of the Axial vehicular scenario, for varying load.

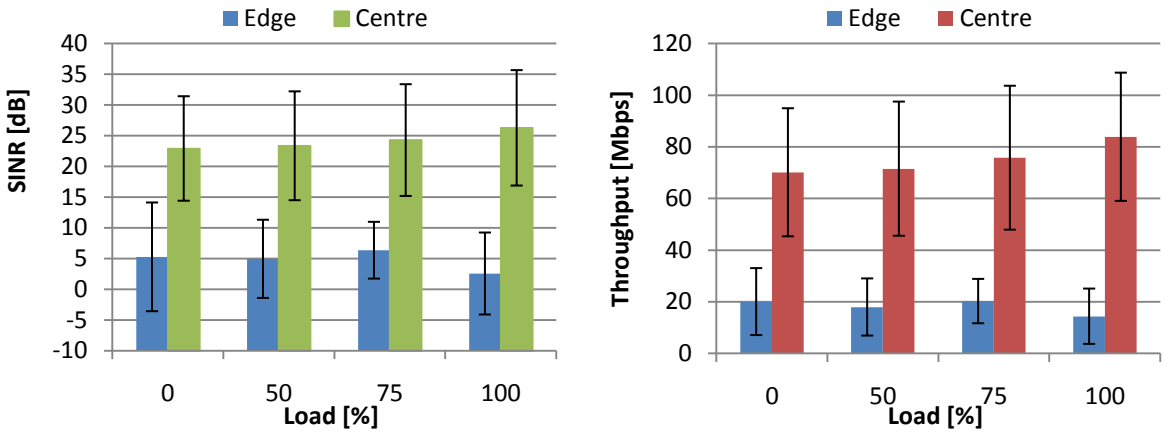

(a) SINR. (b) Throughput.

Figure F.22. Simulated cell edge versus cell centre results for DL of the Urban vehicular scenario, for varying load.

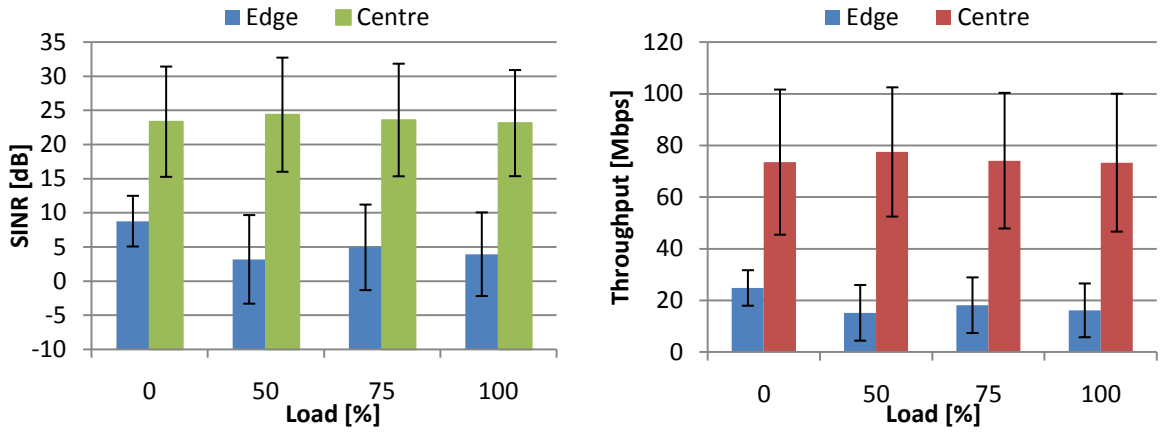

(a) SINR. (b) Throughput.

Figure F.23. Simulated cell edge versus cell centre results for DL of the Dense Urban vehicular scenario, for varying load.

Table F.7. Average throughput ratio as a function of number of cell users, obtained by curve fitting.

Environment	Average throughput ratio	R^2
LTE UFR	$1.8929 \ln(N_u) + 1.3063$	0.9764
LTE ICIC	$2.5531 \ln(N_u) + 2.0143$	0.9829
LTE ICIC 4×4	$4.2162 \ln(N_u) + 3.1559$	0.9814

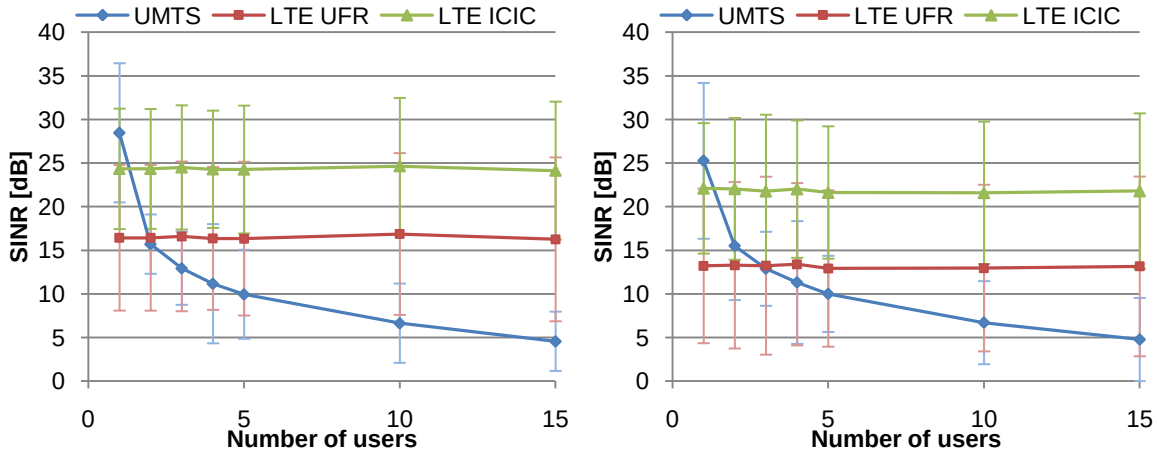

(a) Axial. (b) Dense Urban.

Figure F.24. LTE and UMTS DL SINR for the Axial and Dense Urban pedestrian scenarios, for varying users' number.

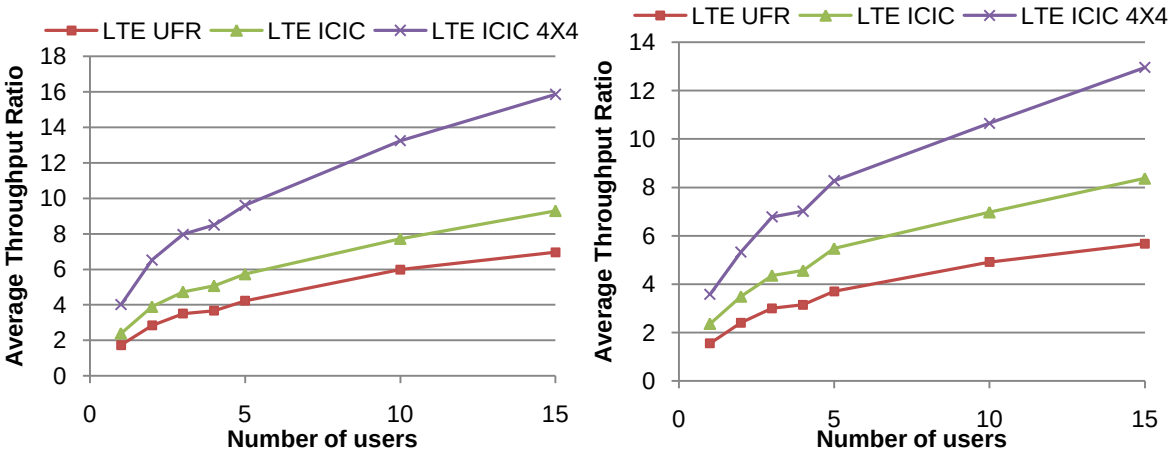

(a) Axial. (b) Dense Urban.

Figure F.25. UMTS to LTE throughput ratio for the Axial and Dense Urban pedestrian scenarios, for varying users' number.

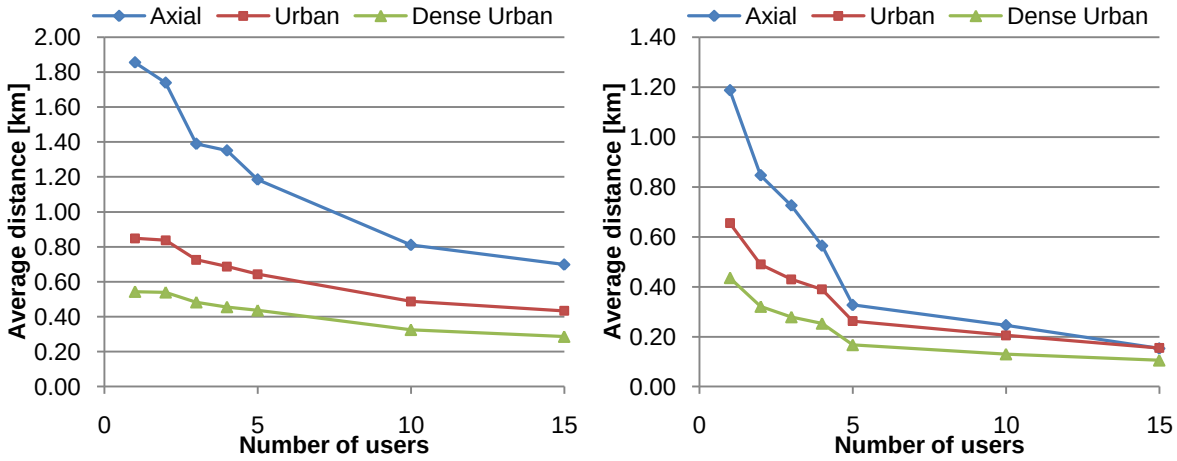

(a) 1Mbps. (b) 5Mbps.

Figure F.26. LTE and UMTS coverage results for LTE UFR's DL in the pedestrian scenario, for required 1Mbps and 5Mbps throughput service.

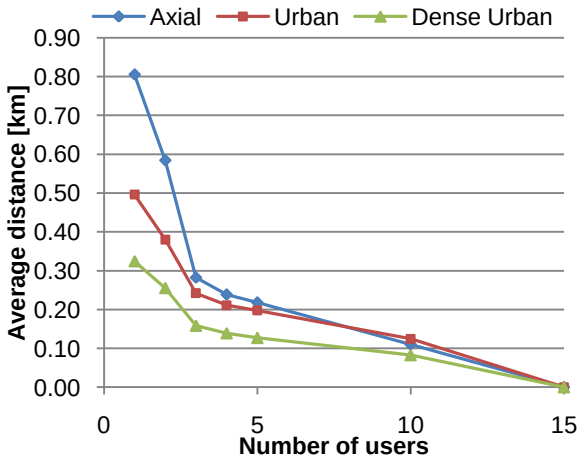

Figure F.27. LTE and UMTS coverage results for LTE UFR's DL in the pedestrian scenario, for required 10Mbps throughput service.

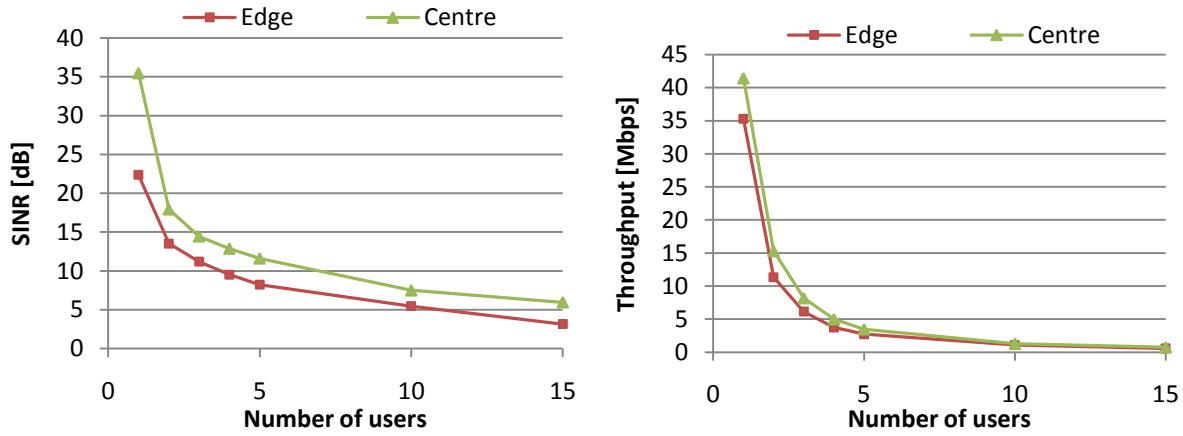

(a) SINR. (b) Throughput.

Figure F.28. Cell centre to cell edge reduction in the Urban pedestrian scenario for UMTS DL, when varying number of users.

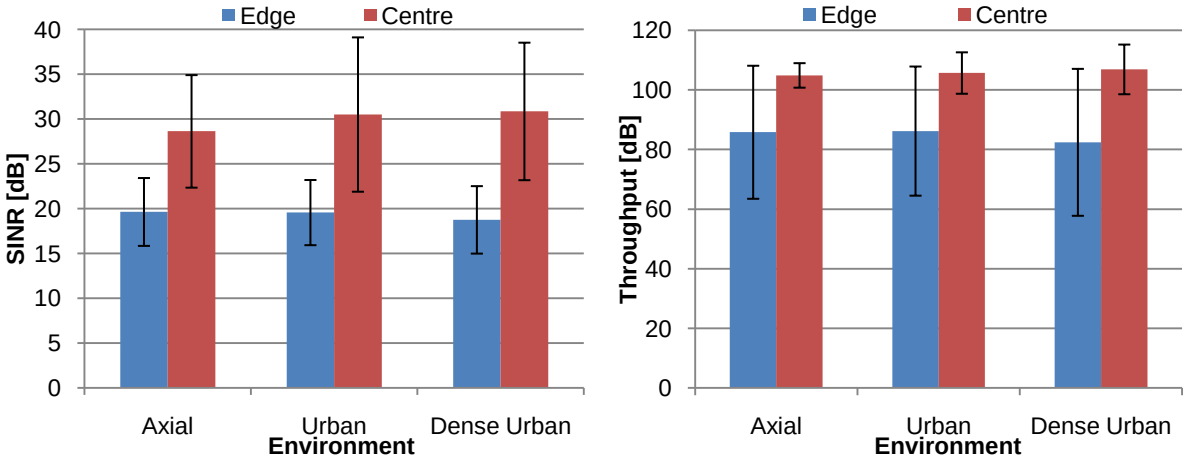

(a) SINR. (b) Throughput.

Figure F.29. Performance difference between cell centre to cell edge DL in the LTE ICIC Urban pedestrian scenario, for varying number of users in the cell.

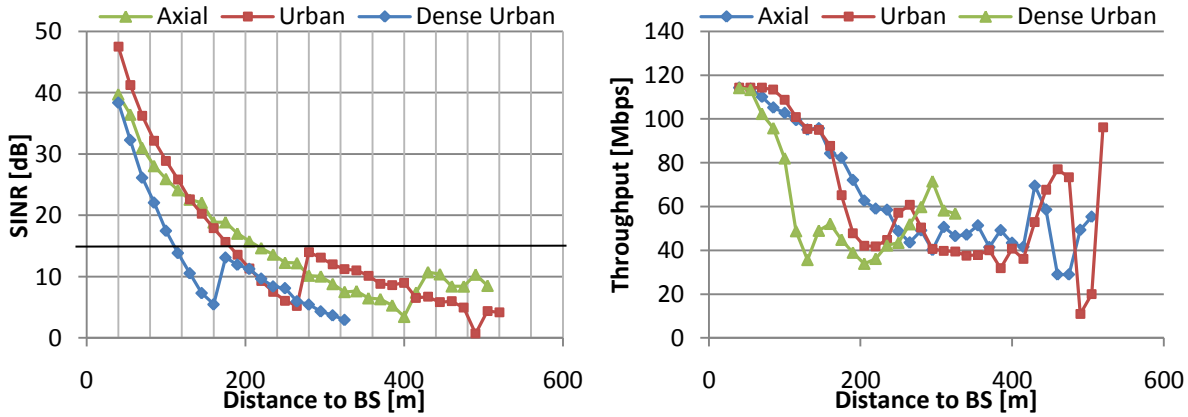

(a) SINR. (b) Throughput.

Figure F.30. SINR and throughput, in DL, as a function of distance to BS, for the Urban pedestrian scenario with a single cell user.

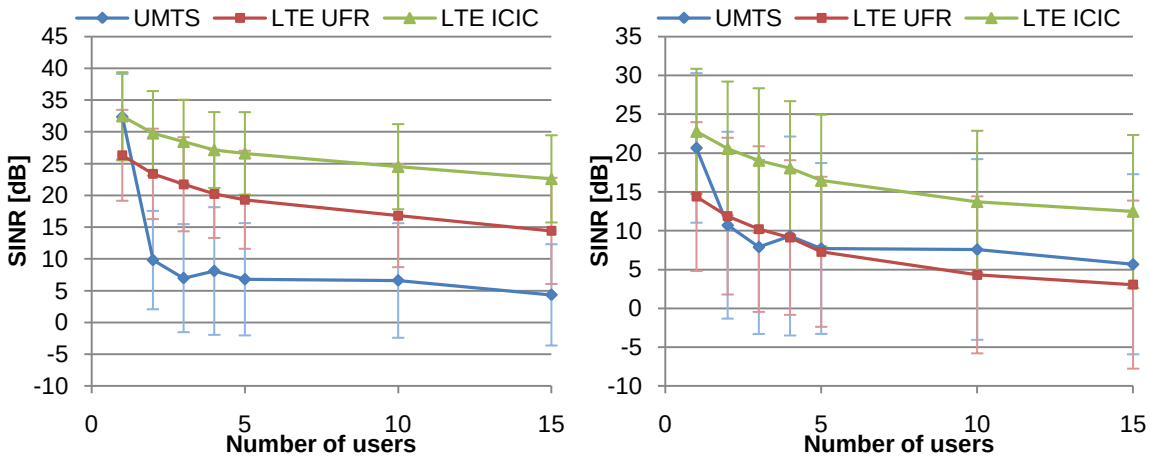

(a) Axial. (b) Dense Urban.

Figure F.31. LTE and UMTS UL SINR for the Axial and Dense Urban pedestrian scenarios, for varying users' number.

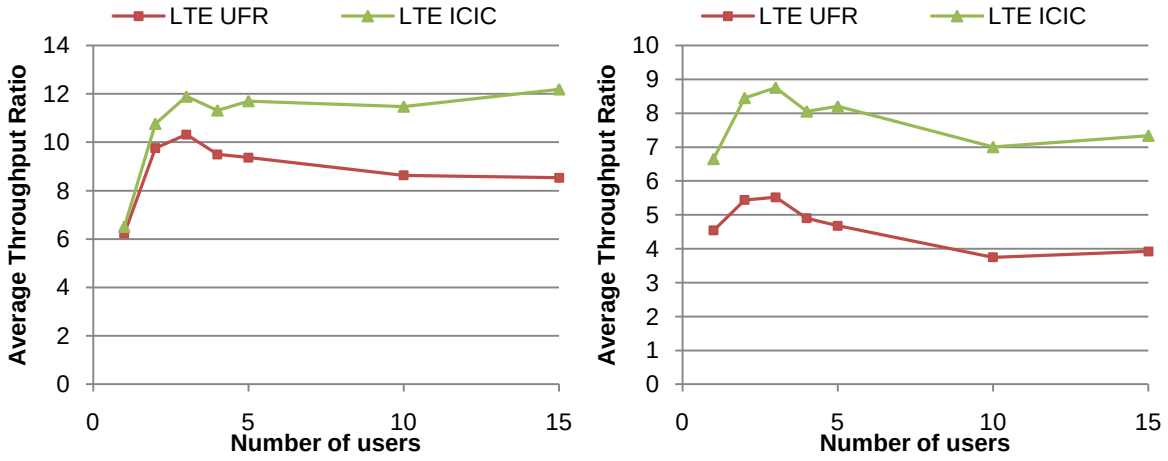

(a) Axial. (b) Dense Urban.

Figure F.32. UMTS to LTE throughput ratio for the Axial and Dense Urban pedestrian scenarios, for varying users' number.

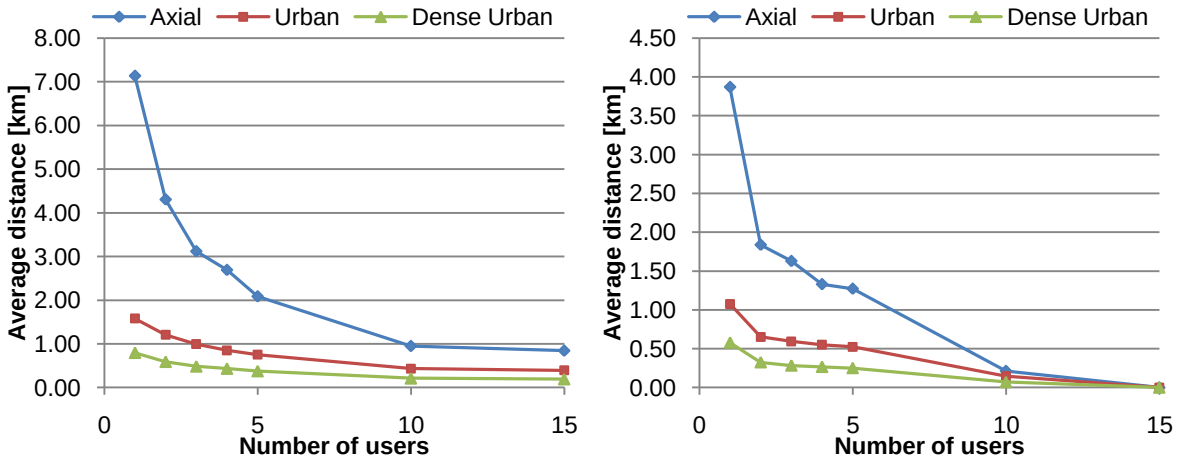

(a) 1Mbps. (b) 5Mbps.

Figure F.33. LTE and UMTS coverage results for LTE UFR's UL in the pedestrian scenario, for required 1Mbps and 5Mbps throughput service.

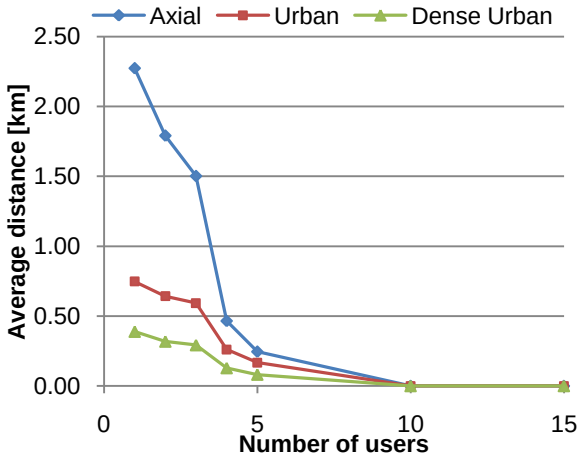

Figure F.34. LTE and UMTS coverage results for LTE UFR's UL in the pedestrian scenario, for required 10Mbps throughput service.

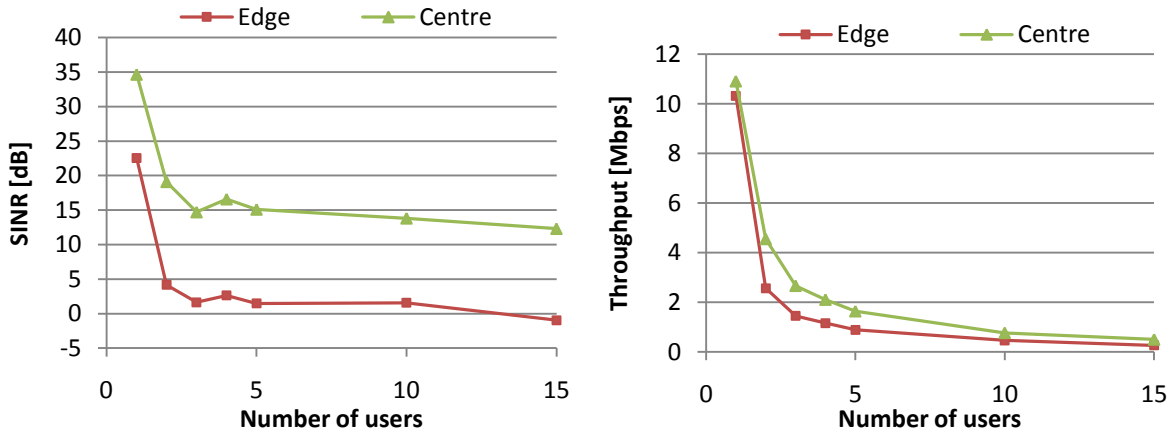

(a) SINR. (b) Throughput.

Figure F.35. Cell centre to cell edge reduction in the Urban pedestrian scenario for UMTS UL, when varying number of users.

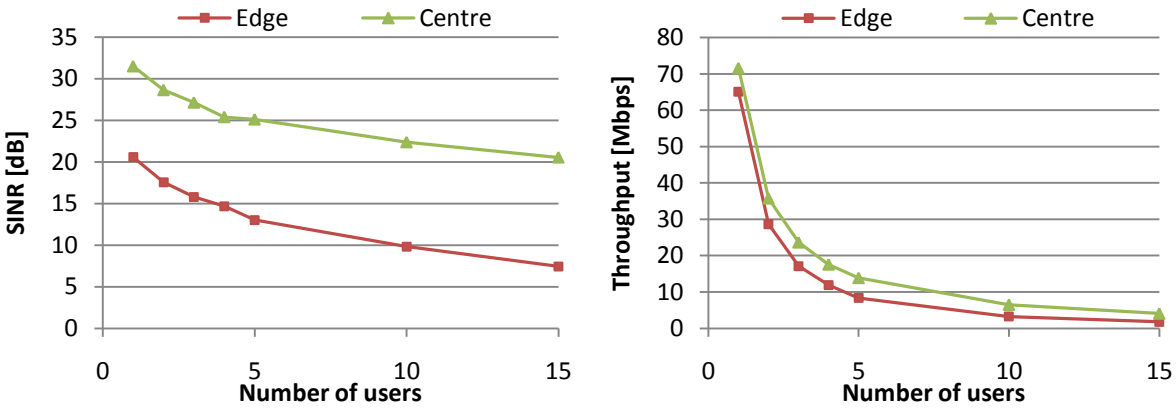

(a) SINR. (b) Throughput.

Figure F.36. Cell centre to cell edge reduction in the Axial pedestrian scenario for LTE, for varying number of users in the cell.

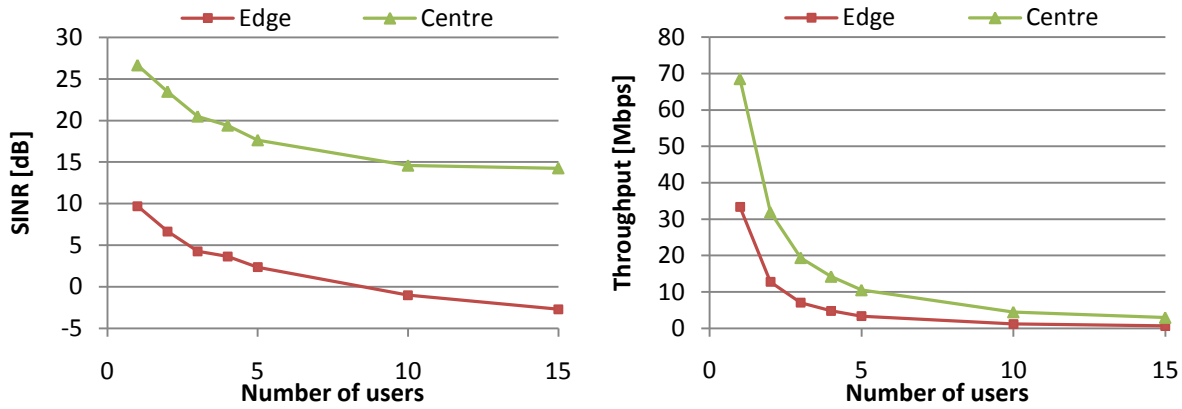

(a) SINR. (b) Throughput.

Figure F.37. Cell centre to cell edge reduction in the Dense Urban pedestrian scenario for LTE, for varying number of users in the cell.

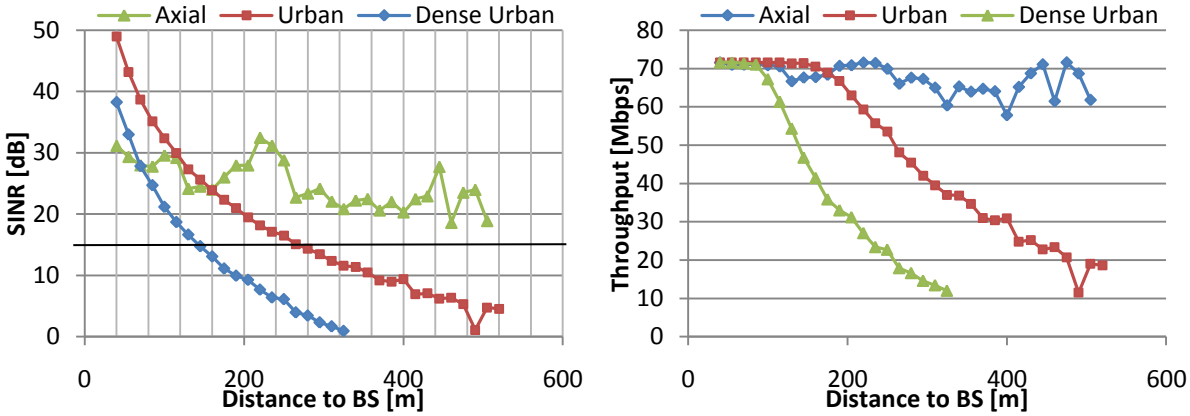

(a) SINR. (b) Throughput.

Figure F.38. SINR and throughput, in UL, as a function of distance to BS, for the Urban pedestrian scenario with a single cell user.

Annex G – LTE Coverage Maps

Additional information regarding the scenarios considered for LTE measurements, namely the maps of LTE covered regions, is presented in this annex. These were previously referenced throughout previous analyses and are a complement to them.

The LTE cluster has been deployed in the city of Porto, in the north of Portugal, composed by a total of 18 BSs, namely an indoor cell and 17 outdoor cells.

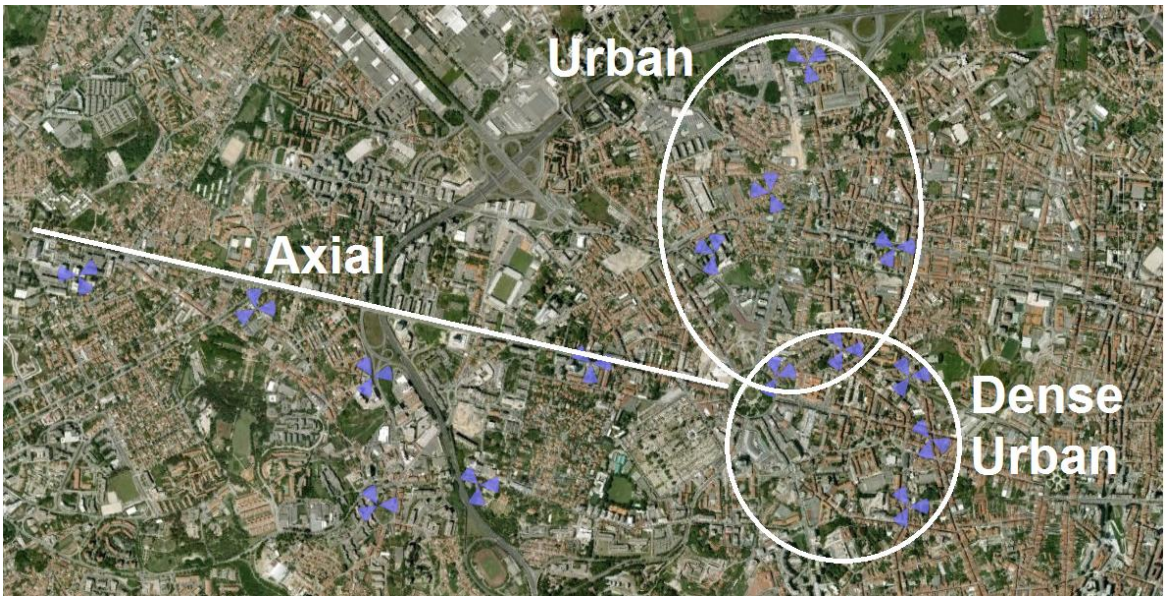

Figure G.1. Outdoor LTE Cluster in Porto (extracted from [GoEa11]).

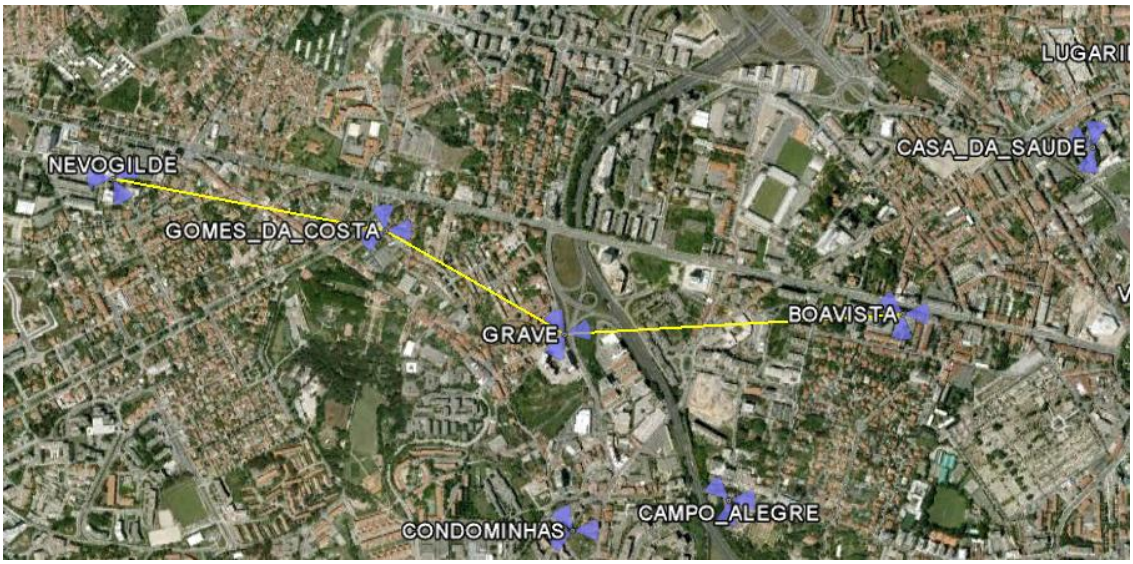

Figure G.2. Inter-BS distance, measured as the distance to the closest detected cell, for the Axial environment (extracted from [GoEa11]).

Figure G.3. Inter-BS distance, measured as the distance to the closest detected cell, for the Urban environment (extracted from [GoEa11]).

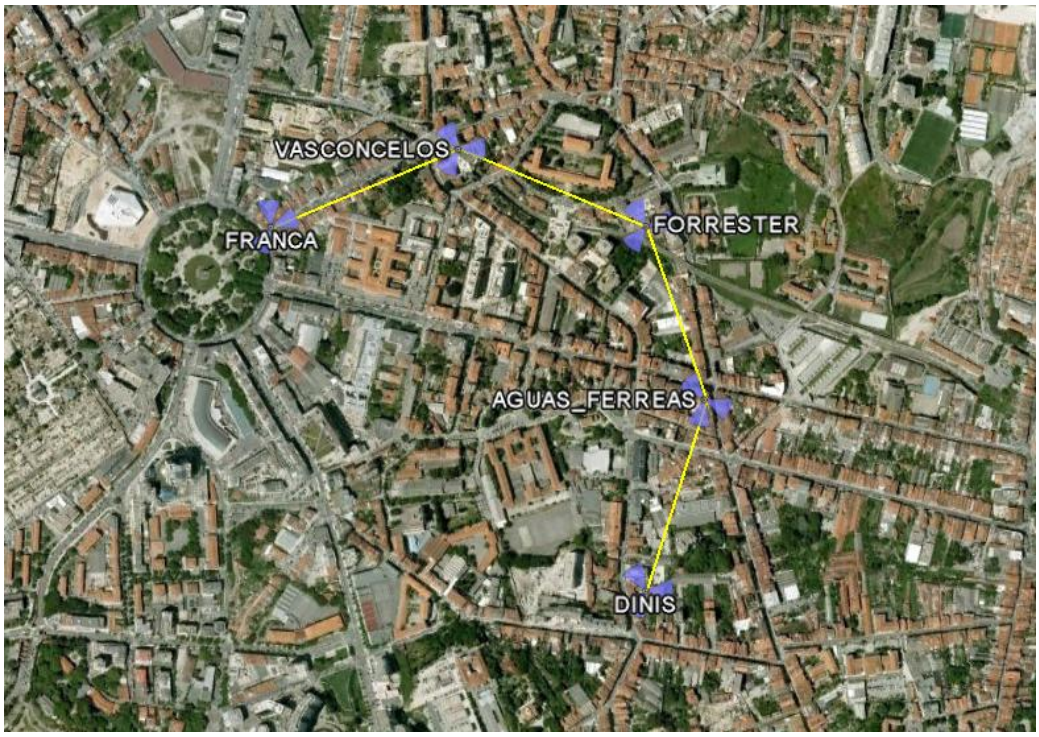

Figure G.4. Inter-BS distance, measured as the distance to the closest detected cell, for the Dense Urban environment (extracted from [GoEa11]).

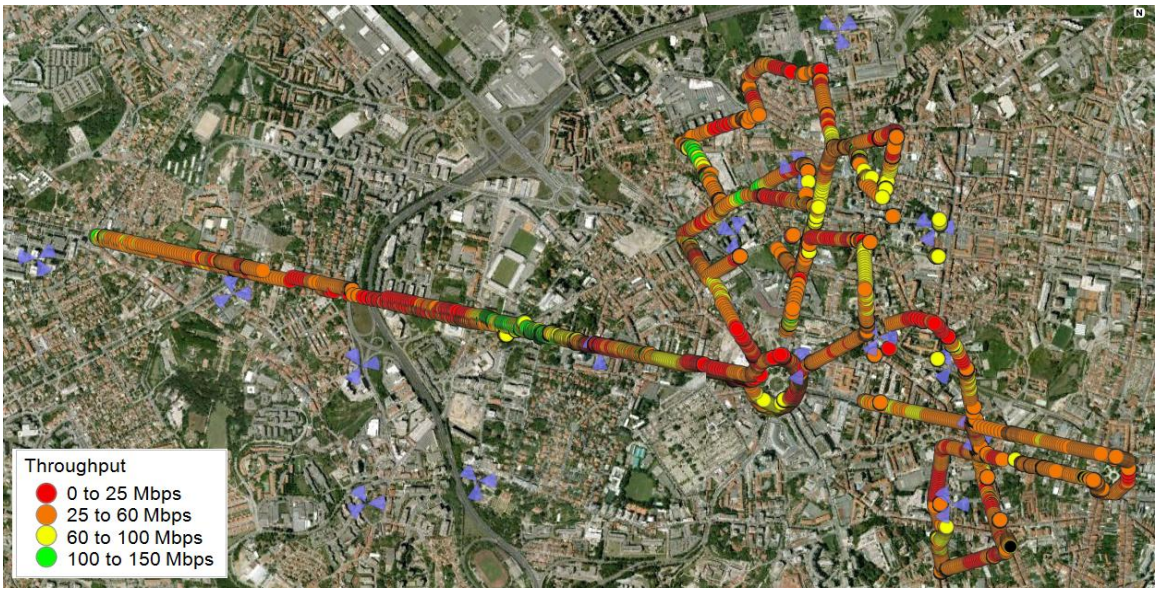

Figure G.5. Drive tests' and static measurements' spots results, sorted by DL throughput (extracted from [GoEa11]).

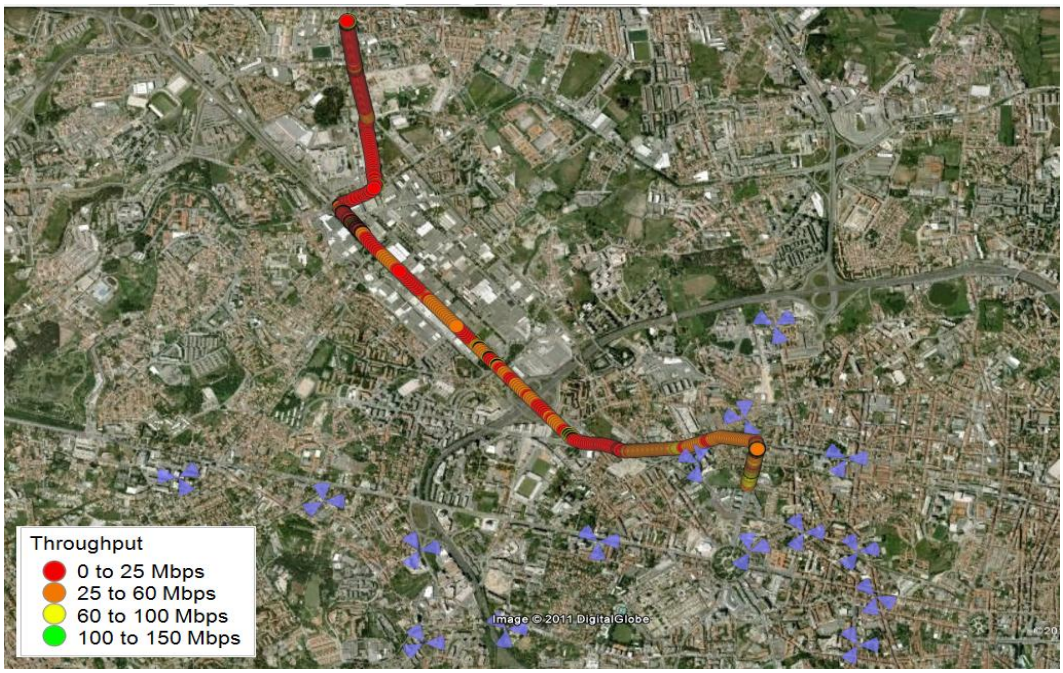

Figure G.6. Drive tests' route for coverage analysis, sorted by DL throughput (extracted from [GoEa11]).

References

[3GPP07] 3GPP, Technical Specification Group - Radio Access Network Working, *Collection of PDSCH results*, Report R4-072218, Jeju, Korea, Nov. 2007.

[3GPP08a] 3GPP, Technical Specification Group - Radio Access Network Working, *PDSCH Demodulation Ideal Results*, Report R4-080194, Sorrento, Italy, Feb. 2008.

[3GPP08b] 3GPP, Technical Specification Group - Radio Access Network Working, *PDSCH 2x2 MCW Ideal Simulation Results*, Report R4-081792, Jeju, Korea, Aug. 2008.

[3GPP08c] 3GPP, Technical Specification Group - Radio Access Network Working, *LTE UE PDSCH demodulation results with impairments for MIMO-FDD case*, Report R4-081439, Munich, Germany, Jun. 2008.

[3GPP08d] 3GPP, Technical Specification Group - Radio Access Network Working, *PDSCH MIMO FDD results*, Report R4-081129, Kansas City, USA, May 2008.

[3GPP08e] 3GPP, Technical Specification Group - Radio Access Network Working, *PUSCH Simulation Results*, Report R4-071730, Shangai, China, Oct. 2007.

[3GPP09] 3GPP, Technical Specification Group Radio Access Network, *Feasibility study for evolved Universal Terrestrial Radio Access (UTRA) and Universal Terrestrial Radio Access Network (UTRAN) (Release 9)*, Report TS 25.912, V9.0.0, Sep. 2009 (http://www.3gpp.org/ftp/specs/html-info/25912.htm).

[3GPP10a] 3GPP, Technical Specification Group Radio Access Network, *BS Radio transmission and Reception (FDD) (Release 99)*, Report TS 25.14.0, V9.6.0, Dec. 2010 (http://www.3gpp.org/ftp/Specs/html-info/25104.htm).

[3GPP10b] 3GPP, Technical Specification Group Radio Access Network, *User Equipment (UE) radio transmission and reception (FDD) (Release 9)*, Report TS 25.101, V9.6.0, Dec. 2010 (http://www.3gpp.org/ftp/specs/html-info/25101.htm).

[3GPP10c] 3GPP, Technical Specification Group Radio Access Network, *Evolved Universal Terrestrial Radio Access (E-UTRA) and Evolved Universal Terrestrial Radio Access Network (E-UTRAN), Overall description, Stage 2 (Release 9)*, Report TS 36.300, V.9.6.0, Dec. 2010 (http://www.3gpp.org/ftp/Specs/html-info/36300.htm).

[3GPP10d] 3GPP, Technical Specification Group Radio Access Network, *Evolved Universal*

Terrestrial Radio Access (E-UTRA); Base Station (BS) radio transmission and reception (Release 9), Report TS 36.104, V.9.6.0, Dec. 2010 (http://www.3gpp.org/ftp/Specs/html-info/36104.htm).

[Agil07] Agilent, Agilent Technologies Solutions for 3GPP LTE, White Paper, USA, September 2007 (http://cp.literature.agilent.com/litweb/pdf/5989-6331EN.pdf).

[Agil11] Agilent, *Transforming MIMO Test With Fast, Accurate Signal Creation and Channel Emulation*, Press Release, USA, Mar. 2011 (http://www.agilent.com/about/newsroom/tmnews/background/2008/01oct2008_pxb.html)

[ANAC11] ANACOM, *Draft rules of the auction for allocation of rights for use of the frequency bands of 450MHz, 900MHz, 1800MHz, 2.1GHz and 2.6 GHz*, Public Consultation, Lisbon, Portugal, 17th Mar. 2011 (http://www.anacom.pt/streaming/Regulation_auction_consultationDUF.pdf?contentId=1093325&field=ATTACHED_FILE).

[Bati08] Batista,T.R., *Capacity Increase in UMTS/HSPA+ Through the Use of MIMO Systems*, M.Sc. Thesis, Technical University of Lisbon, Lisbon, Portugal, 2008.

[Bati11] Batista,R.S., *Performance Evaluation of UMTS/HSPA+ Data Transmission for Indoor Coverage*, M.Sc. Thesis, Technical University of Lisbon, Lisbon, Portugal, 2011.

[BEGG08] Bergman,J., Ericson,M., Gerstenberger,D., Göransson,B., Peisa,J. and Wager,S., "HSPA Evolution – Boosting the performance of mobile broadband access", *Ericsson Review*, Vol.85, No.1, 2008.

[Carv09] Carvalho,G.N., *Data Rate Performance Gains in UMTS Evolution at the Cellular Level*, M.Sc. Thesis, Technical University of Lisbon, Lisbon, Portugal, 2009.

[Cisc11] Cisco, *Cisco Visual Networking Index: Global Mobile Data Traffic Forecast Update, 2010-2015*, White Paper, Cisco Systems, San Jose, California, USA, Feb. 2011 (http://www.cisco.com/en/US/solutions/collateral/ns341/ns525/ns537/ns705/ns827/white_paper_c11-520862.pdf).

[Corr10] Correia,L.M., *Mobile Communication Systems – Course Notes*, IST-UTL, Lisbon, Portugal, 2010.

[DEFJ06] Dahlman, E., Ekstrom, H., Furuskar, A., Jading, Y., Karlsson, J., Lundevall, M., Parkvall, S., "3G Long-Term Evolution – Radio Interface Concepts and Performance Evaluation", in *Proc. of VTC'06 Spring – 63rd IEEE Vehicular Technology Conference*, Melbourne, Australia, May 2006.

[Duar08] Duarte, S., *Analysis of Technologies for Long Term Evolution in UMTS*, M.Sc. Thesis, Technical University of Lisbon, Lisbon, Portugal, Sep.2008.

[Eric08] Ericsson, *Initial field performance measurements of LTE*, White Paper, Ericsson, Stockholm, Sweden, Mar. 2008

(http://www.ericsson.com/res/thecompany/docs/publications/ericsson_review/2010/lte-mimo.pdf).

[Eric10] Ericsson, *Field trials of LTE with 4×4 MIMO*, White Paper, Ericsson, Stockholm, Sweden, Jan. 2010 (http://www.ericsson.com/res/thecompany/docs/publications/ericsson_review/2010/lte-mimo.pdf).

[Eric11] Ericsson, *Ericsson Achieves Three HSPA World Firsts*, Press Release, Ericsson, Stockholm, Sweden, Jan. 2011 (http://hugin.info/1061/R/1483840/419356.pdf).

[EsPe06] Esteves, H. and Pereira M., *Impact of Intra- and Inter-Cellular Interference in UMTS Capacity* (in Portuguese), Dipl. Thesis, Technical University of Lisbon, Lisbon, Portugal, June 2006.

[GGEM09] Greenstein, L.J., Ghassemzadeh, S.S., Erceg, V., Michelson, D.G., "Ricean K Factors in Narrow-Band Fixed Wireless Channels: Theory, Experiments, and Statistical Models", *IEEE Transactions on Vehicular Technology*, Vol. 58, No. 8, Oct. 2009, pp. 4000-4012.

[GoEa11] http://earth.google.com/, May 2011.

[HoTo06] Holma, H. and Toskala, A., *HSDPA/HSUPA for UMTS* (1st Edition), John Wiley & Sons, Chichester, UK, 2006.

[HoTo07] Holma, H. and Toskala, A., *WCDMA for UMTS – HSPA Evolution and LTE* (4th Edition), John Wiley & Sons, Chichester, UK, 2007.

[HoTo09] Holma, H. and Toskala, A., *LTE for UMTS – OFDMA and SC-FDMA Based Radio Access* (1st Edition), John Wiley & Sons, Chichester, UK, 2009.

[IkWR10] Ikuno, J.C., Wrulich, M., Rupp, M., "System Level Simulation of LTE Networks", in *Proc. of VTC'10* Spring – *71st IEEE Vehicular Technology Conference*, Taipei, Taiwan, June 2010.

[Jaci09] Jacinto, N.M., *Performance Gains Evaluation from UMTS/HSPA+ to LTE at the Radio Network Level*, M.Sc. Thesis, Technical University of Lisbon, Lisbon, Portugal, 2009.

[JBGB09] Johansson, K., Bergman, J., Gerstenberger, D., Blomgren, M., Wallén, A., "Multi-Carrier HSPA Evolution", in *Proc. of VTC'09 Spring – 69th IEEE Vehicular Technology Conference*, Barcelona, Spain, Apr. 2009.

[Khan09] Khan, F., *LTE for 4G Mobile Broadband – Air Interface Technologies and Performance* (1st Edition), Cambridge University Press, Cambridge, UK, 2009.

[KuCo08] Kuipers, M., Correia, L.M., "Modelling the Relative MIMO Gain", in *Proc. of PIMRC'08 – IEEE Personal, Indoor and Mobile Radio Communications*, Cannes, France, Sep. 2008.

[LZZY07] Lei, H., Zhang, L., Zhang, X., Yang, D., "A Novel Multi-Cell OFDMA System Structure using Fractional Frequency Reuse", in *Proc. of PIMRC'07 – IEEE Personal, Indoor and Mobile Radio Communications*, Athens, Greece, Sep. 2007.

[Mora10] Morais, M.C., *Probability and Statistics – Course Notes* (in Portuguese), Technical University of Lisbon, Lisbon, Portugal, 2010 (http://www.math.ist.utl.pt/~mjmorais/2010-09-12-NotasApoioPE-EdRevista-SeccaoFolhas.pdf).

[Moto07] Motorola, *Long Term Evolution (LTE): Overview of LTE Air-Interface Technical White Paper*, White Paper, Motorola, USA, 2007 (http://business.motorola.com/experiencelte/pdf/LTEAirInterfaceWhitePaper.pdf).

[Moto09] Motorola, *UMTS/HSPA to LTE Migration*, White Paper, Motorola, USA, 2009 (http://www.motorola.com/web/Business/_Documents/static%20files/UMTS_to_LTE_Migration_White_Paper.pdf).

[Moto10] Motorola, *Motorola LTE Solution*, LTE Systems Overview Brochure, Motorola, USA, 2010 (http://www.motorola.com/web/Business/Solutions/Industry%20Solutions/Service%20Providers/Network%20Operators/LTE/_Document/LTE_Documents/Static_Files/LTE%20Systems%20Overview%20Brochure.pdf).

[MWIB09] Mehlfuhrer, C., Wrulich, M., Ikuno, J.C., Bosanska, D., Rupp, M., "Simulating the Long Term Evolution Physical Layer", in *Proc. of 17th European Signal Processing Conference*, Glasgow, UK, Aug. 2009.

[Neag11] http://www.gifted.uconn.edu/siegle/research/Correlation/alphaleve.htm, July, 2011.

[Noki09] Nokia Siemens Networks, *LTE performance for initial deployments*, White paper, Finland, 2009 (http://w3.nokiasiemensnetworks.com/NR/rdonlyres/46DBDFFE-0B36-40E8-8279-5A56AADB8F6C/0/LTE_measurement_A4_1302.pdf).

[OeCl08] Oestges, C., Clerckx, B., *MIMO Wireless Communications – From Real-World Propagation to Space-Time Code Design* (1st Edition), Elsevier, Oxford, UK, 2008.

[Open10] OPENET, *Closing the Mobile Data Revenue Gap*, White Paper, OPENET Telecom, Dublin, Ireland, 2010 (http://ibmtelconewsletter.files.wordpress.com/2011/02/wp_closing_mobile_data_revenue_gap_a4.pdf).

[Opti11] Private Communication, Optimus, 2011.

[Pede05] Pedersen, K.I., "Quality Based HSDPA Access Algorithms", in *Proc. of VTC'05 Fall – 62nd IEEE Vehicular Technology Conference*, Dallas, TX, USA, Sep. 2005.

[PeMo02] Pedersen, K.I., Mogensen, P.E., "The downlink orthogonality factors influence on WCDMA system performance", in *Proc. of VTC'02 Fall – 56th IEEE Vehicular Technology Conference*, Vancouver, Canada, Dec. 2002.

[Pere11] Pereira, F., *Audio and Video Communications – Course Notes*, Technical University of Lisbon, Lisbon, Portugal, 2011.

[Perg08] Perguiça, R., *Comparison between UMTS/HSPA+ and WiMAX/IEEE 802.16e in Mobility Scenarios*, M.Sc. Thesis, Technical University of Lisbon, Lisbon, Portugal, Sep. 2008.

[PGBC10] Piro, G., Grieco, L.A., Boggia, G., Capozzi, F., Camarda, P., "Simulating LTE Cellular

Systems: an Open Source Framework", *IEEE Transactions on Vehicular Technology*, Vol. 60, No. 2, Feb. 2011, pp.498-513.

[PoMa09] Poikselkä, M. and Mayer, G., *The IMS: IP Multimedia Concepts and Services* (3rd Edition), John Wiley & Sons, Chichester, UK, 2009.

[PoPo10] Porjazoski, M., Popovski, B., "Analysis of Intercell interference coordination by Fractional frequency reuse in LTE", in *Proc. of SoftCOM 2010 International Conference on Software, Telecommunications and Computer Networks (SoftCOM)*, Split, Croatia, Sep. 2010.

[PWST07] Peisa, J., Wager, S., Sågfors, M., Torsner, J., Göransson, B., Fulghum, T., Cozzo, C. and Grant, S., "High Speed Packet Access Evolution – Concept and Technologies", in *Proc. of VTC'07 - 65th IEEE Vehicular Technology Conference*, Dublin, Ireland, Apr. 2007.

[Rysa10] Rysavi, *Transition to 4G – 3GPP Broadband Evolution to IMT-Advanced*, Reserach Report, Rysavi Research, Hood River, USA, Sep. 2010 (http://www.4gamericas.org/documents/3G_Americas_RysavyResearch_HSPA-LTE_Advanced_FINALv1.pdf).

[SaNC10] Salo, J., Nur-Alam, M., Chang, K., *Pratical Introduction to LTE Radio Planning*, White Paper, European Communications Engineering (ECE) Ltd, Espoo, Finland, Nov. 2010 (http://www.eceltd.com/lte_rf_wp_02Nov2010.pdf).

[Seid09] Seidel, E., *Standardization updates on HSPA Evolution*, Research Report, Nomor Research GmbH, Munich, Germany, Mar. 2009 (http://www.3g4g.co.uk/Hspa/HSPAE_WP_0903_Nomor.pdf).

[SeTB09] Sesia, S., Toufik, I., Baker, M., *LTE – The UMTS Long Term Evolution, From Theory to Practice* (1st Edition), John Wiley & Sons, Chichester, UK, 2009.

[Tele09] Telesystem Innovations, *The Seven Modes of MIMO in LTE*, White Paper, Telesystem Innovations (TSI), Toronto, Canada, 2009 (http://www.slideshare.net/allabout4g/the-seven-modes-of-mimo-in-ltepdf).

[VeCo11] Venes, J., Correia, L.M., "Performance of a Heterogeneous Network with UMTS, Wi-Fi and WiMAX", in *Proc. of EUROCON – IEEE International Conference on Computer as a Tool*, Lisbon, Portugal, Apr. 2011.

[Voda10] Vodafone Portugal, *Vodafone Portugal rolls out Mobile Broadband at speeds up to 43.2 Mbps*, Press Release, Vodafone, Lisbon, Portugal, Oct. 2010 (http://www.vodafone.pt/main/A+Vodafone/EN/Press+Releases/pressreleases.htm?id=2396&year=2010&quarter=4).

[XuMK08] Xuehong M., Maaref, A., Koon H. T., "Adaptive Soft Frequency Reuse for Inter-Cell Interference Coordination in SC-FDMA Based 3GPP LTE Uplinks", in *Proc. of GLOBECOM'08 – IEEE Global Communications Conference*, New Orleans, L.A., USA, Dec. 2008.

[Zeme08] Zemen, T., *OFDMA/SC-FDMA Basics for 3GPP LTE (E-UTRA)*, Internal Report, Forschungszentrum Telekommunikation Wien, Vienna, Austria, Apr. 2008 (http://www.nt.tuwien.ac.at/fileadmin/users/wkarner/OFDMA_SCFDMA.pdf).